

APPENDIX B

HYDROLOGY AND HYDRODYNAMICS STUDIES

THIS PAGE INTENTIONALLY LEFT BLANK

Appendix B – Hydrology and Hydrodynamics

This appendix is divided into two sections: 1) the initial Masonville hydrology and hydrodynamics assessment and 2) Seagirt dredging area modeling and dredging depth presentations that were presented to the Bay Enhancement Working Group (BEWG) on December 5th. The report and the presentations are independent of one another and are separated by dividers.

THIS PAGE INTENTIONALLY LEFT BLANK

Masonville Hydrology and Hydrodynamics Study

THIS PAGE INTENTIONALLY LEFT BLANK

TABLE OF CONTENTS

B-1. COASTAL HYDRODYNAMICS.....4

B-1.1 Existing Conditions and Data Sources5

 B-1.1.1 Freshwater Inflow5

 B-1.1.2 Water Levels6

B-2. HYDRODYNAMIC MODELING.....31

B-2.1 Model Description31

B-2.2 Model Development32

 B-2.2.1 Regional Model32

 B-2.2.2 Local Model38

B-2.3 Hydrodynamic Calibration43

 B-2.3.1 Water Levels43

 B-2.3.2 Currents45

B-2.4 Morphological Sediment Model47

 B-2.4.1 Sediment Data and Model Parameters47

 B-2.4.2 Morphological Calibration48

B-2.5 STORM SURGE MODELING50

 B-2.5.1 Model Description.....51

 B-2.5.2 Model Parameters.....55

 B-2.5.3 Storm Surge Calibration.....62

 B-2.5.4 Water Levels63

B-3. IMPACT ASSESSMENT68

B-3.1 Hydrology and Hydrodynamics.....68

 B-3.1.1 Hydrodynamics69

 B-3.1.2 Water Levels69

 B-3.1.3 Currents73

 B-3.1.4 Residence Time80

B-3.2 Sedimentation Impacts82

B-3.3 STORM SURGE IMPACTS84

 B-3.3.1 Water Levels85

TABLES

Table 1.1 Astronomical Tidal Datum Characteristics for Baltimore, Fort McHenry6

Table 1.2 Storm Induced Water Levels7

Table 1.3 Design Wind Speeds per Direction and Return Period (mph)9

Table 1.4 Radially-Averaged Fetch Distances and Water Depth for Wave Hindcasting12

Table 1.5 Offshore Significant Wave Heights (ft) – Masonville13

Table 1.6 Peak Spectral Wave Periods (sec) – Masonville.....13

Table 1.7 Measured Current Speeds (cm/sec) – Patapsco River19

Table 2.1 Water Surface Elevation Statistical Comparison, Model to Predicted.....44

Table 2.2 Peak Storm Surge Water Levels for Baltimore Harbor67

Table 3.1 Water Surface Elevation Statistical Comparison, With and Without Project72

Table 3.2 Residence Time of Patapsco, Upstream of Fort McHenry80

Table 3.3 Peak Storm Surge Water Levels for Baltimore Harbor89

FIGURES

Figure 1.1 Site Map of Masonville Dredged Material Containment Facility	4
Figure 1.2 Design Water Levels per Return Period	8
Figure 1.3 Chesapeake Bay PORTS stations	10
Figure 1.4 Wind Rose at Tolchester Beach	11
Figure 1.5 Wind Direction Frequency Distribution at Tolchester Beach	11
Figure 1.6 CBP Semi-monthly CTD monitoring locations.....	15
Figure 1.7 Current Meter and CTD Profile Locations in Patapsco River	17
Figure 1.8 Current Meter Deployment Locations Near Masonville	18
Figure 1.9 Frequency of Current Speeds at Location No. 5	19
Figure 1.10 Frequency of Current Directions at Location No. 5	20
Figure 1.11 Frequency of Current Directions on Aerial Photograph at Location No. 5	20
Figure 1.12 Current Speed vs. Direction at Location No. 5.....	21
Figure 1.13 Frequency of Current Speeds at Location No. 6.....	22
Figure 1.14 Frequency of Current Directions at Location No. 6	23
Figure 1.15 Frequency of Current Directions on Aerial Photograph at Location No. 6	23
Figure 1.16 Current Speed vs. Direction at Location No. 6.....	24
Figure 1.17 Frequency of Current Speeds at Location No. 7.....	25
Figure 1.18 Frequency of Current Directions at Location No. 7	26
Figure 1.19 Frequency of Current Directions on Aerial Photograph at Location No. 7	26
Figure 1.20 Current Speed vs. Direction at Location No. 7.....	27
Figure 1.21 Frequency of Current Speeds at Location No. 8.....	28
Figure 1.22 Frequency of Current Directions at Location No. 8	29
Figure 1.23 Frequency of Current Directions on Aerial Photograph at Location No. 8	29
Figure 1.24 Current Speed vs. Direction at Location No. 8.....	30
Figure 2.1 Regional Model Grid.....	33
Figure 2.2 Regional Model Bathymetry	35
Figure 2.3 Regional Model Boundary Conditions	37
Figure 2.4 Local Model Grid.....	39
Figure 2.5 Local Model Bathymetry.....	41
Figure 2.6 Local Model Boundary Conditions	42
Figure 2.7– Water Surface Elevation Calibration.....	44
Figure 2.8 Current Velocity at Location 2, Curtis Bay Angle, Surface and Bottom	46
Figure 2.9 Current Velocity at Location 3, Fort McHenry Angle, Surface and Bottom.....	46
Figure 2.10 Current Velocity at Location 4, Fort Masonville Cove	47
Figure 2.11 – Patapsco River Streamflow and TSS.....	49
Figure 2.12 Predicted 20-year Sedimentation/Erosion Patterns	50
Figure 2.13 Model Bathymetry 270m X 270m Grid	52
Figure 2.14 Project Vicinity Bathymetry 270m X 270m Grid.....	53
Figure 2.15 1933 Hurricane Storm Track.....	56
Figure 2.16 Hurricane Fran Storm Track.....	57
Figure 2.17 Hurricane Isabel Storm Track	58
Figure 2.18 Peak Wind Speed in Chesapeake Bay for 1933 Hurricane.....	60
Figure 2.19 Peak Wind Speed in Chesapeake Bay for Hurricane Fran	61
Figure 2.20 Peak Wind Speed in Chesapeake Bay for Hurricane Isabel	62
Figure 2.21 Observation Points within Model.....	63
Figure 2.22 Without-Project Peak Storm Surge in Chesapeake Bay for 1933 Hurricane.....	64
Figure 2.23 Without-Project Peak Storm Surge in Chesapeake Bay for Hurricane Fran	65
Figure 2.24 Without-Project Peak Storm Surge in Chesapeake Bay for Hurricane Isabel	66
Figure 3.1 With-Project Model Bathymetry	68
Figure 3.2 Observation Points Within Model.....	70
Figure 3.3 Water Surface Elevation Comparison, With and Without Project (1 of 2)	71
Figure 3.4 Water Surface Elevation Comparison, With and Without Project (2 of 2)	72
Figure 3.5 Ebb Tide Current Pattern, Surface, With and Without Project.....	74
Figure 3.6 Ebb Tide Current Pattern, Mid Depth, With and Without Project.....	75

Figure 3.7 Ebb Tide Current Pattern, Bottom, With and Without Project.....	76
Figure 3.8 Flood Tide Current Pattern, Surface, With and Without Project.....	77
Figure 3.9 Flood Tide Current Pattern, Mid Depth, With and Without Project.....	78
Figure 3.10 Flood Tide Current Pattern, Bottom, With and Without Project.....	79
Figure 3.11 Residence Time at Observation Points, with and without project.....	81
Figure 3.12 Sedimentation/Erosion Patterns, With Project (bottom) and Without Project (top).....	83
Figure 3.13 Relative annual sedimentation rate of proposed Masonville DMCF project.....	84
Figure 3.14 With-Project Model Bathymetry	85
Figure 3.15 With-Project Peak Storm Surge in Chesapeake Bay for 1933 Hurricane.....	86
Figure 3.16 With-Project Peak Storm Surge in Chesapeake Bay for Hurricane Fran	87
Figure 3.17 With-Project Peak Storm Surge in Chesapeake Bay for Hurricane Isabel	88
Figure 3.18 Surface Elevation Difference Plot for 1933 Hurricane Peak Storm Surge.....	89
Figure 3.19 Surface Elevation Difference Plot for Hurricane Fran Peak Storm Surge.....	90
Figure 3.20 Surface Elevation Difference Plot for Hurricane Isabel Peak Storm Surge	90

B-1. COASTAL HYDRODYNAMICS

This appendix provides detailed information on the coastal processes near the Masonville site shown in Figure 1.1. Sources of data are reviewed and a summary of numerical model development is provided for the hydrodynamic and sedimentation impact assessment.



Figure 1.1 Site Map of Masonville Dredged Material Containment Facility

B-1.1 EXISTING CONDITIONS AND DATA SOURCES

B-1.1.1 Freshwater Inflow

The drainage area of the Chesapeake Bay is approximately 64,000 square miles and includes portions of Maryland, Virginia, West Virginia, Pennsylvania, New York and the District of Columbia. Freshwater enters the system via approximately 150 major rivers and streams at a rate of approximately 80,000 cubic feet per second (Schubel and Pritchard 1987). The primary rivers within the Chesapeake Bay drainage basin are the Susquehanna, Chester, Severn, Choptank, Patuxent, Nanticoke, Potomac, Rappahannock, York, and James Rivers. The Susquehanna River provides, on average, 48 percent of the total freshwater inflow into the Bay. Additional rivers on the western shore of the Bay, which contribute significant flows, are the Potomac, James, Rappahannock, York, and Patuxent, contributing 13.6 percent, 12.5 percent, 3.1 percent, 3.0 percent, and 1.2 percent, respectively. Two significant sources of freshwater flow on the eastern shore of Maryland and Virginia are the Choptank and Nanticoke Rivers, contributing 1.2 percent and 1.1 percent, respectively (Schubel and Pritchard 1987).

The project site is located in Baltimore Harbor, which is on the Patapsco River. The Harbor portion of the Patapsco River is a tributary embayment, receiving very little fresh water inflow from the upper reaches of the Patapsco River, and being influenced primarily by flow from the Bay. United States Geological Survey (USGS) records indicate average freshwater inflow into the Harbor from the Patapsco River to be approximately 430 cubic feet per second, comprising approximately 0.5 percent of total flow into the Bay (USGS 1994).

The North Branch of the Patapsco River originates in Carroll county, north of Westminster and flows south into Liberty Reservoir, then southeast to the Chesapeake Bay. The river flows a total of 65 miles. Of this, the lower 15 are tidally influenced. The Masonville site is approximately nine miles from the mouth of the river. The total drainage area of the watershed is about 550 square miles.

The South Branch of the river originates near Mount Airy and flows east into the main branch about 2 miles south of the Liberty Reservoir. The Middle Branch flows into the main branch at Ferry Bar and Harbor Hospital; the origin of the Middle Branch is at Glyndon and is named the

Gwynns Falls. The third major tributary is the Jones Falls which flows from Owings Mills south into the Northwest Branch at the Baltimore Inner Harbor. Curtis Creek flows north into Curtis Bay, which flows east into the Patapsco River about 2 miles bayward of Masonville. Bear Creek is primarily a relatively large, 800 acre, embayment of the Patapsco River; it is about 5 miles from Masonville and near the mouth of the river. These areas are shown in Figure 2-1.

B-1.1.2 Water Levels

Normal water level variations in the Patapsco River are generally dominated by astronomical tides, although wind effects and freshwater discharge can be important. Extreme water levels, on the other hand, are dictated by storm tides.

B-1.1.2.1 Astronomical Tides

Astronomical tides in the Patapsco River are semi-diurnal; datums near the study area reported from National Ocean Service (NOS) are presented in Table 1.1, for the tidal epoch 1983-2001. The mean sea and mean tide level are about 0.8 ft above MLLW; the mean tidal range is 1.1 ft and the spring tidal range is 1.7 ft (NOS 2003). The difference in elevation between North American Vertical Datum 1988 (NAVD) and National Geodetic Vertical Datum 1929 (NGVD) is approximately 0.55 ft. MLLW will serve as the datum for this project.

Table 1.1 Astronomical Tidal Datum Characteristics for Baltimore, Fort McHenry

Tidal Datum	(ft, MLLW)
Mean Higher High Water (MHHW)	1.66
Mean High Water (MHW)	1.36
North American Vertical Datum – 1988 (NAVD)	0.83
Mean Sea Level (MSL)	0.80
Mean Tide Level (MTL)	0.79
National Geodetic Vertical Datum – 1929 (NGVD)	0.28
Mean Low Water (MLW)	0.22
Mean Lower Low Water (MLLW)	0.00

B-1.1.2.2 Storm Surge

Design water levels for the study area are dominated by storm effects (i.e. storm surge and wave setup) in combination with astronomical tides. Storm surge is a temporary rise in water level

generated either by large-scale extra-tropical storms known as northeasters, or by hurricanes. The rise in water level results from wind action, the low pressure of the storm disturbance and the Coriolis force. A comprehensive evaluation of storm-induced water levels for several Chesapeake Bay locations has been conducted by the Virginia Institute of Marine Science (VIMS) (1978) as part of the Federal Flood Insurance Program. Results of this study, summarized in Table 1.2, were used to generate the water level vs. return period curve presented in Figure 1.2, which provides water levels in feet above MLLW for various return periods. Data in Figure 1.2 are for the closest station location for the project site, which is Baltimore (Fort McHenry). The Fort McHenry station in Baltimore is located at 39° 16' north latitude and 76° 34.7' west longitude, less than one mile northeast of Masonville. The graph shows that water level elevation for a 25-year return period at Baltimore is 5.4 ft MLLW and for a 100-year return period is 8.4 ft MLLW.

Table 1.2 Storm Induced Water Levels

Return Period	Water Level (ft, NGVD)
10	4.1
50	6.8
100	8.4
500	10.7

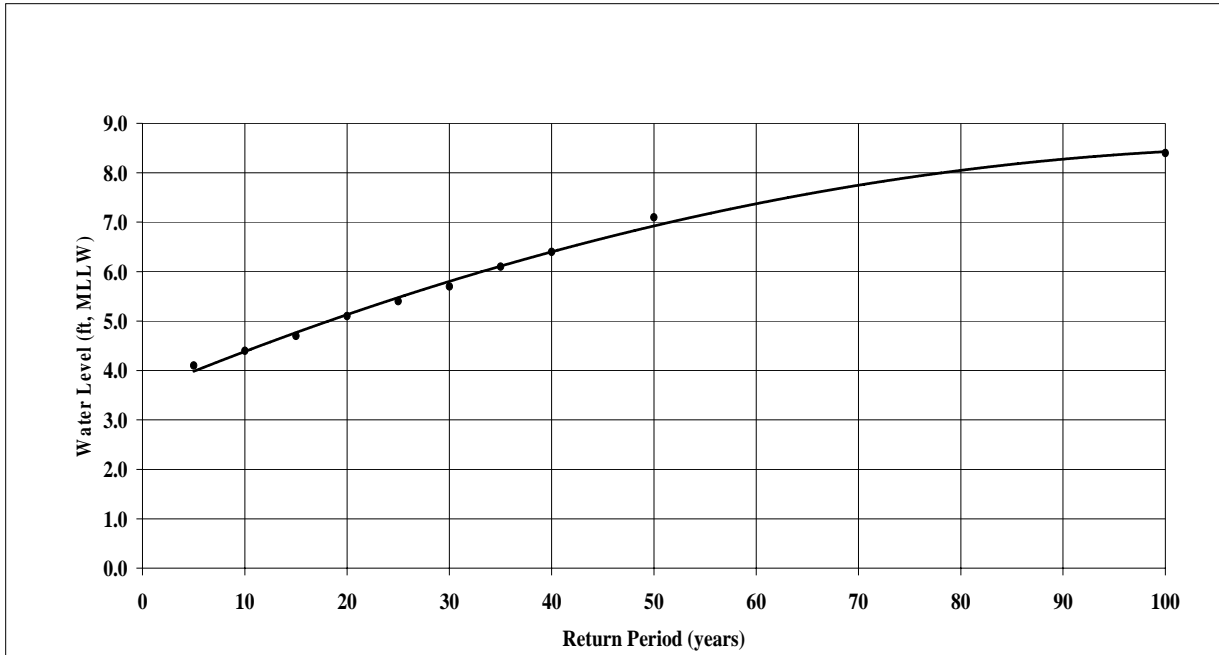


Figure 1.2 Design Water Levels per Return Period

B-1.1.2.3 Wind Conditions

B-1.1.2.3.1 Extreme Wind Conditions

Winds are a significant hydrodynamic force in the Patapsco River and affect both water levels and wave conditions. Annual extreme wind speed data from the National Oceanic and Atmospheric Administration, National Climatic Data Center (NOAA, NCDC) for Baltimore-Washington International (BWI) Airport, for the period 1951 through 1982, were used in computing design wind conditions for this study that will be used for sizing armor stone and dike crest elevations (NOS 1982 and NCDC 1994). The BWI data were used to develop wind speed-return period relationships based on a Type I (Gumbel) distribution for eight directions, namely: North (N), Northeast (NE), East (E), Southeast (SE), South (S), Southwest (SW), West (W) and Northwest (NW). Return period is defined as the average time between wind events which equal or exceed a given value. The specific return periods examined were 5, 10, 15, 20, 25, 30, 35, 40, 50 and 100 years. Table 1.3 contains the design winds.

Table 1.3 Design Wind Speeds per Direction and Return Period (mph)

Return Period	Direction							
	N	NE	E	SE	S	SW	W	NW
5	40	37	32	37	36	47	50	54
10	48	44	38	45	43	56	54	59
15	52	48	41	50	47	61	56	62
20	56	52	45	55	51	67	59	65
25	59	55	47	58	54	70	60	67
30	62	57	49	61	56	73	61	68
35	64	60	51	63	58	76	62	70
40	66	62	53	65	60	78	63	71
50	69	66	55	69	63	82	64	73
100	81	76	65	82	74	97	69	81

B-1.1.2.3.2 Prevailing Wind Conditions

Wind speed and direction are available at a number of stations along the Chesapeake Bay from several sources. Recent data have been collected by the Chesapeake Bay Physical Oceanographic Real-Time System (PORTS) program of National Oceanic and Atmospheric Administration's (NOAA's) NOS Center for Operational Oceanographic Products and Services (CO-OPS). The closest station for which wind data are available is the Francis Scott Key Bridge, shown in Figure 1.3. However the station data collection at this station has been ongoing for only one year. Hourly wind speed and direction is available for the station located at Tolchester Beach for the period from 1995 to 2001., Data was been collected at a 6 minute intervals from spring 2002 to 2005.

Wind speed and direction were analyzed for the 7 year period of 1995 through 2001. The wind rose presented in Figure 1.4 summarizes the percent occurrence of wind speeds and directions at the Tolchester Beach Station. Findings presented in previous studies of hydrodynamic and sediment transport modeling indicate that only winds with speeds higher than 13 mph (11.3 knots) will cause sediment suspension for cohesive sediments (M&N 2003). For non-cohesive sediments it was found that even higher wind speeds are necessary in order to produce any noticeable sediment transport. Analysis of the data shows that the wind speed at the Tolchester

Beach Station is above 11 knots approximately 20 percent of the time. The data is shown in Figure 1.5, which that presents the frequency distribution by direction. Figure 1.5 also shows the frequency distribution of wind speeds below and above 11 knots. For wind speeds higher than 11 knots, in 90 percent of the cases, the wind direction is between W to NNE.

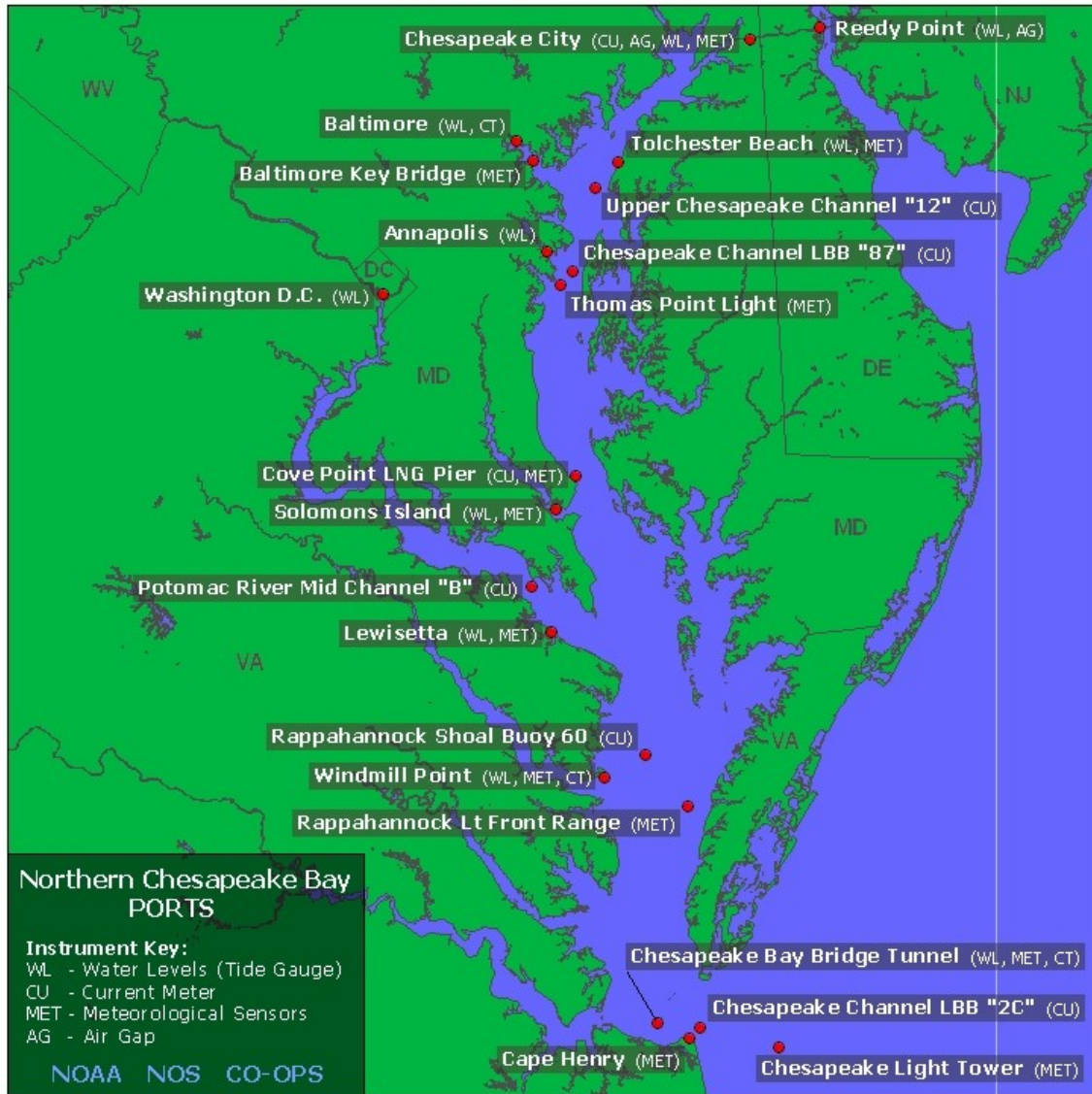


Figure 1.3 Chesapeake Bay PORTS stations

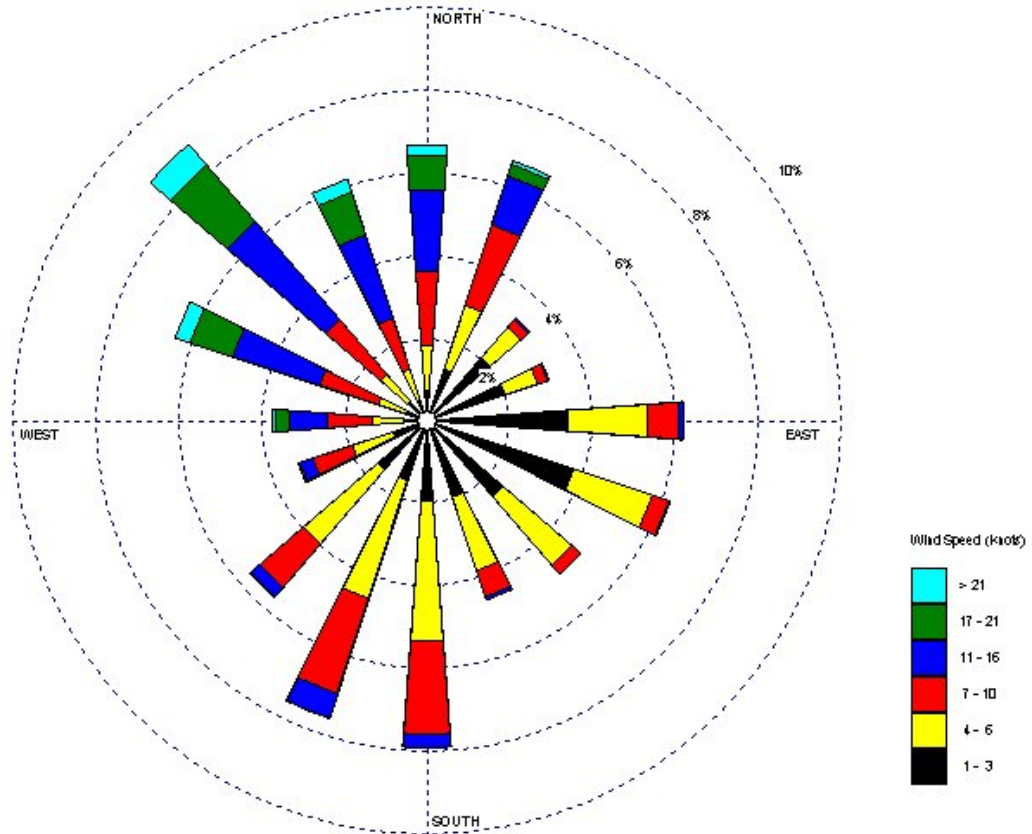


Figure 1.4 Wind Rose at Tolchester Beach

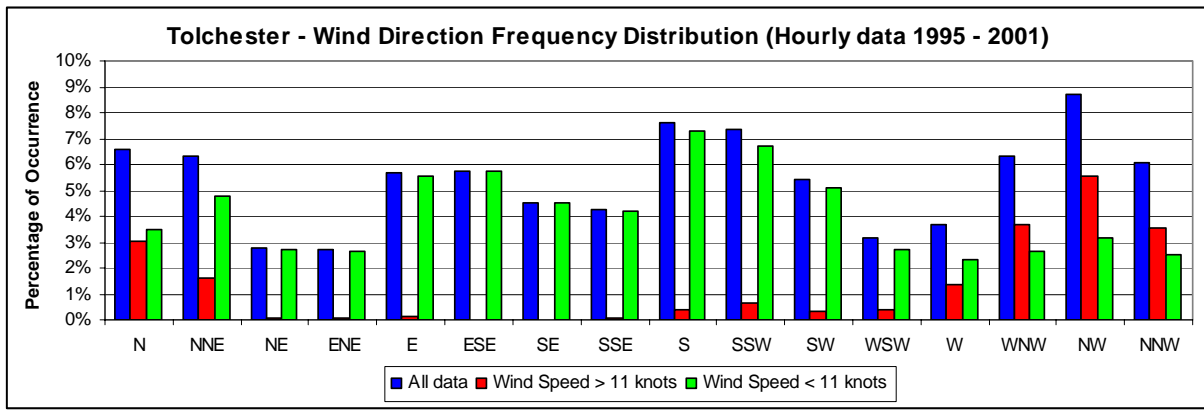


Figure 1.5 Wind Direction Frequency Distribution at Tolchester Beach

4.2.4.4 Wave Conditions

The Masonville site is exposed to wind-generated waves from all directions except the south. Thus, wind-generated wave calculations were completed for the southwest, west, northwest, north, northeast, east and southeast directions.

In accordance with procedures recommended by the U.S. Army Corps of Engineers (USACE), Coastal Engineering Manual (CEM) (USACE 2001), a radially averaged fetch distance was computed for each direction. Table 1.4 presents the radially averaged fetch distances and mean water depths corresponding to each direction.

Table 1.4 Radially-Averaged Fetch Distances and Water Depth for Wave Hindcasting

Direction	Mean Fetch Distance (Miles)	Mean Water Depth (ft, MLLW)
North	0.70	25.3
Northeast	1.1	30.9
East	1.9	30.2
Southeast	1.3	23.1
South	N/A	N/A
Southwest	0.62	6.2
West	1.1	4.7
Northwest	0.95	26.4

A sea state is normally composed of a spectrum of waves with varying heights and periods which may range from relatively long waves to short ripples. In order to summarize the spectral characteristics of a sea state it is customary to represent that wave spectrum in terms of a distribution of wave energy over a range of wave periods. Having made this distribution, known as a wave spectrum, it is convenient to represent the wave spectrum by a single representative wave height and period. The significant wave height (H_s) is defined as the average of the highest one-third of the waves in the spectrum. Depending on the duration of the storm condition represented by the wave spectrum, maximum wave heights may be as high as 1.8 to 2 times the significant wave height. The peak spectral wave period (T_p) corresponds to the maximum wave energy level in the wave spectrum.

Wave conditions were hindcast along each fetch direction for the design winds presented in Table 1.3 (adjusted appropriately for duration) and the water levels presented in Figure 1.2 using methods published in the CEM. Wave hindcast results are presented in Table 1.5 and Table 1.6

Table 1.5 Offshore Significant Wave Heights (ft) – Masonville

Return Period (years)	N	NE	E	SE	S	SW	W	NW
5	1.2	1.3	1.4	1.4	N/A	1.3	1.7	1.9
10	1.4	1.6	1.7	1.7	N/A	1.5	1.8	2.1
15	1.6	1.7	1.9	2.0	N/A	1.7	1.9	2.2
20	1.7	1.9	2.1	2.2	N/A	1.9	2.0	2.3
25	1.8	2.0	2.2	2.3	N/A	2.0	2.0	2.4
30	1.9	2.1	2.3	2.4	N/A	2.1	2.1	2.4
35	2.0	2.2	2.4	2.5	N/A	2.2	2.1	2.5
40	2.0	2.3	2.5	2.6	N/A	2.2	2.2	2.5
50	2.1	2.5	2.6	2.8	N/A	2.4	2.2	2.6
100	2.6	2.9	3.1	3.4	N/A	2.9	2.4	2.9

Table 1.6 Peak Spectral Wave Periods (sec) – Masonville

Return Period (years)	N	NE	E	SE	S	SW	W	NW
5	1.7	1.9	2.2	2.0	N/A	1.8	2.1	2.1
10	1.9	2.1	2.3	2.2	N/A	1.9	2.2	2.2
15	1.9	2.2	2.4	2.3	N/A	1.9	2.2	2.3
20	2.0	2.2	2.5	2.4	N/A	2.0	2.2	2.3
25	2.0	2.3	2.5	2.4	N/A	2.0	2.3	2.3
30	2.1	2.3	2.6	2.5	N/A	2.1	2.3	2.3
35	2.1	2.3	2.6	2.5	N/A	2.1	2.3	2.4
40	2.1	2.4	2.6	2.5	N/A	2.1	2.3	2.4
50	2.2	2.4	2.7	2.6	N/A	2.2	2.3	2.4
100	2.3	2.6	2.9	2.8	N/A	2.3	2.4	2.5

B-1.1.2.4 Tidal Currents

NOAA Tidal Current Tables (1996) state that currents in the Patapsco River from the mouth at North Point, Brewerton Channel to the Middle Branch entrance at the Hanover Street Bridge are weak and variable, with a maximum velocity of less than 30 cm/sec.

B-1.1.2.5 Salinity and Temperature

Boicourt and Olson (1982) performed hydrodynamic studies of the Baltimore Harbor that included field measurements of current velocity, temperature and salinity at several locations in the Patapsco River. These measurements were used to provide data for their development of a two-dimensional numerical model of Baltimore Harbor. The two-dimensional model was oriented in a vertical direction along the axis of the main shipping channels. Results from the study's current measurements indicated the existence of a three-layer, density-driven circulation that can dominate flow such that typical semi-diurnal tidal current direction reversals (shifting between high and low tide) do not necessarily occur. The study also determined that wind events often dominate circulation patterns, especially within the Middle Branch and the tributaries; however, high flow events from the Patapsco River often produce a typical two-layer estuarine circulation. Two-layer circulation consists of fresh river water flowing out on the surface and higher salinity bay water flowing in at the bottom. The study determined that the short-term variability of circulation and density is as significant as seasonal variability.

As part of the semi-monthly Chesapeake Bay Program (CBP) monthly monitoring cruises, water quality parameters are measured over the water column depth at various points within the bay. These data provide snapshots of the stratification of the Harbor and the main Bay which changes seasonally. Figure 1.6 displays the locations of the CBP monitoring stations within the project vicinity.

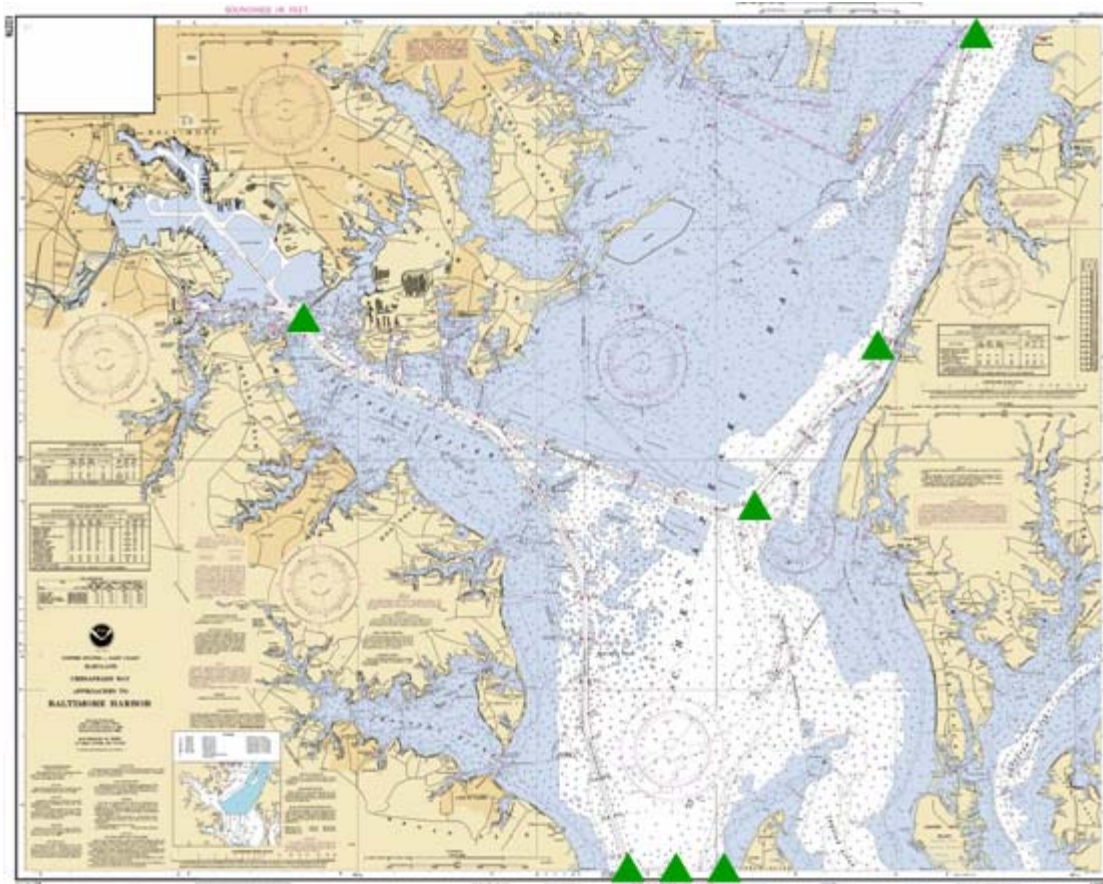


Figure 1.6 CBP Semi-monthly CTD monitoring locations

B-1.1.2.6 Additional Project Data Collection

One of the recommendations from the Boicourt and Olson (1982) study was to collect additional data using continuous vertical-profiling current measurements for a period of time greater than three weeks. As part of this EIS, a field data collection program was developed to use Acoustic Doppler Current Profilers (ADCP) to collect current measurements. These were completed by Science Applications International Corporation (SAIC) and Moffatt & Nichol (M&N) in 2004 and 2005. In addition, three-dimensional hydrodynamic numerical modeling was performed to evaluate existing conditions as regards tidal currents, suspended sediment movement, and salinity.

Current meters were deployed in eight locations to collect data to evaluate typical current speed and direction. The meters were located in the Patapsco River, including several locations in the vicinity of the Masonville project location. The locations in meters are shown in Figure 1.7 and

Figure 1.8. The eight locations include:

- 1) The mouth of the Patapsco River at the Brewerton Cutoff Angle;
- 2) The Curtis Bay Channel Angle;
- 2A) Curtis Bay
- 3) The Fort McHenry Angle;
- 4) The mouth of Masonville Cove;
- 5) North of the existing Masonville site, about 50 ft from a point feature along the shoreline, east of the derelict vessels;
- 6) Within Masonville Cove about 150 ft from the shoreline;
- 7) The approximate middle of the mouth of the main branch of the Patapsco River, about 20 ft downstream of the bridge crossing Hanover Street, halfway between two bridge pilings to avoid their effects on the flow; and
- 8) The main branch Patapsco River, about 1,250 ft upstream from the mouth.

ADCPs were deployed at Stations 1 thru 4 for the period 21 April 2005 to 7 July 2005. These meters collected current speed and direction at several intervals throughout the water column. In addition, conductivity-temperature-depth (CTD) profilers were employed to collect salinity and temperature data at Stations 1 thru 4 on 21 April 2005 and 25 May 2005, to supplement the limited stations available from the CBP cruises. Analysis of the data from Stations 1 thru 4 as well as the CTD profiles may found in Attachment A.1. An Aanderaa ADCP recording current meter RCM-9 was deployed at Station 5 for the period 3 September 2004 to 1 October 2004, at Station 6 for the period 7 October 2004 to 5 November 2004, at Station 7 for the period 5 November 2004 to 8 December 2004, and at Station 8 for the periods 20 April 2005 to 22 May 2005 and 14 June 2005 to 16 July 2005.

Statistical analysis was performed to compute mean speed and directions for flood and ebb tides for Stations 1 thru 8. The minimum, maximum, mean, median, and mode of the current speeds at the eight locations are presented in Table 1.7. These data show that mean speeds near Masonville are very low, at about 3.5 to 4.4 cm/sec, with occasional highs from 14.2 to 24.4 cm/sec. These low values can be attributed to two factors: 1) Most of the tidal influence from the Chesapeake Bay remains in the main part of the Bay and does not enter the Patapsco River; and 2) The freshwater discharge from the Patapsco River is not significantly large. Values in the upstream Patapsco River are slightly higher with means of 6.5 to 7.4 cm/sec and maximum

speeds of 38.1 to 47.4 cm/sec. Values in the Patapsco River increase in velocity moving closer to the Bay, with velocities up to 18.2 cm/sec and maximum measurements of 88 cm/sec.

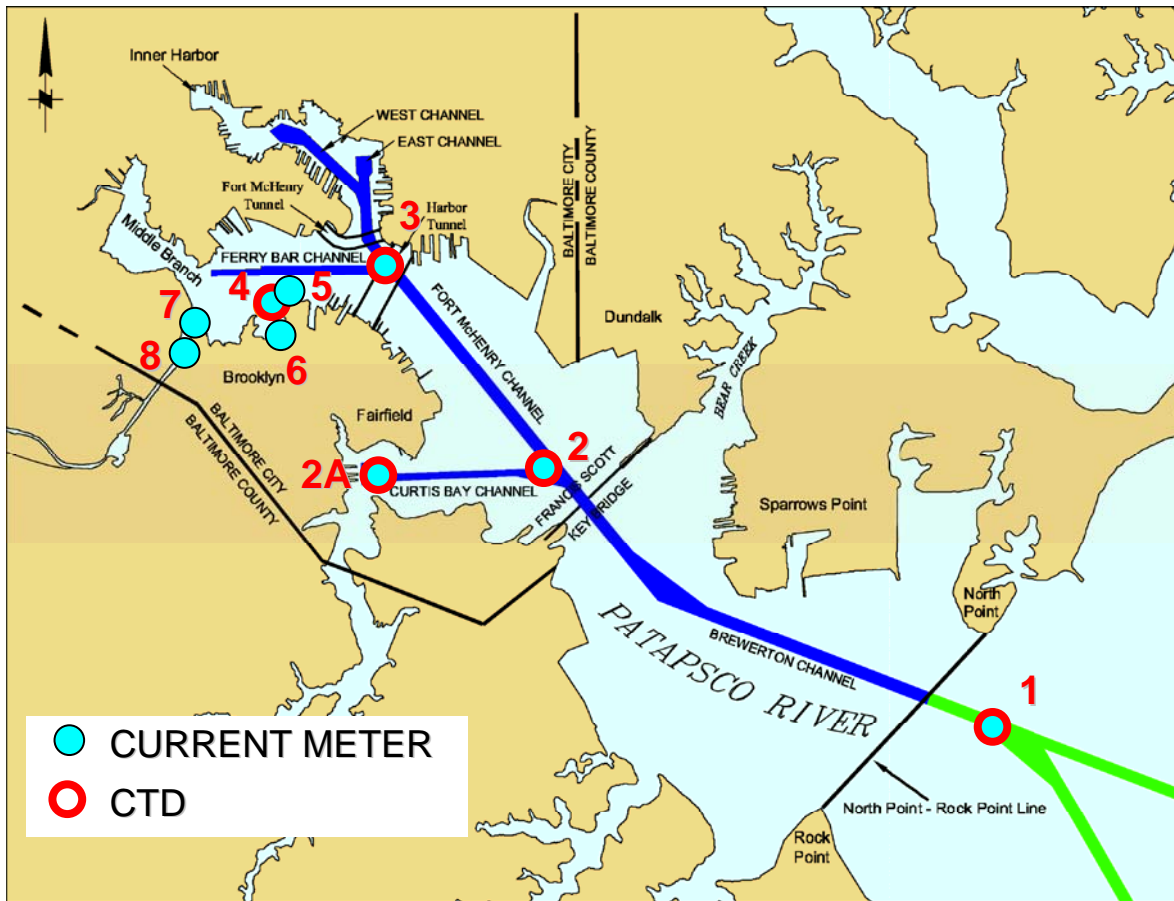


Figure 1.7 Current Meter and CTD Profile Locations in Patapsco River

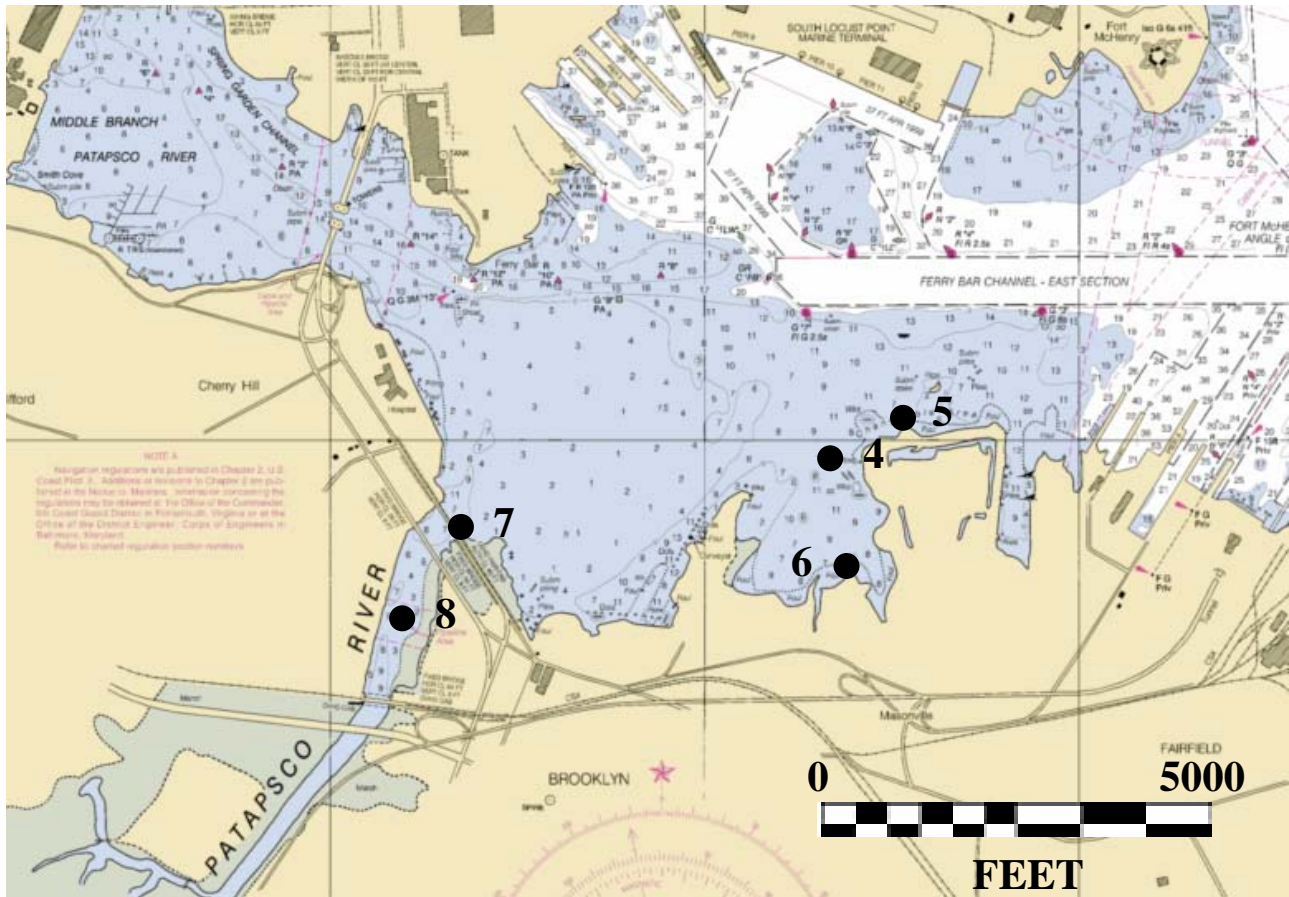


Figure 1.8 Current Meter Deployment Locations Near Masonville

The minimum, maximum, mean (average), median (middle value of data set), and mode (most frequent) of the current speeds at the eight locations are presented in Table 1.7. These data show that typical speeds are very low at about 2 to 5 cm/sec, with occasional highs from 14 to 38 cm/sec. These low values can be attributed to two factors: 1) most of the tidal influence from the Chesapeake Bay remains in the main part of the Bay and does not enter the Patapsco River, and 2) the freshwater discharge from the Patapsco River is not significantly large (see above Section B-1.1.1).

Table 1.7 Measured Current Speeds (cm/sec) – Patapsco River

Location No.	Minimum	Maximum	Mean	Median	Mode
1 – Surface	0	88.0	13.4	11.4	2.9
1 – Mid-Depth	0	74.5	18.2	16.7	4.7
1- Bottom	0	51.9	10.1	9.2	9.7
2 – Surface	0	54.3	6.5	5.0	2.5
2 – Mid-Depth	0	46.1	8.0	7.0	4.3
2- Bottom	0	37.2	6.2	5.4	3.6
3 – Surface	0	27.9	8.0	7.2	3.6
3 – Mid-Depth	0	27.3	6.4	5.8	3.9
3- Bottom	0	38.0	6.4	5.6	5.5
4 – Mid-Depth	0	14.3	4.4	4.1	3.8
5 – Mid-Depth	0	14.2	3.5	3.4	2.4
6 – Mid-Depth	0	24.4	4.2	3.4	2.9
7 – Mid-Depth	0	38.1	6.5	5.4	3.9
8 – Mid-Depth	0	47.4	7.4	5.9	2.9

Figure 1.9 presents a current speed vs. frequency of occurrence plot for location no. 5 that shows graphically that most of the speeds are in the 2 to 5 cm/sec range and practically all are less than 10 cm/sec. Higher speeds are likely attributable to wind-generated or boat-generated waves.

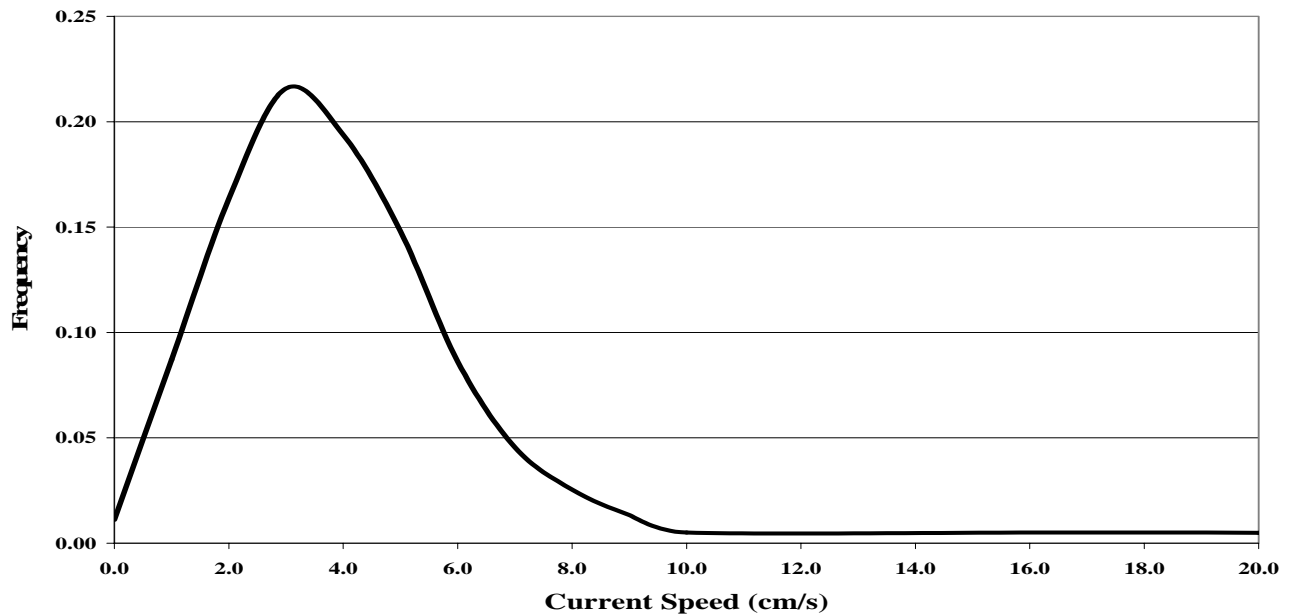


Figure 1.9 Frequency of Current Speeds at Location No. 5

Figure 1.10 presents a polar plot showing current direction vs. frequency of occurrence for location no. 5. This figure shows that predominant ebb direction is towards the east-southeast (112.5 to 135 degrees) and the predominant flood direction is towards the west-southwest (225 to 247.5 degrees). Figure 1.11 contains the polar plot overlaid on an aerial photograph which shows that these predominant directions are due to the current following the existing shoreline.

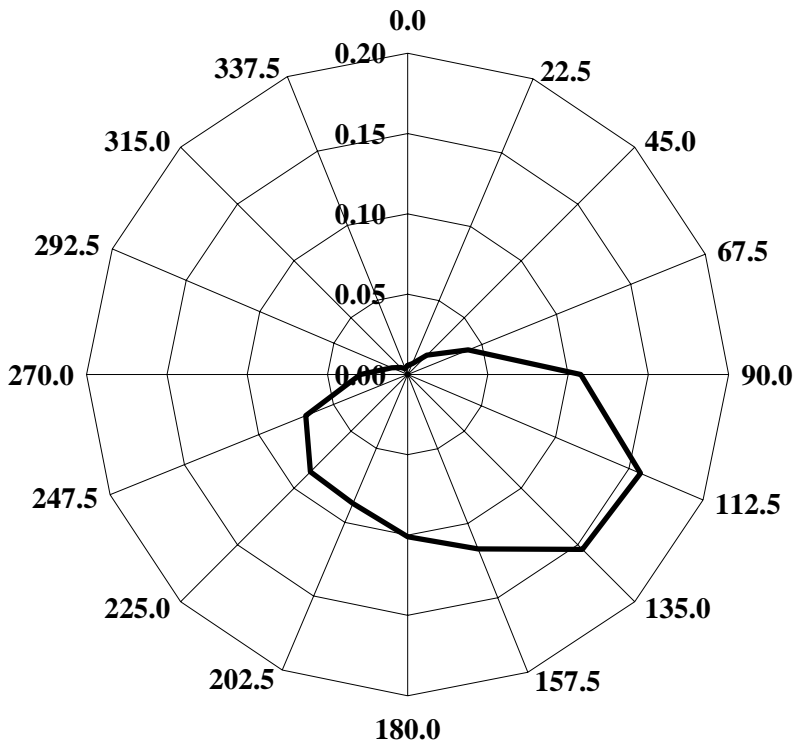


Figure 1.10 Frequency of Current Directions at Location No. 5

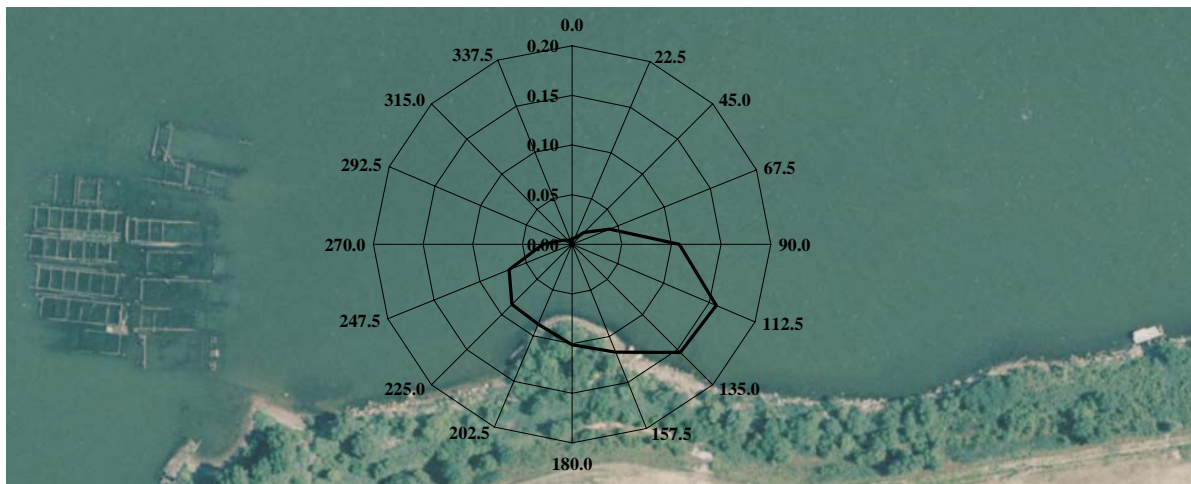


Figure 1.11 Frequency of Current Directions on Aerial Photograph at Location No. 5

Figure 1.12 presents a scatter plot graph of the current speed vs. direction for location no. 5. This graph shows that the highest speeds tend to match the most common ebb and flood directions, however, there is a lot of variability in direction, i.e. there is not a defined ebb-flood direction. This variability is probably due to wind-generated flow conditions as the location is relatively exposed to open water.

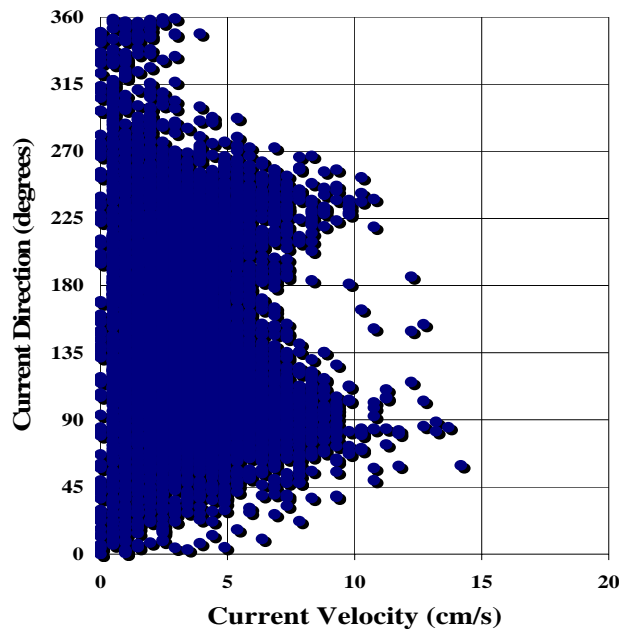


Figure 1.12 Current Speed vs. Direction at Location No. 5

Figure 1.13 presents a current speed vs. frequency of occurrence plot for location no. 6 that shows (similarly to location no. 5) most of the speeds are in the 2 to 5 cm/sec range. Unlike location no. 5, however, there are more frequent occurrences of speeds greater than 10 cm/sec. Table 1.7 contains data that show this location has a slightly higher mean speed and significantly higher measured maximum speed (24 cm/sec). Higher speeds for location no. 6 can be attributed to wind-generated waves from the northwest to northeast pushing water into the cove, and because there is no outlet, the trapped water would increase in speed as it flowed within and along the shoreline of the cove.

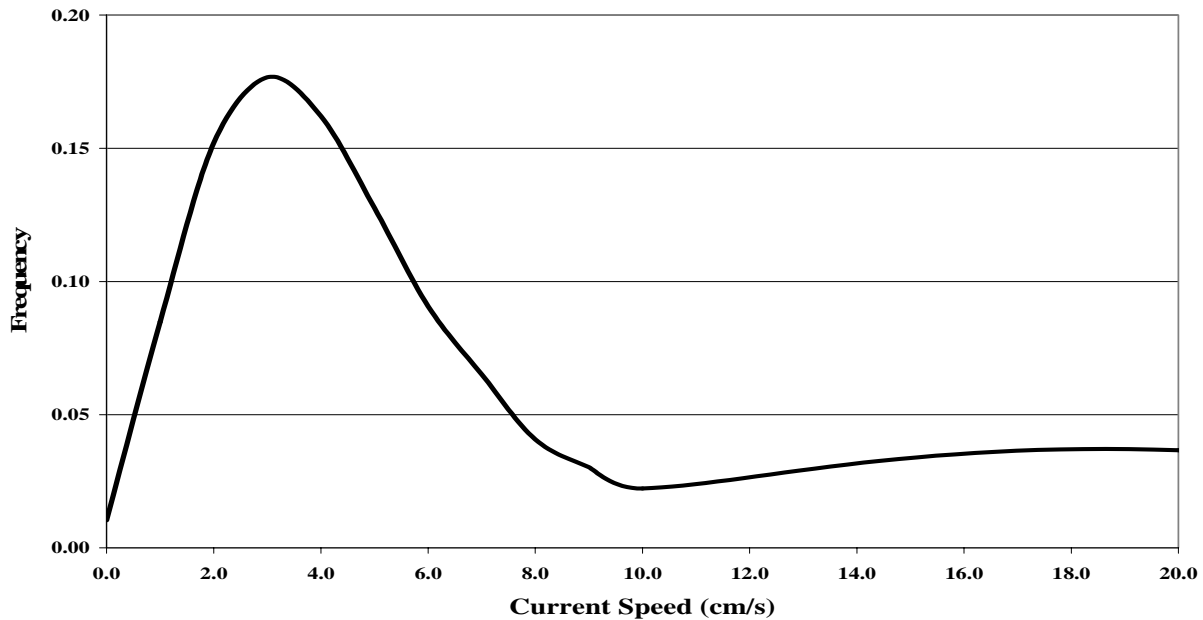


Figure 1.13 Frequency of Current Speeds at Location No. 6

Figure 1.14 presents a polar plot showing current direction vs. frequency of occurrence for location no. 6. This figure shows that predominant ebb direction is towards the east-northeast (67.5 degrees) and the predominant flood direction is towards the west-northwest (270 to 292.5 degrees). Figure 1.15 contains the polar plot overlaid on an aerial photograph which shows that these predominant directions are due to the current following the existing shoreline.

Figure 1.16 presents a scatter plot graph of the current speed vs. direction for location no. 6. This graph shows that the highest speeds match the most common ebb and flood directions, and unlike location no. 5, there is a well-defined ebb-flood direction. This distinct pattern is primarily due to the fact that flow into the cove is trapped and follows a circular movement along the shoreline.

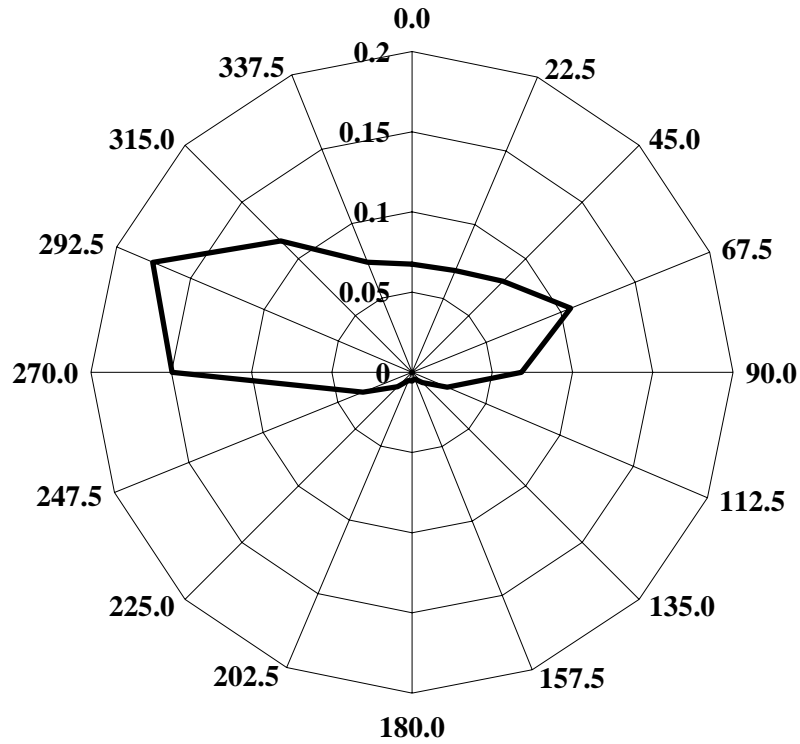


Figure 1.14 Frequency of Current Directions at Location No. 6

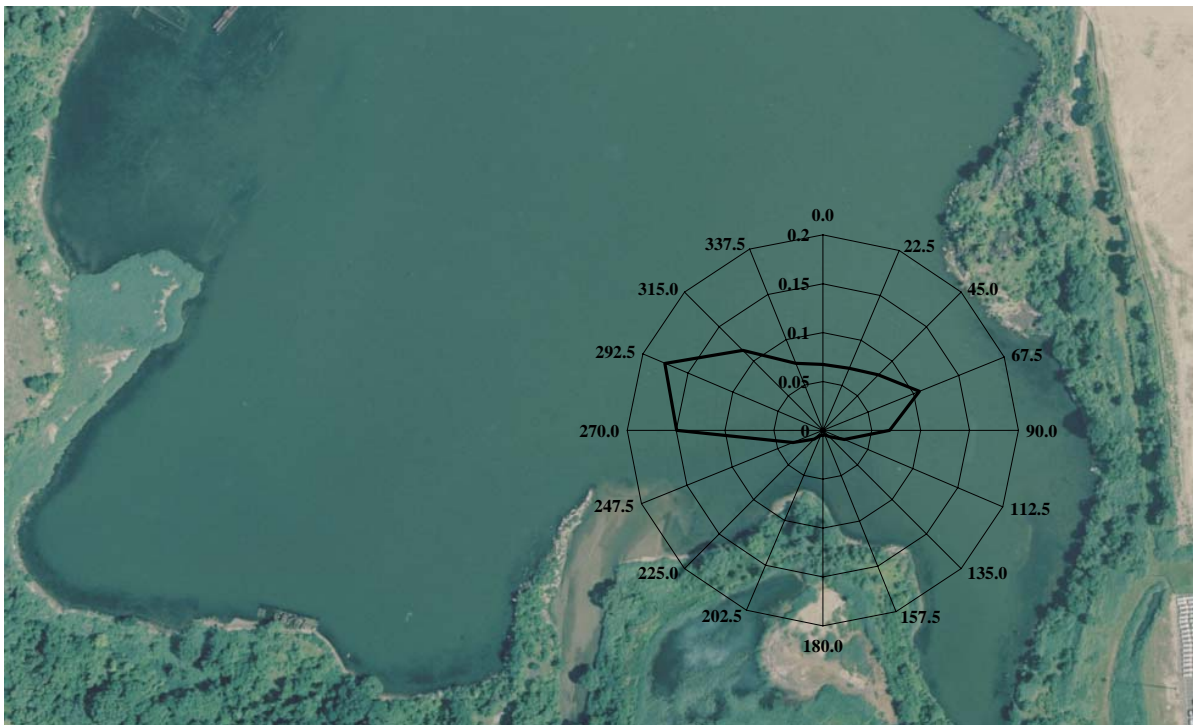


Figure 1.15 Frequency of Current Directions on Aerial Photograph at Location No. 6

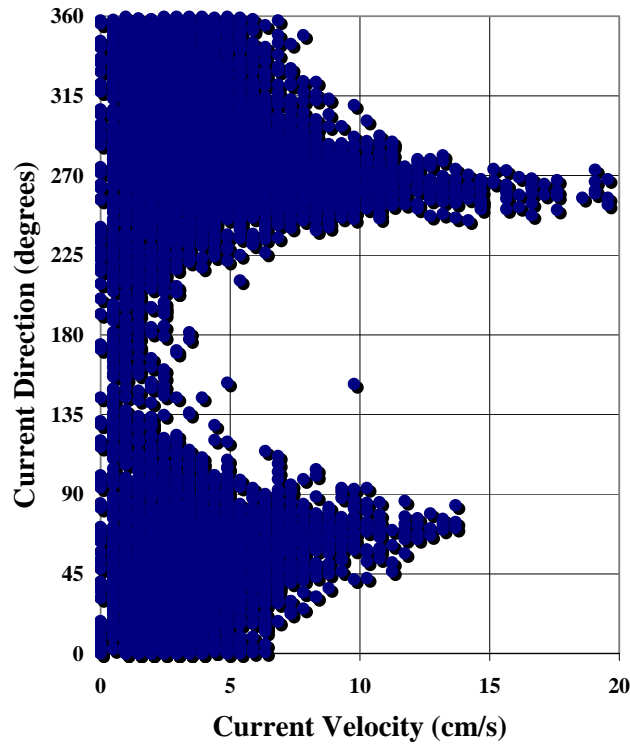


Figure 1.16 Current Speed vs. Direction at Location No. 6

Figure 1.17 presents a current speed vs. frequency of occurrence plot for location no. 7 that shows graphically that most of the speeds are in the 2 to 6 cm/sec range and practically all are less than 20 cm/sec. At this location there is a greater frequency of speeds in the 10 to 20 cm/sec range than at location no. 5 and 6.

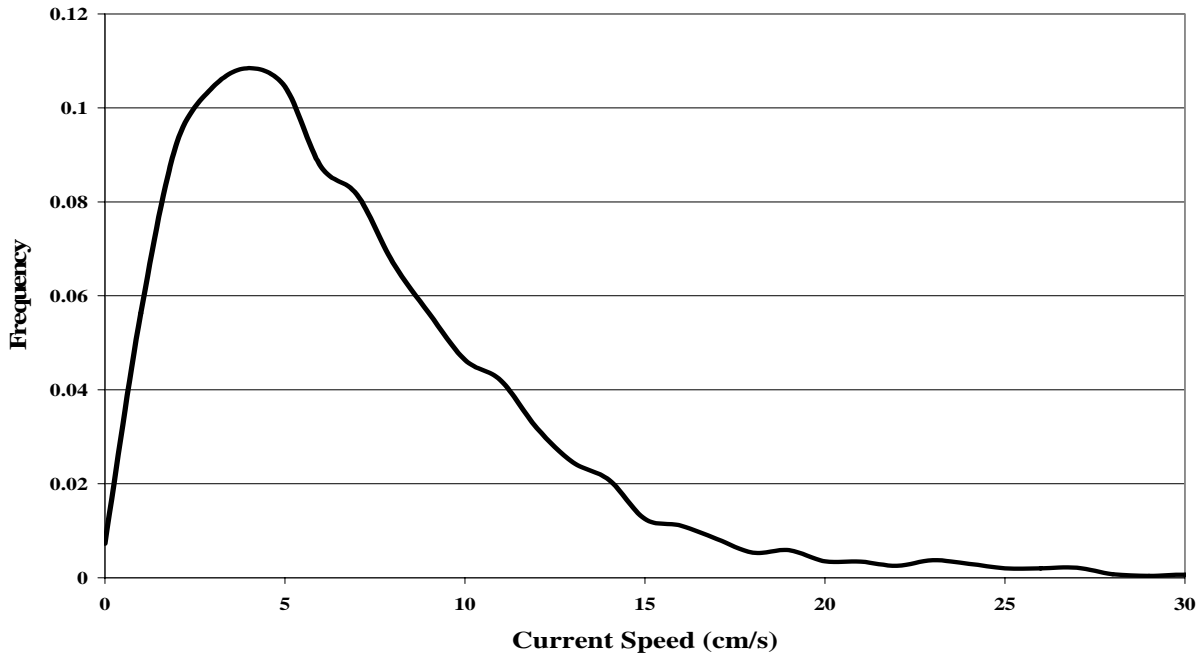


Figure 1.17 Frequency of Current Speeds at Location No. 7

Figure 1.18 presents a polar plot showing current direction vs. frequency of occurrence for location no. 7. This figure shows that predominant ebb direction is towards the northeast (45 degrees) and the predominant flood direction is towards the southwest (225 degrees).

Figure 1.19 contains the polar plot overlaid on an aerial photograph which shows that these predominant directions flow into and out of the Patapsco River.

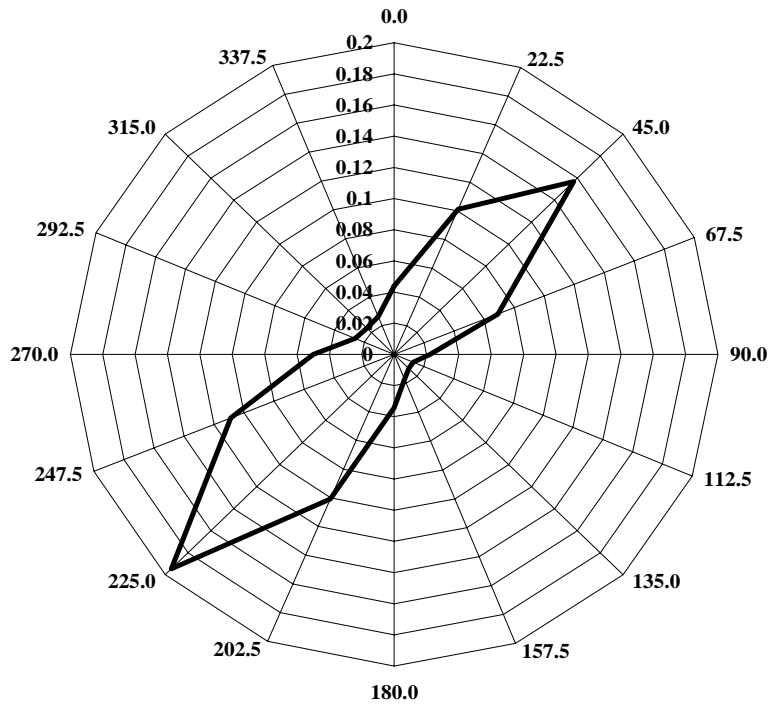


Figure 1.18 Frequency of Current Directions at Location No. 7

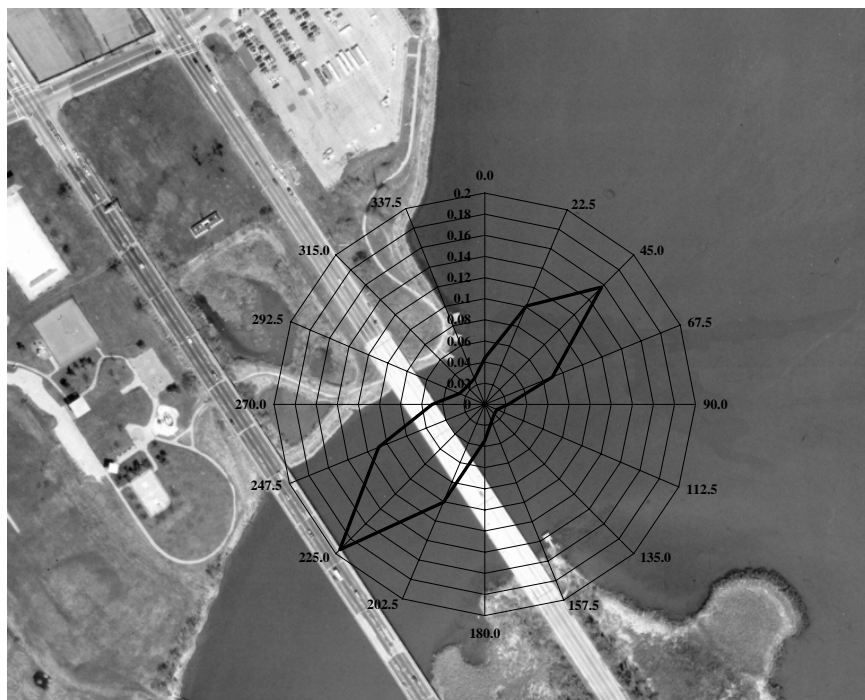


Figure 1.19 Frequency of Current Directions on Aerial Photograph at Location No. 7

Figure 1.20 presents a scatter plot graph of the current speed vs. direction for location no. 7. This graph shows that the highest speeds tend to match the most common ebb and flood directions and that there is a predominant ebb and flood direction.

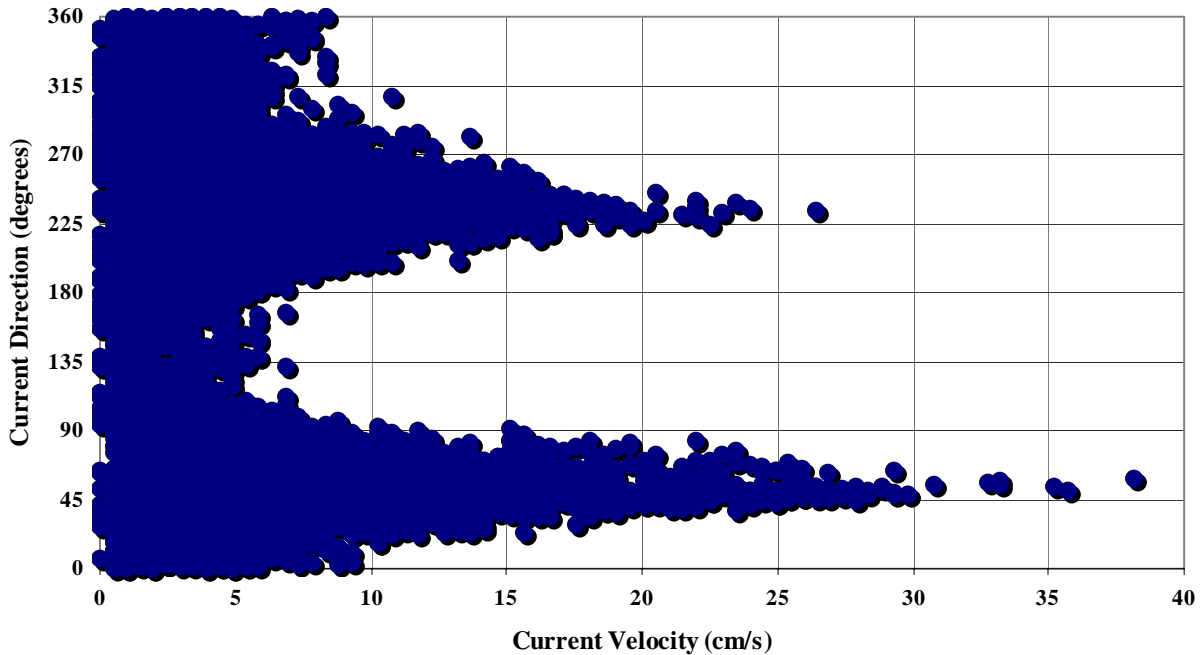


Figure 1.20 Current Speed vs. Direction at Location No. 7

Figure 1.21 presents a current speed vs. frequency of occurrence plot for location no. 8. The results for location no. 8 are consistent with location no. 7 in that most speeds are in the 2 to 6 cm/sec range and practically all are less than 20 cm/sec. Location no. 8, is also consistent with location no. 7, in that it shows a greater frequency of speeds in the 10 to 20 cm/sec range than at location no. 5 and 6.

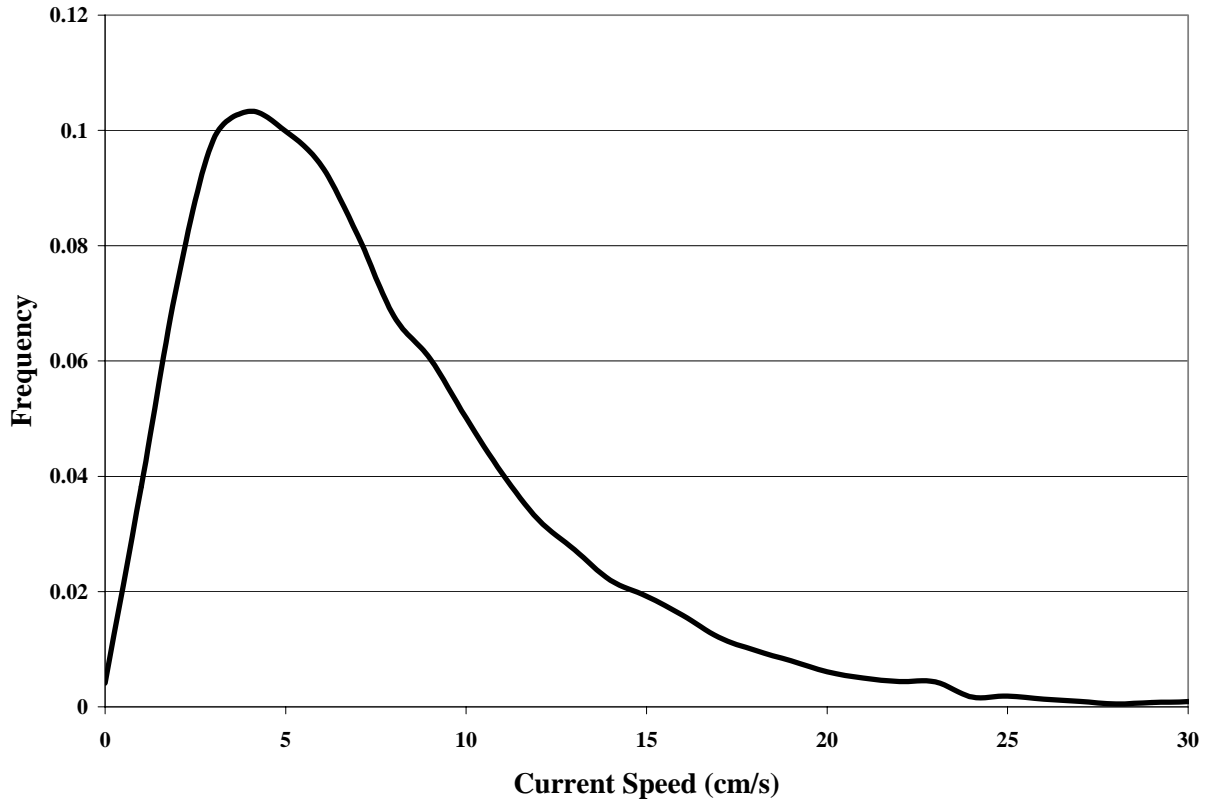


Figure 1.21 Frequency of Current Speeds at Location No. 8

Figure 1.22 presents a polar plot showing current direction vs. frequency of occurrence for location no. 8. This figure shows that predominant ebb direction is towards the north-northeast (22.5 degrees) and the predominant flood direction is towards the south-southwest (337.5 degrees). Figure 1.23 contains the polar plot overlaid on an aerial photograph which shows that these predominant directions generally follow the shoreline of the Patapsco River.

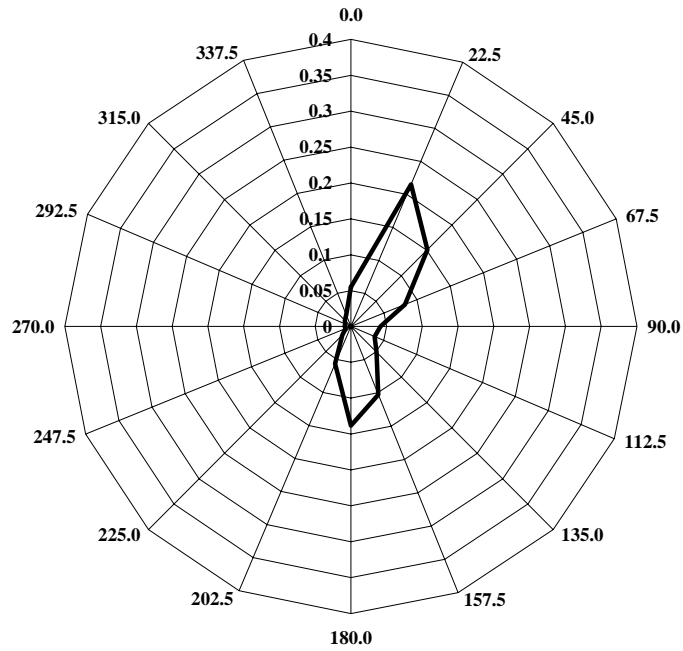


Figure 1.22 Frequency of Current Directions at Location No. 8



Figure 1.23 Frequency of Current Directions on Aerial Photograph at Location No. 8

Figure 1.24 presents a scatter plot graph of the current speed vs. direction for location no. 8. This graph shows that the highest speeds tend to match the most common ebb and flood directions and that there is a predominant ebb and flood direction.

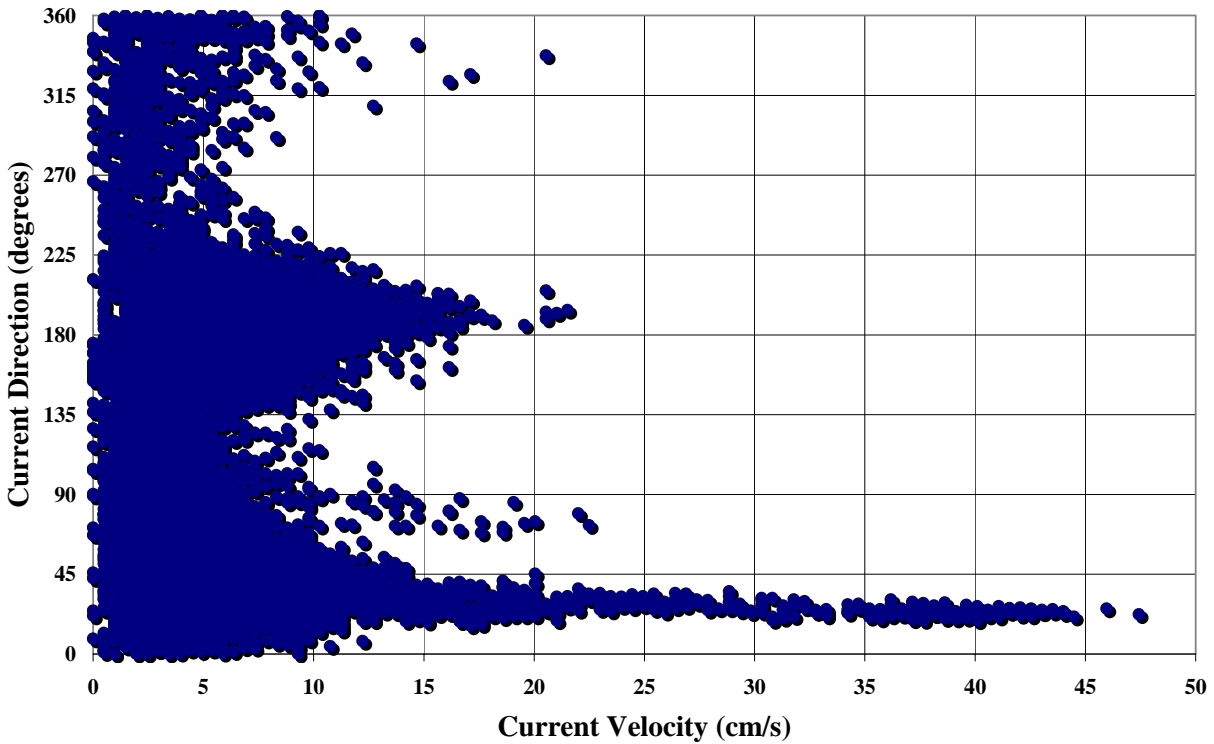


Figure 1.24 Current Speed vs. Direction at Location No. 8

B-2. HYDRODYNAMIC MODELING

This section summarizes the numerical modeling work completed to date, including hydrodynamic model development and calibration. Specifically, a state-of-the-art surface water modeling system, Delft3D, is being used to simulate hydrodynamics and sediment transport in the Study Area. Once model development and calibration is complete, the impact of different construction alternatives relative to base conditions will be evaluated.

B-2.1 MODEL DESCRIPTION

The Delft3D morphological model, developed at Delft University of Technology in Netherlands, integrates the effects of waves, currents, sediment transport and salinity on morphological developments. It can simulate the morphodynamic behavior of rivers, estuaries and coastal areas due to the complex interactions between waves, currents, sediment transport and bathymetry. Each of the included processes is described in the following sections.

The hydrodynamic module Delft3D-FLOW simulates two-dimensional (2D, depth averaged) or three-dimensional (3D) unsteady flow and transport resulting from tidal and/or meteorological forcing, including the effect of density differences due to a non-uniform temperature and salinity distribution (density-driven flow). The flow is forced by tide at the open boundaries, wind stress at the free surface, and pressure gradients due to free surface gradients (barotropic) or density gradients (baroclinic).

The DELFT3D hydrodynamic model determines salinity using the Navier Stokes equations for an incompressible fluid, under the shallow water and the Boussinesq assumption. In addition, the model uses a fully implicit method to solve the equations in the vertical. The model allows the wetting and drying of tidal flats, which is a very common phenomenon in tidal estuaries (such as Chesapeake Bay).

The Delft3D-FLOW Sediment Transport and Morphology Add-on includes cohesive and non-cohesive suspended sediment, bed-load transport, influence of waves and bed-level feedback. The local flow velocities and eddy diffusivities are based on the results of the hydrodynamic computations. The elevation of the bed is dynamically updated at each computational time-step,

meaning that the hydrodynamic flow calculations are always carried out using the correct bathymetry. The hydrodynamic model implementation used in the sediment transport and morphology model includes the effects of the waves on both nearshore hydrodynamics and sediment transport. It should be noted, however, that the model does not include all of the physics affecting beach profile changes during storm conditions, such as the three-dimensional wave and hydrodynamic processes that generate undertow.

B-2.2 MODEL DEVELOPMENT

A two-dimensional version of an existing M&N Chesapeake Bay model was used to provide boundary conditions to a higher-resolution local model of Baltimore Harbor. The local model was used to predict hydrodynamic conditions, wind-generated waves, sediment transport and salinity. Using data extracted from the larger “regional” model to force the smaller and more detailed “local” model is referred to as “nesting”. Modeling efficiency can be significantly increased by the nesting the models.

The Geographical Coordinate system selected for this modeling task was the Maryland State Plane system 1900. The associated datum was North American Datum of 1983 (NAD 83). The units used in the modeling and presentation of results are meters.

B-2.2.1 Regional Model

B-2.2.1.1 Grid

The Chesapeake Bay Model extends from the north at the entrance of the Chesapeake and Delaware (C&D) Canal on the Elk River to approximately 200 miles south to the Chesapeake Bay bridge tunnel and then approximately further 100 miles off shore into the Atlantic Ocean. The regional grid is presented in Figure 2.1.

The model is built on a curvilinear computational grid. Over 27,000 computational grid points define the model. The grid resolution is variable throughout the model domain, with a minimum resolution of 4 km grid spacing offshore and a maximum resolution of approximately 100 m within the bay itself.

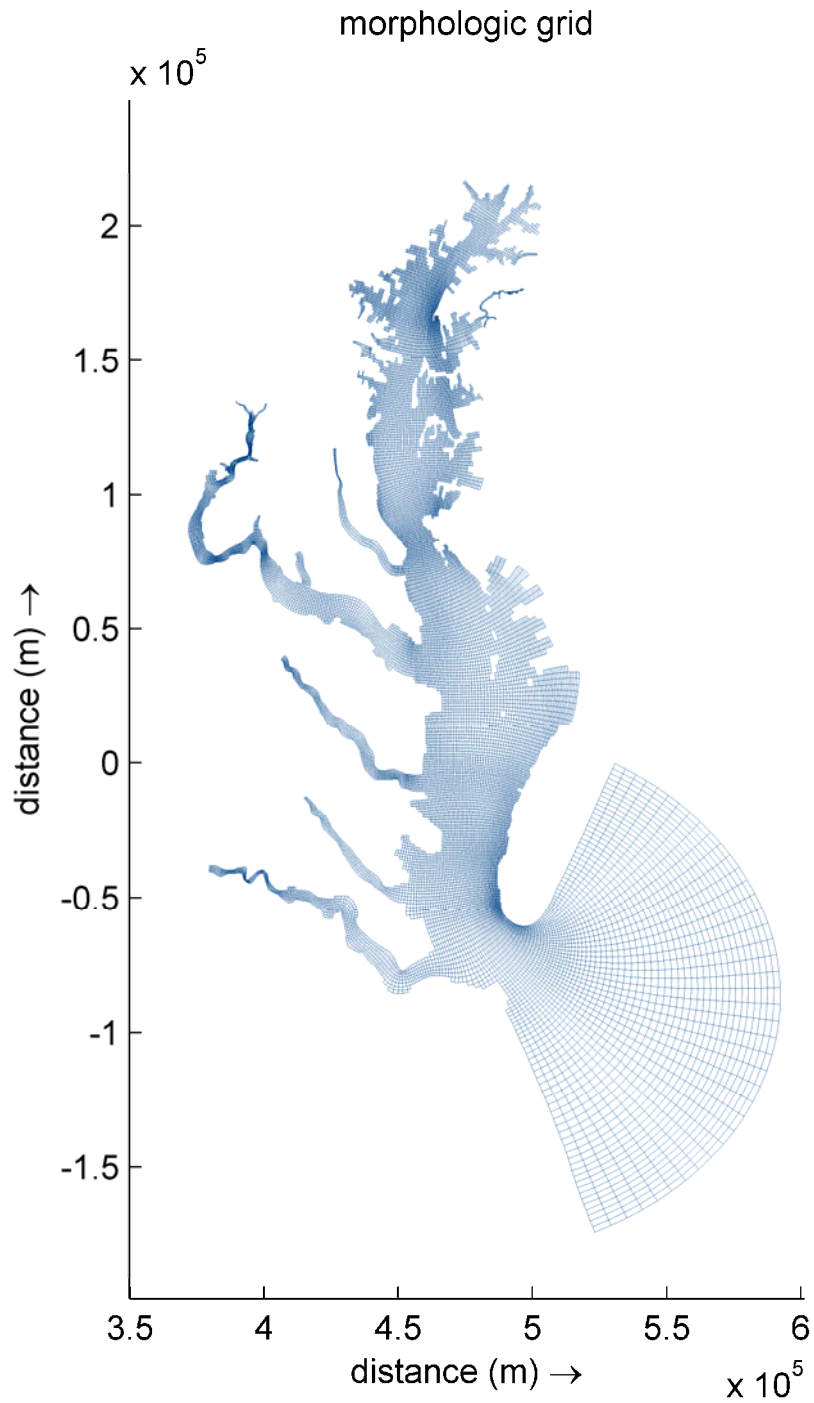


Figure 2.1 Regional Model Grid

B-2.2.1.2 Regional Model Bathymetry

The bathymetry for the regional model was developed from two National Oceanic and Atmospheric Administration (NOAA) data sources – (i) the National Ocean Service (NOS) estuarine bathymetry for the bay area and (ii) the National Geophysical Data System's (GEODAS) data sets.

The estuarine bathymetry data used were extracted from a single, large format Digital Elevation Map (DEM) file for 3-arc second gridded (90m) bathymetry data. Bathymetric elevations within these data sets are referenced to the local tidal datum which typically is Mean Lower Low Water (MLLW) averaged over a 19-year tidal epoch. However, as the model bathymetry was referenced to the Mean Tide Level (MTL), the NOS bathymetry was converted to the MTL based on a spatial datum transformation, which was developed on the information from the NOAA tidal benchmark information of 66 stations. The bathymetry developed for the model is presented in Figure 2.2.

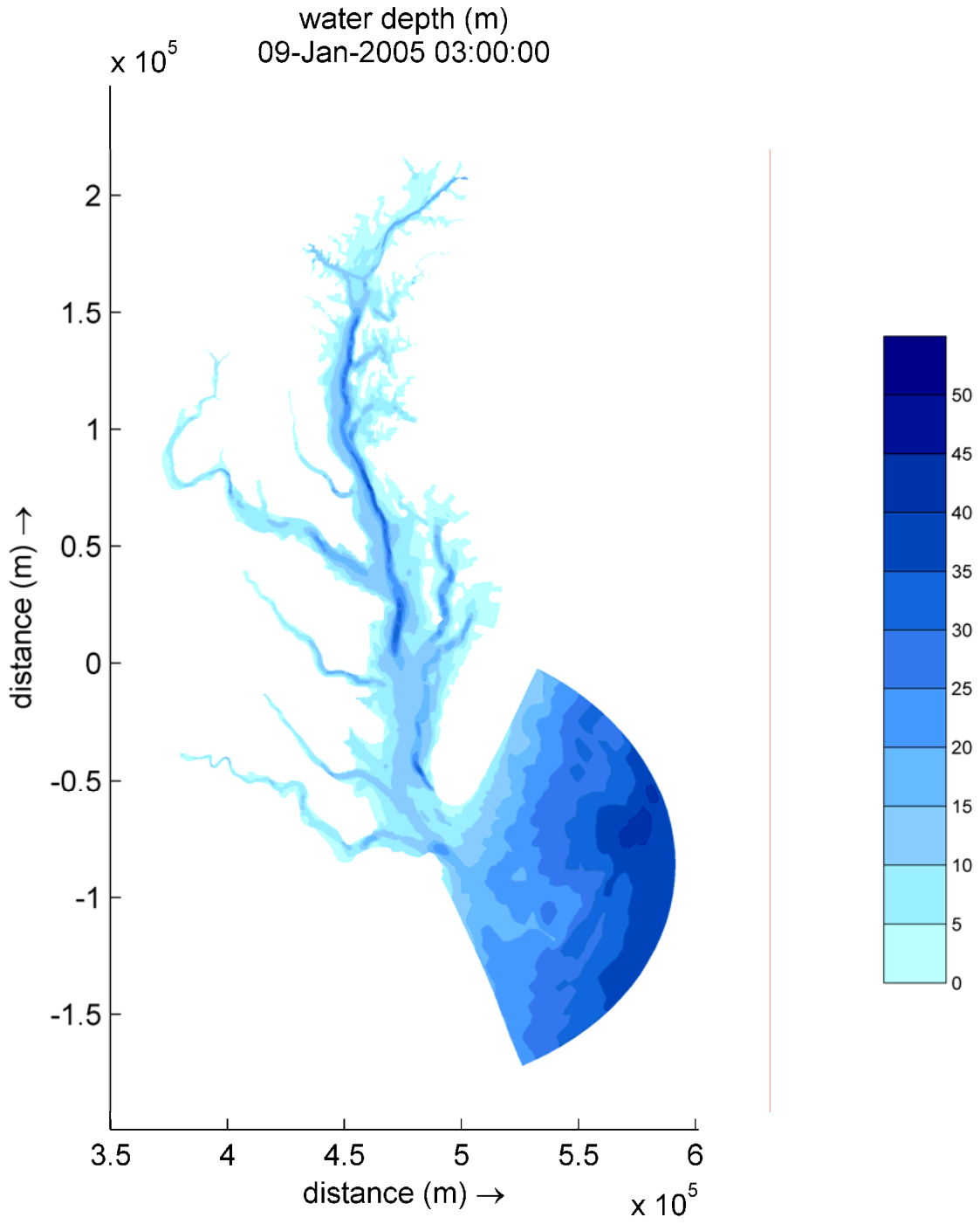


Figure 2.2 Regional Model Bathymetry

B-2.2.1.3 Regional Model Boundaries

Open boundaries to the model were defined at two locations – at the southern offshore boundary and at the northern most location at the junction of the Elk River with the C&D Canal. Figure 3 shows the model boundaries located on the grid. The offshore boundaries are defined as time series of water surface elevations constructed from 9 major tidal constituents extracted from the high-resolution Advanced Circulation (ADCIRC) East Coast 2001, finite-element tidal model. The northern most boundary location of the model is where the C&D Canal joins the Elk River at Welch point. Current velocity time series based on NOAA constituents were applied at the boundary.

Fresh water inflow stations were used as inflow points on the Susquehanna, Potomac and James Rivers. The inflows use daily average flow data from USGS gages. The locations of the inflows are shown in Figure 2.3.

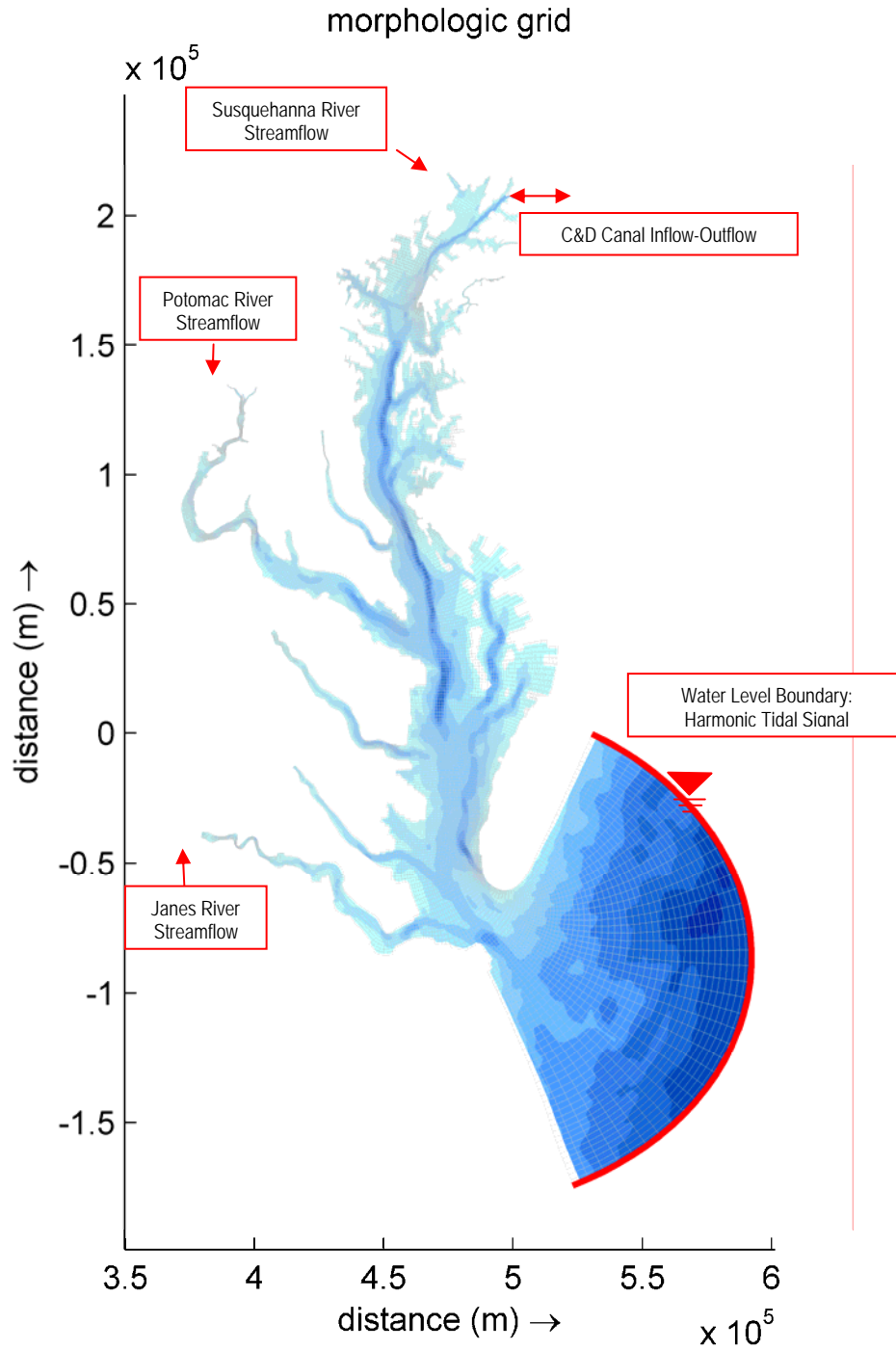


Figure 2.3 Regional Model Boundary Conditions

B-2.2.2 Local Model

A high-resolution local grid covering the area in the vicinity of the Patapsco River was developed to run nested within the Regional Model. The local model was developed to increase detail in the project vicinity while maintaining model efficiency and reducing run time.

B-2.2.2.1 Grid

The local grid includes the Chesapeake Bay from Pooles Island south to Sandy Point, including the Patapsco, Chester, Middle and Back Rivers. The local Baltimore Harbor grid, shown in Figure 2.4, has 21,626 grid cells. The grid resolution is variable throughout the local model, with a maximum resolution of 11 km grid spacing along the axis of the shoreline and 3.5 km spacing in the immediate vicinity of the proposed project.

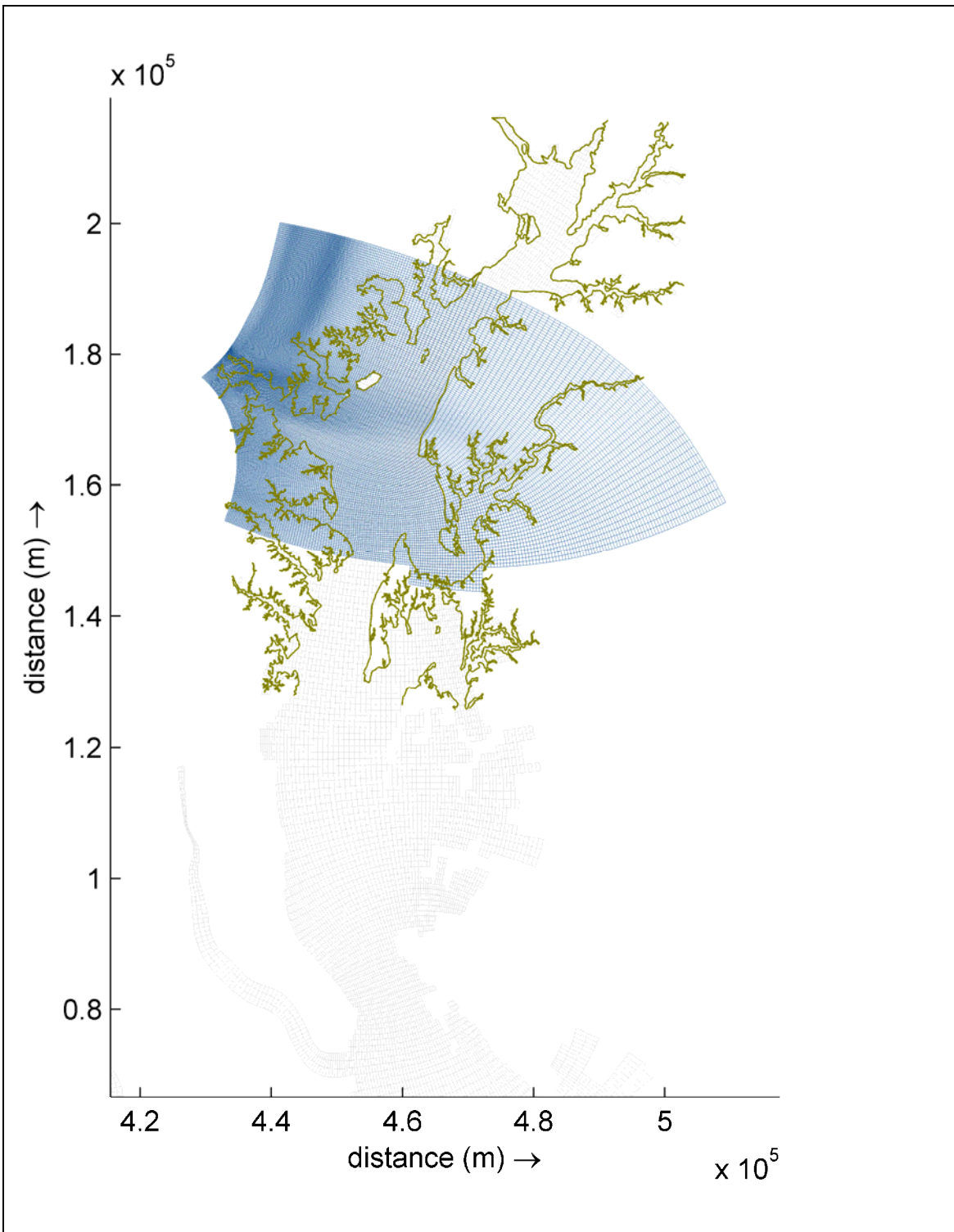


Figure 2.4 Local Model Grid

B-2.2.2.2 Local Model Bathymetry and Grid

The bathymetry data for the local model was extracted from a single DEM for 1-arc second gridded (30m) bathymetry data. Where the resolution of the DEM is not sufficient to capture bathymetric details such as shipping channels, bathymetric data were obtained from the NOAA, NOS Charts 12278 and 12281. Bathymetric elevations within these data sets are referenced to the local tidal datum which typically is MLLW averaged over a 19-year tidal epoch. However, the bathymetry was converted to the MTL as described in Section B-2.2.1. The bathymetry developed for the model is presented in Figure 2.5. The finest resolution of the model is approximately 30m in the immediate vicinity of Masonville. The resolution of the model is sufficient to define the major shipping channels within the Harbor area.

The local model was operated in three-dimensional mode to replicate the effect of winds and density on the flows in the harbor area. The local model was specified with 5 layers in the vertical dimension throughout the model domain. Therefore, the thickness of the layers varies with water depth at each grid point. The layers are defined such that the thickness of the top and bottom layers (layer 1 and 5, respectively) are each 10% of the water depth, the second and fourth layers are 25% of the water depth, and the third layer (middle of water column) is 30% of the water depth. This schematization allows the model to define the flow in the boundary layers at the water surface and seabed.

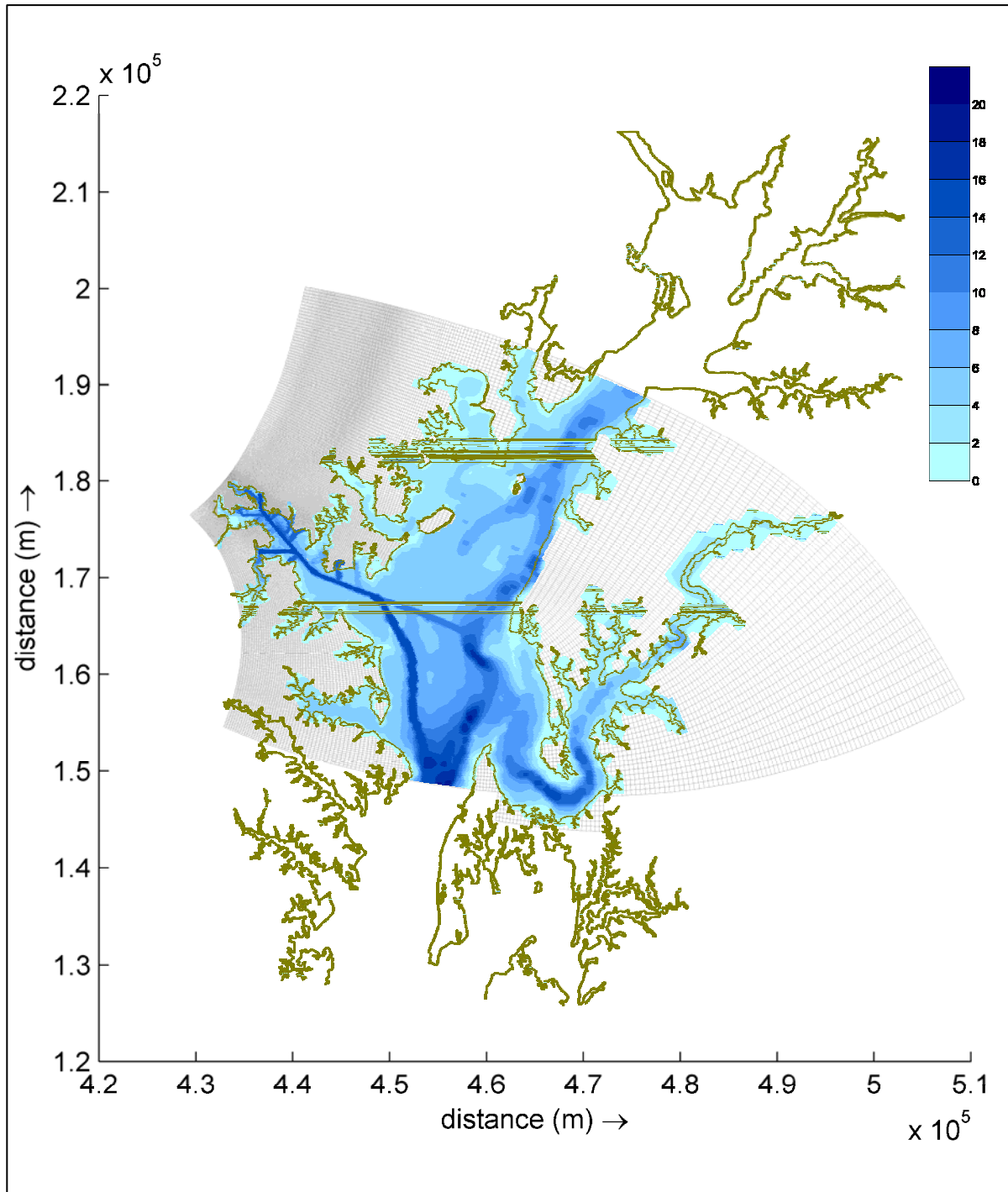


Figure 2.5 Local Model Bathymetry

B-2.2.2.3 Model Boundaries

B-2.2.2.3.1 Hydrodynamic Boundaries

The boundary conditions for the local model were generated from the regional hydrodynamic model and USGS data sources. Water levels at the northern boundary and velocities at the southern boundary are transferred from the regional model to the local model. Inflows were assigned on the Jones Falls, Gwen’s Falls and Curtis Creek. The inflows use daily average flow data from USGS gages. In addition, the daily discharge from the 2 regional WWTP outfalls were included in the model: Patapsco WWTP and Back River WWTP. The locations of the boundary conditions are shown in Figure 2.6.

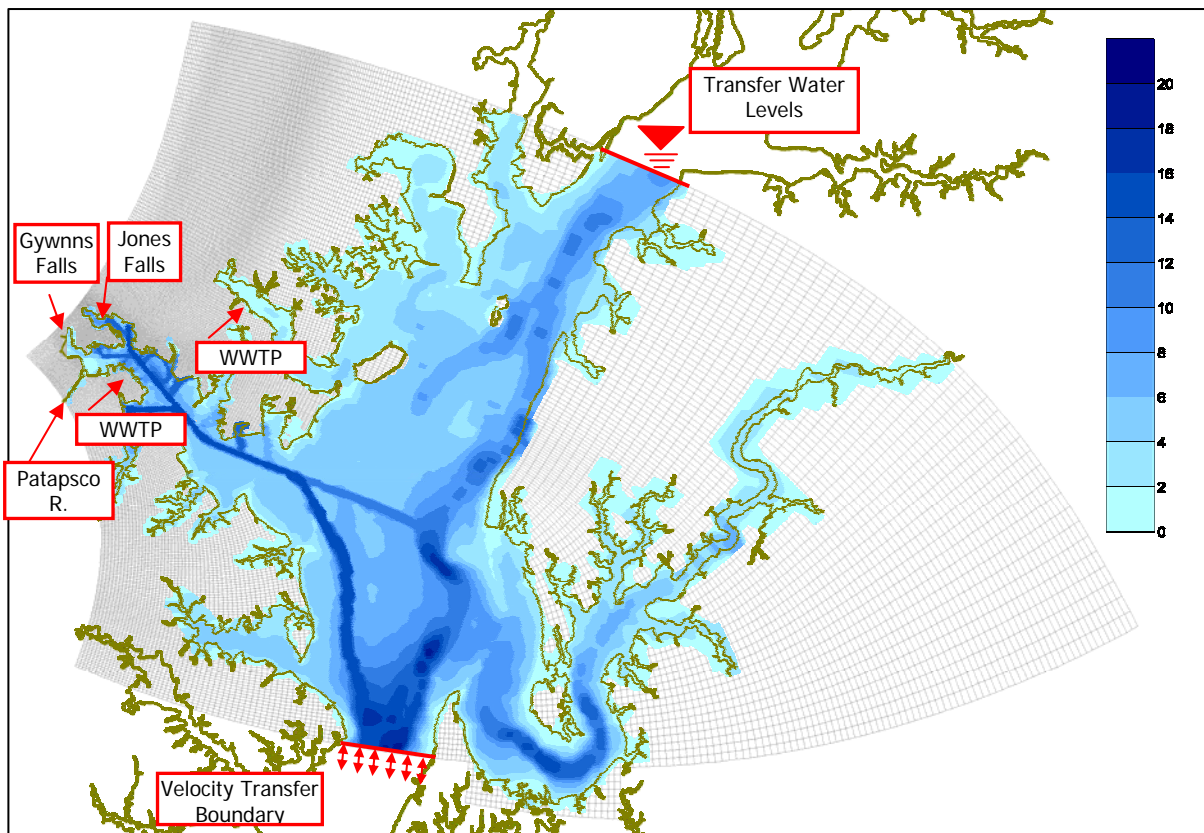


Figure 2.6 Local Model Boundary Conditions

B-2.2.2.3.2 Salinity and Temperature Boundaries

The salinity and temperature at the northern and southern boundaries were defined from the

semi-monthly CBP monitoring cruises. See Figure 1.6 for locations of CBP data gathering stations. Three stations along the southern boundary and one station on the northern boundary were used to define depth-varying salinity temperature. For time between cruises, the data were linearly interpolated.

B-2.2.2.3.3 Wind

Wind was applied as a uniform field over the local model domain. Wind data from the PORTS Francis Scott Key Bridge station were used to force the model. For time periods prior to the installation of the Key Bridge Gage, data from Thomas Point Light was used in the model.

B-2.3 HYDRODYNAMIC CALIBRATION

B-2.3.1 Water Levels

The Local Model was calibrated to tidal water level elevations (water levels) and tidal current velocities (currents) at fixed stations throughout the estuary over the period 20 April – 25 May 2005. Two harmonic tidal prediction and measurement stations were available within the model domain: Tolchester Beach and Fort McHenry. In order to calibrate the Model, bed roughness and eddy viscosity were tuned until an acceptable calibration was obtained.

Calibration was assessed graphically and using a statistical analysis that computed root mean square error and the correlation coefficient. The graphical plots compare the actual time series of predicted tidal elevation and modeled results over the one month calibration period. It should also be noted that some of the difference may due to the inclusion of wind in the model versus the predicted tide which is based solely on long-term tidal data. The statistical measures used in calibration are defined as follows:

- Root Mean Square (RMS) Error: Compares the root of the average square of the difference (error) between the extremes of the two data sets.
- RMS Error Percentage: Computes the RMS error as a percentage of the range of the measured data. This gives perspective on the magnitude of the RMS error.

- Correlation Coefficient: Uses the Pearson product moment correlation coefficient, r , (a dimensionless index that ranges from -1.0 to 1.0) to reflect the extent of a linear relationship between two data sets. This parameter indicates how closely the modeled data is in phase with the calibration data. An index of 1.0 indicates that the two data sets are linearly perfectly in phase; an index of -1.0 indicates that the data are 180 degrees out of phase.

Figure 2.7 presents the comparison of the modeled tide signal compared to the predicted tide at the two stations. Table 2.1 presents the statistical calibration for both stations. RMS error for both stations is on the order 4 cm (1.6 inches) which is a satisfactory calibration.

Table 2.1 Water Surface Elevation Statistical Comparison, Model to Predicted

	Correlation Coefficient	RMS Error (cm)	RMS Error (%)
Tolchester	0.87	4.0	10.5%
Fort McHenry	0.95	3.8	11.0%

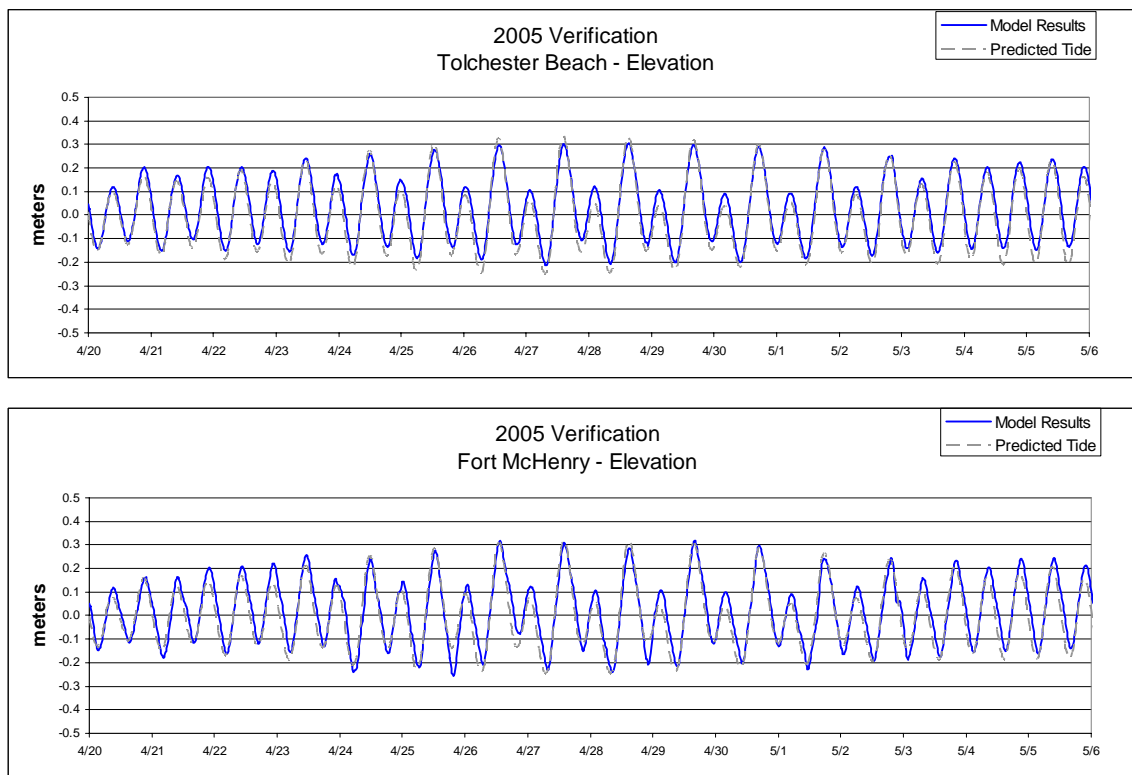


Figure 2.7– Water Surface Elevation Calibration

B-2.3.2 Currents

Currents within the harbor are weak and are subject not only to tidal forces, but are equally influenced by wind and stratification of salinity and temperature. The three-dimensional framework allows the comparison of measurements taken at various depths with model results. Currents are difficult to compare statistically because small-scale variations in bathymetry, channel geometry and flow patterns can significantly affect current velocity and direction. These variations are difficult to reproduce in a model with finite resolution. However, the magnitude of current and the general directions of flow can be compared. The calibration period for model currents was 21 April 2005 to 25 May 2005. Currents were calibrated to match measurement stations within the Patapsco River, namely Stations 2,3, and 4.

Figure 2.8 displays the current velocity in the model compared to velocities measured at Location 2, the entrance to Curtis Bay. Both surface and bottom currents are displayed. Surface currents are well matched in magnitude in direction by the model. Bottom currents match in ebb magnitude, underpredict slightly on flood currents. Measured direction shows more scatter than the model. Discrepancies are likely due to variations in bathymetry between the model and the actual channel bottoms and differences in density stratification (see next section).

Figure 2.9 displays the current velocity in the model compared to velocities measured at Location 3, the Fort McHenry Angle, for both surface and bottom. Predominant directions are reproduced well by the. On the surface, the model matches ebb speed well, but underpredicts flood magnitude. On the bottom, the opposite is true; the model matches flood magnitude but underpredicts ebb magnitude.

Figure 2.10 compares measured and modeled velocities at Masonville Cove. Both datasets show scattered direction and low velocities (less than 20 cm/s). The model reproduces the measured flow behavior well, with highly variable, weak currents.

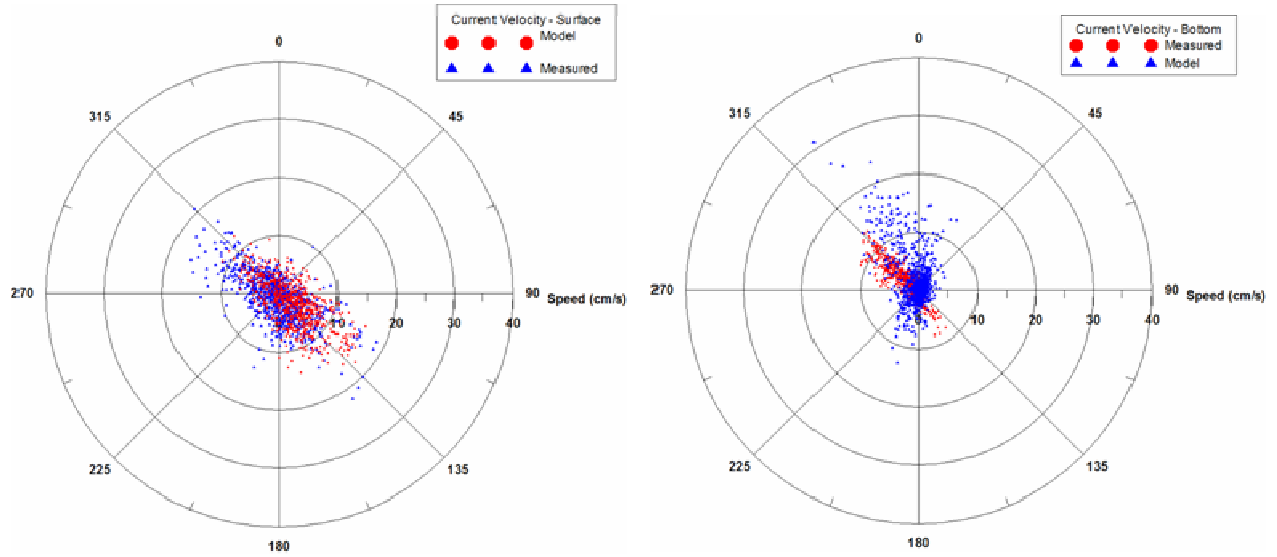


Figure 2.8 Current Velocity at Location 2, Curtis Bay Angle, Surface and Bottom

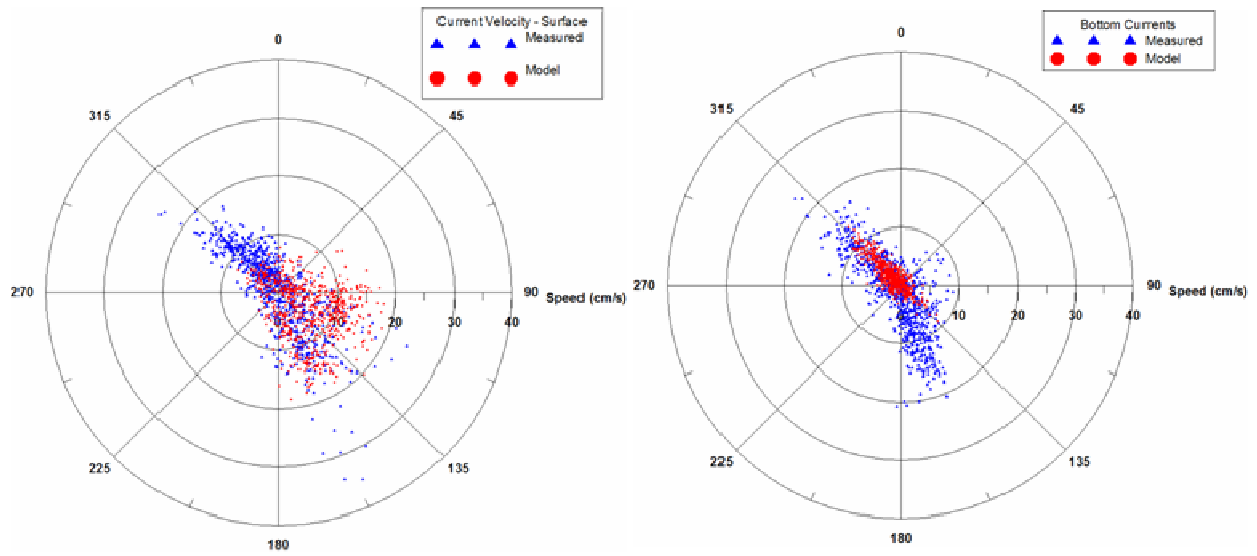


Figure 2.9 Current Velocity at Location 3, Fort McHenry Angle, Surface and Bottom

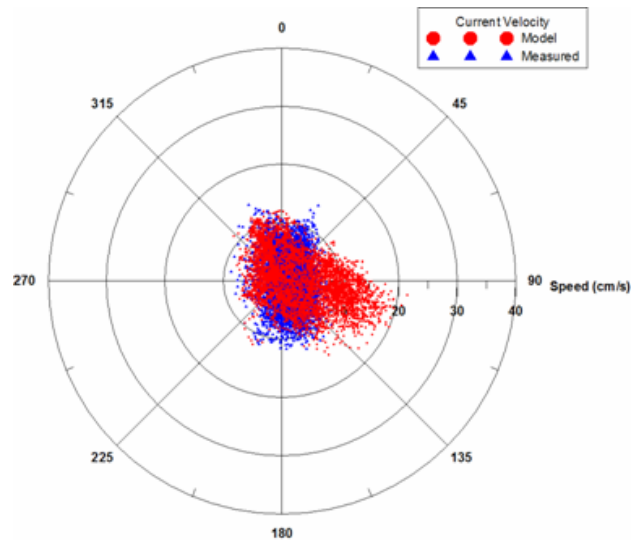


Figure 2.10 Current Velocity at Location 4, Fort Masonville Cove

B-2.4 MORPHOLOGICAL SEDIMENT MODEL

This section describes the set up and calibration of the morphological sediment model of the Masonville vicinity. The rationale developed herein is based on the sediment data described in Section B-2.4.1. The available data was used to develop and assess the morphological model in the vicinity of the proposed Masonville DMCF.

B-2.4.1 Sediment Data and Model Parameters

Sediment characteristics have been obtained from the available data and from previous reports (M&N, 2003) (GBA and M&N, 1995). In general, the site is characterized by very fine silt and clay sediments with a very low percentage of sands. Surveys of bottom sediments by the Chesapeake Biological Laboratory in 1997 found that the sediments in the Patapsco near Masonville consisted of 90-95% silts and clays, while sediments closer to the mouth of the Patapsco were comprised mainly of sand. This pattern indicates that sediment deposited in the Masonville area is carried there mainly by stream and rivers flowing into the harbor.

The sediment parameters in the model were assigned based on the Chesapeake Biological Laboratory testing. The sediment parameters implemented in the model are as follows:

- All sediments cohesive
- Critical Shear stress for erosion 0.1 N/m^2
- Critical Shear stress for deposition 0.07 N/m^2
- Erosion rate constant $0.01 \text{ g/m}^2/\text{s}$
- Cohesive sediment dry density 500 kg/m^3
- Settling velocity 0.02 mm/s
- Initial layer thickness of cohesive sediment set to 1 m throughout the Harbor

B-2.4.2 Morphological Calibration

Initial simulations of the morphological model showed little or no movement of sediment under normal tidal and wind conditions, i.e. during the hydrodynamic calibration period. It was determined that strong winds (greater than 16 m/s) create currents strong enough to resuspend sediment. It was postulated for the purposes of this investigation (and later corroborated by calibration) that storm events drive sedimentation in the Patapsco upstream of the Fort McHenry-Fairfield line. To model long term sedimentation, a strategy was adopted to run several large high wind-high flow events through the model to develop sedimentation and erosion patterns during storm flows, the results are then factored to match historical dredging records in the Ferry Bar Channel.

Suspended sediment concentrations in the model are determined based on resuspension of bed sediments and concentration on the four freshwater inflows to the harbor: Jones Falls, Gwynns Falls, Patapsco River, and Curtis Creek. Suspended sediments on each inflow are collected as part of the semi-monthly CBP monitoring. Total suspended solids (TSS) concentrations are generally relatively low, less than 20 mg/L . Samples are rarely collected during storm events, however a handful of samples were collected during high flow events and provide some data on elevated sediment concentrations. Figure 2.11 displays the freshwater flow for the Patapsco River versus sampled TSS values over the last 10 years. Note several of the samples show

elevated TSS, several on the order of 200-700 mg/L. A function was developed to specify TSS concentration in the inflowing rivers based on streamflow. A separate function was developed for each river discharge based on streamflow records and sampling history.

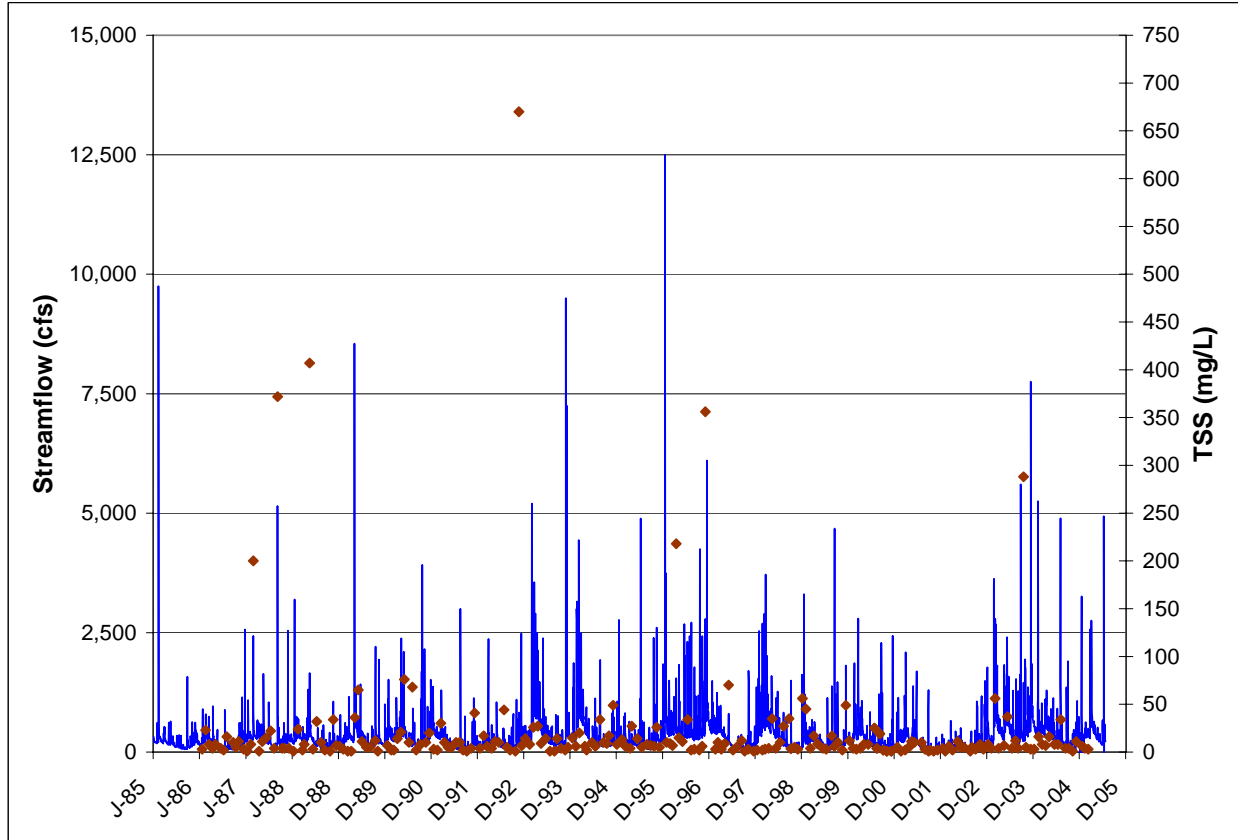


Figure 2.11 – Patapsco River Streamflow and TSS

To simulate the long term sedimentation in the Patapsco five storms from the last 10 years were selected that had either high winds, high discharges or both. These five storms were run through the model simultaneously with the normal tidal conditions from the calibration period. Using a morphological scale factor, the sedimentation results were extrapolated to represent 20-years of sedimentation.

Figure 2.12 displays the model-predicted sedimentation patterns over a 20-year period. Maximum sedimentation rates in the Ferry Bar Channel at the western end are predicted to be approximately 2 feet (0.6 meters). From dredging records, the last major dredging project in the Ferry Bar occurred in 1985. The latest check survey by the Corps of Engineers in September

2005 shows depths at the western end of the Ferry Bar at 37-42 feet. Based on a project depth of 42 feet, this represents sedimentation of 0-5 feet over 20 years. The morphological model is considered reasonably well calibrated to channel sedimentation rate. At the time this report was produced, additional survey records from USACE were pending. Additional calibration may be warranted after examination of the surveys between 1985 and 2005. For the purposes of assessing relative sedimentation impacts, however, the model is satisfactorily calibrated.

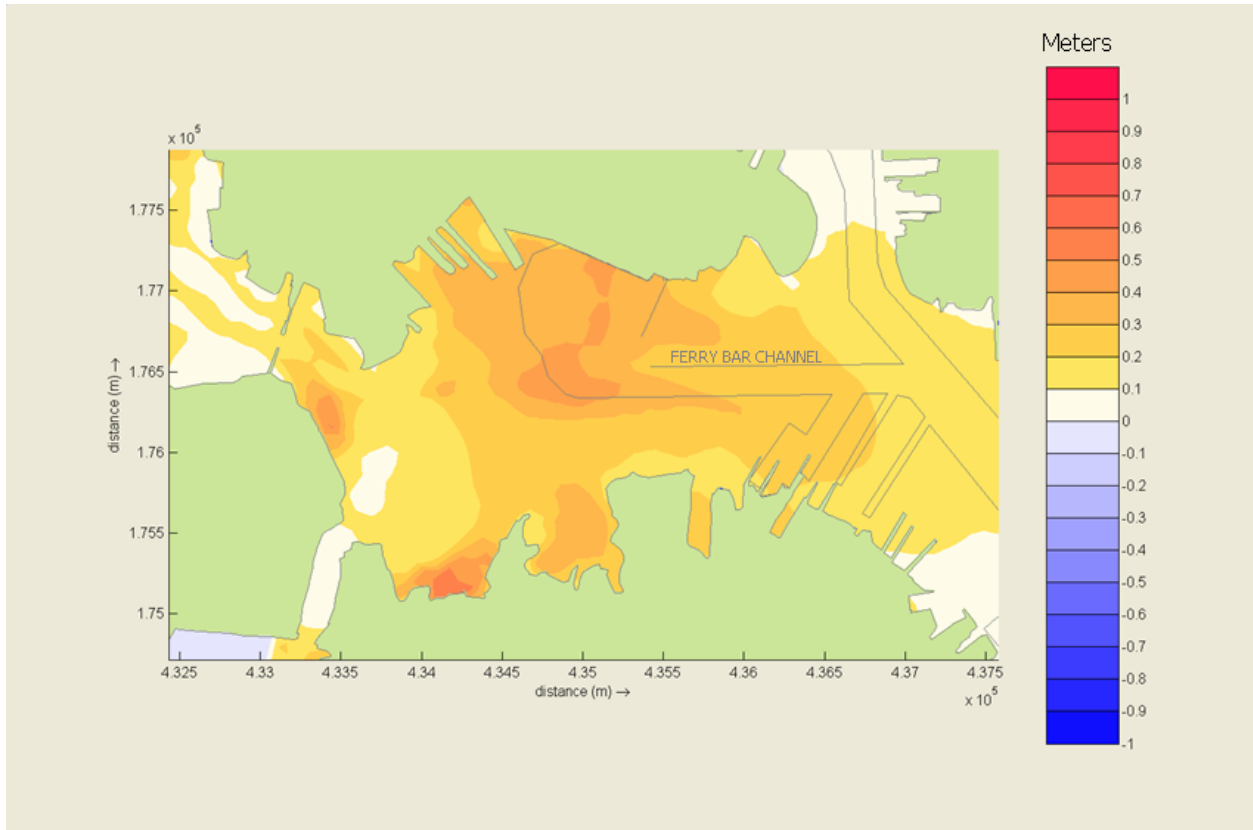


Figure 2.12 Predicted 20-year Sedimentation/Erosion Patterns

B-2.5 STORM SURGE MODELING

This section describes the numerical storm surge modeling work performed using DHI's MIKE21 modeling software. MIKE21 uses hydrodynamic models to determine water surface elevations and hurricane, or cyclone, models to define the driving force wind and pressure fields in the study area. Following model development and calibration, the impact of the proposed Masonville DMCF on existing conditions was evaluated.

B-2.5.1 Model Description

The hydrodynamic model in MIKE21 Flow Model (HD) is a general numerical modeling system for the simulation of water levels and flows in estuaries, bays, and coastal areas. It simulates unsteady two-dimensional flows in one layer (vertically homogenous) fluids when presented with the bathymetry and relevant conditions (e.g. resistance coefficients, wind field, hydrographic boundary conditions). MIKE21 HD uses the Saint Venant equations to describe the flow and water level variations by vertically integrating the equations of conservation of mass and momentum. The system solves the partial differential equations that govern nearly horizontal flow given the following input and boundary data:

- Bathymetry
- Water surface levels at the open boundaries and flux densities parallel to the open boundaries or flux densities both perpendicular and parallel to the open boundaries.
- Bed Resistance
- Wind speed, direction, and friction coefficient
- Barometric pressure

B-2.5.1.1 Bathymetry

MIKE21 Flow Model is a finite difference model with constant grid spacing in the x and y direction. The model grid must be rectangular in shape and include a large enough area for the wind surge to be computed correctly. To accurately model a hurricane surge at the proposed Masonville site, it was determined that the entire Chesapeake Bay should be included in the model. Figure 2.13 and Figure 2.14 show the bathymetry throughout the model and in the project vicinity, respectively.

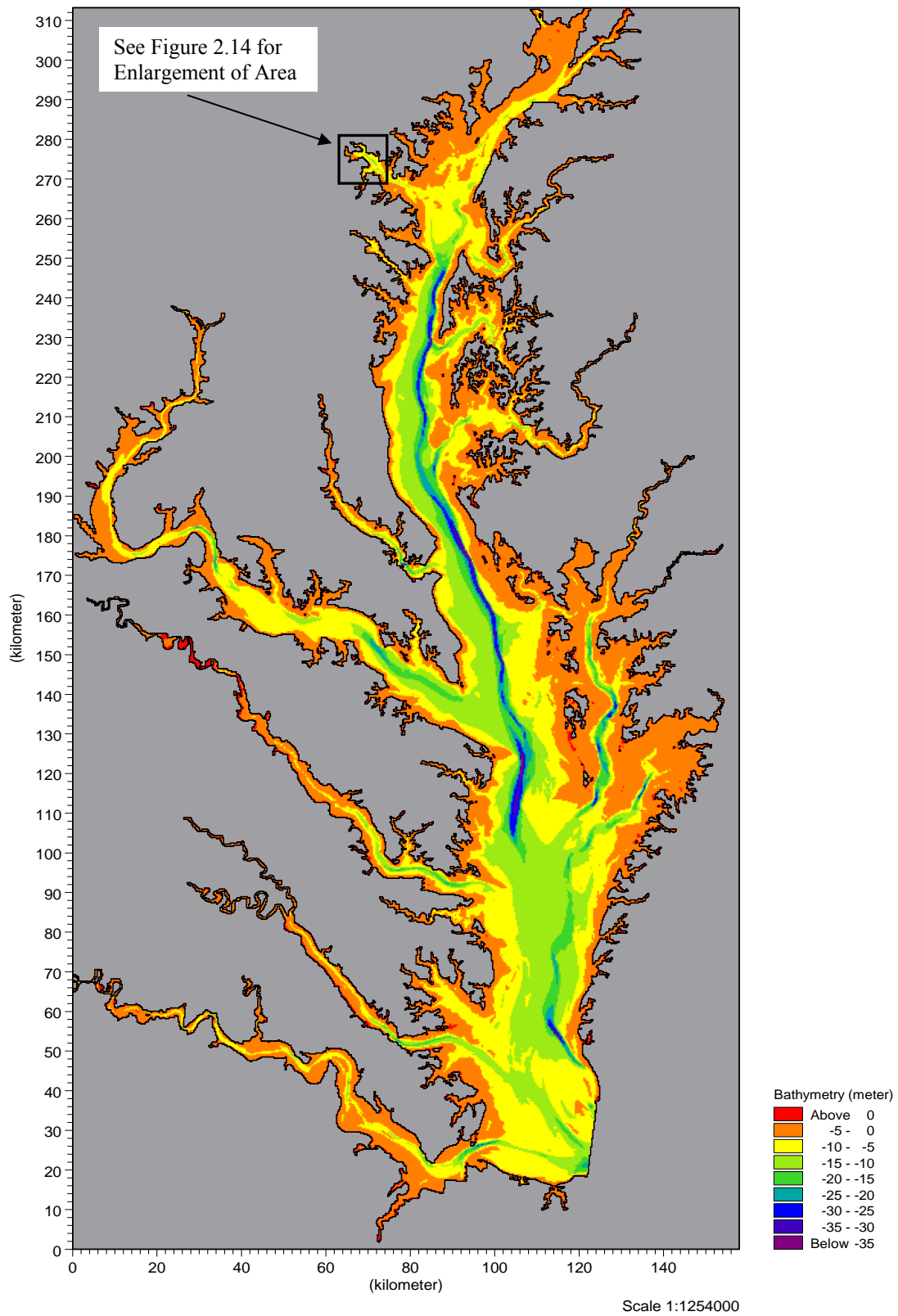


Figure 2.13 Model Bathymetry 270m X 270m Grid

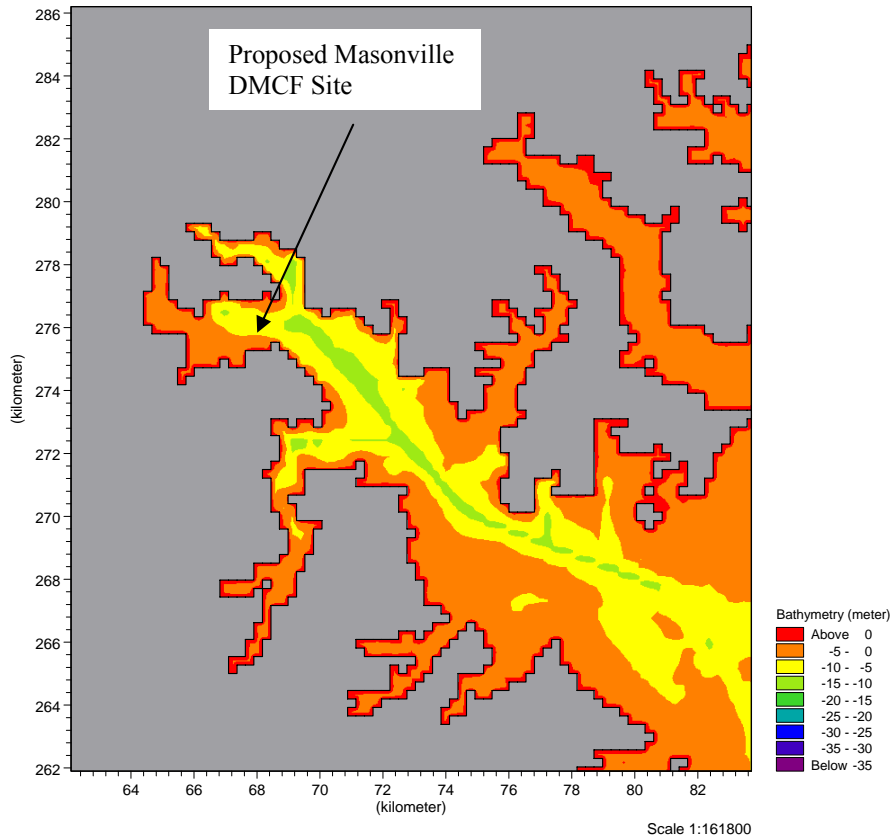


Figure 2.14 Project Vicinity Bathymetry 270m X 270m Grid

Bathymetric data for the grid was obtained from the NOAA CO-OPS (National Oceanic and Atmospheric Administration Center for Operational Oceanographic Products and Services) web site and from various NOAA NOS (National Ocean Service) nautical charts for the Chesapeake Bay area. A 90-meter digital elevation model (DEM) was downloaded from the NOAA web site for the entire Chesapeake Bay in UTM coordinates and MLLW vertical datum. A DEM is an evenly spaced array of elevation data. In this case, the spacing was 90 meters. These points were then imported into MIKE21 and were used to create a 270m X 270m grid. The nautical charts were used to verify the newly created grid. A 270 m spacing was determined to be optimal grid spacing size to provide adequate resolution while maintaining reasonable computational time and HD output file size. This resolution is adequate as the navigation channels and the bathymetry around the site are represented. The 270 meter grid spacing is a multiple of 90 meters, which results in minimal interpolation of the original DEM data. Smaller grid spacing would have resulted in more computational points, which would have increased computation time and HD output file size.

B-2.5.1.2 Open Boundaries

Open boundaries on the grid were eliminated. The tides that would be applied to the open boundaries were determined to have a minimal effect on the storm surge compared to the overall wind surge generated from the hurricane traveling up the Chesapeake Bay. Instead, an initial water surface elevation was applied to the model, and the model was driven by the wind-induced water levels and currents depicting the modeled hurricane.

B-2.5.1.3 Bed Resistance

Bed Resistance was assigned in the model as a map, by defining a Manning's n value for each grid point. The bed resistance values are based on depth and range from 20 to 80 m^{1/3} /s. It is important to take note that the Manning's n values used in MIKE21 are the reciprocal value of the Manning's n values typically used.

B-2.5.1.4 Wind Speed, Direction, and Stress

Wind conditions can be specified such that wind magnitude and direction vary during the simulation period and over the model area. The wind shear stress acting on the water surface is directly related to the density of air over water, the wind velocity 10 meters above the sea surface, and the wind friction coefficient. A wind friction coefficient of 0.0026 was determined to be appropriate for moderate and strong winds. Smaller coefficients are used for weak winds.

For this model, the MIKE21 *Wind Generation from Cyclone Specifications* program, was used to create a wind and pressure field for each hurricane. The bathymetric grid and cyclone parameters must be specified. These parameters include:

- Time in hours from the start of the cyclone period.
- X-coordinate and y-coordinate of the center of the cyclone in km relative to the origin (0,0) of the bathymetry grid.
- Radius of maximum winds in km.

- Maximum wind speed in m/s. This wind is described as the average 10-minute wind, 10 meters above sea level.
- Central pressure in hPa.
- Neutral pressure in hPa, i.e. the pressure outside the area influenced by the cyclone.

The output from the wind generation tool contains:

- Atmospheric pressure in hPa
- X-component and y-component of wind velocity in m/s

B-2.5.2 Model Parameters

Several possible tracks of hurricanes were modeled in order to determine the one resulting in the highest water levels at Baltimore. For this study three historical hurricanes, the unnamed 1933 hurricane occurring on August 17th through 26th, 1933, Hurricane Fran occurring on August 23rd through September 8th, 1996, and Hurricane Isabel, which occurred on September 6th through September 19th, 2003 were simulated to estimate storm surge levels for the study area. Tracks of these three hurricanes are shown in Figure 2.15, Figure 2.16 and Figure 2.17.

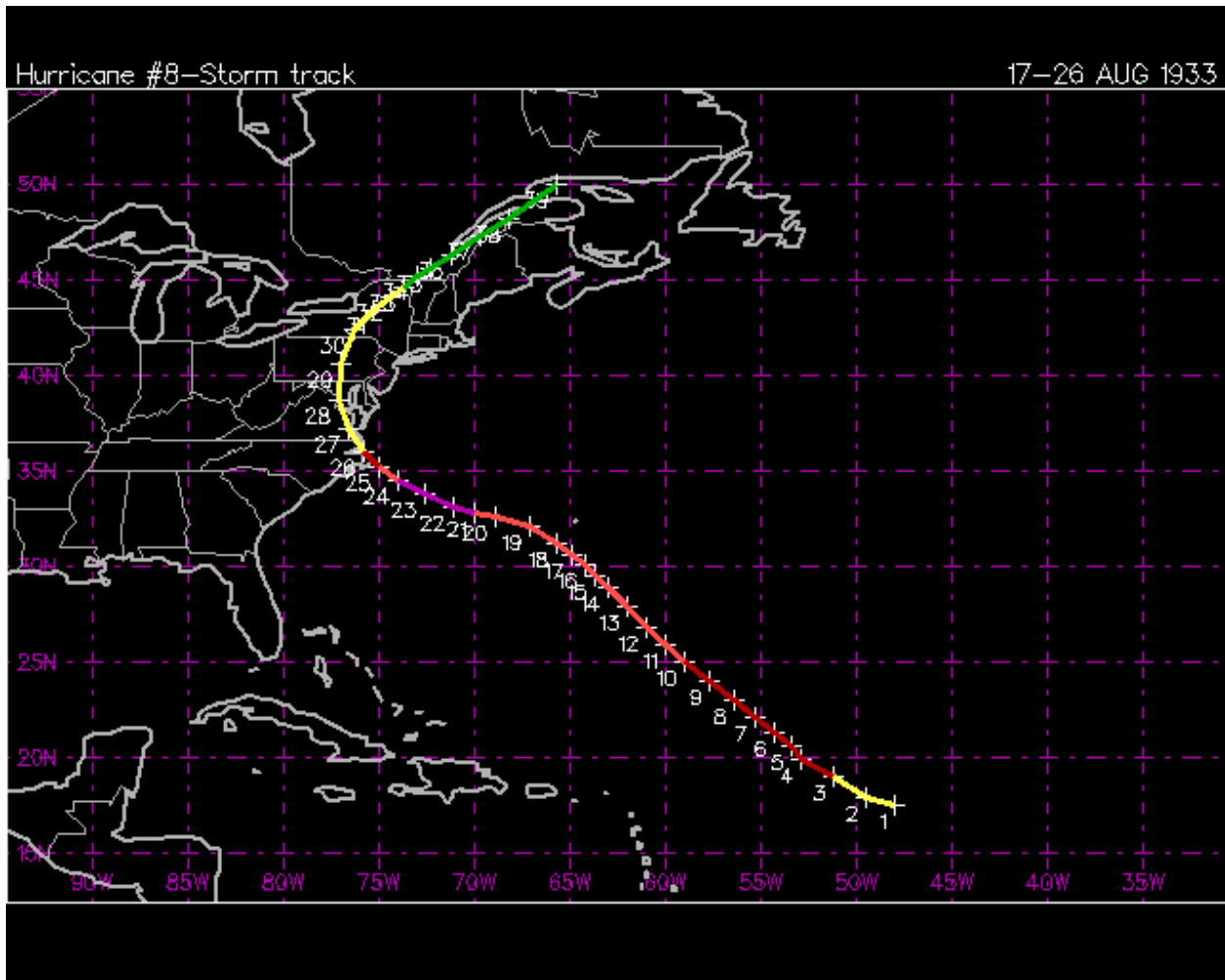


Figure 2.15 1933 Hurricane Storm Track

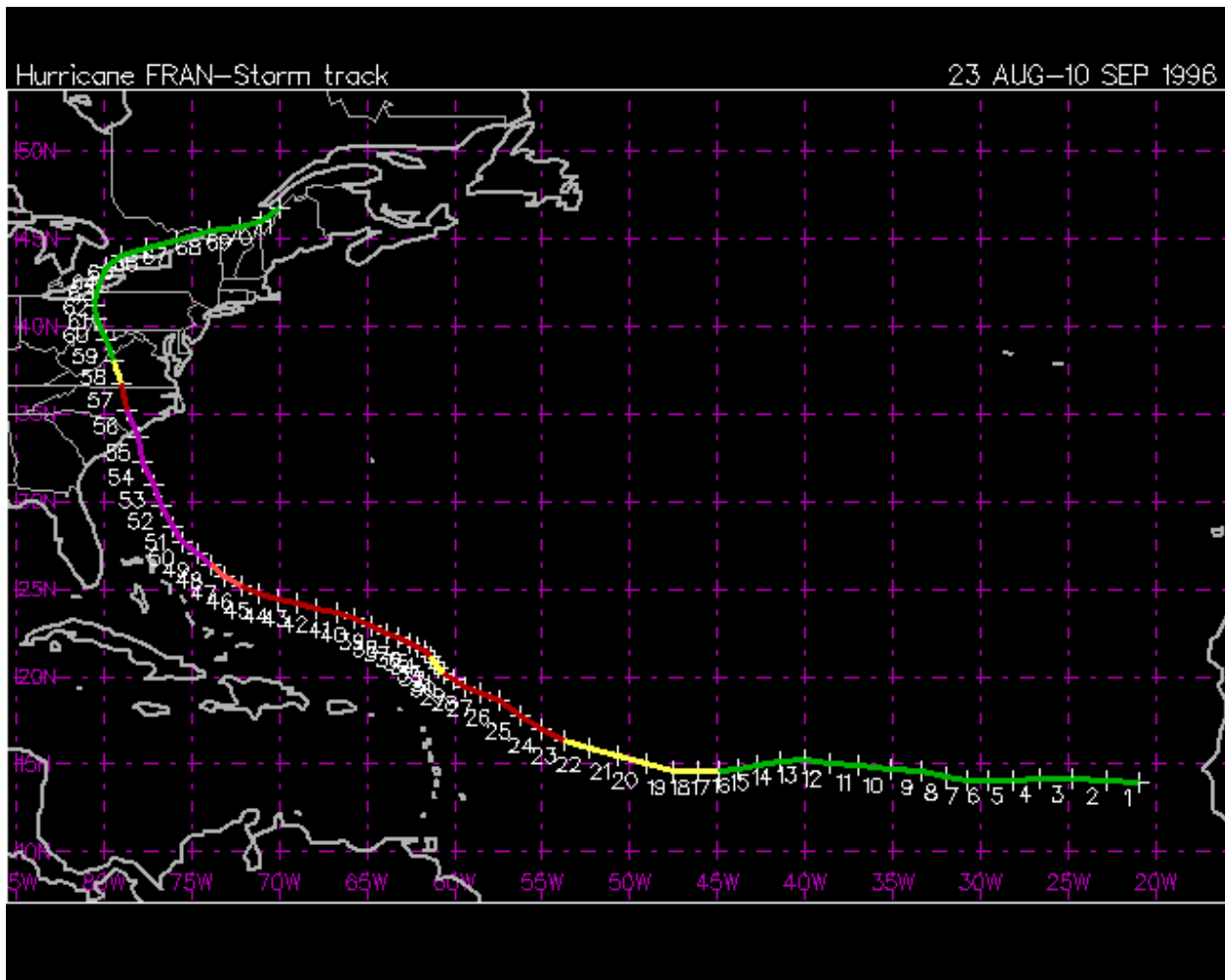


Figure 2.16 Hurricane Fran Storm Track

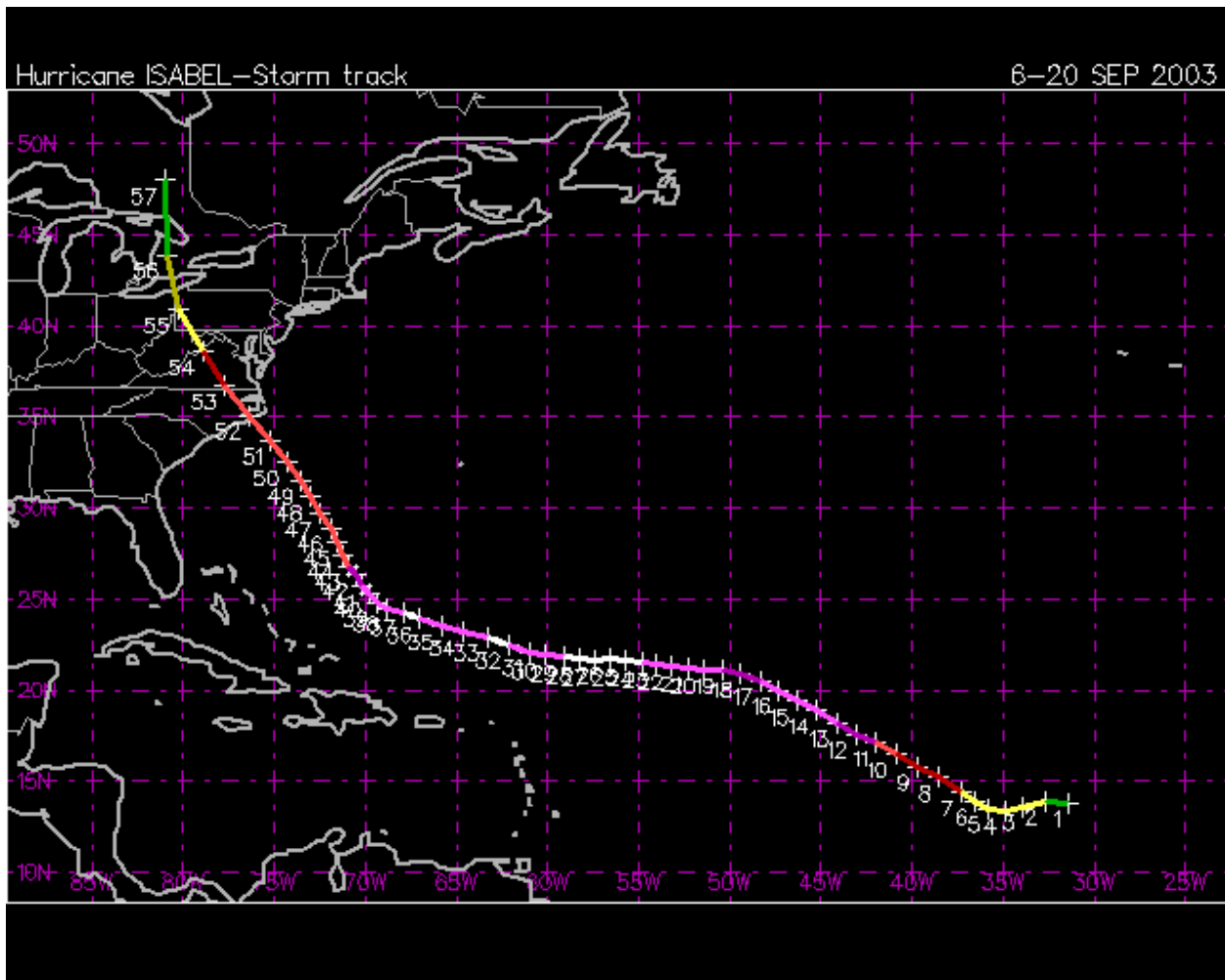


Figure 2.17 Hurricane Isabel Storm Track

For the 1933 hurricane, storm track, wind speed, and central pressure parameters were obtained from NOAA’s National Hurricane Center (NHC). The radius to maximum wind speed was not a given parameter and could not be calculated as recorded winds were not available for the Baltimore area during this time. Thus, this parameter as well as the Manning’s roughness values and eddy viscosity hydrodynamic parameters, were adjusted to obtain a storm surge behavior which corresponded reasonably to the reported magnitudes of the 1933 storm.

Storm Track, wind speed, and central pressure parameters for Hurricane Fran were also obtained from NHC. Additionally, wind speeds at Baltimore’s BWI Airport were obtained from the National Climatic Data Center (NCDC). Using Equation 28.1 from the MIKE21 Toolbox User Guide, 2005, the measured winds at Baltimore were compared to the computed wind speed at Baltimore based on trial radii of maximum wind speeds. The radius of maximum wind speed

was then adjusted until the computed winds at Baltimore were similar to those measured by NCDC during Hurricane Fran. The same bathymetry, Manning's n roughness values, and eddy viscosity from the 1933 model run were used for the model simulation of Hurricane Fran, and storm surge water levels similar to those measured were obtained.

The same input parameters as Hurricane Fran were obtained from NHC for Hurricane Isabel. The radius of maximum winds was not calculated; instead a range of radii was given in a NHC report. The average of this range was used as the radius of maximum winds for the entire duration of the storm. The same bathymetry, Manning's n roughness values, and eddy viscosity from the 1933 model run were used for the model simulation of Hurricane Fran, and results yielded a storm surge behavior similar to the reported magnitudes of Hurricane Isabel.

Figure 2.18 through Figure 2.20 show the peak wind speeds in the Study Area for the final hurricane model simulation.

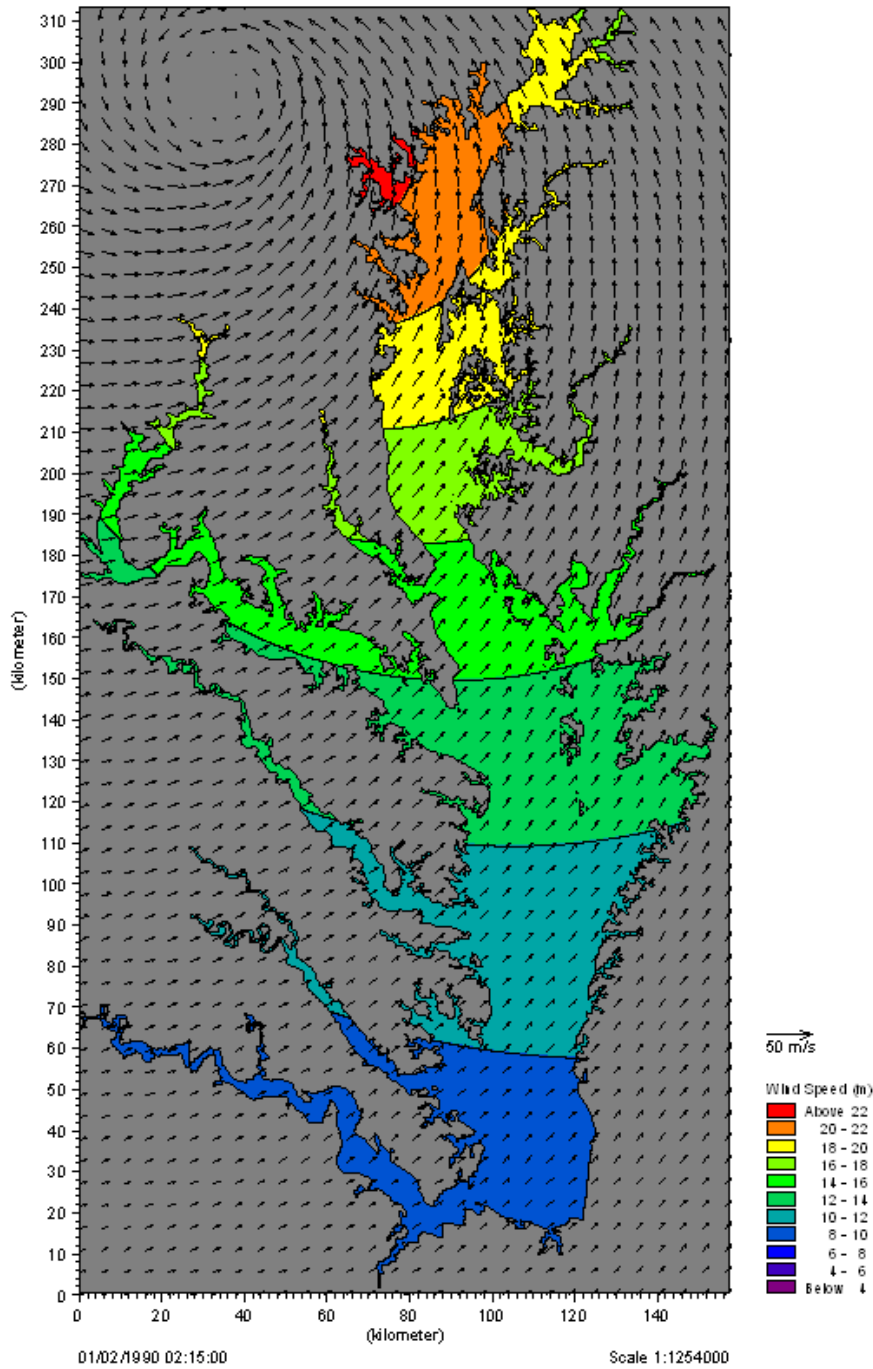


Figure 2.18 Peak Wind Speed in Chesapeake Bay for 1933 Hurricane

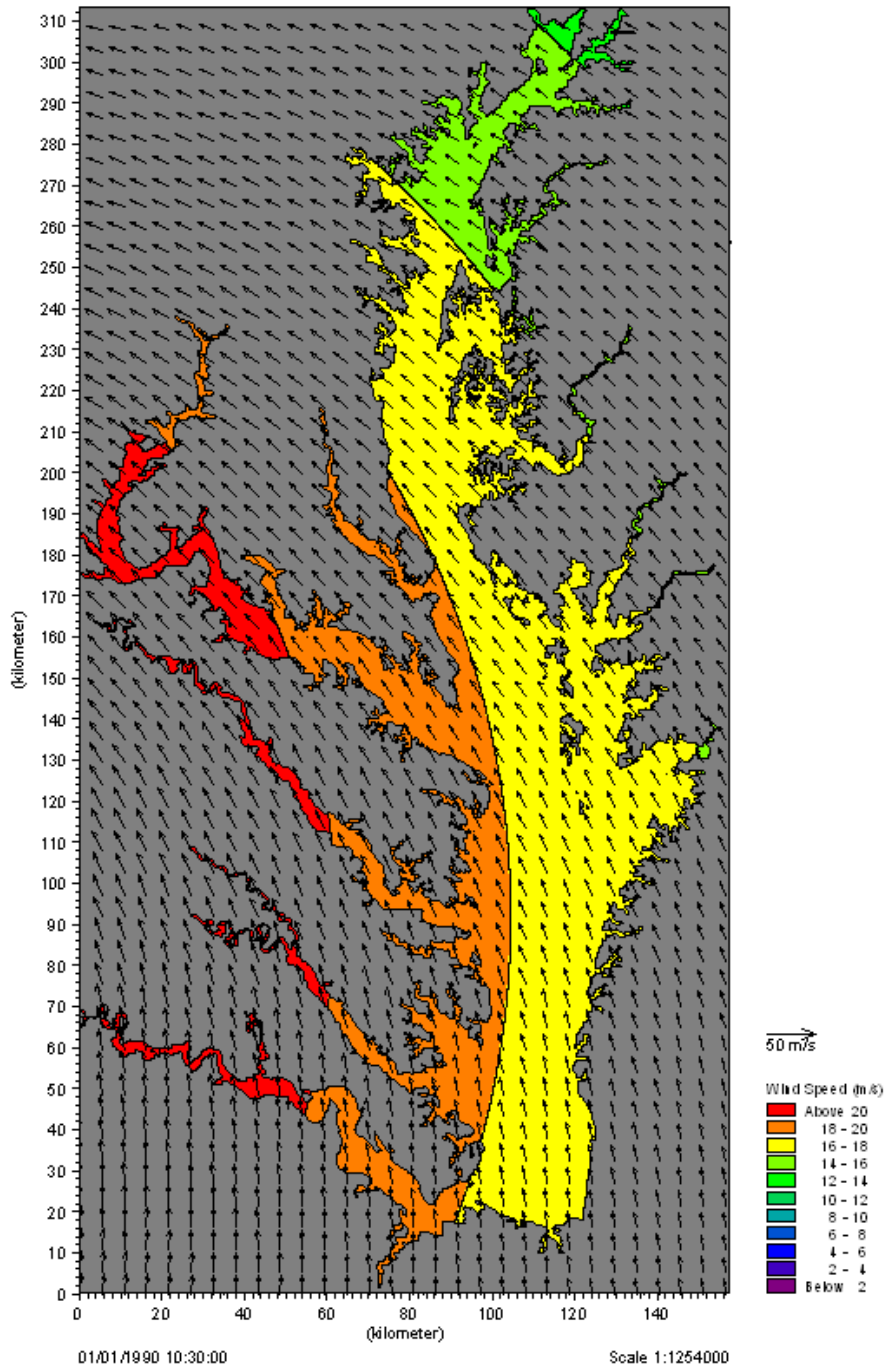


Figure 2.19 Peak Wind Speed in Chesapeake Bay for Hurricane Fran

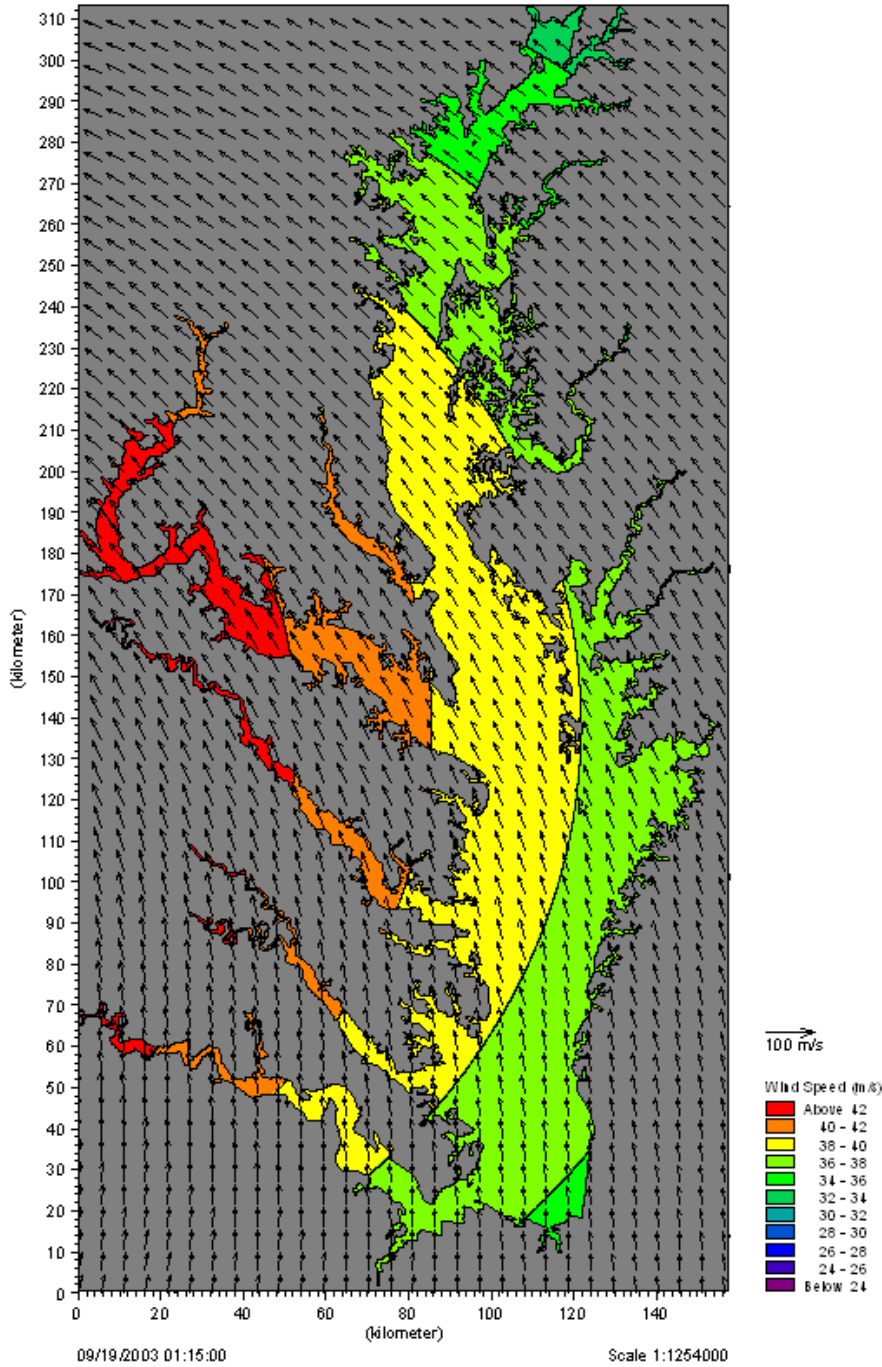


Figure 2.20 Peak Wind Speed in Chesapeake Bay for Hurricane Isabel

B-2.5.3 Storm Surge Calibration

B-2.5.3.1 Water Levels

Tidal water level elevations (water levels) and tidal current velocities (currents) at designated

grid points throughout the Chesapeake Bay were extracted into a time series file from the hydrodynamic model produced by each hurricane simulation. Eight grid points were chosen to accurately observe the impact of the hurricanes in Middle Branch, Fort McHenry, and the Inner Harbor. The following UTM coordinates were selected: (255, 1023), (252, 1024), (243, 1023), (248, 1024), (246, 1021), (256, 1056), (254, 1030), and (251, 1032). Figure 2.21 displays a graphical plot of the coordinates.

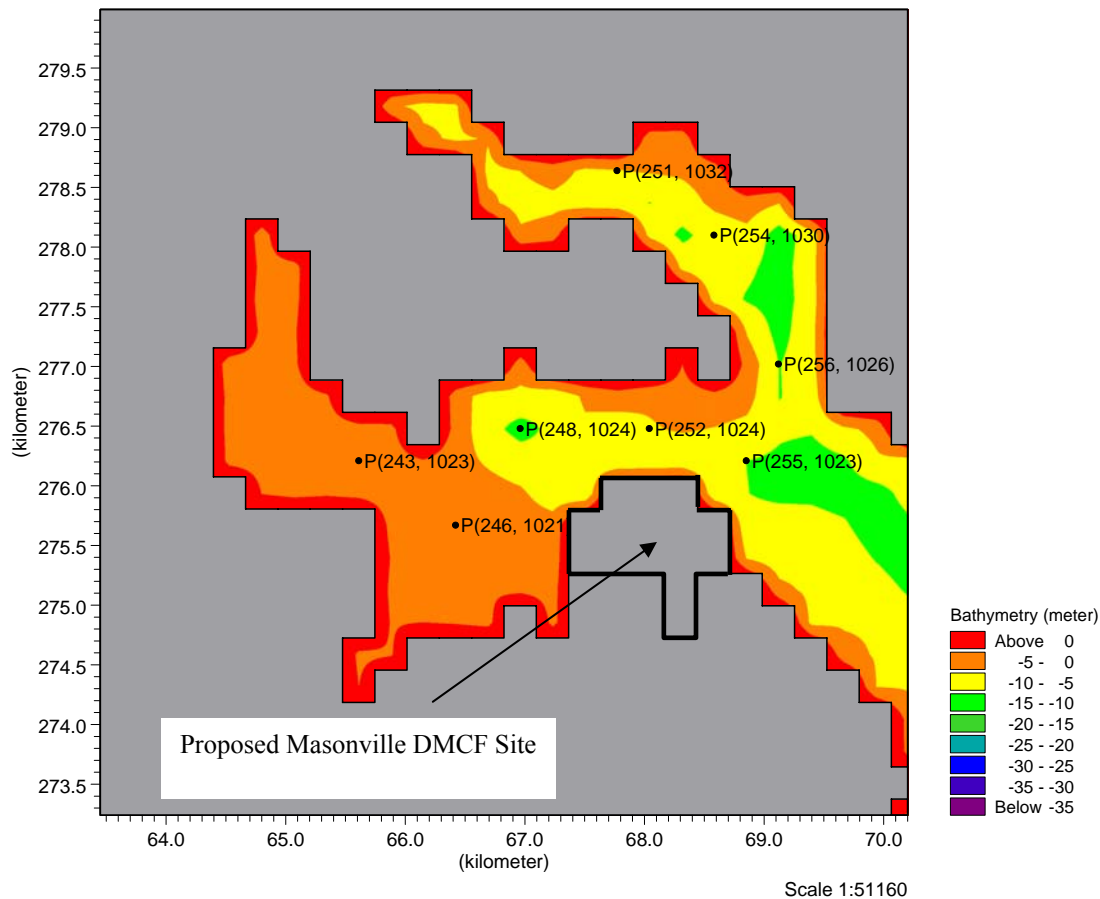


Figure 2.21 Observation Points within Model

B-2.5.4 Water Levels

Figure 2.21 shows observation points within the model domain where the model outputs water level and current magnitude/direction during the simulation. Water surface elevations at the

observation points under existing conditions are shown in Figures 3.15 to 3.20 for each hurricane simulation. The differences in water level between the simulations are visually indistinguishable. As seen in Figure 2.22 through Figure 2.24, Hurricane Isabel produces the largest storm surge.

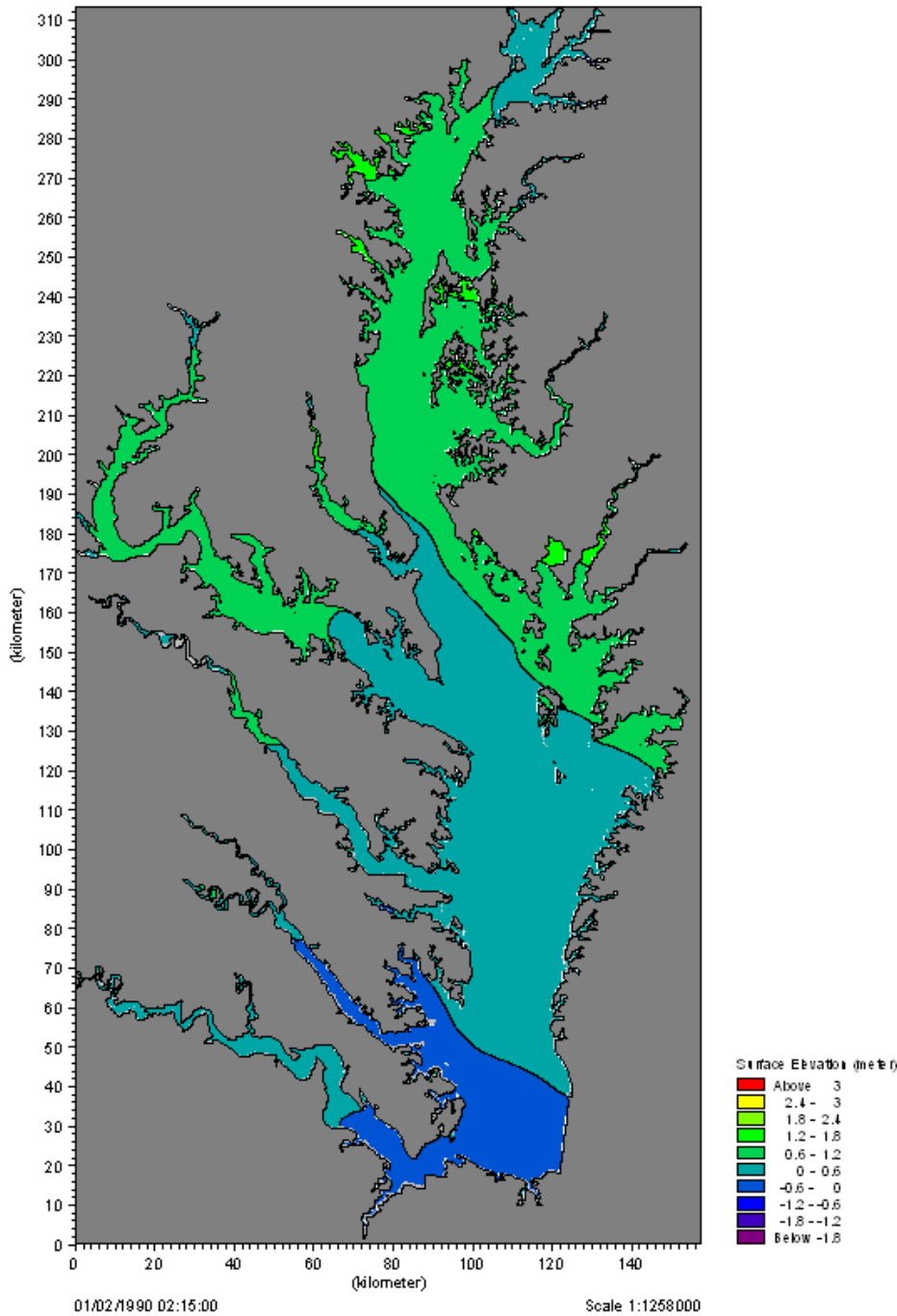


Figure 2.22 Without-Project Peak Storm Surge in Chesapeake Bay for 1933 Hurricane

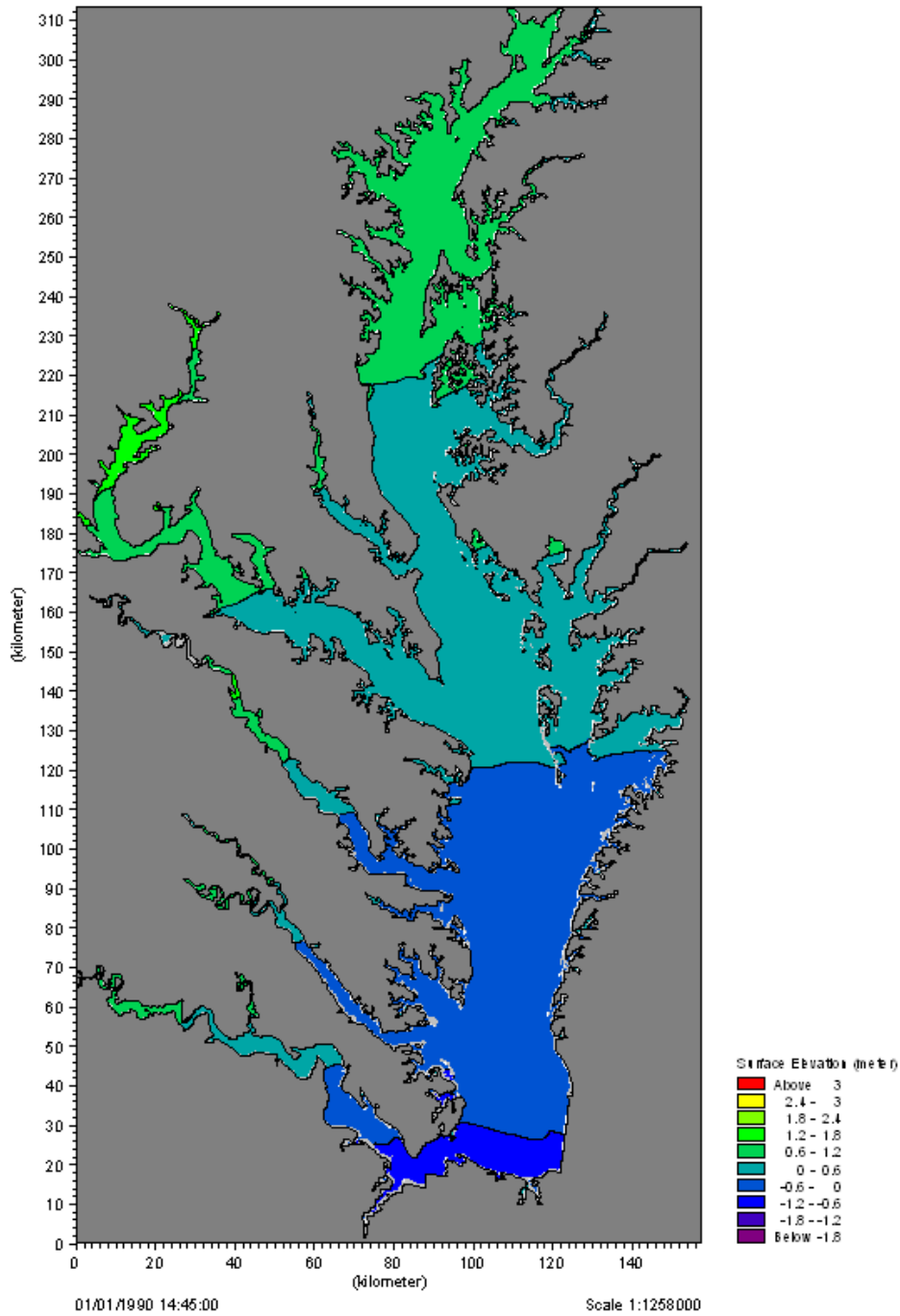


Figure 2.23 Without-Project Peak Storm Surge in Chesapeake Bay for Hurricane Fran

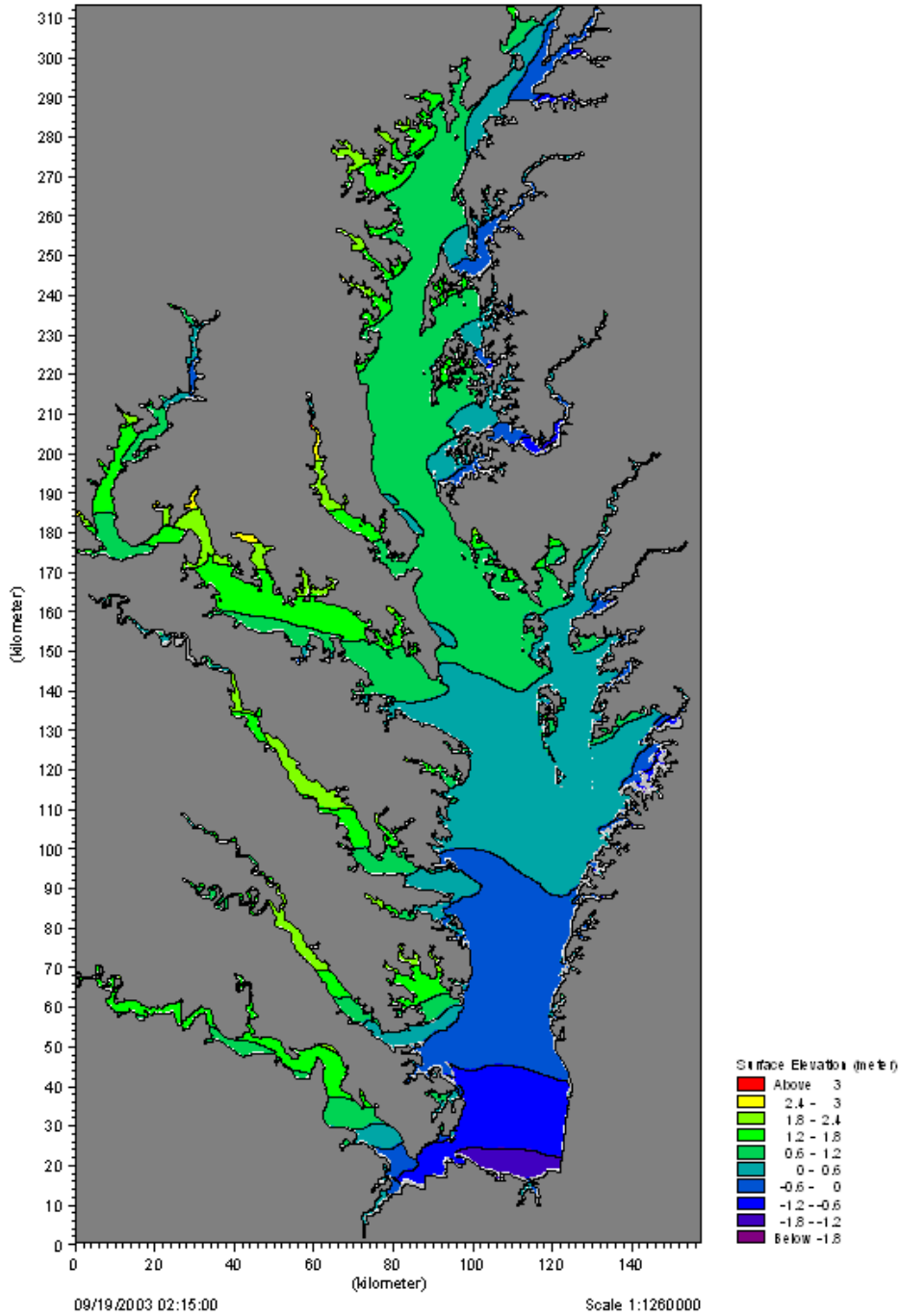


Figure 2.24 Without-Project Peak Storm Surge in Chesapeake Bay for Hurricane Isabel

Table 2.2 shows the water levels modeled during the peak storm surge for the 1933 hurricane, Hurricane Fran, and Hurricane Isabel.

Table 2.2 Peak Storm Surge Water Levels for Baltimore Harbor

Water Surface Elevation Point	Storm Surge Water Level (m)		
	1933 – Without Project	Fran – Without Project	Isabel – Without Project
P(255, 1023)	1.418	0.980	2.031
P(252, 1024)	1.427	0.984	2.056
P(243, 1023)	1.449	1.010	2.167
P(248, 1024)	1.435	0.991	2.089
P(246, 1021)	1.415	0.991	2.073
P(256, 1026)	1.435	0.983	2.056
P(254, 1030)	1.460	0.990	2.107
P(251, 1032)	1.476	0.997	2.146

B-3. IMPACT ASSESSMENT

B-3.1 HYDROLOGY AND HYDRODYNAMICS

The impact of the proposed Masonville DMCF on hydrodynamics and sedimentation within the Middle Branch of the Patapsco River was assessed using the three-dimensional numerical model described in Section B-2.1. The impacts were measured by comparing model simulations with identical boundary forcing and comparing selected parameters. The proposed Masonville DMCF was represented by creating “dry” computational points within the dike outline as shown in Figure 3.1. A full description of the model development, calibration, and impact assessment scenario development can be found in Section B-2.

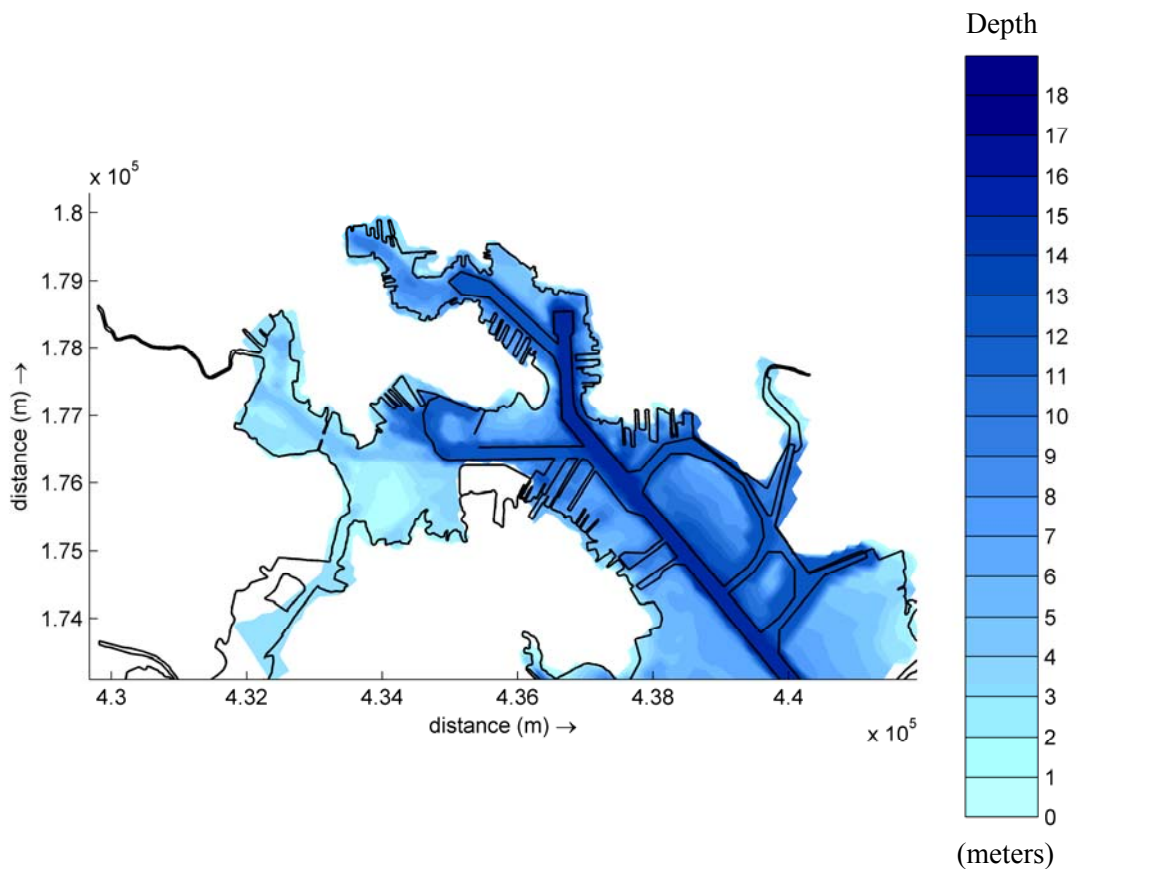


Figure 3.1 With-Project Model Bathymetry

B-3.1.1 Hydrodynamics

Hydrodynamics were assessed over a 30-day simulation corresponding to the data collection program used for model calibration (April-May 2005). The tides within Baltimore harbor have small amplitude, less than 2 feet average range, and therefore wind and density currents have an equal or greater influence on circulation and water levels.

B-3.1.2 Water Levels

Figure 3.2 displays observation points within the model domain where the model outputs water level and current magnitude/direction during the simulation. Water surface elevations at the observation points with and without project are compared in Figure 3.3 to Figure 3.4 for a two week cycle. The differences in water level between the simulations is visually indistinguishable. Table 3.1 lists the correlation and Root Mean Squared (RMS) error between with- and without-project simulations.

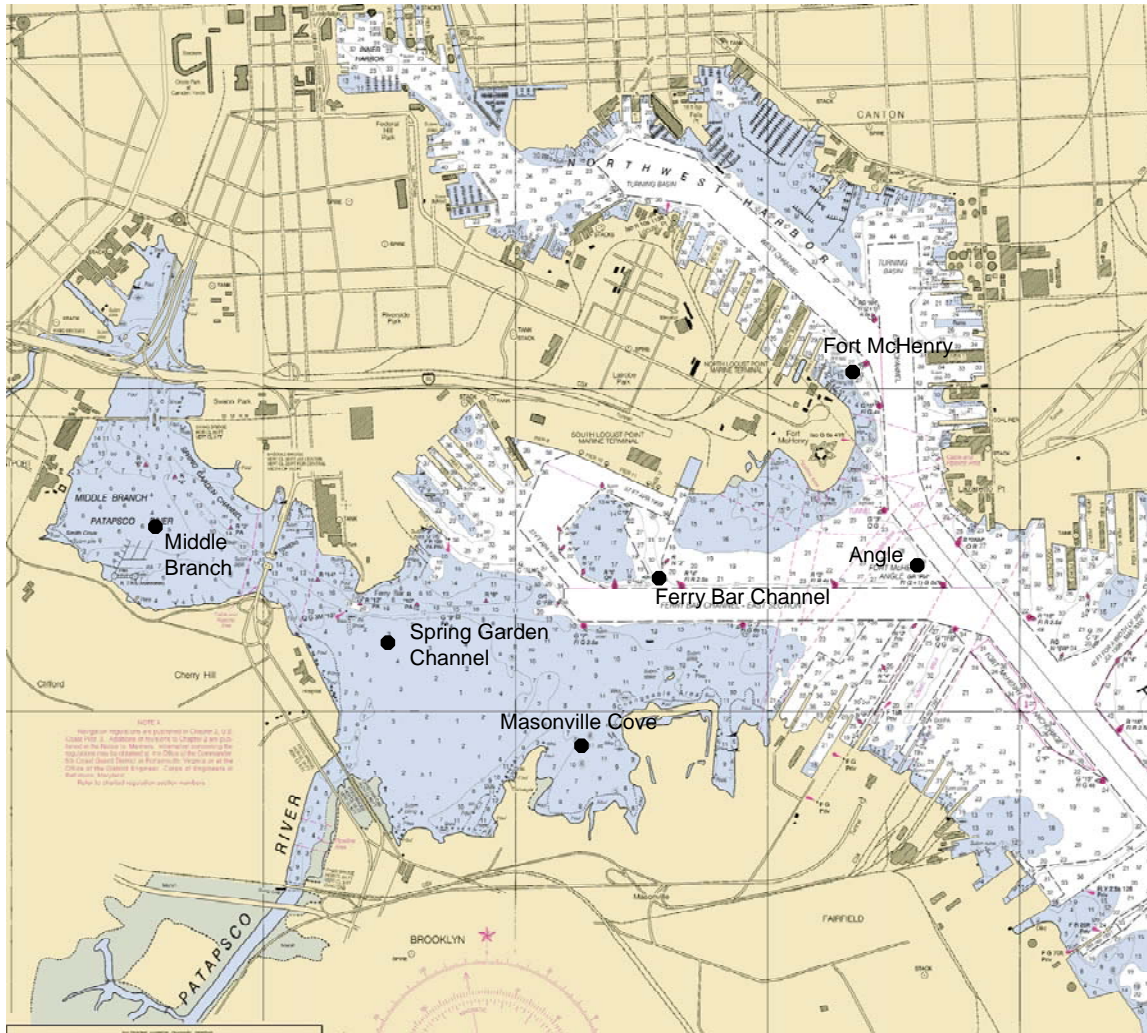


Figure 3.2 Observation Points Within Model

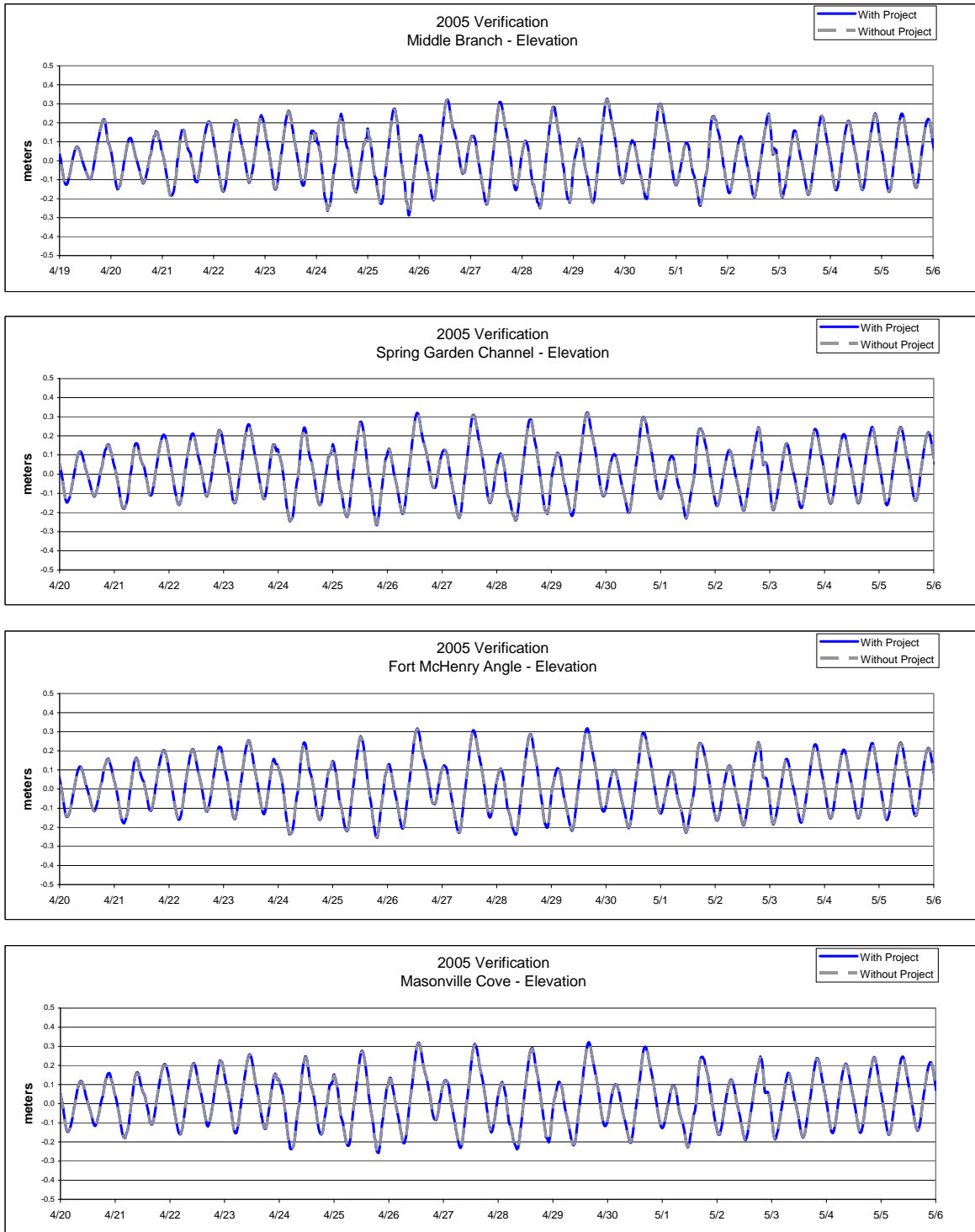


Figure 3.3 Water Surface Elevation Comparison, With and Without Project (1 of 2)

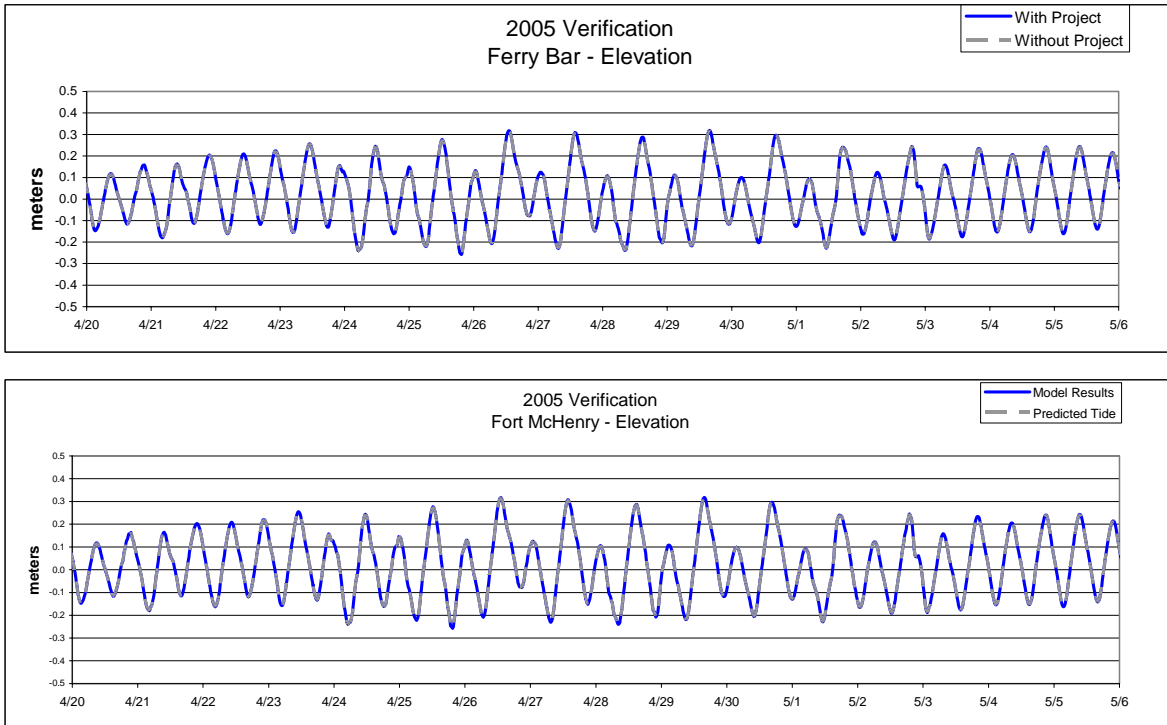


Figure 3.4 Water Surface Elevation Comparison, With and Without Project (2 of 2)

Table 3.1 Water Surface Elevation Statistical Comparison, With and Without Project

Observation Point	Correlation	RMS Error, cm
Fort McHenry	1.00	0.02
Fort McHenry Angle	1.00	0.04
Ferry Bar	1.00	0.07
Masonville Cove	1.00	0.09
Spring Garden Channel	1.00	0.06
Middle Branch	1.00	0.09

The RMS errors between the two datasets are less than 1 cm. Water surface elevations under typical tide and wind conditions, with and without project, are by all measures essentially identical.

B-3.1.3 Currents

Currents show more variation than the water surface elevations. The proposed Masonville DMCF does appear to alter the prevailing currents, especially in the immediate vicinity of the project. Figure 3.5 to Figure 3.7 depict surface, mid-depth, and bottom current fields, respectively, during ebb tide at one time step during the simulation, with and without project. Note that under without-project conditions, the flow out of the Patapsco travels mainly at the surface along the south shore with a maximum velocity of 0.25 m/s (~1 ft/s). The flows on the channel bottom are weaker and do not necessarily follow the surface currents, depending on wind conditions and density stratification. However, under with-project conditions, the proposed Masonville DMCF blocks the outflow and diverts the surface flows out over the main Ferry Bar Channel. Inflows along the channel bottom increase slightly in strength.

Figure 3.8 to Figure 3.10 display surface, mid-depth, and bottom current fields during flood tide, for with- and without-project conditions. Like the ebb tide, surface and bottom currents flow in opposite directions. The surface currents continue to flow outward, though at reduced velocity. The mid-depth and bottom currents flow inward. Under with-project conditions the strength of the inflowing bottom currents is increased.

Model results show that current patterns may be altered by the construction of the proposed Masonville DMCF, though current strengths are on the same order as without-project conditions.

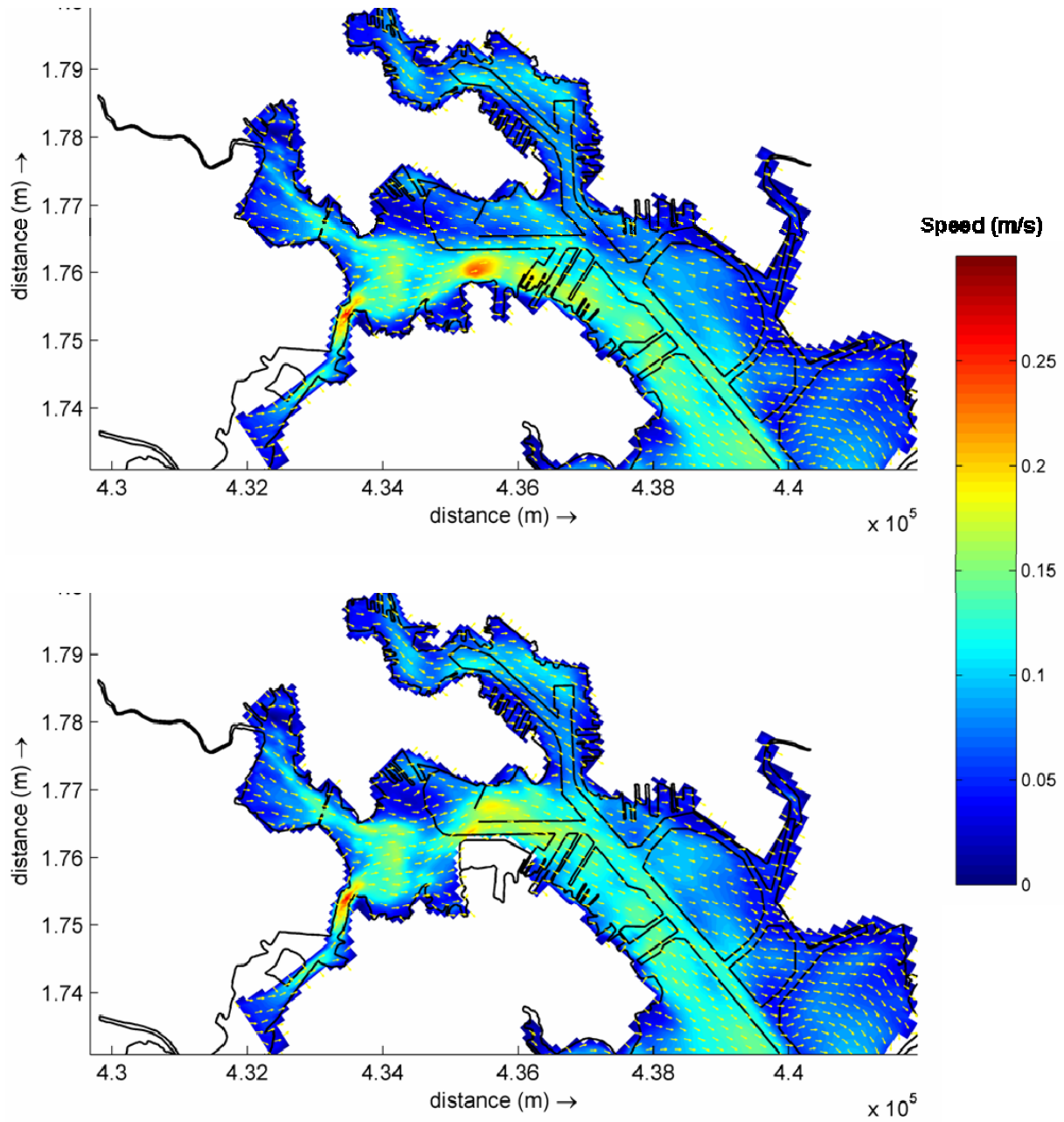


Figure 3.5 Ebb Tide Current Pattern, Surface, With and Without Project

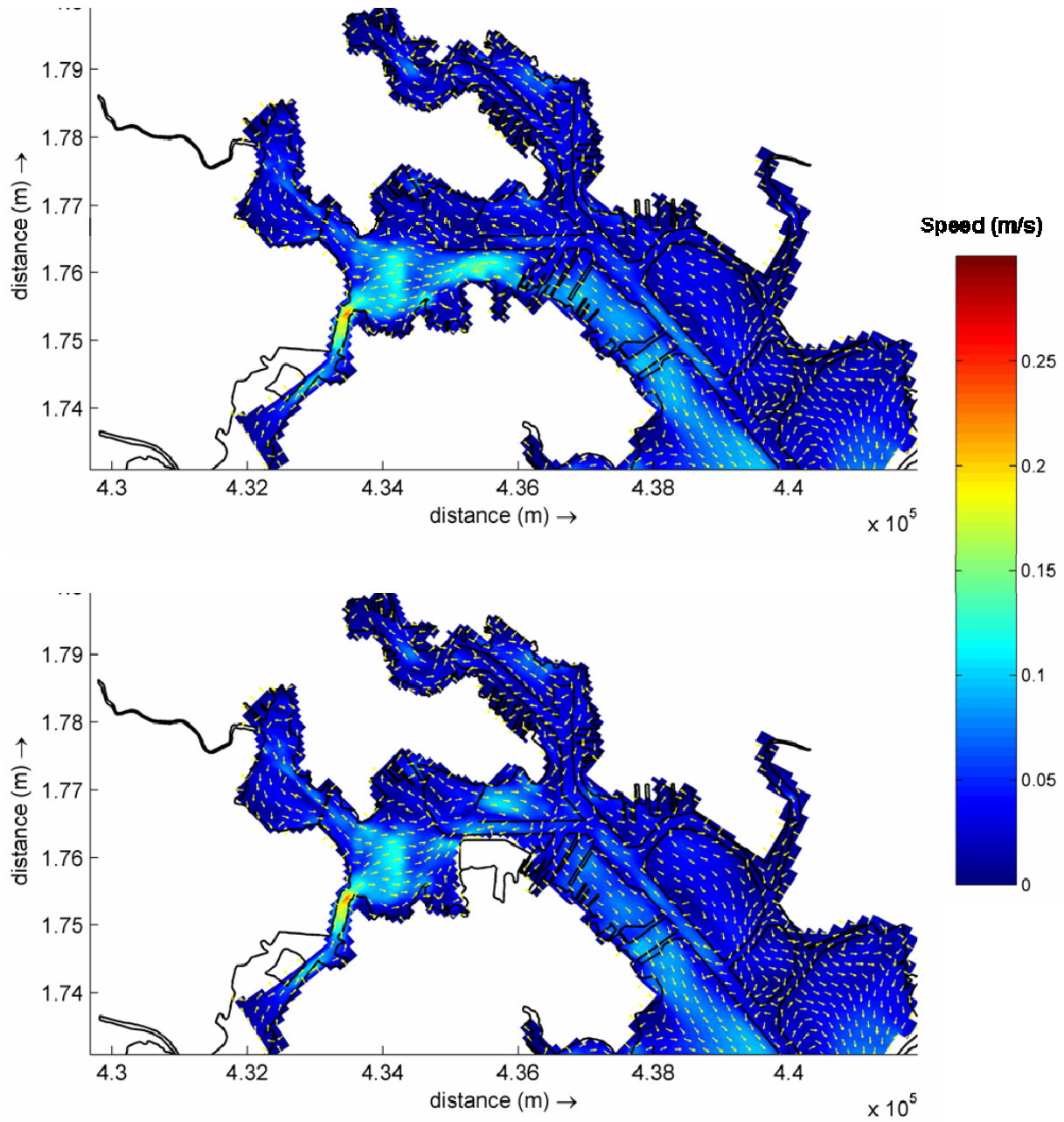


Figure 3.6 Ebb Tide Current Pattern, Mid Depth, With and Without Project

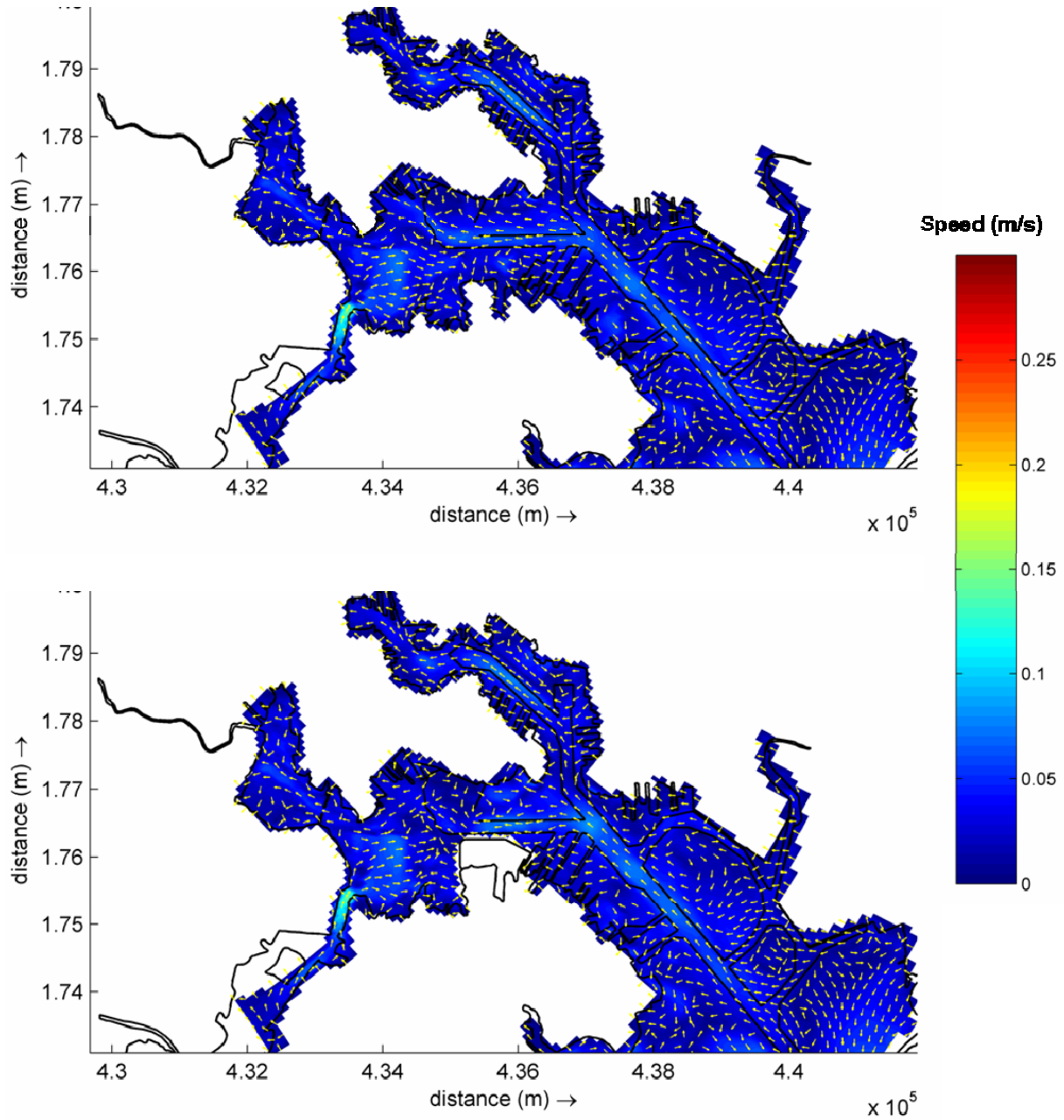


Figure 3.7 Ebb Tide Current Pattern, Bottom, With and Without Project

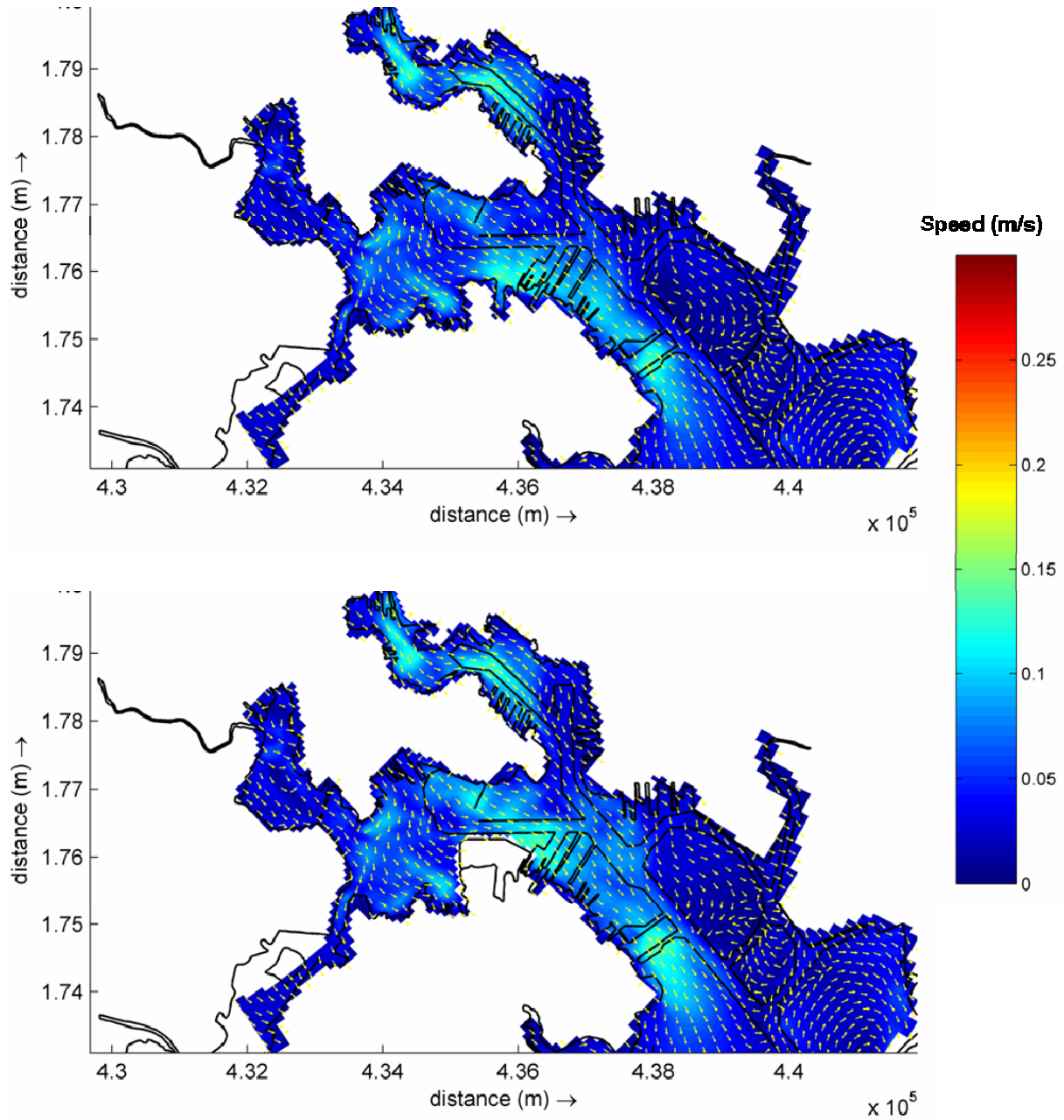


Figure 3.8 Flood Tide Current Pattern, Surface, With and Without Project

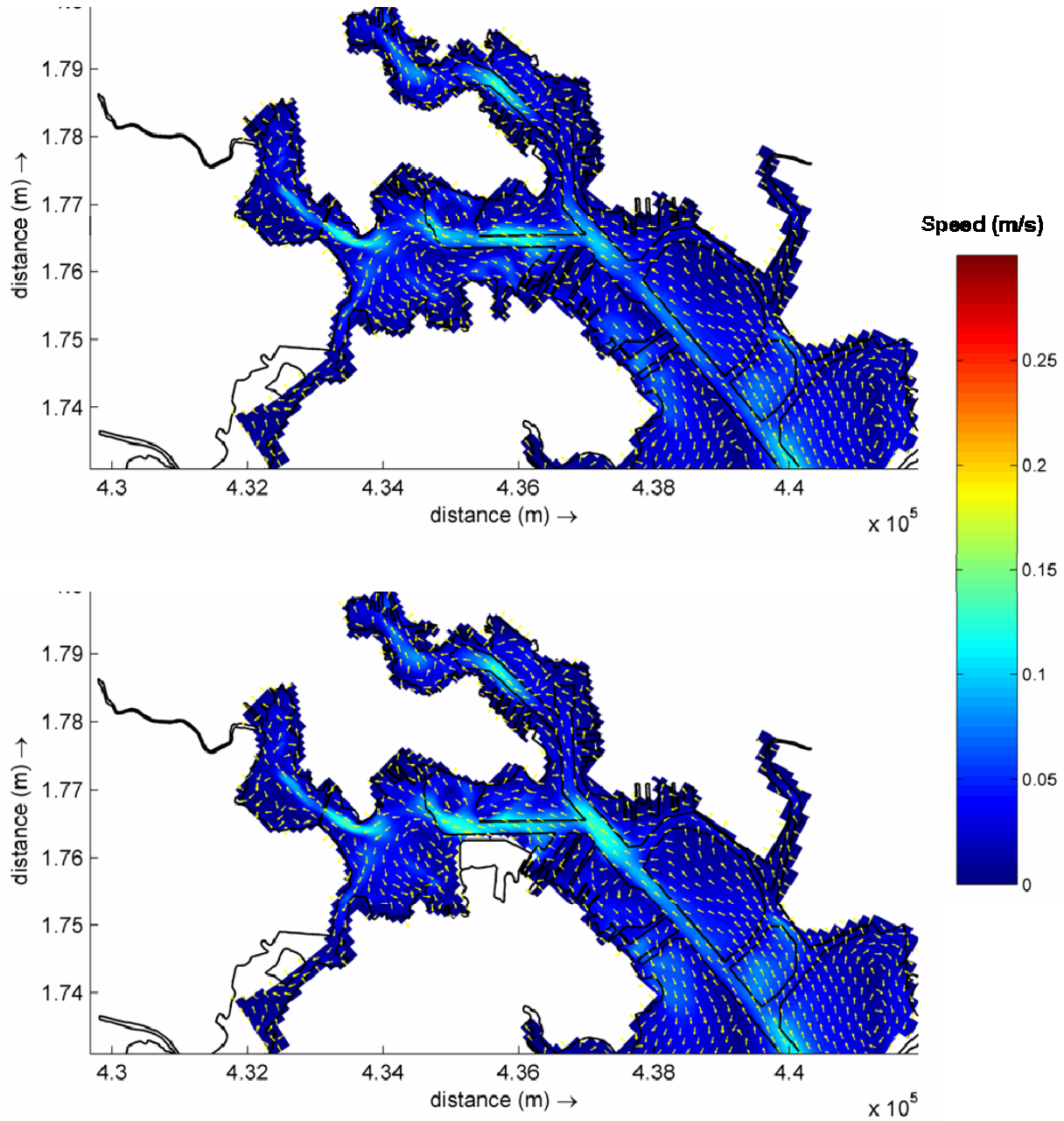


Figure 3.9 Flood Tide Current Pattern, Mid Depth, With and Without Project

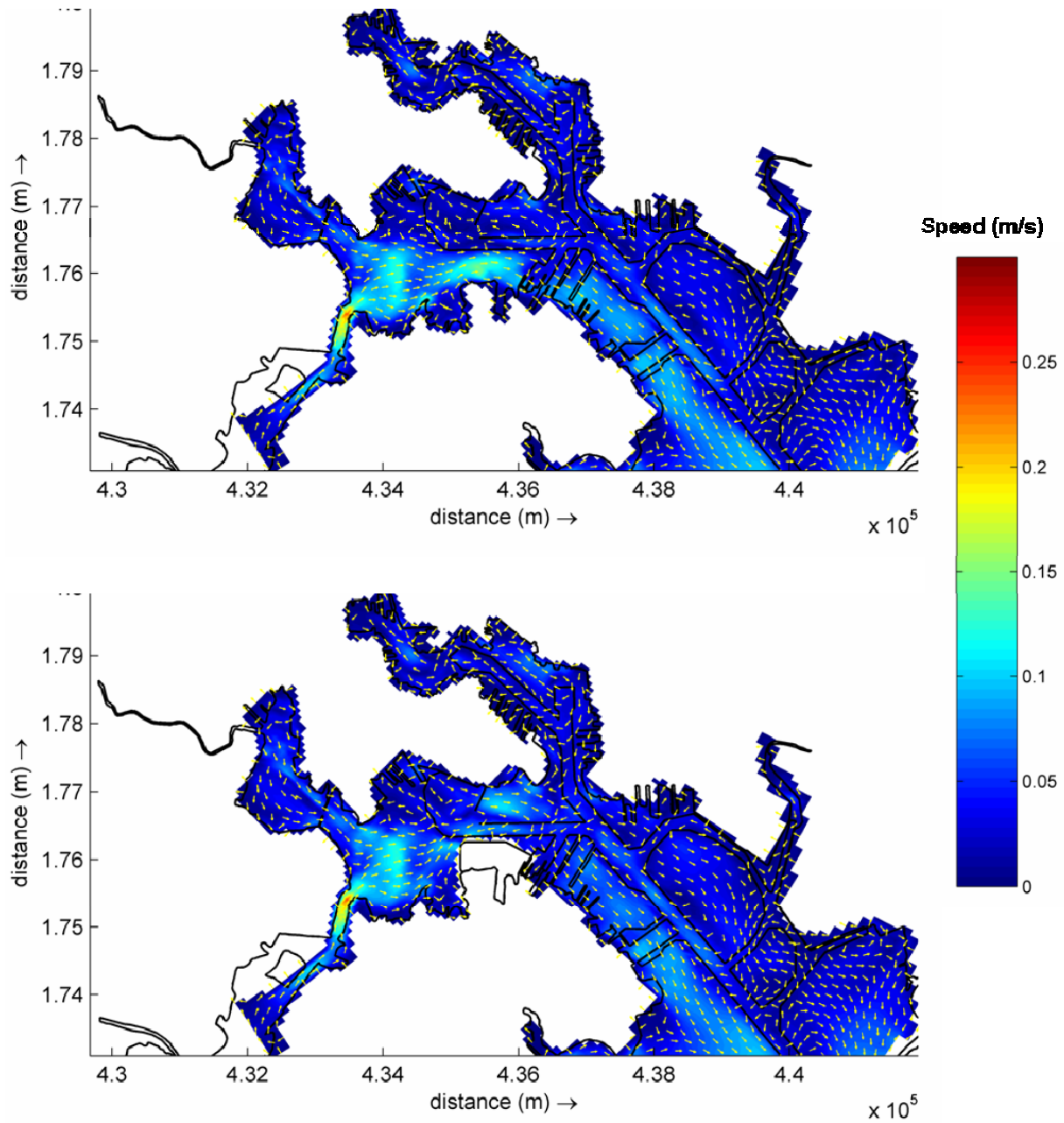


Figure 3.10 Flood Tide Current Pattern, Bottom, With and Without Project

B-3.1.4 Residence Time

Residence time is a typical measure used to assess the flushing characteristics of an enclosed water body. To assess the impact of the proposed Masonville DMCF on water exchange within the Middle Branch, the three-dimensional model was run using a tracer concentration to measure residence time, with and without project. The model initiated with a unit concentration of a tracer constituent within the main branch of the Patapsco upstream of Fort McHenry. The boundary of the basin was defined as a line drawn between Fort McHenry and Fairfield. As the simulation progresses, the water from the basin will mix with water in the outer harbor and the tracer concentration will become diluted. The residence time is reached when the average concentration within the embayment reaches $1/e$, where e is the natural exponent (USACE, 2001).

Figure 3.11 displays the concentration at the observation points within the Middle Branch over the course of a two-week simulation for both with- and without-project conditions. Due to the change in current patterns described above, the dispersion of the tracer concentration has been slowed slightly resulting in marginally longer residence times. Table 3.2 lists the computed residence times for the Middle Branch embayment, with and without project. The residence time vary from approximately 5 days in the Ferry Bar Channel to over 10 days in the Middle Branch. With the proposed Masonville DMCF in place, residence times are increased by 2-4 hours or 1-2 percent.

Table 3.2 Residence Time of Patapsco, Upstream of Fort McHenry

	Residence Time (days)	
	Without Project	With Project
Ferry Bar	5.0	5.1
Masonville Cove	6.0	6.2
Spring Garden Channel	6.9	7.0
Middle Branch	10.4	10.5

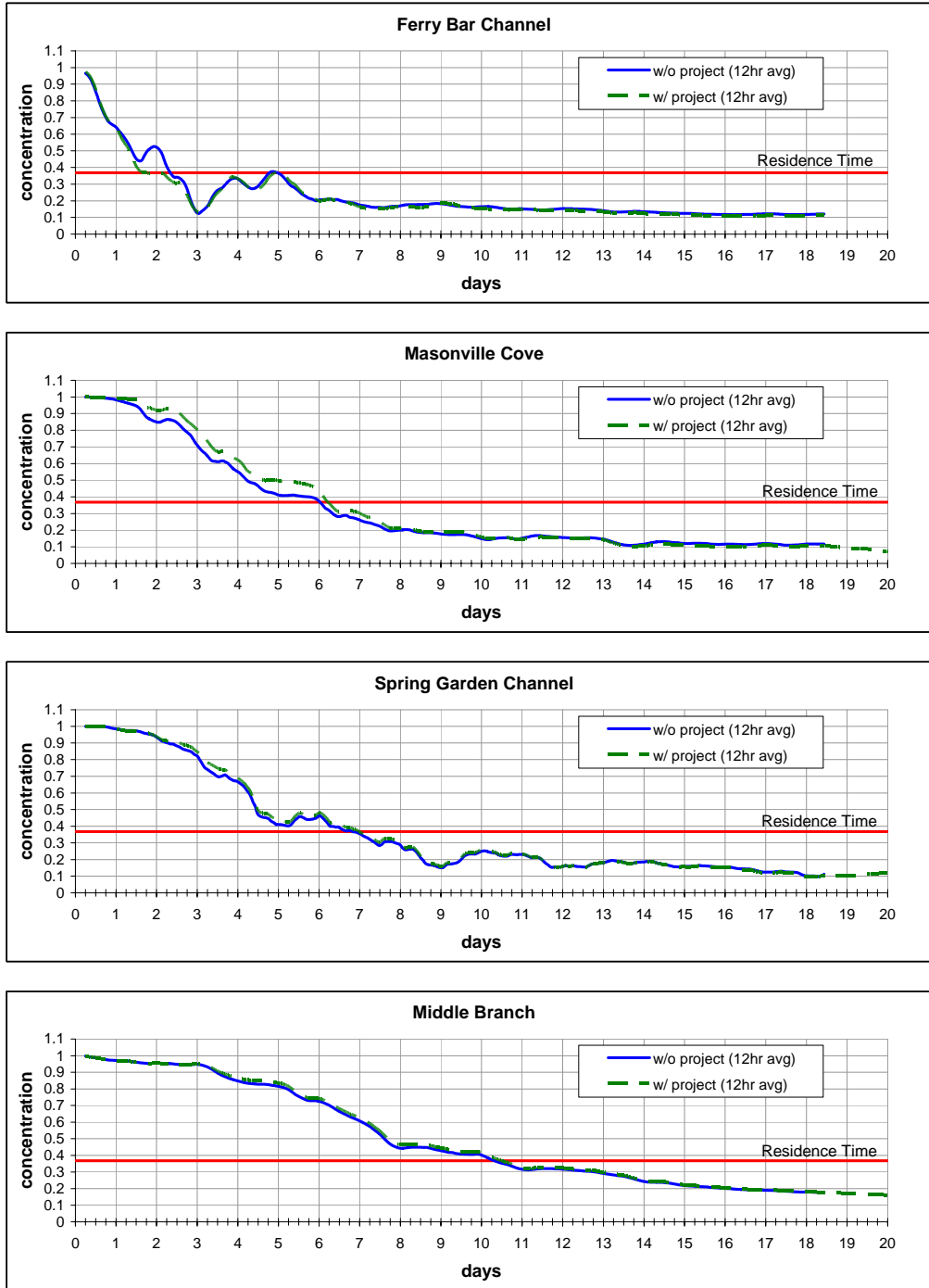


Figure 3.11 Residence Time at Observation Points, with and without project

B-3.2 SEDIMENTATION IMPACTS

The influence of the proposed Masonville DMCF on the erosion and deposition in the project area was assessed using the calibrated long-term morphological model. The model simulates the deposition of harbor sediments over a 20-year cycle by simulating sequential storm events which carry sediment load through high freshwater inflows and resuspend harbor sediments due to high winds. The model was calibrated to reproduce the 20-year deposition rate in the Ferry Bar Channel. Details of model calibration and sediment parameters implemented are given in B-2.4.

Figure 3.12 displays the sedimentation/erosion patterns in the Patapsco River for with and without project conditions. Rates are presented as annual depth. Sedimentation rates are generally slow with maximum rates of 1-2 inches per year. The highest rates under without project conditions are in the upstream end of the Ferry Bar Channel and in Masonville Cove. Under with-project conditions, the model predicts increased sedimentation in both these areas. The model predicts that no erosion occurs in the Patapsco upstream of Fort McHenry (ie, the system is depositional).

Figure 3.13 presents the relative sedimentation rate between with-project and without-project conditions. Sedimentation at the upstream end of the Ferry Bar Channel and at the north end of Masonville Cove increases by 0.4-0.8 inches per year. The net increase in sediment depth over 20 years in the Ferry Bar Channel is projected to be 8-16 inches. The sedimentation rate near the northwest corner of the DMCF decreases due to increase flow velocities near the structure.

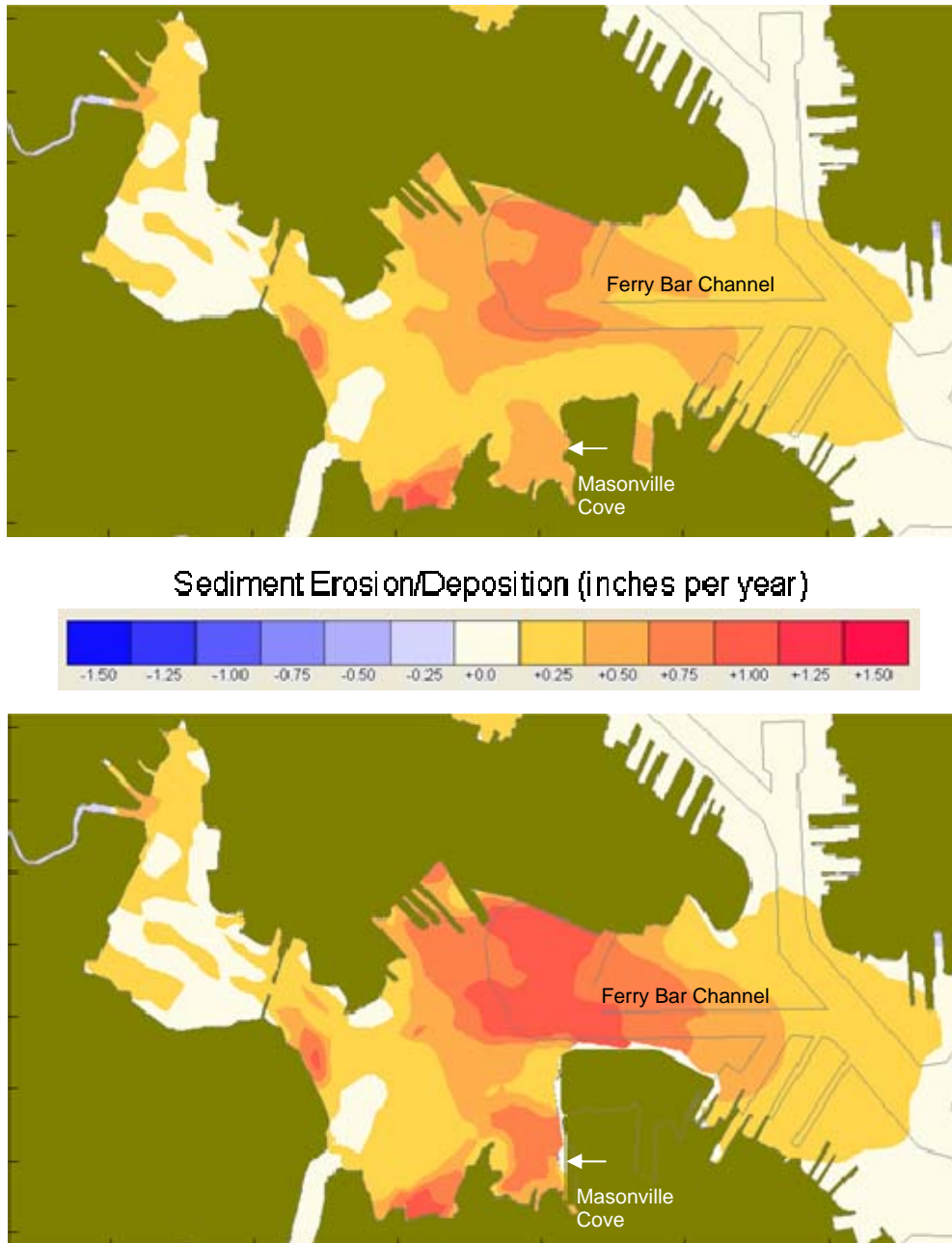


Figure 3.12 Sedimentation/Erosion Patterns, With Project (bottom) and Without Project (top)

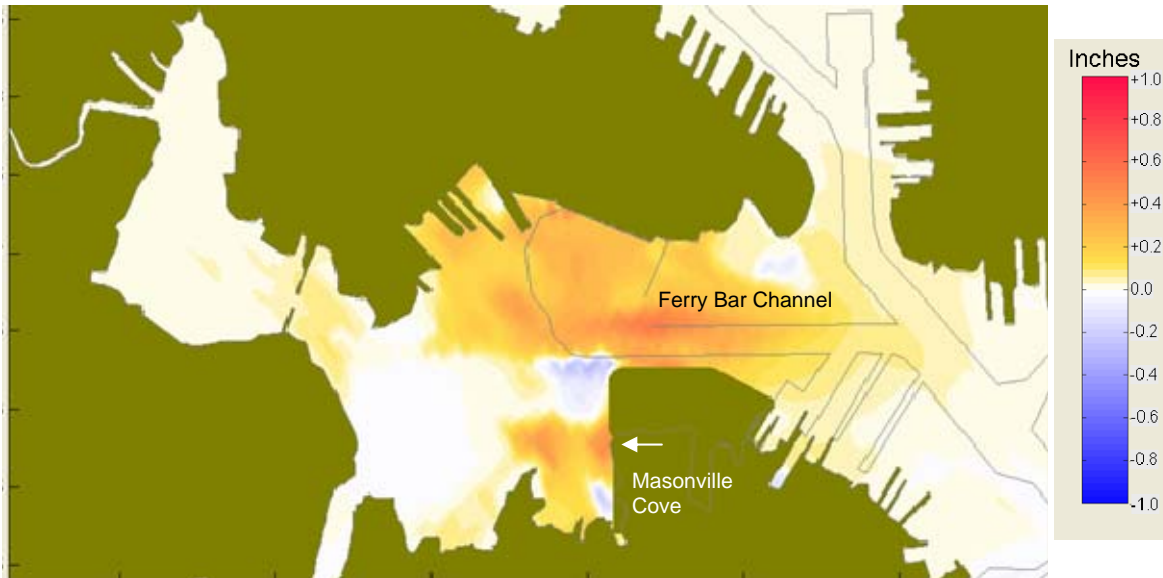


Figure 3.13 Relative annual sedimentation rate of proposed Masonville DMCF project

B-3.3 STORM SURGE IMPACTS

The impact of the proposed Masonville DMCF on the water surface elevations within the Baltimore Harbor was assessed using the two-dimensional numerical model described in Section B-2.5. The impacts were measured by comparing model simulations with identical boundary forcing and comparing selected hurricane parameters. The proposed Masonville DMCF was represented by creating “dry” computational points within the dike outline as shown in Figure 3.14. A full description of the model parameters, calibration, and impact assessment scenario development can be found in Section B-2.5.

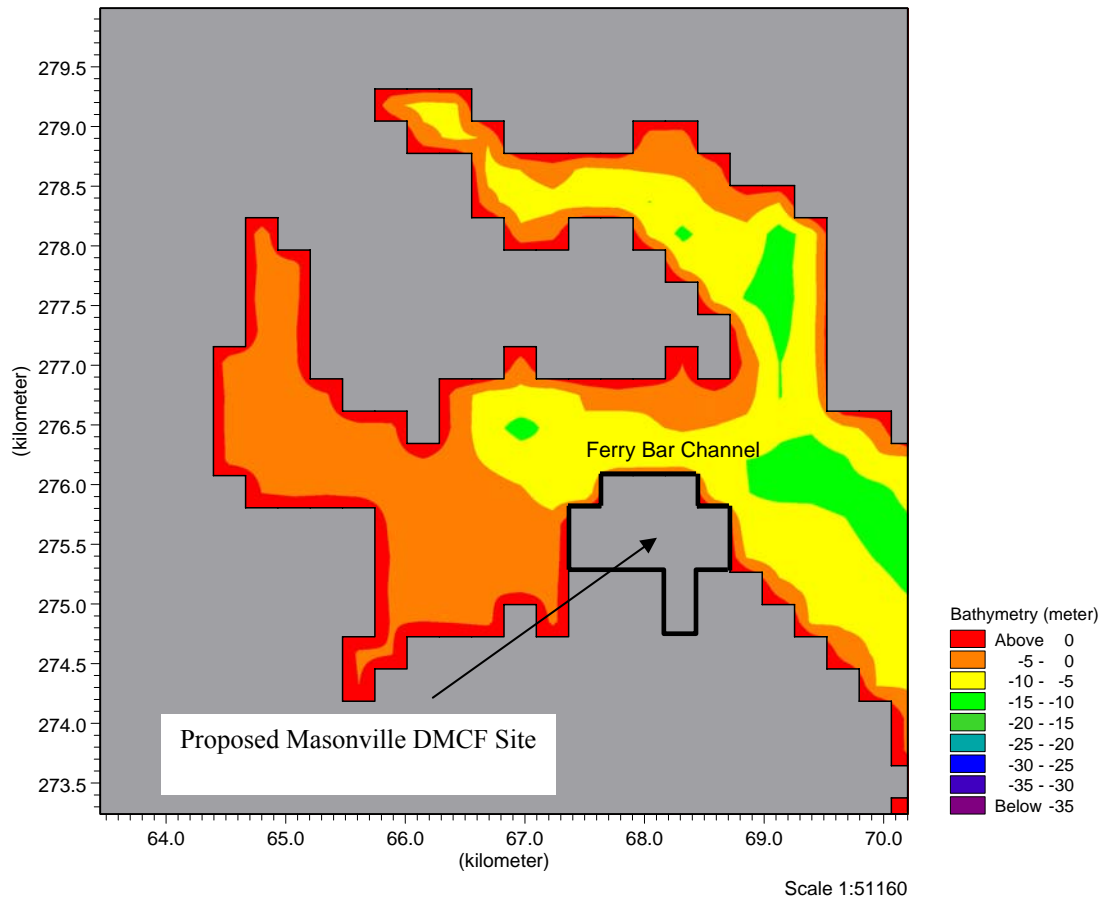


Figure 3.14 With-Project Model Bathymetry

B-3.3.1 Water Levels

Figure 2.21, displays observation points within the model domain where the model outputs water level and current magnitude/direction during the simulation. Water surface elevations for the entire model, under with project conditions are shown in Figure 3.15 through Figure 3.17 for each hurricane simulation. As seen in the figures, Hurricane Isabel produces the largest storm surge.

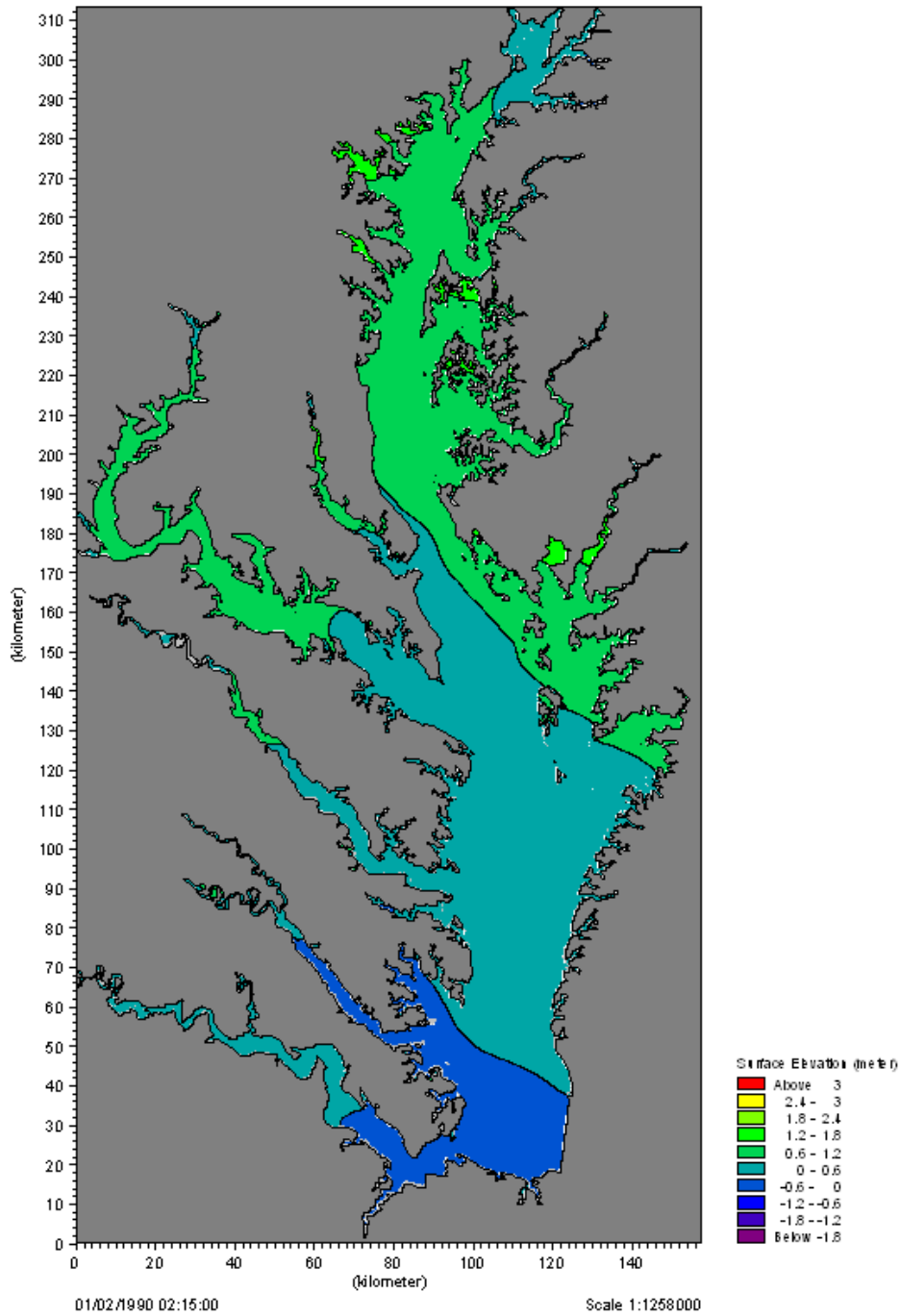


Figure 3.15 With-Project Peak Storm Surge in Chesapeake Bay for 1933 Hurricane

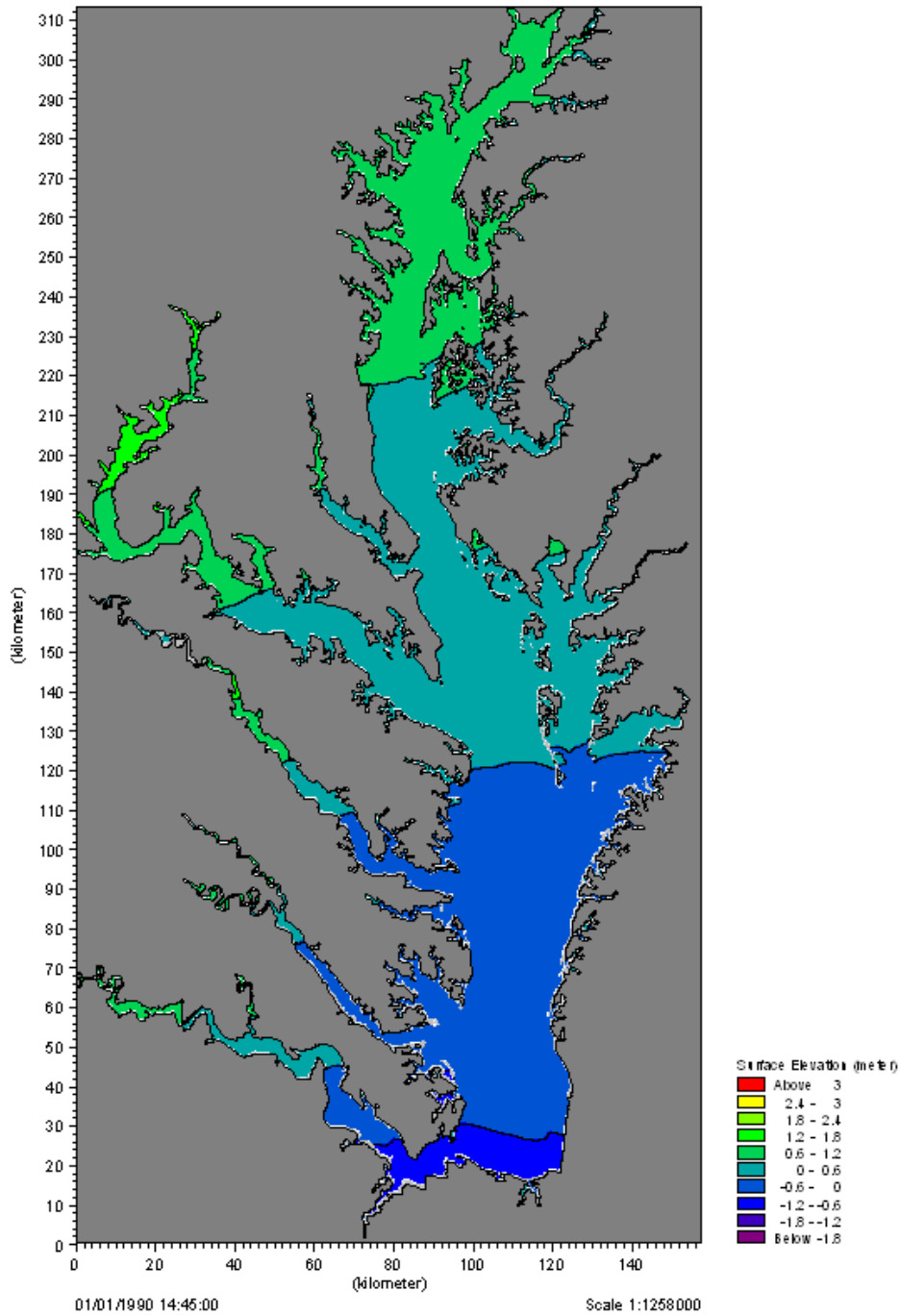


Figure 3.16 With-Project Peak Storm Surge in Chesapeake Bay for Hurricane Fran

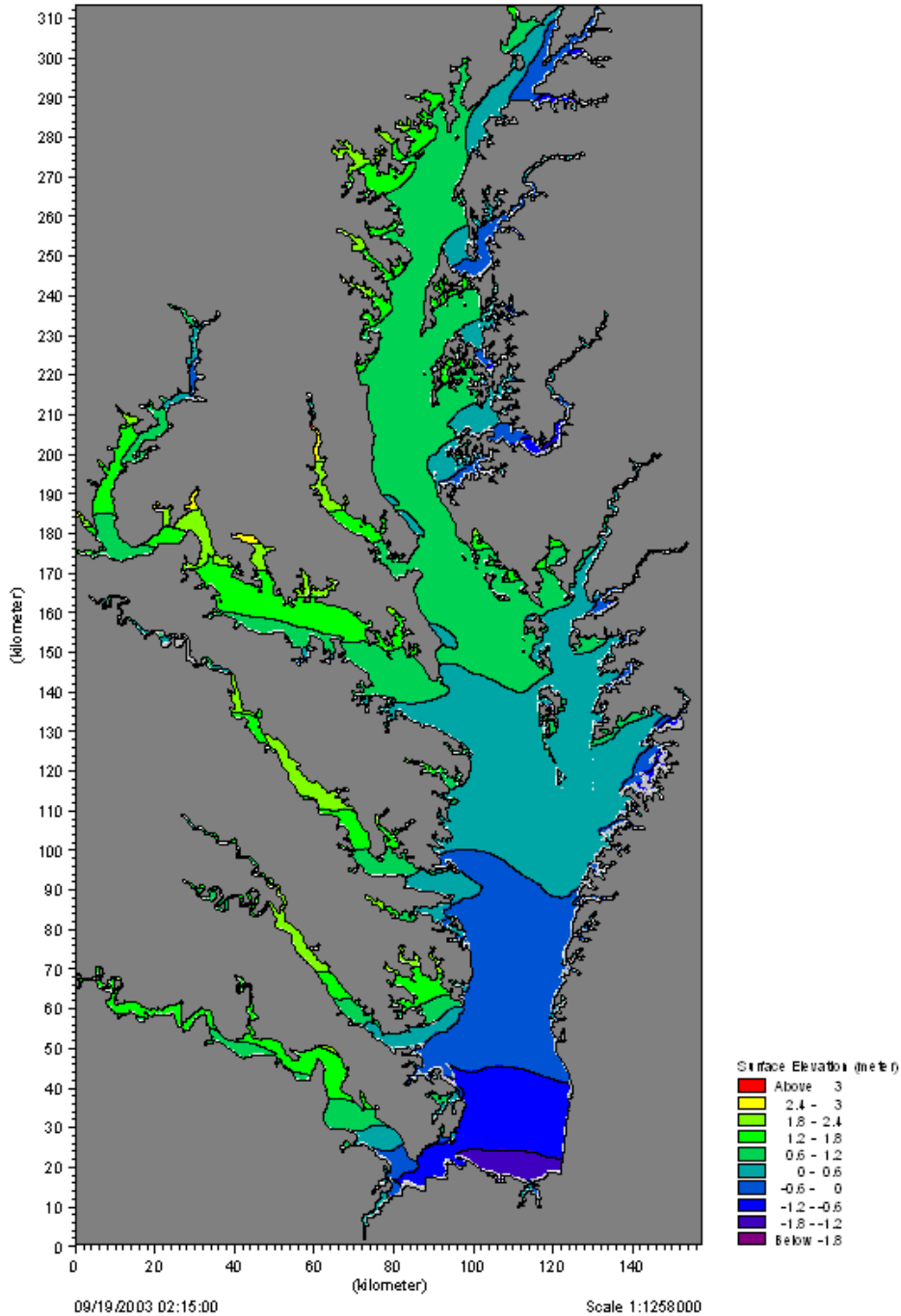


Figure 3.17 With-Project Peak Storm Surge in Chesapeake Bay for Hurricane Isabel

Table 3.3 shows the water levels measured during the peak storm surge for the 1933 hurricane, Hurricane Fran, and Hurricane Isabel. The comparison of the with- and without-project water elevation in Table 3.3 reveals that the with-project water elevation is within millimeters of the without-project water levels and is considered acceptable.

Table 3.3 Peak Storm Surge Water Levels for Baltimore Harbor

Water Surface Elevation Point	Storm Surge Water Level (m)					
	1933		Fran		Isabel	
	Without	With	Without	With	Without	With
P(255, 1023)	1.418	1.418	0.980	0.980	2.031	2.033
P(252, 1024)	1.427	1.430	0.984	0.985	2.056	2.059
P(243, 1023)	1.449	1.454	1.010	1.009	2.167	2.166
P(248, 1024)	1.435	1.440	0.991	0.990	2.089	2.093
P(246, 1021)	1.415	1.421	0.991	0.990	2.073	2.070
P(256, 1026)	1.435	1.435	0.983	0.983	2.056	2.057
P(254, 1030)	1.460	1.460	0.990	0.990	2.107	2.108
P(251, 1032)	1.476	1.477	0.997	0.997	2.146	2.147

In order to fully observe the changes in water surface elevation, a difference plot was created for each storm surge. Figure 3.18, Figure 3.19 and Figure 3.20 show the difference plots for the 1933 Hurricane, Hurricane Ran and Hurricane Isabel, respectively. All three plots show that the proposed Masonville Site will decrease water levels in the Middle Branch area and will increase water levels in the Fort McHenry and Inner Harbor area.

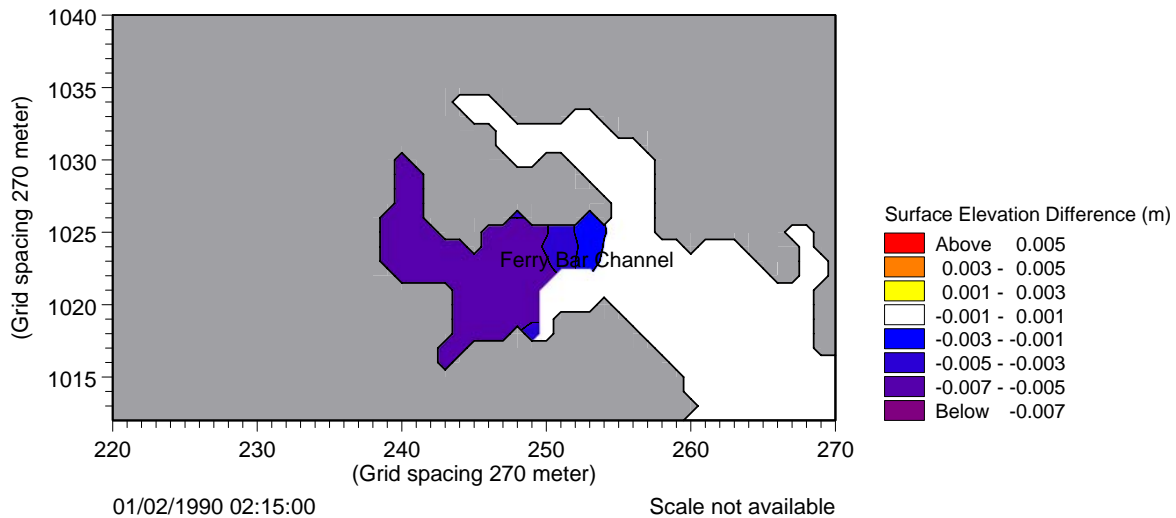


Figure 3.18 Surface Elevation Difference Plot for 1933 Hurricane Peak Storm Surge

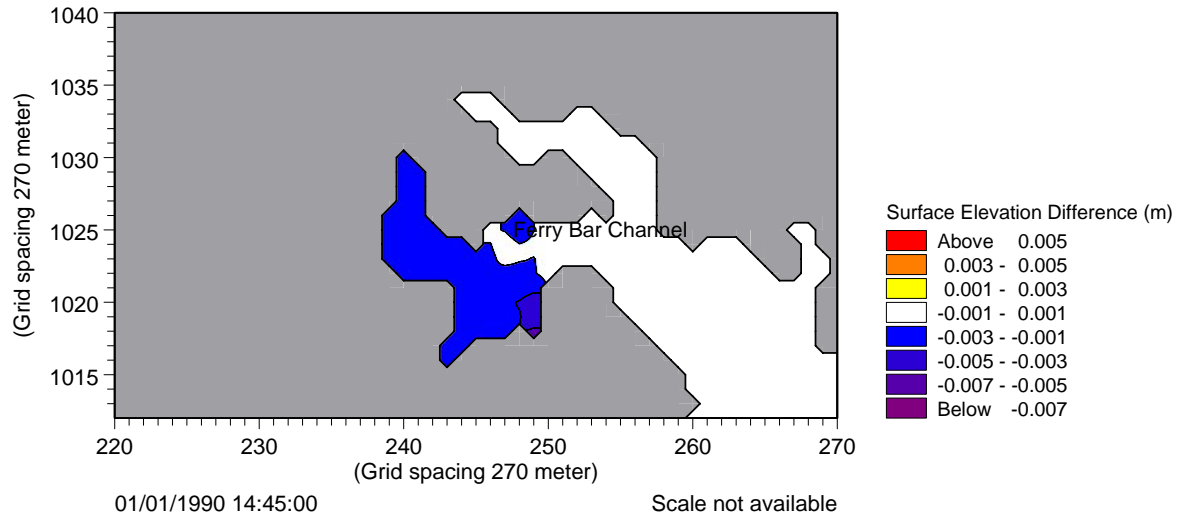


Figure 3.19 Surface Elevation Difference Plot for Hurricane Fran Peak Storm Surge

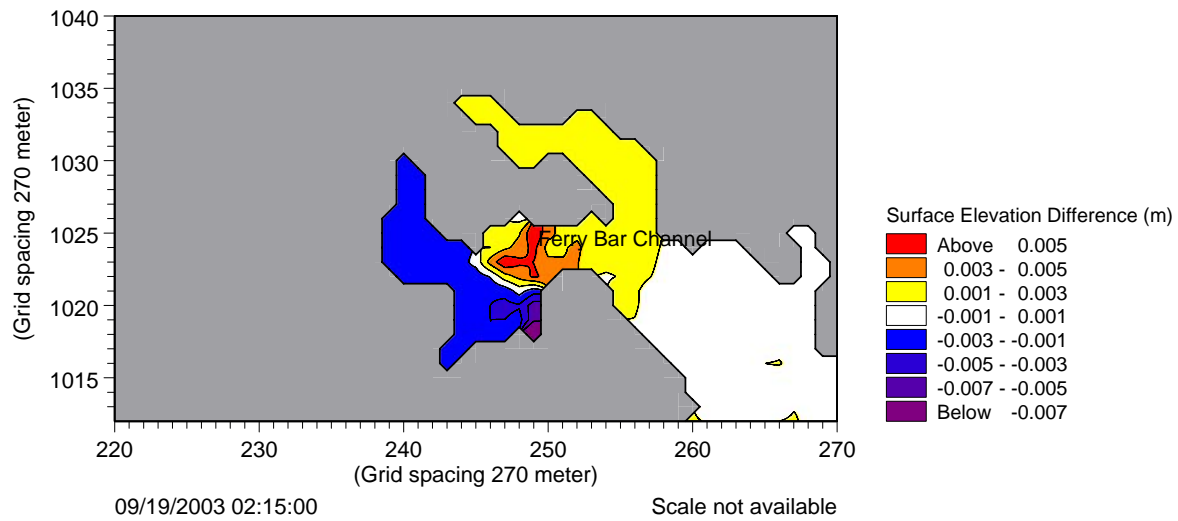


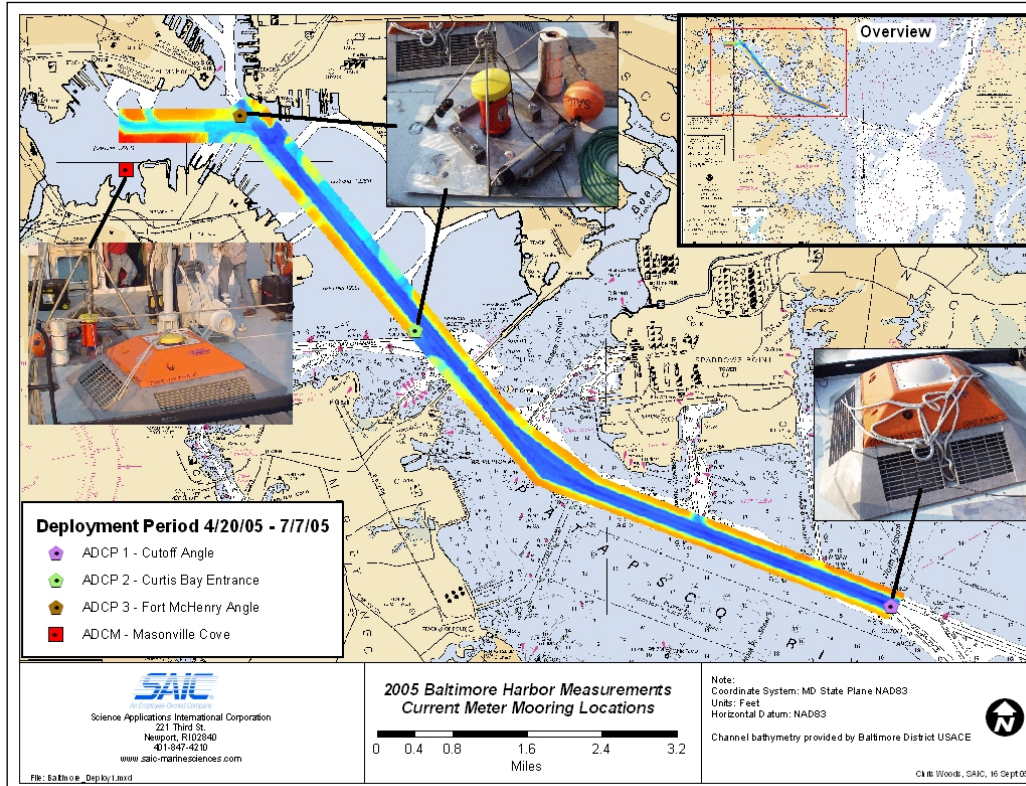
Figure 3.20 Surface Elevation Difference Plot for Hurricane Isabel Peak Storm Surge

ATTACHMENT B.1

DATA REPORT FOR THE 2005 WATER COLUMN MEASUREMENT PROGRAM IN THE PATAPSCO RIVER, BALTIMORE HARBOR

THIS PAGE INTENTIONALLY LEFT BLANK

DATA REPORT FOR THE 2005 WATER COLUMN MEASUREMENT PROGRAM IN THE PATAPSCO RIVER, BALTIMORE HARBOR



Prepared by:
Science Applications International Corporation
Admiral's Gate
221 Third Street
Newport, RI 02840

Prepared for:
Moffatt & Nichol
2700 Lighthouse Point East
Suite 501
Baltimore, MD 21224

September 2005
Contract No: 520820C
SAIC Project No. 01-0440-00-8918-500

SAIC REPORT NO. 695

TABLE OF CONTENTS

1.0	INTRODUCTION & OBJECTIVES.....	1
2.0	METHODS	2
2.1	Oceanographic Mooring Deployment / Recovery	2
2.2	Water-Column Sampling and Underway ADCP Profiling.....	3
2.3	Data Processing	3
3.0	RESULTS	5
3.1	Mooring Results.....	5
3.2	Underway ADCP Results	7
3.3	CTD Profile and Water Sampling Results.....	9
4.0	REFERENCES	12
	TABLES	
	FIGURES	

LIST OF TABLES

- Table 2.0-1. Overview of Field Activities during the 2005 Water Column Measurement Program in the Patapsco River
- Table 3.1-1. Summary current statistics computed during both deployment periods from the Cutoff Angle ADCP data
- Table 3.1-2. Summary current statistics computed during both deployment periods from the Curtis Bay Entrance ADCP data
- Table 3.1-3. Summary current statistics computed during both deployment periods from the Fort McHenry Angle ADCP data
- Table 3.1-4. Summary current statistics computed during both deployment periods from the Masonville Cove ADCM data

LIST OF FIGURES

- Figure 2.1-1 Location of the four current meter moorings within Baltimore Harbor during the 2005 measurement program.
- Figure 2.2-1 Location of the underway ADCP transects and the discrete CTD / water sample stations within Baltimore Harbor during the 2005 measurement program
- Figure 3.1-1 Scatter plots of raw ADCP vector data at each mooring for both deployments providing an indication of the number of useable bins.
- Figure 3.1-2 3-HLP current magnitude time-series from the Cutoff Angle ADCP during the first deployment (4/20 thru 5/26/05).
- Figure 3.1-3 3-HLP current direction time-series from the Cutoff Angle ADCP during the first deployment (4/20 thru 5/26/05).
- Figure 3.1-4 40-HLP current magnitude and direction time-series from the Cutoff Angle ADCP during the first deployment (4/20 thru 5/26/05).
- Figure 3.1-5 3-HLP current magnitude time-series from the Curtis Bay Entrance ADCP during the first deployment (4/20 thru 5/26/05).
- Figure 3.1-6 3-HLP current direction time-series from the Curtis Bay Entrance ADCP during the first deployment (4/20 thru 5/26/05).
- Figure 3.1-7 40-HLP current magnitude and direction time-series from the Curtis Bay Entrance ADCP during the first deployment (4/20 thru 5/26/05).
- Figure 3.1-8 3-HLP current magnitude time-series from the Fort McHenry Angle ADCP during the first deployment (4/21 thru 5/24/05).
- Figure 3.1-9 3-HLP current direction time-series from the Fort McHenry Angle ADCP during the first deployment (4/21 thru 5/24/05).
- Figure 3.1-10 40-HLP current magnitude and direction time-series from the Fort McHenry Angle ADCP during the first deployment (4/21 thru 5/24/05).
- Figure 3.1-11 Near-bottom 3-HLP current magnitude and direction time-series from the Masonville Cove Aquadopp during the first deployment (4/20 thru 5/24/05).
- Figure 3.1-12 3-HLP current magnitude time-series from the Cutoff Angle ADCP during the second deployment (5/27 thru 7/7/05).
- Figure 3.1-13 3-HLP current direction time-series from the Cutoff Angle ADCP during the second deployment (5/27 thru 7/7/05).
- Figure 3.1-14 40-HLP current magnitude and direction time-series from the Cutoff Angle ADCP during the second deployment (5/27 thru 7/7/05).

- Figure 3.1-15 3-HLP current magnitude time-series from the Curtis Bay Entrance ADCP during the second deployment (5/27 thru 7/7/05).
- Figure 3.1-16 3-HLP current direction time-series from the Curtis Bay Entrance ADCP during the second deployment (5/27 thru 7/7/05).
- Figure 3.1-17 40-HLP current magnitude and direction time-series from the Curtis Bay Entrance ADCP during the second deployment (5/27 thru 7/7/05).
- Figure 3.1-18 3-HLP current magnitude time-series from the Fort McHenry Angle ADCP during the second deployment (5/26 thru 7/7/05).
- Figure 3.1-19 3-HLP current direction time-series from the Fort McHenry Angle ADCP during the second deployment (5/26 thru 7/7/05).
- Figure 3.1-20 40-HLP current magnitude and direction time-series from the Fort McHenry Angle ADCP during the second deployment (5/26 thru 7/7/05).
- Figure 3.1-21 Near-bottom 3-HLP current magnitude and direction time-series from the Masonville Cove Aquadopp during the second deployment (5/24 thru 7/7/05).
- Figure 3.2-1 Close-up view of the WinADCP screen depicting the current magnitude and direction along-track contour and profile results from an ADCP transect acquired on 5/25/2005.
- Figure 3.2-2 Indication of the Fort McHenry tidal stage relative to the underway ADCP transects that were conducted on 4/21/05.
- Figure 3.2-3 Current magnitude and direction along-track contour and profile results collected along underway ADCP Transect 1 on 4/21/05
- Figure 3.2-4 Current magnitude and direction along-track contour and profile results collected along underway ADCP Transect 2 on 4/21/05
- Figure 3.2-5 Current magnitude and direction along-track contour and profile results collected along underway ADCP Transect 3 on 4/21/05
- Figure 3.2-6 Current magnitude and direction along-track contour and profile results collected along underway ADCP Transect 4 on 4/21/05
- Figure 3.2-7 Current magnitude and direction along-track contour and profile results collected along underway ADCP Transect 5 on 4/21/05
- Figure 3.2-8 Indication of the Fort McHenry tidal stage relative to the underway ADCP transects that were conducted on 5/25/05.
- Figure 3.2-9 Current magnitude and direction along-track contour and profile results collected along underway ADCP Transect 1 on 5/25/05

- Figure 3.2-10 Current magnitude and direction along-track contour and profile results collected along underway ADCP Transect 2 on 5/25/05
- Figure 3.2-11 Current magnitude and direction along-track contour and profile results collected along underway ADCP Transect 3 on 5/25/05
- Figure 3.2-12 Current magnitude and direction along-track contour and profile results collected along underway ADCP Transect 4 on 5/25/05
- Figure 3.2-13 Current magnitude and direction along-track contour and profile results collected along underway ADCP Transects 5 and 6 on 5/25/05
- Figure 3.3-1 Indication of the Fort McHenry tidal stage relative to the CTD and water sample casts that were collected on 4/21/05
- Figure 3.3-2 Salinity profile results from Stations 2, 3, 4, and 5 for the CTD casts collected on 4/21/05
- Figure 3.3-3 Water temperature profile results from Stations 2, 3, 4, and 5 for the CTD casts collected on 4/21/05
- Figure 3.3-4 Transmissometer profile results from Stations 2, 3, 4, and 5 for the CTD casts collected on 4/21/05
- Figure 3.3-5 Turbidity profile results from Stations 2, 3, 4, and 5 for the CTD casts collected on 4/21/05
- Figure 3.3-6 Turbidity, transmissometer, water temperature, and salinity profile results from Station 1 for the CTD cast collected on 4/21/05
- Figure 3.3-7 Indication of the Fort McHenry tidal stage relative to the CTD and water sample casts that were collected on 5/25/05
- Figure 3.3-8 Salinity profile results from Stations 1, 2, 3, and 5 for the CTD casts collected on 5/25/05
- Figure 3.3-9 Water temperature profile results from Stations 1, 2, 3, and 5 for the CTD casts collected on 5/25/05
- Figure 3.3-10 Transmissometer profile results from Stations 1, 2, 3, and 5 for the CTD casts collected on 5/25/05
- Figure 3.3-11 Turbidity profile results from Stations 1, 2, 3, and 5 for the CTD casts collected on 5/25/05
- Figure 3.3-12 Total Suspended Solids (TSS) versus Turbidity and Transmission from the water samples and CTD profiles collected on 4/21//05
- Figure 3.3-13 Total Suspended Solids (TSS) versus Turbidity and Transmission from the water samples and CTD profiles collected on 5/25/05

1.0 INTRODUCTION & OBJECTIVES

In support of the on-going effort by the Maryland Port Administration (MPA) to identify potential dredged material placement sites needed to support future Port dredging needs, Moffatt & Nichol (M&N) has recently begun a study to investigate possible enhancements to an existing placement site in the vicinity of Masonville Cove along the south shore of the Patapsco River. An initial phase of this study will require M&N to develop a water-column hydrodynamic model that will enable a better assessment of potential water-column impacts in the Harbor due to possible expansion of the existing upland placement site near Masonville Cove.

Due to a lack of existing historical data on currents and other water-column properties within Baltimore Harbor, M&N needed to initiate a field program to acquire water-column boundary condition data within the Harbor that would help to parameterize the model and to assess the model results. Science Applications International Corporation (SAIC) worked with M&N in the early spring 2005 to develop an economical water-column measurement program that would help provide the data to support M&N's hydrodynamic modeling effort. The 2005 measurement program that was developed involved the following sampling techniques and objectives:

- Three upward-looking Acoustic Doppler Current Profiler (ADCP) moorings were deployed on the river bottom in or near the main Baltimore Harbor entrance channel to provide high-resolution water-column current data for at least a sixty-data observation period.
- An Acoustic Doppler Current Meter (ADCM) mooring was also deployed in shallow water near the Masonville Cove site that is being evaluated as part of the dredged material placement study. In addition to near-bottom currents, this mooring provided long-term time-series data on water-level, water temperature, and turbidity.
- During the periods of mooring deployment and servicing operations, an additional two days of water column survey and sampling was conducted. Underway ADCP data were collected along transects run across the channel in the vicinity of each of the moorings. In addition, discrete water column conductivity-temperature-depth (CTD) profiles and water samples were collected periodically throughout the day at each of the mooring sites.

2.0 METHODS

All of the mooring and water column sampling operations conducted under this study were completed during three separate field periods (Table 2.0-1). Initial mooring deployment and the first water column sampling survey occurred from 19 to 21 April 2005. Servicing of the four deployed moorings and the second water column sampling survey occurred from 24 to 27 May 2005. The final mooring recovery operation was conducted from 7 to 8 July 2005. Vessel support for mooring deployment / recovery, underway ADCP surveys, and water column sampling was provided by the State of MD's *R/V Kerhin* and EA Engineering's *R/V Beast* and *R/V Brenda*. Some equipment storage logistical support was also provided at the U.S. Army Corps of Engineers Fort McHenry field facility. Specific details about the main field measurement components of this study are presented below.

2.1 Oceanographic Mooring Deployment / Recovery

SAIC constructed and deployed three (3) bottom-mounted instrument packages for the acquisition of high-resolution water-column current information over an approximately 75-day period from 20 April through 7 July 2005 within the main channel portions of the Patapsco River in Baltimore (Figure 2.1-1 and Table 2.0-1). The eventual mooring locations were selected in consultation with M&N and after due consideration of potential problems associated with interference from deep-draft ships in the channel. Each of the channel mooring packages consisted of an upward-looking 300-kHz RD Instruments (RDI) Workhorse Acoustic Doppler Current Profiler (ADCP). The two inshore ADCP moorings, located just out of the main channel (near the Curtis Bay Entrance and the Fort McHenry Angle), consisted of a weighted low-profile stainless steel-bottom housing. The offshore ADCP mooring, located in the middle of the Cutoff Angle Channel, consisted of a heavily weighted, low-profile, trawl-resistant bottom mount (TRBM) housing (Figure 2.1-1).

In addition to the three in-channel ADCP moorings, a single bottom-mounted current meter mooring was also deployed for the same period at the entrance of the cove near the proposed Masonville site (Figure 2.1-1). This mooring consisted of a Nortek Aquadopp sensor interfaced with a D&A Instruments optical backscatter sensor (OBS) and a WetLabs transmissometer that provided time-series water-column data on currents, temperature, pressure, transmission, and turbidity at a single near-bottom depth (i.e., the mounting height of the instrument above the river bottom).

To minimize potential interference from vessel traffic and/or fishing activity in the area, all of the moorings were deployed without surface representation or up-haul lines. The three ADCP moorings included acoustic releases with recovery floats and lines. The shallow-water Aquadopp mooring was shallow enough that it could be recovered from the surface. Acoustic pingers were also included on all four of the mooring packages to assist with recovery in the event that the releases did not operate properly. Though mooring recovery was impacted somewhat due to bottom suction within the very soft sediments or high sedimentation around the acoustic releases, all of the moorings were successfully recovered as planned.

The ADCPs and the Aquadopp were set to record data in six-minute increments throughout the length of each deployment. Each ADCP six-minute ensemble value was based on a total of 60 acoustic pings at a 4-second interval over a 4-minute sampling period. The ADCPs were able to begin collecting useable data at 2 m above the instrument head in multiple, vertical, one-meter bins. Because the velocities within the depth bins were vertically averaged, the data represented

the velocity at the center of the one-meter bins. The Aquadopp six-minute values were based on a total of 60 samples at a 1-second interval over a 1-minute sampling period.

2.2 Water-Column Sampling and Underway ADCP Profiling

SAIC also conducted two separate one-day water column profiling and sampling surveys during the mooring deployment and servicing periods (Table 2.0-1). During each of these one-day sampling surveys, SAIC acquired underway ADCP data periodically along established transects near the mooring locations (Figure 2.2-1). Three of the five transects were aligned to pass over each of three ADCP moorings. Because of rough sea conditions at Transect 5 during the second survey (5/25/05), a Transect 6 was established in a more protected location further into the harbor for the last two underway iterations. The underway ADCP data was acquired with a pole-mounted, downward-looking RDI 300-kHz ADCP (in water-profiling mode) interfaced with differential GPS (DGPS) and a data acquisition system. To provide some redundant underway ADCP data to assist with QA/QC, a few of the transects were run multiple times (in two directions) during a single iteration.

In conjunction with the underway ADCP operations, periodic vertical conductivity-temperature-depth (CTD) profiles and water samples were collected at selected stations near the mooring locations (Figure 2.2-1). The samplings stations were consistent between both surveys with the exception of Station 4, which was relocated during the second survey from the head of the Ferry Bar Channel to a location near the Aquadopp mooring in Masonville Cove. The CTD profiles were collected with a Seabird SBE-19 CTD profiler interfaced with an optical backscatter sensor and a transmissometer. Water samples were collected at the same locations as the CTD profiles with a one-liter Niskin bottle that was tripped approximately 1 m above the river bottom. All water samples were transferred from the Niskin bottle to storage containers and then stored in coolers until they were ready for transport to the laboratory. Total suspended solids (TSS) analysis of the collected water samples was conducted by M&N through a local laboratory.

During the first survey period only a single sampling vessel was used to conduct both the underway ADCP operations and the CTD profiling survey. Because this limited the total number of samples that could be acquired by each method, we employed a second boat during the second sampling period – one boat was dedicated to CTD profiling and water sampling and the other boat conducted the underway ADCP operations.

2.3 Data Processing

All data from the mooring arrays (primarily currents, but also turbidity, pressure, and temperature for the Aquadopp) were initially run through standard QA/QC processing routines to remove any unreliable data and to interpolate over any short-term periods of questionable data. For the ADCP data, this initial QA/QC review also entailed assessing the number of useable bins based primarily on the quality of the data in the near-surface bins. All current data were initially recorded in earth coordinates as north-south and east-west vector components. Basic processing of the current data included applying a magnetic variation correction to the data, and then calculating a magnitude and direction for each sample.

These data were also run through a series of different low-pass filters (1, 3, and 40-hour). The one- and three-hour filters (1-HLP and 3-HLP) are used to filter out higher-frequency signals and/or noise and help to produce a smoother complete time-series record. The 40-hour filter (40-HLP) is used to help with the evaluation of longer-term trends (e.g., non-tidal) in the data by effectively removing lower-frequency signals (e.g., daily or diurnal) in the data. In addition,

based on the 3-HLP results, overall mean speed and direction and other relevant statistics were also computed for each separate deployment period. For the ADCP data, these computations were made for each useable bin within the full profile. To assist with data interpretation, all of the mooring data were displayed in a wide-range of time-series plots, using both filtered and raw data. Eventually, all of these data were exported in a variety of ASCII formats at differing densities based primarily on the needs of M&N. All of the moored-data processing, analysis, plotting, and exporting were conducted using customized Matlab routines.

The underway ADCP data were processed using standard RDI data processing (VMDas), viewing (WinADCP), and exporting software. The initial processing of the underway ADCP data entailed applying the magnetic variation to the heading data and also selecting the bottom-tracking data as the primary reference for the current magnitude and direction data. In addition, different along-track averaging schemes were examined for generating the processed geo-referenced current profile data. For these datasets, we used both a 10-second and 20-second along-track averaging scheme to produce the final versions of the underway ADCP datasets. In the instances where multiple datasets were acquired along the same transect at the same time, each dataset was processed independently to verify the consistency of the results. To assist with visualization and interpretation of the underway ADCP results, the RDI WinADCP software was used to generate cross-sectional views of each ADCP transect.

Vertical CTD profile data were processed using standard Seabird conversion and processing software. For each of the CTD casts, profile data on water temperature, salinity, turbidity, and transmission were averaged within 1-m bins for the full depth of the cast. These bin-averaged datasets were stored within separate spreadsheet tables and grouped by sampling station. After the laboratory TSS results were obtained, the near-bottom TSS values associated with each of the casts were also included with the CTD data. To assist with data interpretation, all of the vertical profiling results were displayed in a series of plots, depicting all of the results for a particular parameter at each of the sampling stations.

3.0 RESULTS

Though limited historical hydrodynamic data is available for Baltimore Harbor, a rather extensive field measurement program was conducted from late 1978 through late 1979 to help assess potential water quality impacts within the Harbor (Boicourt 1982a). This late-70's measurement program and the subsequent analyses and model formulation effort helped to characterize the complexity of the hydrodynamic structure within the Harbor (Boicourt 1982b). It helped to better characterize the density-driven, three-layer flow within the Harbor and showed that this three-layer circulation often dominates the flow to the point that semi-diurnal tidal current reversals are eliminated.

Though the recently completed 2005 measurement program was much smaller in scope than the late-70s program, the 2005 data do help to fill-in some of the gaps identified in the previous program. Specifically, the 2005 ADCP datasets provide high-resolution current measurements on the full water column that were not available during the previous program; the late-70s program relied on single-point current meter measurements at only a few selected depth intervals. In general, many of the conclusions derived from the late-70s comprehensive study were consistent with the results observed in the datasets acquired during this measurement program

The following results section is primarily intended to provide an overview of the extent of the data acquired and a brief interpretation of some of the results. Most of the results will be presented in a series of figures depicting the data from each of the two deployments and sampling periods. An in-depth interpretation of these results, comparisons with previous study results, and incorporation of additional ancillary environmental data (e.g., winds, fresh-water flow, etc.) is well outside the scope of this basic data measurement effort.

3.1 Mooring Results

Scatter plots of the raw ADCP vector component data were used in conjunction with recorded correlation and echo intensity values at each of the recorded bin-levels to evaluate the number of useable bins at each mooring location (Figure 3.1-1). In most cases, it was quite apparent where the cutoff point should be for shallowest useable bin. Because the Cutoff Angle ADCP was the only instrument deployed within the deeper parts of the channel, this location produced 13 bins of useable data for both deployments. The Curtis Bay Entrance ADCP, deployed in somewhat shallower water, produced nine bins of useable data for both deployments. The Fort McHenry Angle ADCP, deployed in even shallower water, produced five bins of useable data for both deployments.

As discussed in section 2.3, the raw ADCP and ADCM data were run through various low-pass filters to smooth the records and to evaluate longer-term trends in the data. Based primarily on the 3-HLP filtered data, summary statistics were computed at each mooring location for each bin-level over both deployments (Tables 3.1-1 thru 3.1-3). In addition, a series of time-series plots were generated based on the raw, 3-HLP, and 40-HLP datasets for each mooring during both deployments. In this report, we have provided 3-HLP time-series plots and 40-HLP stick plots for each dataset (Figure 3.1-2 thru 3.1-21). While the 3-HLP plots essentially provided a short-term averaged view of the raw data, the 40-HLP plots provided an indication of longer term trends in the net flow at different levels in the water-column.

At the Cutoff Angle ADCP, a maximum 3-HLP current magnitude of 70.9 cm/sec was observed in the mid-water column during the first deployment (Table 3.1-1). During this deployment, the

highest 3-HLP mean magnitudes of around 17 cm/sec were also found in the mid-water column. The lowest mean and maximum current magnitudes were found at the two near-surface bins. During the second deployment, both maximum and mean 3-HLP current magnitudes were consistently lower than during the first deployment; a maximum 3-HLP current magnitude of 51.4 cm/sec was observed in the mid-water column. The mid-water column mean 3-HLP current magnitudes during the second deployment were around 13 cm/sec. At the two near-surface bins, maximum and mean current magnitudes were very similar during both deployments. As expected, the orientation of the principal axis showed that the primary direction of flow was focused along the same alignment as the main navigation channel. The ratio between the 40-HLP and 3-HLP variances provided an indication of how much of the signal variability was attributable to high- and low-frequency sources. The lower ratios observed in the two near-surface bins was reflective of the influence of the higher-frequency semi-diurnal tidal signal that was primarily confined to these two bins. This was also reflected in the time-series 3-HLP current-direction plot that showed the tidal signal primarily confined to the two surface bins (Figure 3.1-1).

At the Curtis Bay Entrance ADCP, a maximum 3-HLP current magnitude of 30.6 cm/sec was observed in the mid-water column during the first deployment (Table 3.1-2). During this deployment, the 3-HLP mean magnitudes varied from about 4 to 7 cm/sec, with only slightly higher values noted in the mid-water column. The lowest mean and maximum current magnitudes were found at lowest bin, though the differences between any of the records were negligible. During the second deployment at this site, both maximum and mean 3-HLP current magnitudes were generally consistent with values observed during the first deployment. The mean 3-HLP current magnitudes during the second deployment again varied from about 4 to 7 cm/sec, with the lowest mean values found in the lower water column. A maximum 3-HLP current magnitude of 33.6 cm/sec was observed in the mid-water column. The orientation of the principal axis again showed that the primary direction of flow was focused along the same alignment as the main navigation channel. The 40-HLP and 3-HLP variance ratio indicated a less pronounced semi-diurnal signal at any particular bins in the water column.

At the Fort McHenry Angle ADCP, a maximum 3-HLP current magnitude of 21.8 cm/sec was observed in the lower water column during the first deployment (Table 3.1-3); an only slightly lower value of 20.8 cm/sec was in the near-surface bin. During this deployment, the 3-HLP mean magnitudes varied from about 4 to 7 cm/sec, with only slightly higher values noted in the lower water column. In general, the differences in the computed mean and maximum current magnitudes between any of the bin levels were negligible. During the second deployment at this site, both maximum and mean 3-HLP current magnitudes were generally consistent with values observed during the first deployment. The mean 3-HLP current magnitudes during the second deployment again varied from about 4 to 5 cm/sec. A maximum 3-HLP current magnitude of 18.7 cm/sec was observed in the upper water column. The orientation of the principal axis again showed that the primary direction of flow was focused along the same alignment as the main navigation channel. The 40-HLP and 3-HLP variance ratio indicated a less pronounced semi-diurnal signal at any particular bins in the water column.

As these results indicate, the maximum and mean current magnitudes were consistently higher at the Cutoff Angle mooring, in comparison to either the Curtis Bay or Fort McHenry locations. Mean current magnitudes were similar between Curtis Bay and Fort McHenry, though the Curtis Bay ADCP did record somewhat higher maximum current magnitudes. As mentioned previously, both the Curtis Bay and Fort McHenry ADCPs were located just outside the main navigation channel in somewhat shallower water. With just the mooring data, it was difficult to evaluate

whether the lower current magnitudes were primarily a function of the mooring location relative to the channel or to the overall location of the mooring within the Harbor. The supplemental underway ADCP data (see Section 3.2 below) provided some additional insight into these observed differences in current magnitude.

The internally-recording Aquadopp ADCM sensor deployed in Masonville Cove provided data on currents, water temperature, and turbidity at a depth approximately 0.5 m above the river bottom. Basic processing of the current data included calculating a magnitude and direction for each sample as well as a mean and maximum speed (Table 3.1-4). The computed 3-HLP mean and maximum current magnitude results were very similar between both deployments at the Masonville Cove site. The maximum observed current magnitude during both deployments was around 11.5 cm/sec and the mean current magnitude was around 4 cm/sec. Both the computed maximum and mean current magnitude values were somewhat lower at the Masonville site in comparison to the computed values from the Fort McHenry Angle ADCP. These differences were more pronounced during the first deployment, when the Fort McHenry Angle site experienced somewhat higher mean and maximum current magnitudes.

The time-series data on water temperature, turbidity, and pressure provided an indication of general water-column trends during the two deployment periods (Figures 3.1-11 and 3.1-21). The pressure data during both deployment periods was reflective of the semi-diurnal tides; these data were very similar to the observed tide data from the primary NOAA tide station at Fort McHenry. The water-temperature data showed generally increasing or steady temperatures throughout the period, with a couple of periods of relatively sharp increases. From around 9 May to 13 May, the water temperature increased from a low of around 12°C up to a 20°C; these represented the lowest and highest temperature observed over the entire 34-day first deployment period. During the second deployment period, from around 31 May until 15 June, there was a more gradual, though steady, increase in temperature from around 16°C up to around 24°C .

Though there were some minor fluctuations in the Aquadopp turbidity data during the first half of both deployments, the observed turbidity values were generally consistently low during these early periods. During the first deployment, turbidity values varied from around 8 to 20 NTUs until after 12 May or so, when the values began to slowly and fairly consistently rise. Though some of this increase was likely due to actual water-column conditions (particularly the periodic steeper increases), much of it was also undoubtedly due to increasing marine growth on the OBS sensor. The period of increasing turbidity values also coincided with the period when water temperatures began to rise. Upon recovery after the first deployment, the OBS sensor was covered with a thin layer of biofouling. During the second deployment, the likely marine growth impact on turbidity happened much quicker and was far more extensive. For the first week or so, turbidity values remained below 20 NTUs, and then gradually increased up to around 100 NTUs through the first 10 days of June. From around 10 June until 17 June, the turbidity rapidly increased until it peaked at the measurement limit of the sensor (around 2000 NTUs). Again, this increase coincided with a steady increase in water temperature and was likely a result of rapidly increasing marine growth on the sensor. Upon recovery after the second deployment, the OBS sensor was thoroughly covered with biofouling, including extensive barnacle coverage.

3.2 Underway ADCP Results

As discussed in Section 2.2, underway ADCP data was acquired along pre-selected transects in conjunction with water-sampling operations that were conducted during each of the two mooring-deployment periods. The data were first processed in VMDas to determine the number of useable bins, to apply the magnetic variation, and to conduct along-track averaging. The processed

transects were then visualized and further analyzed within WinADCP. A close-up view of a WinADCP transect has been provided to illustrate the contents of the screens that will be provided subsequently for each of the datasets (Figure 3.2-1). The top panel of this screen provides a color contour view of the current magnitude across the entire length of the transect for the full water-profile depth. The acoustically detected river bottom is also indicated below the last useable bins of current-profile data. The bottom panel of the screen shows the along-track profile view of current magnitude and current direction for three selected bins (e.g., upper, mid-, and lower water column). Because mostly shallow water depths prevail outside the navigation channels in the Harbor, the mid and lower water-column profiles generally extended only across the main channel portions of each transect.

During the first sampling day (4/21/05), two underway ADCP datasets were obtained along each transect over the course of the sampling period (Figure 3.2-2). The first series of transects were collected during the mid-phase of an ebb tide and the second series of transects began just after the low tide and ran through the middle part of the following flood tide. During this period, the underway ADCP results were generally consistent with the stage of the tide (Figures 3.2-3 thru 3.2-7). For Transects 1 and 2, across the inner portions of the Fort McHenry Channel, the currents were weak (around 10 cm/sec) and variable throughout most of the water column (Figures 3.2-3 and 3.2-4). Transect 1A showed general outward flow and Transect 2B showed general inward flow, consistent with the stage of tide; Transects 1B and 2A showed a more mixed flow. For Transect 3, across the inner portions of the Curtis Bay Channel, the flow was more clearly split between the upper and lower water column, though the magnitude was still weak (Figure 3.2-5). Transect 3A showed the mid- and lower water column flowing outward (or towards the east) while upper water column flow was inward; approximately six hours later during Transect 3B, the conditions were reversed, with the mid- and lower water column flowing inward and the upper water column flowing out.

Transect 4, aligned over the Fort McHenry Channel and the entrance to the Curtis Bay Channel, also showed low magnitude and split flow, though not the same reversal seen along Transect 3 (Figure 3.2-6). Transect 4A showed the lower and upper water column generally flowing outward, while the mid-water column flowed inward; during Transect 4B, the mid- and lower water column were flowing inward while the upper water column continued to flow outward. Transect 5, aligned over the Cutoff Angle Channel, also showed weak and split flow, though at this station the upper water-column magnitudes were somewhat higher, particularly to the south of the channel (Figure 3.2-7). Transect 5A showed the mid- and lower water column flowing inward, while the upper water column flowed outward.

During the second deployment water-column sampling day (5/25/05), three underway ADCP datasets were obtained along each transect over the course of the sampling period (Figure 3.2-8). The first series of transects was collected just after high tide during the first part of the ebb, the second series was collected during the last part of the ebb, and the third series were collected during the mid-phase of the following flood tide. In comparison with the first underway sampling period, the results during this period showed some noticeably stronger current magnitudes, particularly in the mid-water column at the outer sampling locations (Transects 4, 5, and 6). With the exception of Transect 3, aligned across the Curtis Bay Channel, all of the transects occupied during this period showed the mid- and lower water column flowing inward, regardless of the tidal stage (Figures 3.2-9 thru 3.2-13).

This consistent inward flow was particularly evident in Transects 4A, 4B, and 4C, where a strong pulse of inward-flowing water was clearly seen in the lower to mid-water column; the highest

magnitudes of over 50 cm/sec (flowing inward) were recorded during Transect 4B, towards the end of the ebb (Figure 3.2-12)). This pulse of relatively strong inward-flowing water was confined to the deeper waters of the Fort McHenry Channel, with no indications of a similar flow in the adjacent Curtis Bay Channel. The near-surface currents were much weaker over these transects, and flowed either outward or to the south. A similar flow pattern was also observed over Transects 5 and 6, located further outside the Harbor across the Cutoff Angle or Brewerton Channel. Transects 5A, 6B, and 6C showed the mid- and lower water column flowing consistently inward, with peak magnitudes approaching 50 cm/sec (Figure 3.2-13). Over each of these same three transects the near-surface flow was weaker and consistently towards the south. This southerly upper-water-column flow was likely a surface response to the relatively strong northerly winds that were blowing that day.

For Transect 3, across the inner portions of the Curtis Bay Channel, the flow was generally weak and variable during most of the period (Figure 3.2-11). On Transect 3A there were some indications of a somewhat higher-magnitude inward flow in the mid-water column. For Transects 1 and 2, across the inner portions of the Fort McHenry Channel, the currents were generally weak (around 10 cm/sec) throughout most of the water column (Figures 3.2-9 and 3.2-10). During Transects 1A and 2A there were some current magnitudes greater than 25 cm/sec focused in the mid-water column. The mid and lower water-column flow were consistently inward during the period, and the near-surface flow was more variable.

Though the underway ADCP transects were not of a sufficient temporal or spatial density to enable cross-section water-mass flow analysis, they did provide a useful qualitative dataset to help characterize the current flow in the Harbor (at least during the two days of measurements). During these periods, the underway ADCP datasets clearly indicated that the highest current magnitudes were confined to the mid-water column within the main channel areas. This result does have an impact on the interpretation of the results from the moored ADCP datasets. It seems likely that the higher mean and maximum current magnitudes measured at the Cutoff Angle ADCP were mostly a function of its placement within the main channel, as opposed to both the Curtis Bay Entrance and Fort McHenry Angle ADCPs that were placed in somewhat shallower waters adjacent to the channel edge. Based on the consistently higher mid-depth current magnitudes measured in the Fort McHenry Channel (very near to the Curtis Bay Entrance ADCP) during the second underway ADCP survey, it seems likely that this area would experience currents similar to those observed at the Cutoff Angle. During both of the underway surveys, the currents outside of the channels were mostly weak and variable, and far more influenced by the semi-diurnal tides and the surface winds.

3.3 CTD Profile and Water Sampling Results

As discussed in Section 2.2, in conjunction with the underway ADCP operations, periodic CTD profiles and water samples were collected at selected stations near the mooring locations (Figure 2.2-1). The sampling stations were consistent between both surveys with the exception of Station 4, which was relocated during the second survey from the Ferry Bar Channel to a location near the Aquadopp mooring in Masonville Cove. During the first survey, two profiles were collected at most stations and during the second survey up to five casts were collected per station. For each of the CTD casts, profile data on water temperature, salinity, turbidity, and transmission were averaged within 1-m bins for the full depth of the cast. These bin-averaged datasets were stored within separate spreadsheet tables and grouped by sampling station. After the laboratory TSS results were obtained, the near-bottom TSS values associated with each of the casts were also

included with the CTD data. To assist with data interpretation, all of the vertical-profiling results were displayed in a series of plots, depicting all of the results for a particular parameter at each of the sampling stations (Figures 3.3-1 through 3.3-11). In addition, visual comparisons were made between the laboratory-derived total suspended solids (TSS) results from the water samples and the observed transmissometer and optical backscatter results from the vertical CTD casts (Figures 3.3-12 and 3.3-13).

During the first sampling day (4/21/05), two series of vertical profile data were obtained at each sampling station (except Station 1) over the course of the sampling period (Figure 3.3-1). The first series of vertical profiles were collected during the later phase of an ebb tide and the second series of profiles were collected during the later phases of the following flood tide. In general, the vertical CTD cast results observed during this period were quite variable and difficult to interpret given the spatial and temporal spacing of the data (Figures 3.3-2 thru 3.3-6). The salinity and water-temperature profiles varied greatly between the two sampling periods, and seemed to indicate the introduction of a cold, fresh, and denser layer during the second sampling period in conjunction with the incoming tide (Figure 3.3-2 and 3.3-3). At three of the four afternoon sampling stations there was a prominent salinity drop at around the 3 to 5-m depth, and at the fourth station (Station 3 near the Fort McHenry Angle), the salinity was low throughout the profile. Though we did not attempt to retrieve any ancillary water flow or rainfall data from this period, we know that there had been heavy rainfall in this area in advance of the sampling period, and we suspect that there was a significant inflow of freshwater into the Chesapeake Bay (and the Patapsco River).

The transmission results collected during these two sampling periods were similar, though the optical backscatter results indicated a noticeable increase in the turbidity during the second set of profiles (Figures 3.3-4 and 3.3-5). Visually, the water had a brownish-yellowish color and appeared very turbid during this sampling period; it was difficult to see any of the sampling instruments even a few centimeters below the water surface. The water clarity actually appeared better further up the Patapsco River and in the vicinity of Masonville Cove. We suspect that this off-color water may have been a result of the high freshwater inflow during this period. Based on the relatively low laboratory TSS results obtained during this period, it did not appear that the high turbidity was due solely to suspended sediment concentrations (Figure 3.3-12). During this sampling period, the transmissometer data showed a much stronger correlation with the TSS data than the optical backscatter data.

During the second sampling day (5/25/05), five sets of vertical-profile data were obtained at Stations 2 thru 5 and three sets of profile data were obtained at Station 1 over the course of the sampling period (Figure 3.3-7). The first series of vertical profiles were collected at the start of an ebb tide and the final series of profiles were collected during the later stages of the following flood tide. During this survey, Station 4 was relocated to the vicinity of the Masonville Aquadopp mooring, so that the vertical profile extended downward for only 2 m. The results for Station 4 have not been included in the following sets of figures (Figures 3.3-8 thru 3.3-11). In general, the vertical CTD cast results observed during this period were far more coherent and predictable than those seen during the first sampling period. The salinity profiles were still quite variable between sampling periods, and there were indications of both a stratified and well-mixed salinity profile depending on the station and the timing of the cast (Figure 3.3-8). The water temperature profiles were fairly consistent at each station, with some differences noted in the depth of the thermocline and the slope of the temperature gradient below the thermocline (Figure 3.3-9).

The transmission results collected during this sampling period were quite consistent at each station, with the exception of Station 3 (at the Fort McHenry Angle) which showed somewhat greater variability (Figure 3.3-10). Stations 1, 2, and 3 showed a general decrease in transmission with depth, while Station 5 (in Curtis Bay) showed an improvement in transmission with depth. Unlike the transmission results, the optical backscatter results showed a relatively consistent turbidity profile with little change noted throughout the depth of the cast (Figure 3.3-11). Though most of the TSS samples collected during this period were low, there were five samples that showed TSS values above 100 mg/L (Figure 3.3-13). In some cases, these elevated TSS values might have been due to locally resuspended sediment that was caused by the CTD profiler impacting the seafloor before the water sample was collected. The validity of these somewhat elevated TSS results has a big impact on the evaluation of the correlation between TSS and both the optical backscatter and transmissometer data.

4.0 REFERENCES

Boicourt, W. and Olson, P. 1982. A Hydrodynamic Study of the Baltimore Harbor System: Observations on the Circulation and Mixing in Baltimore Harbor. Chesapeake Bay Institute. Reference 82-10, Bulletin 1.

Boicourt, W. and Olson, P. 1982. A Hydrodynamic Study of the Baltimore Harbor System: A Numerical Model of Baltimore Harbor Circulation. Chesapeake Bay Institute. Reference 82-11, Bulletin 2.

TABLES

Table 2.0-1. Overview of Field Activities During the 2005 Water Column Measurement Program in the Patapsco River/ Baltimore Harbor

Date	Daily Activity Type	Daily Operations Overview
4/17/2005	Mob	Prepare mooring and sampling gear for transport from Newport to Baltimore
4/18/2005	Travel / Mob	Transport mooring and sampling equipment to Baltimore via box truck and begin local mob
4/19/2005	Mob	Conduct equipment mob and testing on the <i>R/V Kerhin</i> alongside the pier at Sandy Point Park
4/20/2005	Deploy	Deploy Cutoff Angle and Curtis Creek ADCP moorings and Masonville Cove Aquadopp mooring from the <i>R/V Kerhin</i>
4/21/2005	Sample / Survey / Deploy	Conduct underway ADCP surveying, along with CTD water-column profiling and water sampling from the <i>R/V Brenda</i> ; deploy the Fort McHenry ADCP mooring after completing the underway sampling.
4/22/2005	Travel / Demob	Store sampling equipment at USACE facility in Baltimore; travel back to Newport
5/23/2005	Travel / Mob	Transport personnel and equipment to Baltimore and begin local mob
5/24/2005	Recover / Deploy	Recover the Masonville Cove Aquadopp and the Fort McHenry ADCP from the <i>R/V Beast</i> Redeploy the Masonville Cove Aquadopp after servicing
5/25/2005	Sample / Survey	Conduct underway ADCP surveying, along with CTD water-column profiling and water sampling from the <i>R/V Brenda</i> and the <i>R/V Beast</i>
5/26/2005	Deploy / Recover	Redeploy the Fort McHenry ADCP mooring from the <i>R/V Beast</i> (AM); recover the Cutoff Angle and Curtis Creek ADCP moorings from the <i>R/V Kerhin</i> (PM)
5/27/2005	Deploy / Demob	Redeploy Cutoff Angle and Curtis Creek ADCP moorings from the <i>R/V Kerhin</i>
5/28/2005	Travel / Demob	Store sampling equipment at USACE facility in Baltimore; travel back to Newport
7/6/2005	Travel / Mob	Transport personnel and equipment to Baltimore and begin local mob
7/7/2005	Recover	Recover the Masonville Cove Aquadopp and the Fort McHenry, Curtis Creek, and Cutoff Angle ADCPs from the <i>R/V Kerhin</i>
7/8/2005	Demob	Demob all mooring gear on the <i>R/V Kerhin</i> alongside at Sandy Point Park
7/9/2005	Travel / Demob	Transport mooring equipment back to Newport via leased box truck
7/10/2005	Demob	Unload truck and begin equipment demob at local warehouse facility
7/11/2005	Demob	Complete local demob and return leased gear to vendors

Table 3.1-1. Summary current statistics computed during both deployment periods from the Cutoff Angle ADCP data

Summary Current Statistics - Cutoff Angle ADCP								
(Approximate Water Depth - 16 m)								
Bin #	Approx Depth (m)	St.Dev. (3-HLP)	St.Dev. (40-HLP)	Ratio Var(40-HLP) / Var(3-HLP)	Current Magnitude			Orientation of Principal axis °True, (3-HLP)
					Max (3-HLP) (cm/sec)	Min (3-HLP) (cm/sec)	Mean (3-HLP) (cm/sec)	
Deployment 1: 4/19/2005 - 5/26/2005								
1	13	8.4	7.0	0.7	43.7	0.1	11.5	295.8
2	12	9.1	7.8	0.7	53.8	0.2	12.7	306.9
3	11	9.9	8.7	0.8	62.7	0.2	14.0	306.8
4	10	10.9	9.8	0.8	61.0	0.6	15.3	305.6
5	9	11.2	10.2	0.8	69.7	0.1	16.5	304.4
6	8	11.3	10.1	0.8	70.9	0.1	17.4	303.6
7	7	11.3	9.6	0.7	61.6	0.5	17.7	303.3
8	6	10.9	8.7	0.6	57.0	0.3	17.2	302.2
9	5	10.1	7.8	0.6	61.9	0.2	15.9	303.2
10	4	8.8	6.7	0.6	51.8	0.1	13.3	307.5
11	3	6.9	4.3	0.4	44.3	0.3	10.4	315.4
12	2	5.1	2.5	0.2	29.0	0.2	9.3	322.5
13	1	4.8	2.1	0.2	25.0	0.1	9.8	316.3
Deployment 2: 5/27/2005 - 7/7/2005								
1	13	6.6	5.1	0.6	30.5	0.1	8.7	300.4
2	12	6.9	5.6	0.7	31.4	0.3	9.7	310.3
3	11	7.3	6.3	0.7	33.6	0.2	10.9	309.3
4	10	7.8	7.0	0.8	38.5	0.4	12.0	308.8
5	9	8.5	7.3	0.7	47.9	0.2	12.7	308.2
6	8	9.0	7.3	0.7	49.2	0.3	13.1	307.8
7	7	9.1	7.0	0.6	51.4	0.2	13.2	307.4
8	6	8.5	6.7	0.6	49.8	0.4	13.0	305.3
9	5	7.6	6.2	0.7	50.0	0.3	11.9	307.4
10	4	6.1	4.9	0.6	38.0	0.3	10.2	313.1
11	3	4.9	3.1	0.4	27.3	0.7	9.2	320.9
12	2	4.7	2.3	0.2	23.9	0.7	9.4	322.3
13	1	4.7	2.2	0.2	24.8	0.2	9.1	317.2

Table 3.1-2. Summary current statistics computed during both deployment periods from the Curtis Bay Entrance ADCP data

Summary Current Statistics - Curtis Bay Entrance ADCP (Approximate Water Depth - 12 m)								
Bin #	Approx Depth (m)	St.Dev. (3-HLP)	St.Dev. (40-HLP)	Ratio Var (40-HLP) / Var (3-HLP)	Current Magnitude			Orientation of Principal axis °True, (3-HLP)
					Max (3-HLP) (cm/sec)	Min (3-HLP) (cm/sec)	Mean (3-HLP) (cm/sec)	
Deployment 1: 4/19/2005 - 5/26/2005								
1	9	3.9	2.6	0.4	24.6	0.1	4.1	351.7
2	8	4.9	3.3	0.5	27.6	0.1	5.4	345.2
3	7	5.2	3.8	0.5	30.2	0.0	6.4	337.8
4	6	5.1	3.9	0.6	26.6	0.1	7.1	336.2
5	5	4.7	3.6	0.6	28.4	0.2	7.2	335.0
6	4	4.2	3.2	0.6	30.6	0.5	6.5	328.7
7	3	3.5	2.4	0.5	19.2	0.1	5.6	320.7
8	2	3.6	2.1	0.3	23.5	0.4	5.1	319.9
9	1	4.5	3.2	0.5	25.6	0.3	6.4	323.6
Deployment 2: 5/27/2005 - 7/7/2005								
1	9	3.4	2.0	0.3	23.5	0.0	4.0	348.9
2	8	3.8	2.7	0.5	25.4	0.1	4.5	348.2
3	7	4.3	3.3	0.6	32.9	0.0	5.1	341.7
4	6	4.6	3.6	0.6	33.6	0.1	5.7	337.5
5	5	4.0	3.2	0.6	26.7	0.4	5.8	334.5
6	4	3.1	2.2	0.5	18.1	0.0	5.3	327.0
7	3	2.5	1.3	0.3	14.0	0.1	4.7	328.5
8	2	3.1	2.0	0.4	18.1	0.1	5.0	335.4
9	1	4.1	3.2	0.6	23.0	0.1	6.8	331.6

Table 3.1-3. Summary current statistics computed during both deployment periods from the Fort McHenry Angle ADCP data

Summary Current Statistics - Fort McHenry Angle ADCP (Approximate Water Depth - 9 m)								
Bin #	Approx Depth (m)	St.Dev. (3-HLP)	St.Dev. (40-HLP)	Ratio Var(40-HLP) / Var(3-HLP)	Current Magnitude			Orientation of Principal axis °True, (3-HLP)
					Max (3-HLP) (cm/sec)	Min (3-HLP) (cm/sec)	Mean (3-HLP) (cm/sec)	
Deployment 1: 4/22/2005 - 5/24/2005								
1	5	4.5	3.5	0.6	21.8	0.2	7.3	327.6
2	4	4.1	3.3	0.6	20	0.1	6.7	340.1
3	3	3.3	2.7	0.7	18.4	0.3	5.6	331.7
4	2	2.9	1.8	0.4	16.1	0.1	4.8	325.5
5	1	3.5	2.3	0.4	20.8	0.1	5.4	332.2
Deployment 2: 5/26/2005 - 7/7/2005								
1	5	3.1	2.4	0.6	17.8	0.2	5	321.2
2	4	2.9	2.2	0.6	14.8	0.2	4.7	325.4
3	3	2.7	1.8	0.4	16.7	0.1	4.4	321.8
4	2	2.8	1.6	0.3	18.7	0.1	4.4	320.7
5	1	3.6	1.9	0.3	18.2	0.5	5.3	324.6

Table 3.1-4. Summary current statistics computed during both deployment periods from the Masonville Cove ADCM data

Summary Current Statistics - Masonville Cove ADCM (Approximate Water Depth - 3 m)								
Bin #	Approx Depth (m)	St.Dev. (3-HLP)	St.Dev. (40-HLP)	Ratio Var(40-HLP) / Var(3-HLP)	Current Magnitude			Orientation of Principal axis °True, (3-HLP)
					Max (3-HLP) (cm/sec)	Min (3-HLP) (cm/sec)	Mean (3-HLP) (cm/sec)	
Deployment 1: 4/20/2005 - 5/24/2005								
1	2.5	2	1	0.26	11.6	0.1	4	355.4
Deployment 2: 5/24/2005 - 7/7/2005								
1	2.5	1.9	0.9	0.24	11.7	0.1	3.7	0.5

FIGURES

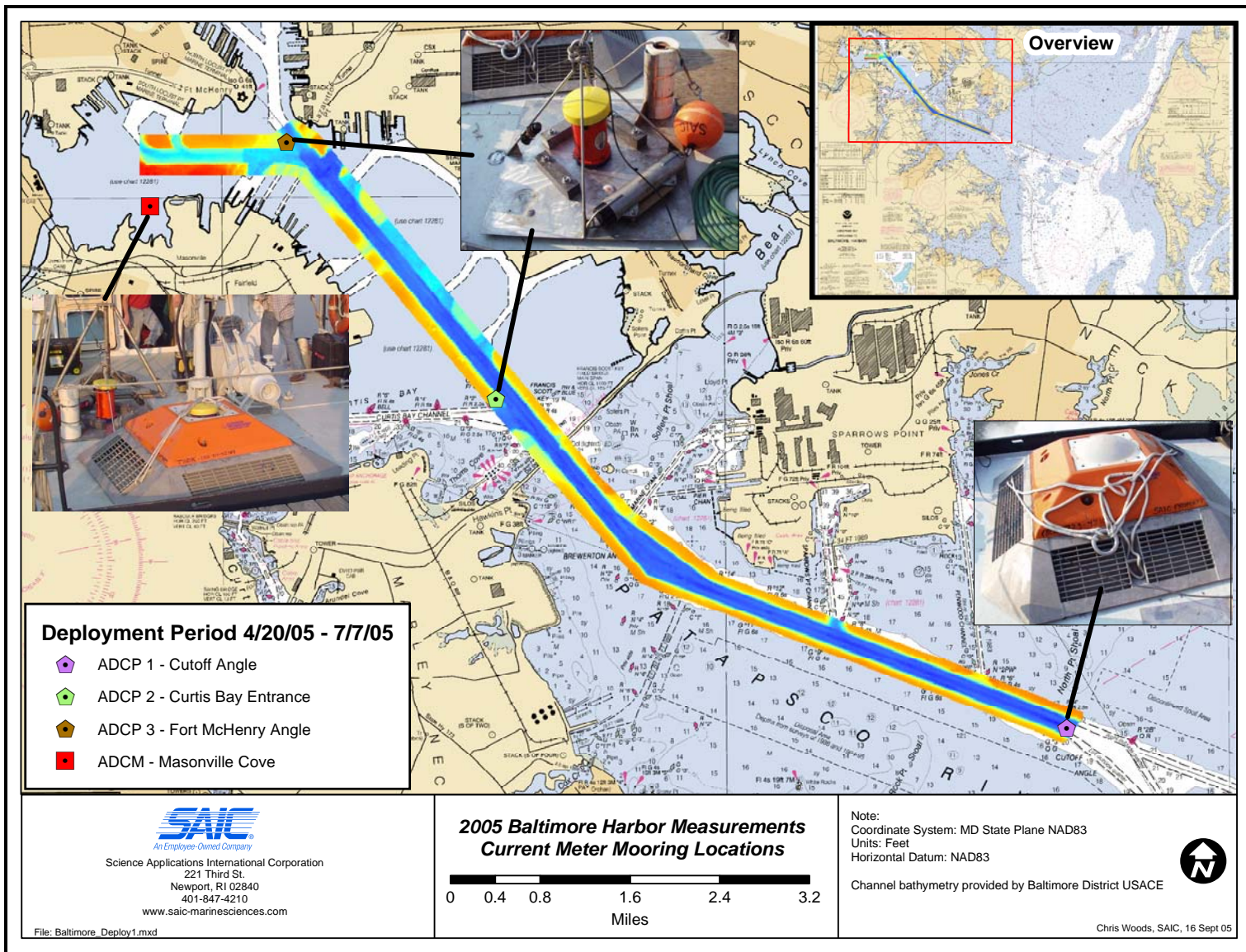


Figure 2.1-1. Location of the four current meter moorings within Baltimore Harbor during the 2005 measurement program.

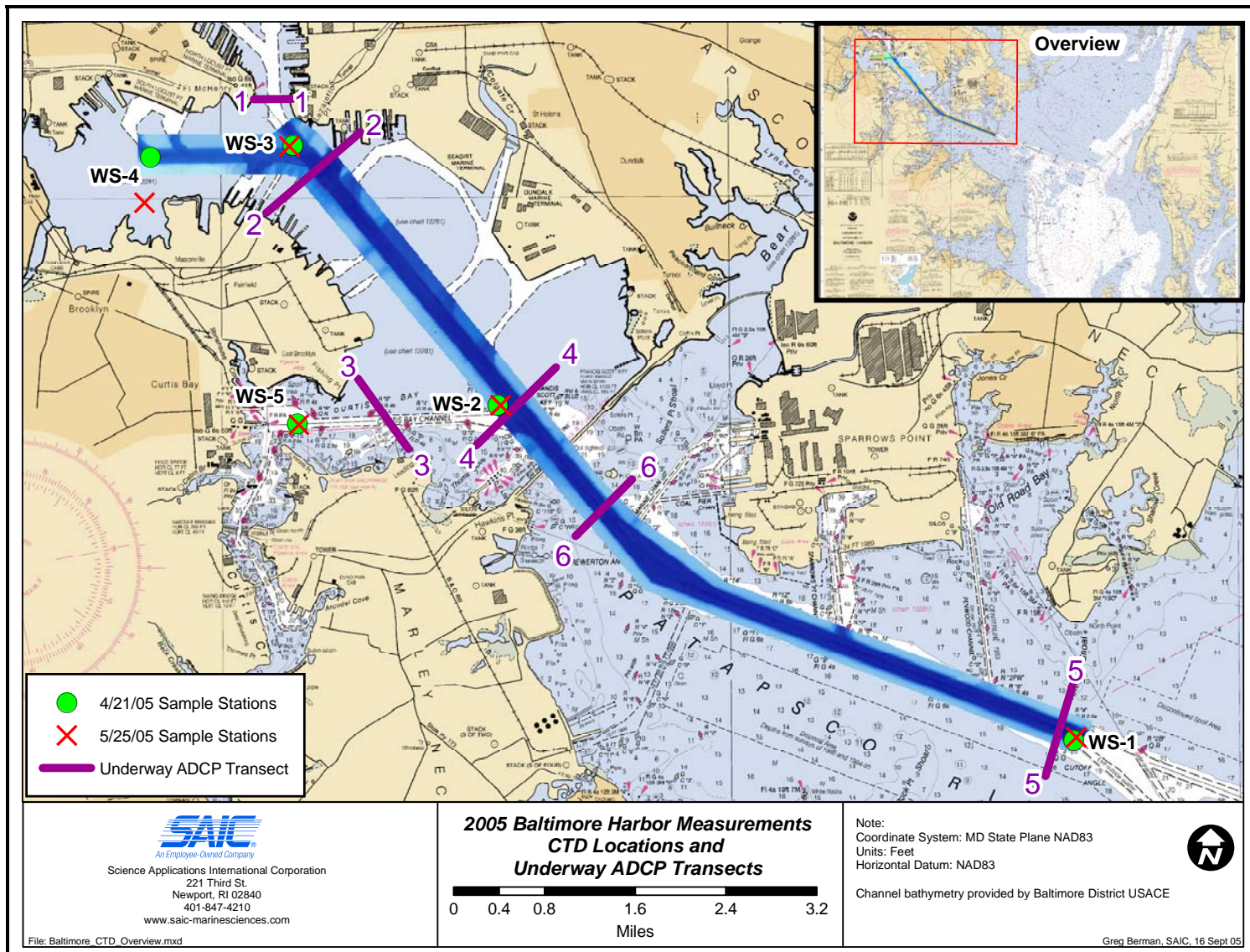


Figure 2.2-1. Location of the underway ADCP transects and the discrete CTD / water sample stations within Baltimore Harbor during the 2005 measurement program

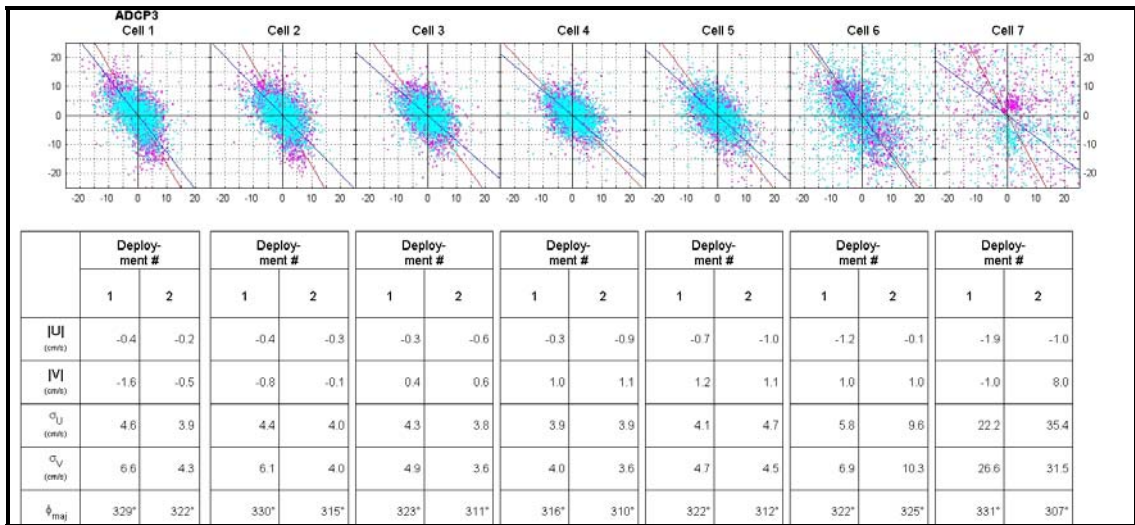
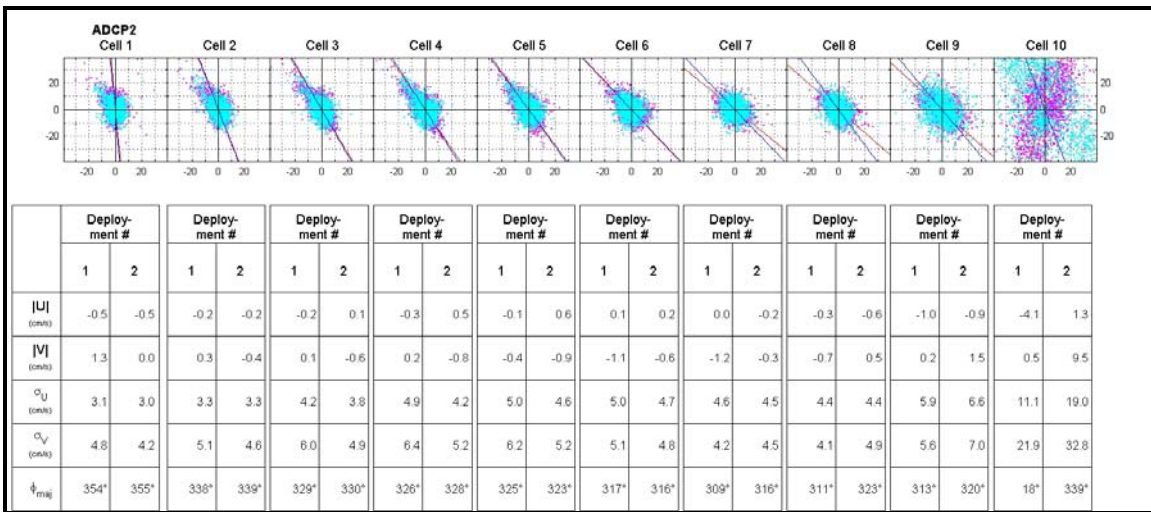
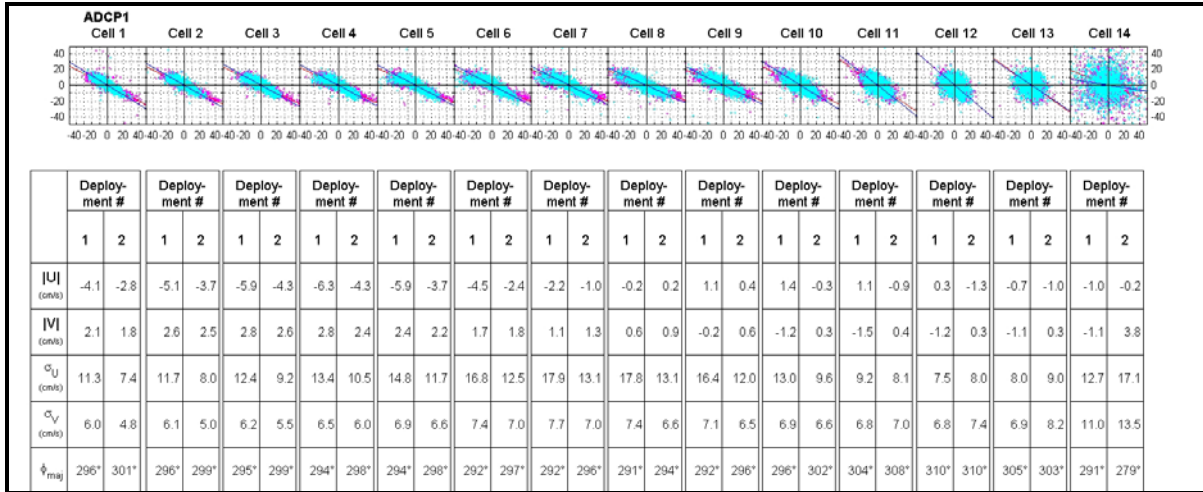


Figure 3.1-1. Scatter plots of raw ADCP vector data at each mooring for both deployments providing an indication of the number of useable bins. Top Panel – Cutoff Angle ADCP; Middle Panel – Curtis Bay Entrance ADCP; Bottom Panel – Fort McHenry Angle ADCP.

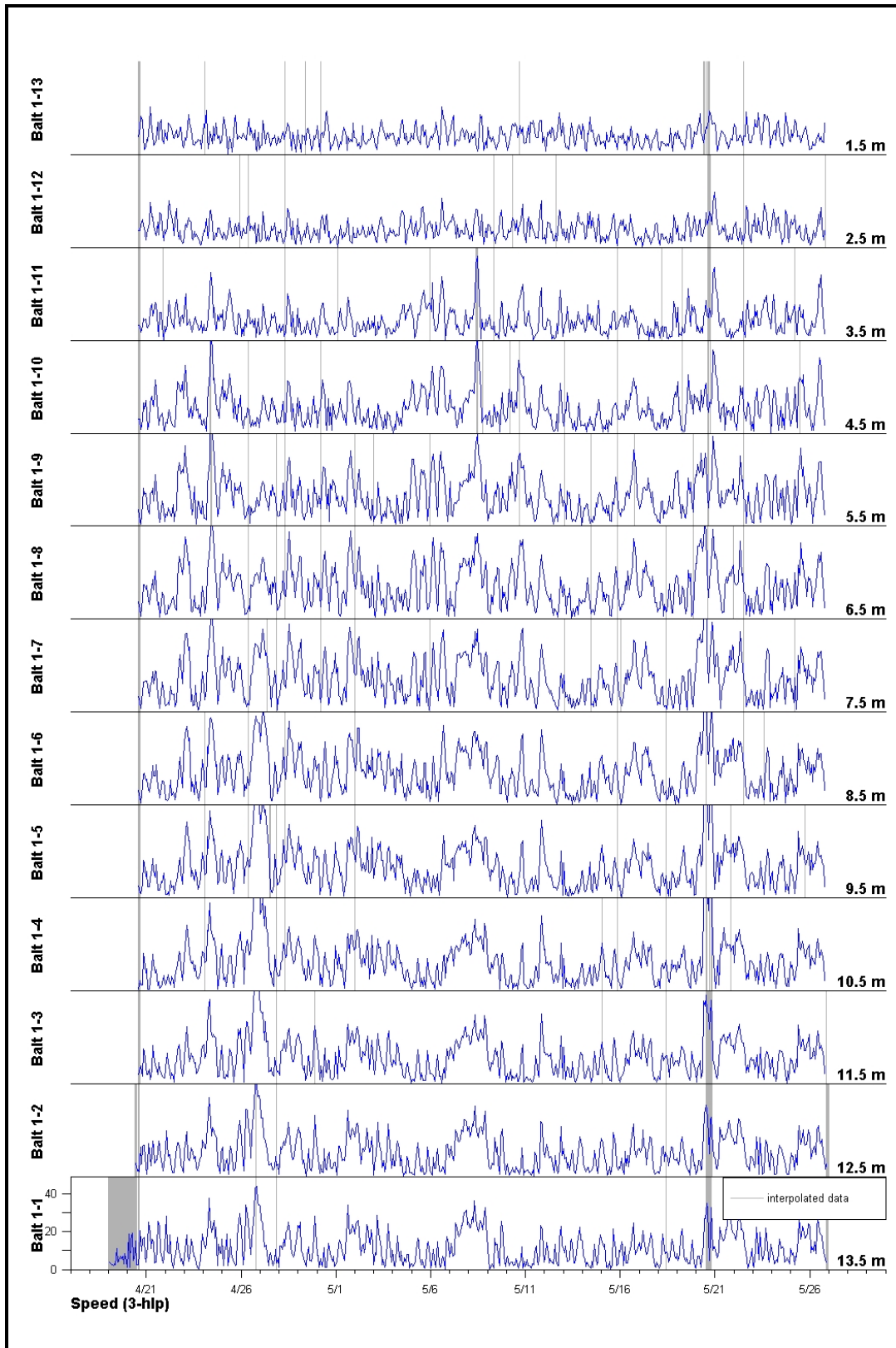


Figure 3.1-2. 3-HLP current magnitude time-series time-series from the Cutoff Angle ADCP during the first deployment (4/20 thru 5/26/05).

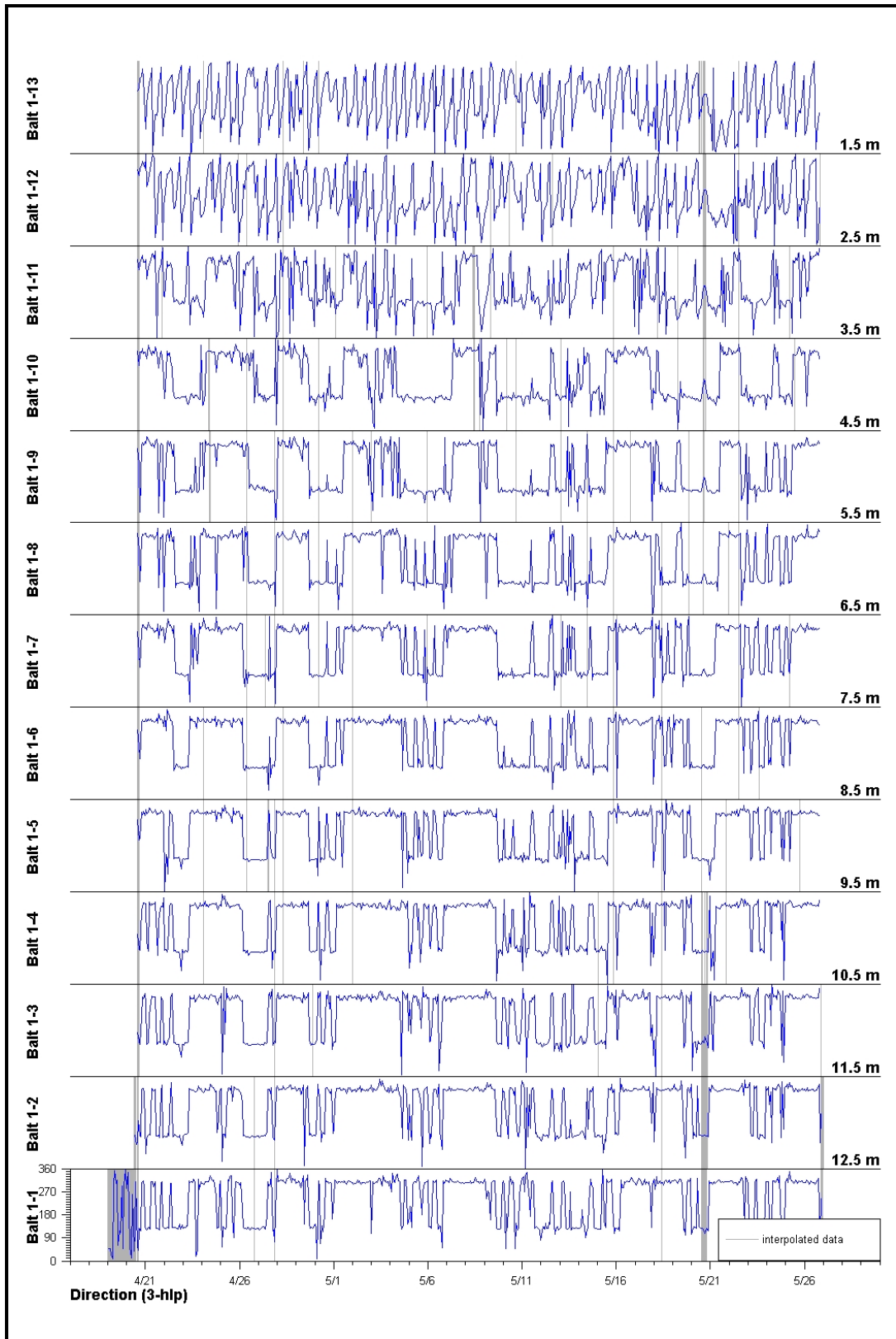


Figure 3.1-3. 3-HLP current direction time-series from the Cutoff Angle ADCP during the first deployment (4/20 thru 5/26/05).

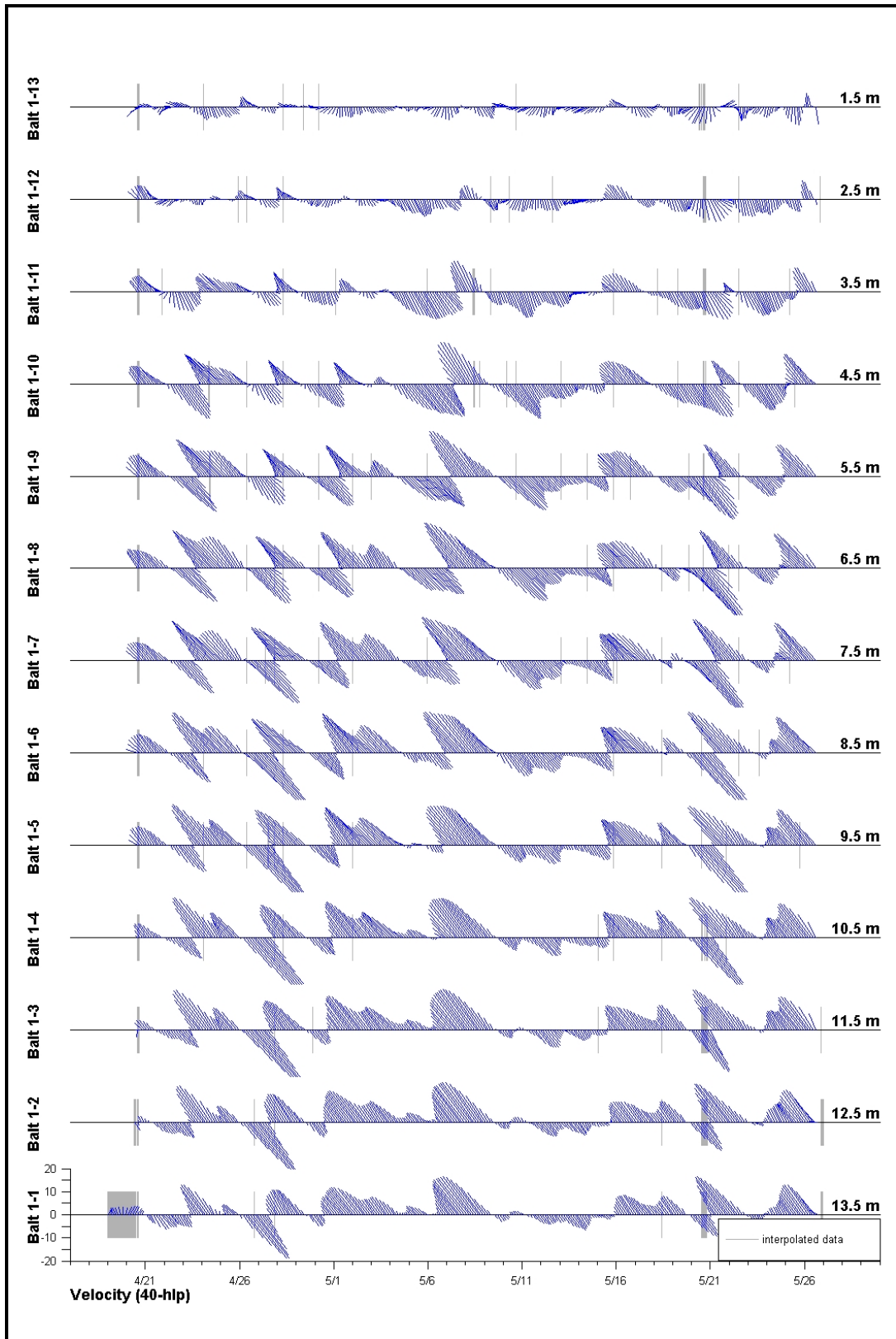


Figure 3.1-4. 40-HLP current magnitude and direction time-series from the Cutoff Angle ADCP during the first deployment (4/20 thru 5/26/05).

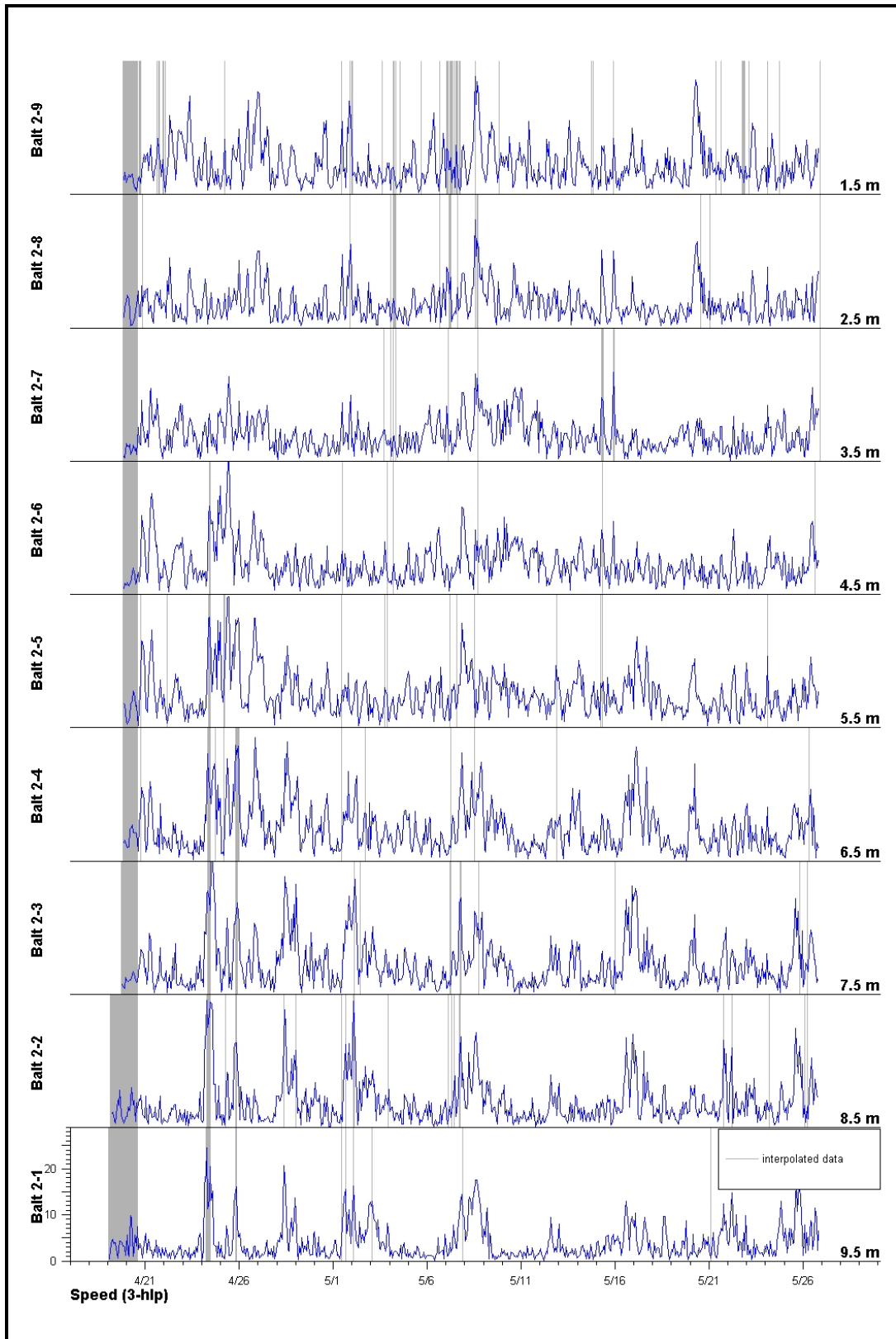


Figure 3.1-5. 3-HLP current magnitude time-series from the Curtis Bay Entrance ADCP during the first deployment (4/20 thru 5/26/05).

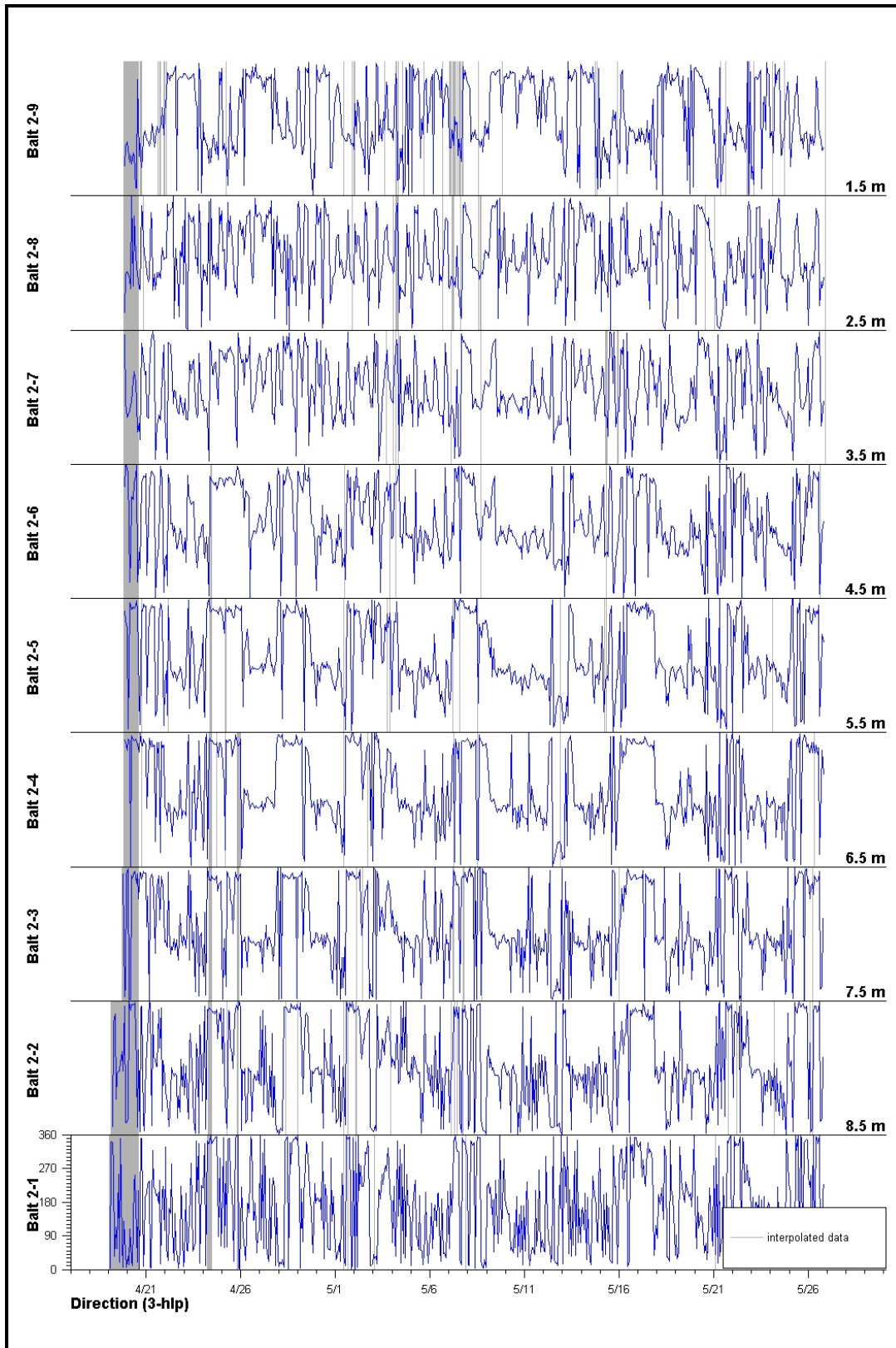


Figure 3.1-6. 3-HLP current direction time-series from the Curtis Bay Entrance ADCP during the first deployment (4/20 thru 5/26/05).

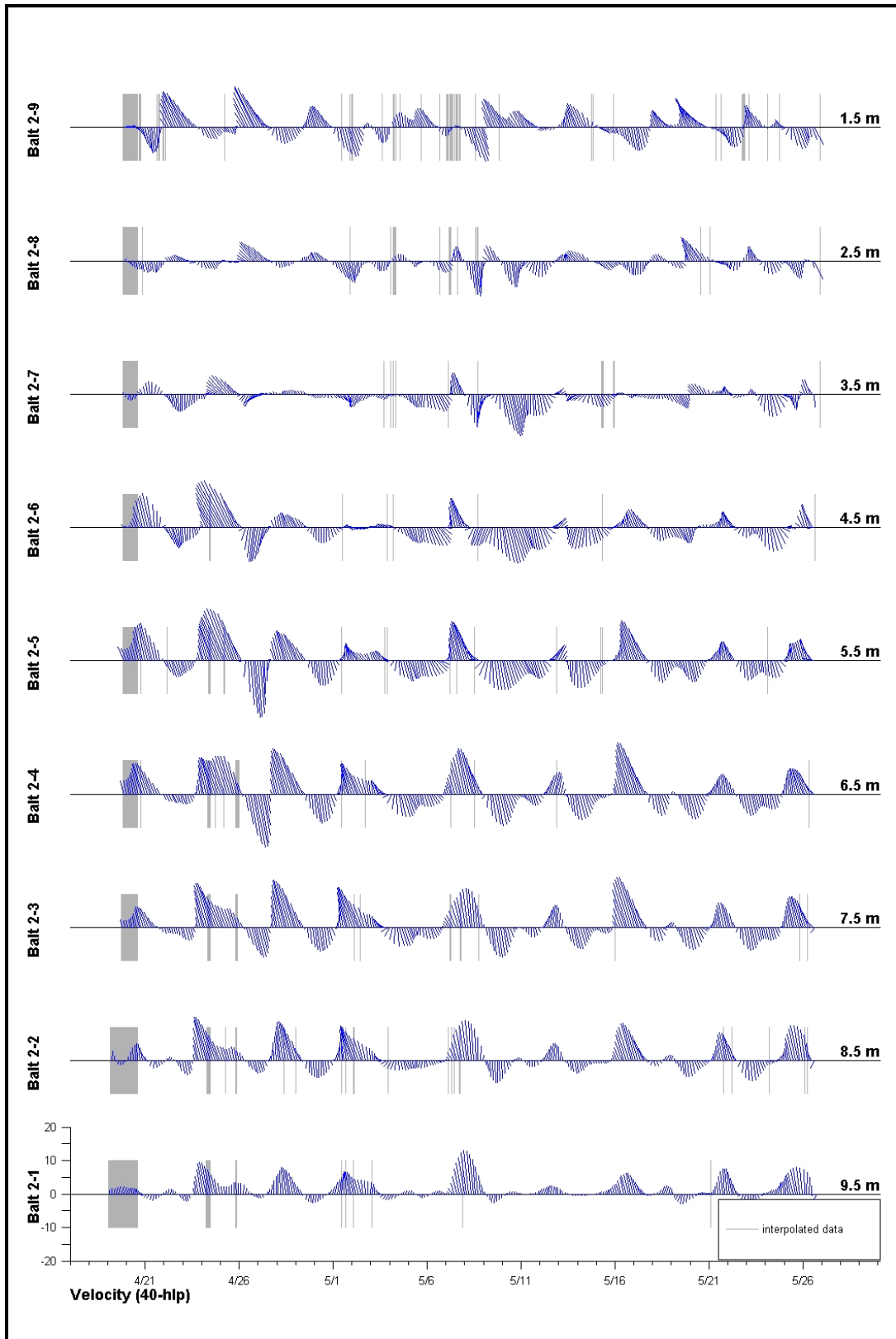


Figure 3.1-7. 40-HLP current magnitude and direction time-series from the Curtis Bay Entrance ADCP during the first deployment (4/20 thru 5/26/05).

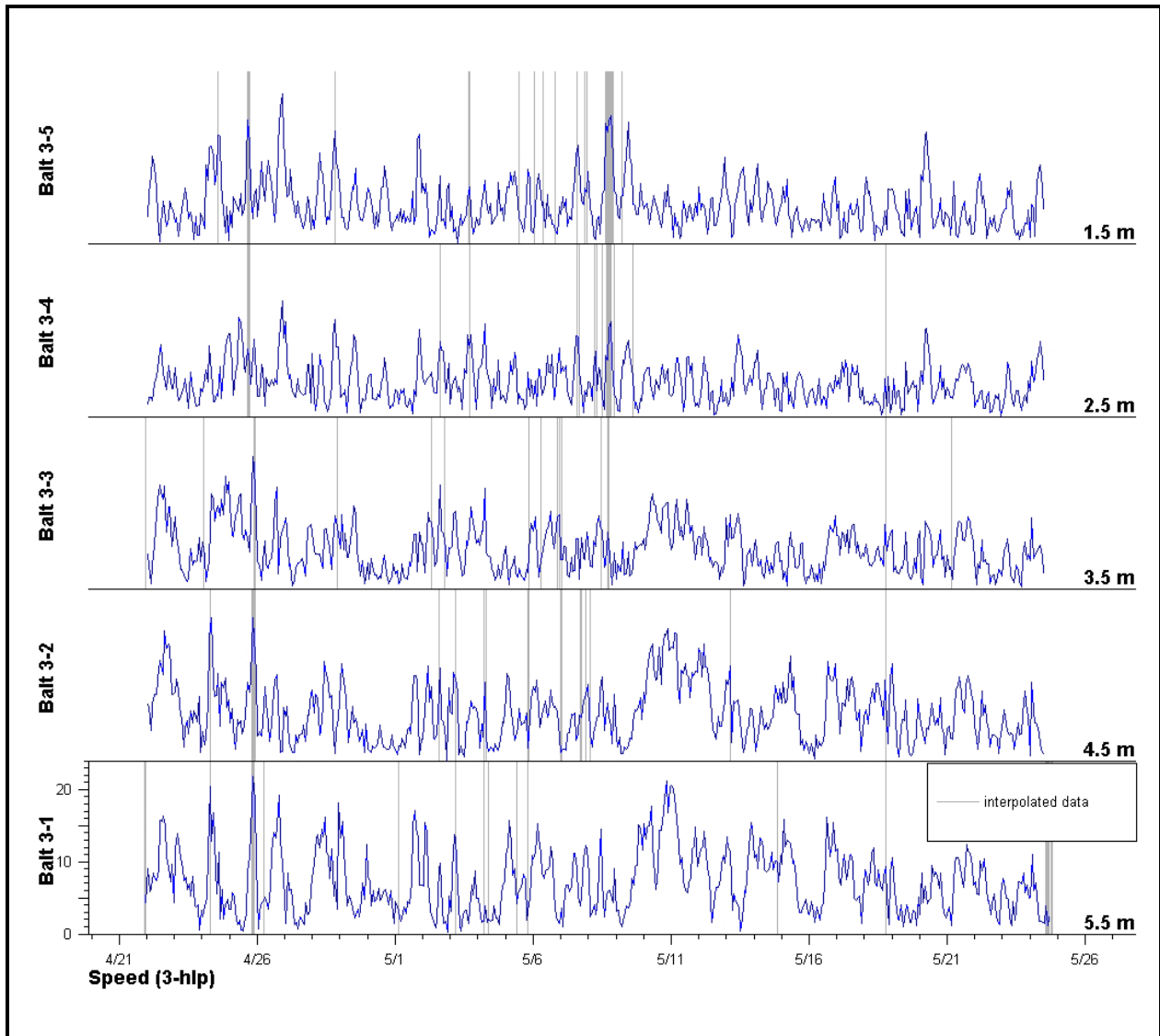


Figure 3.1-8. 3-HLP current magnitude time-series from the Fort McHenry Angle ADCP during the first deployment (4/21 thru 5/24/05).

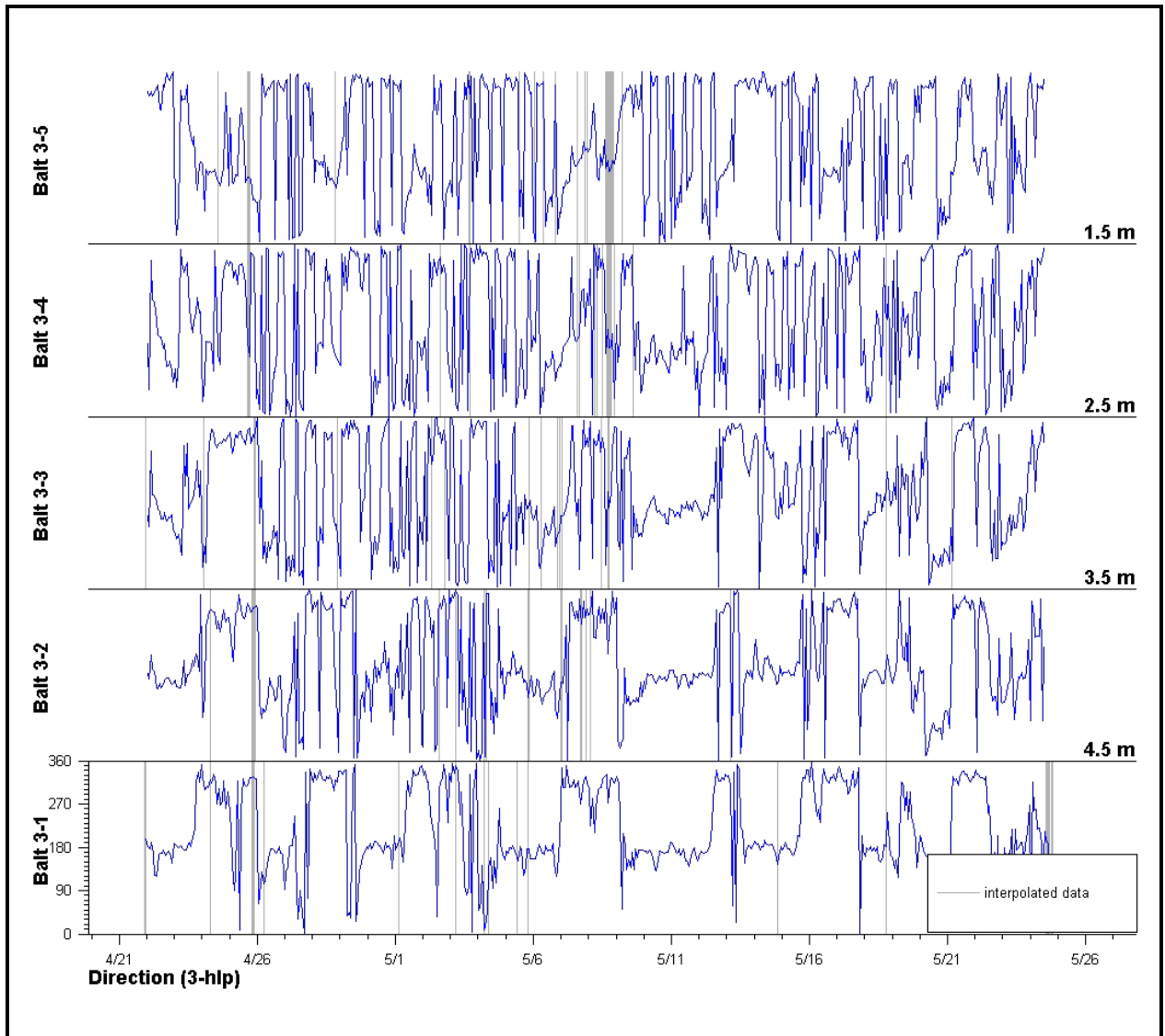


Figure 3.1-9. 3-HLP current direction time-series from the Fort McHenry Angle ADCP during the first deployment (4/21 thru 5/24/05).

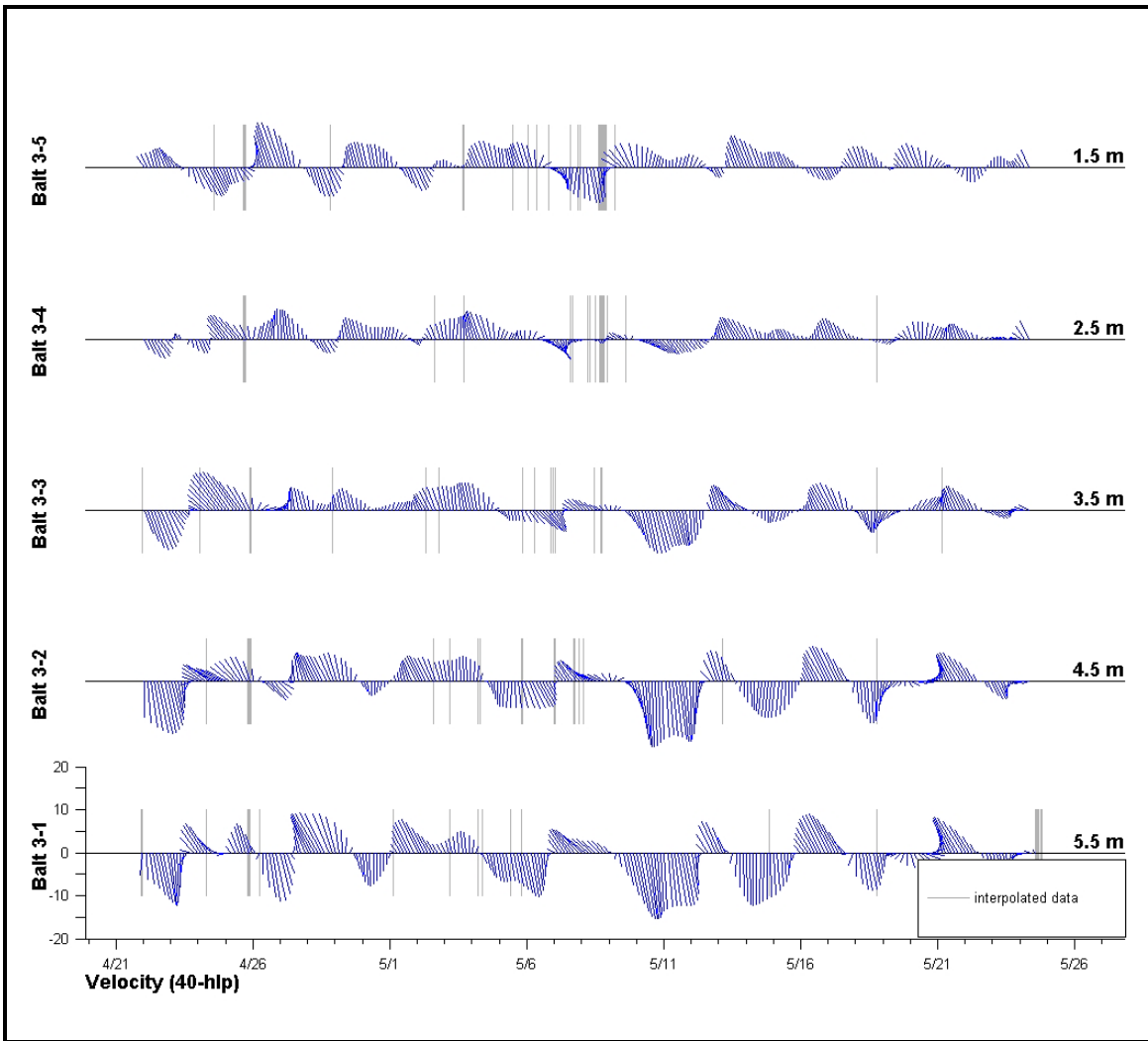


Figure 3.1-10. 40-HLP current magnitude and direction time-series from the Fort McHenry Angle ADCP during the first deployment (4/21 thru 5/24/05).

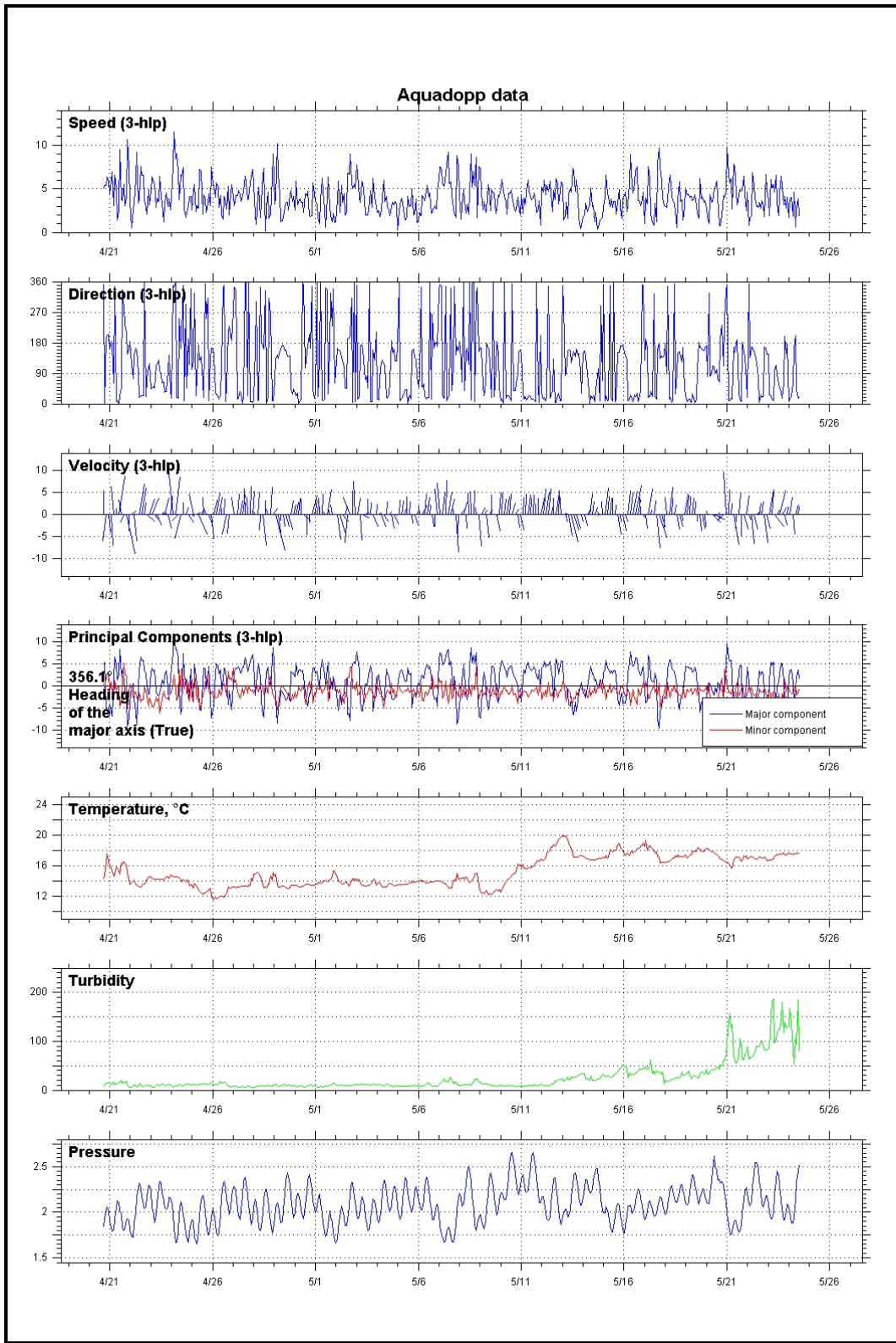


Figure 3.1-11. Near-bottom 3-HLP current magnitude and direction time-series from the Masonville Cove Aquadopp during the first deployment (4/21 thru 5/24/05). Time-series temperature, turbidity, and pressure data are also shown.

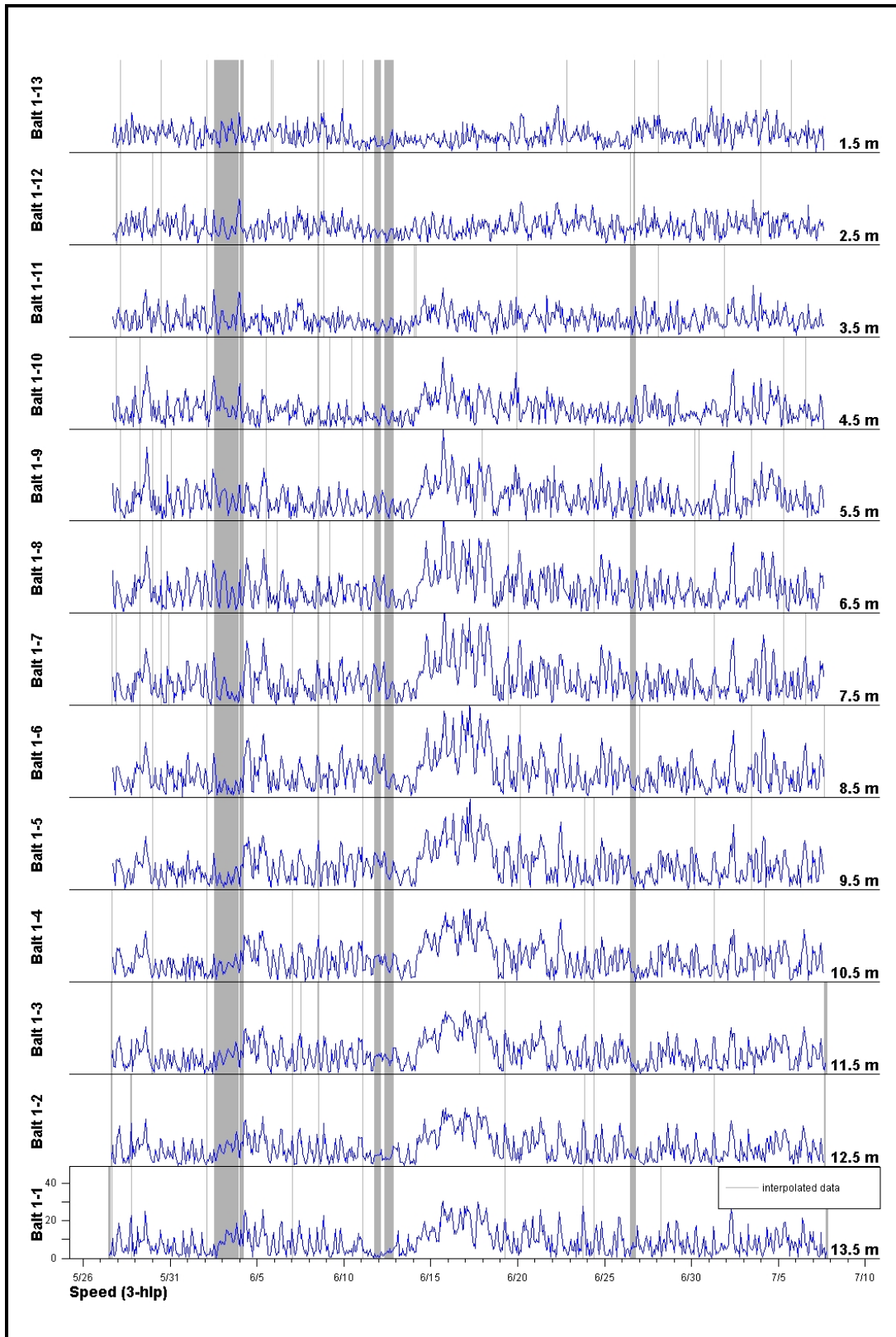


Figure 3.1-12. 3-HLP current magnitude time-series from the Cutoff Angle ADCP during the second deployment (5/27 thru 7/7/05).

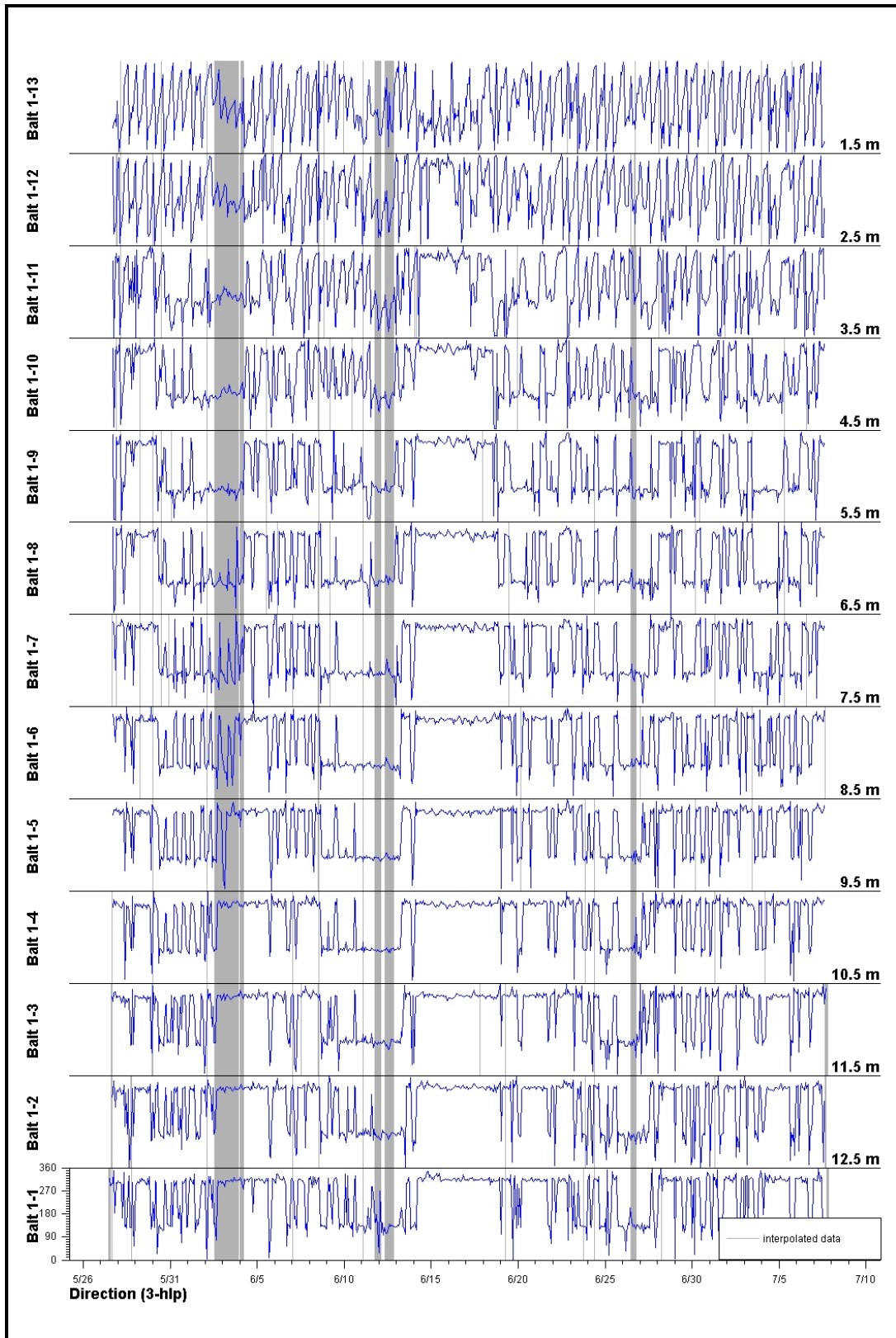


Figure 3.1-13. 3-HLP current direction time-series from the Cutoff Angle ADCP during the second deployment (5/27 thru 7/7/05).

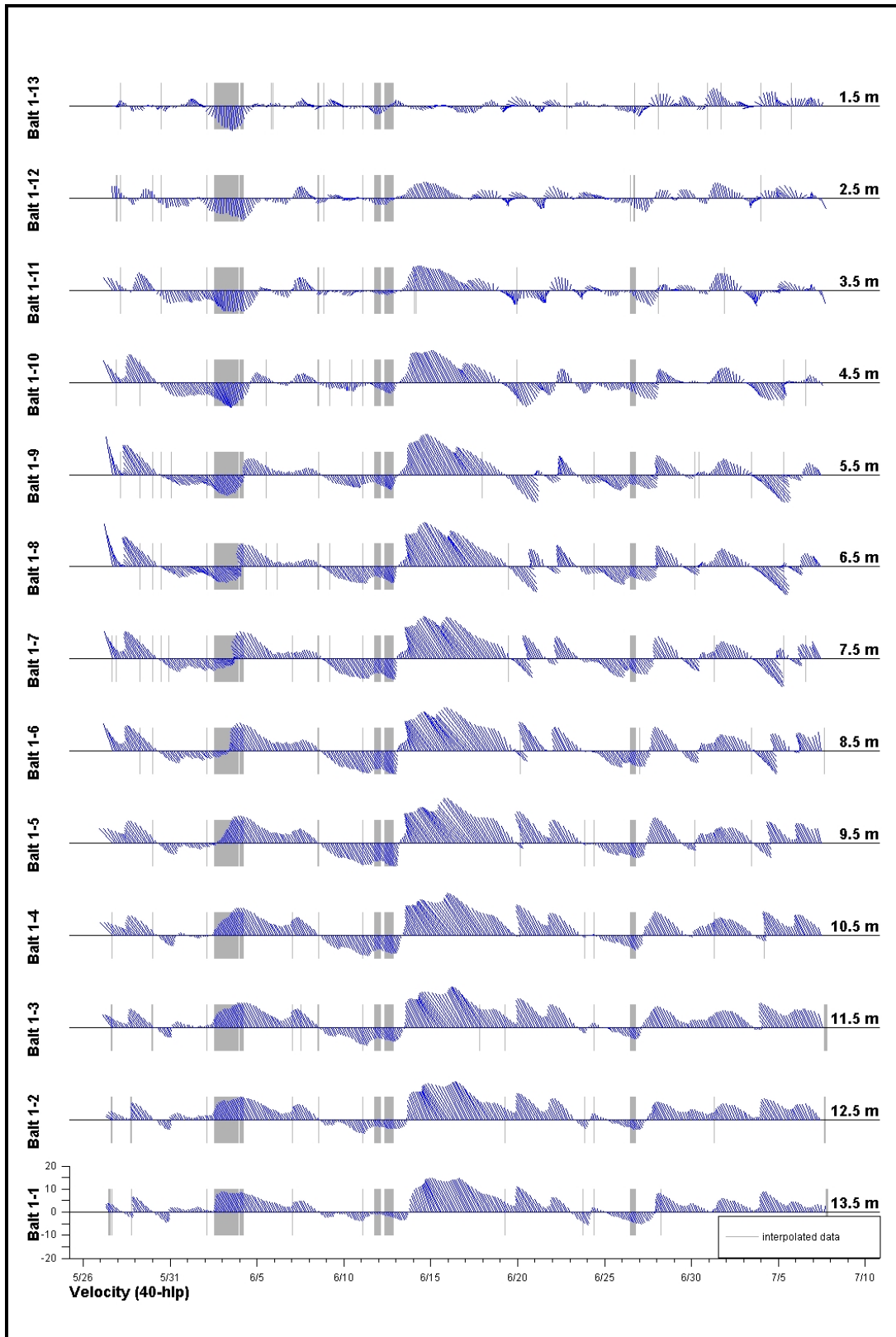


Figure 3.1-14. 40-HLP current magnitude and direction time-series from the Cutoff Angle ADCP during the second deployment (5/27 thru 7/7/05).

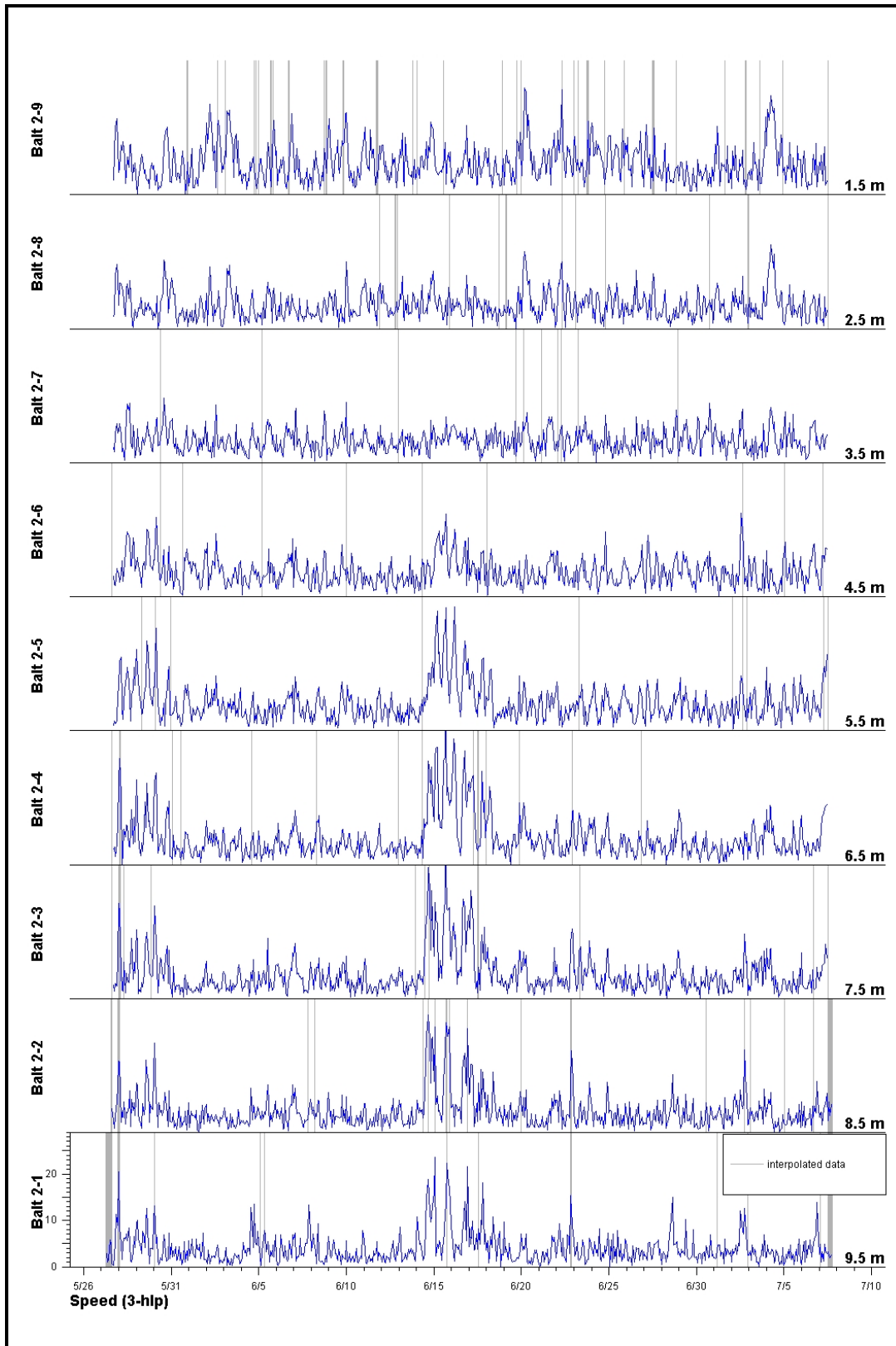


Figure 3.1-15. 3-HLP current magnitude time-series from the Curtis Bay Entrance ADCP during the second deployment (5/27 thru 7/7/05).

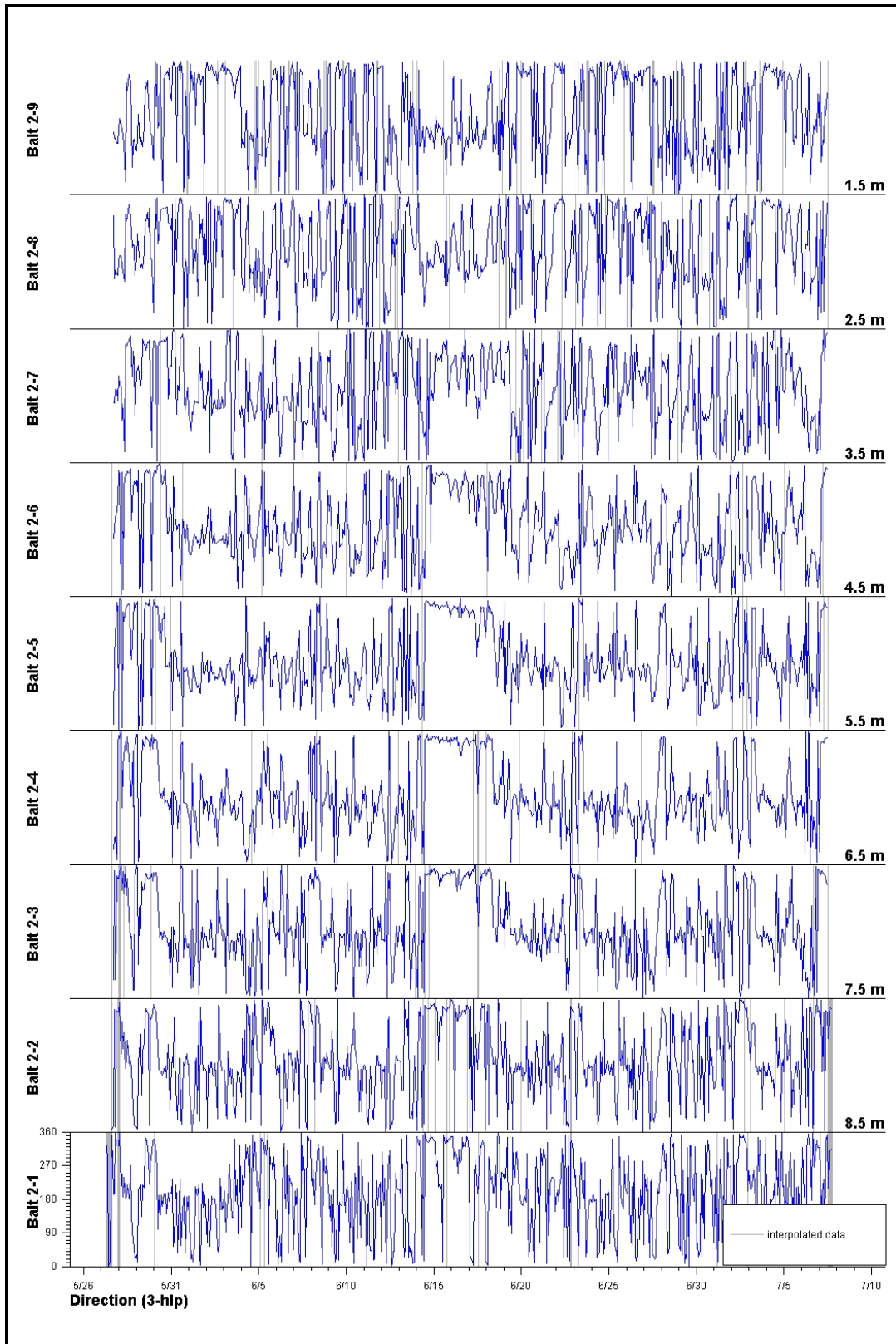


Figure 3.1-16. 3-HLP current direction time-series from the Curtis Bay Entrance ADCP during the second deployment (5/27 thru 7/7/05).

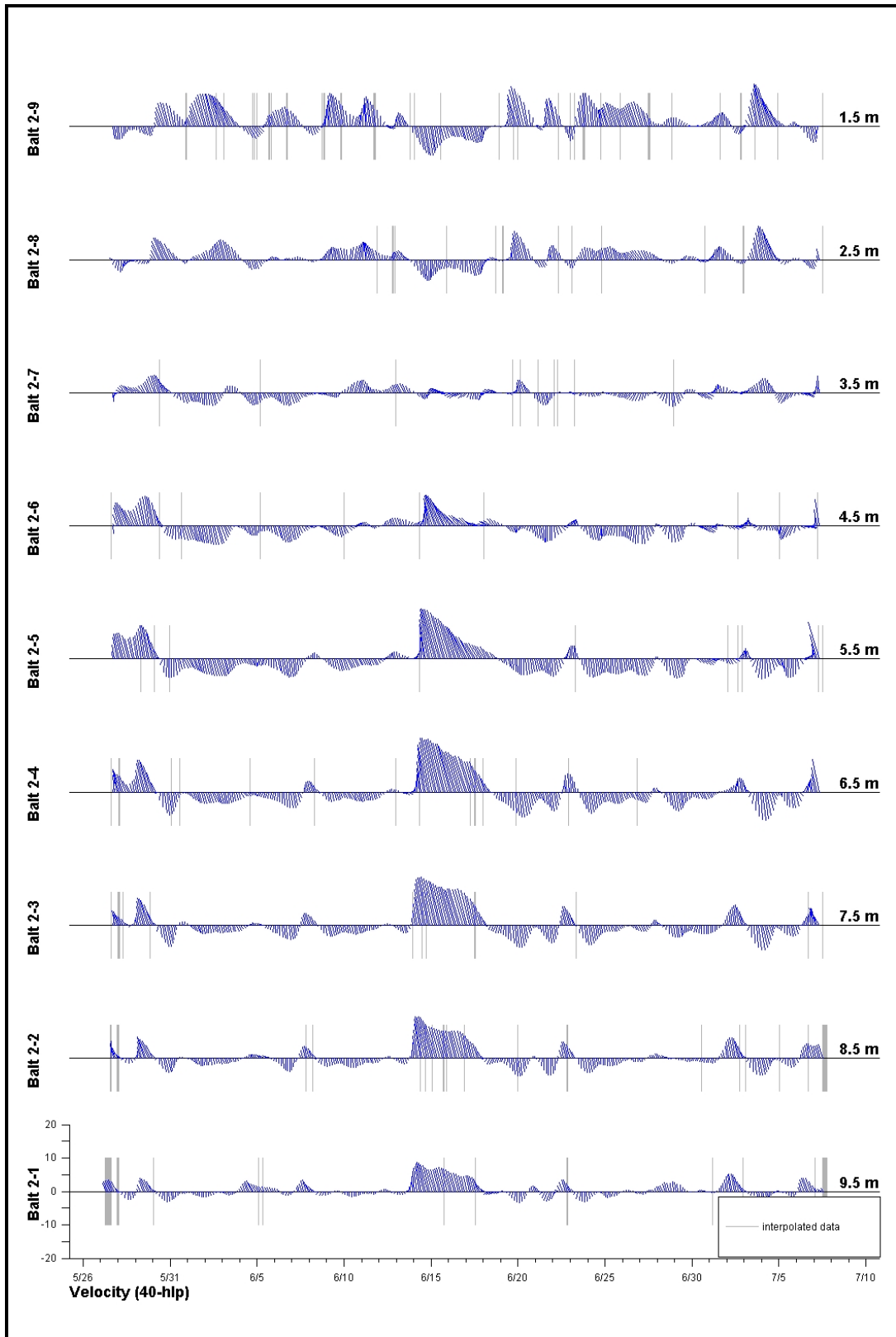


Figure 3.1-17. 40-HLP current magnitude and direction time-series from the Curtis Bay Entrance ADCP during the second deployment (5/27 thru 7/7/05).

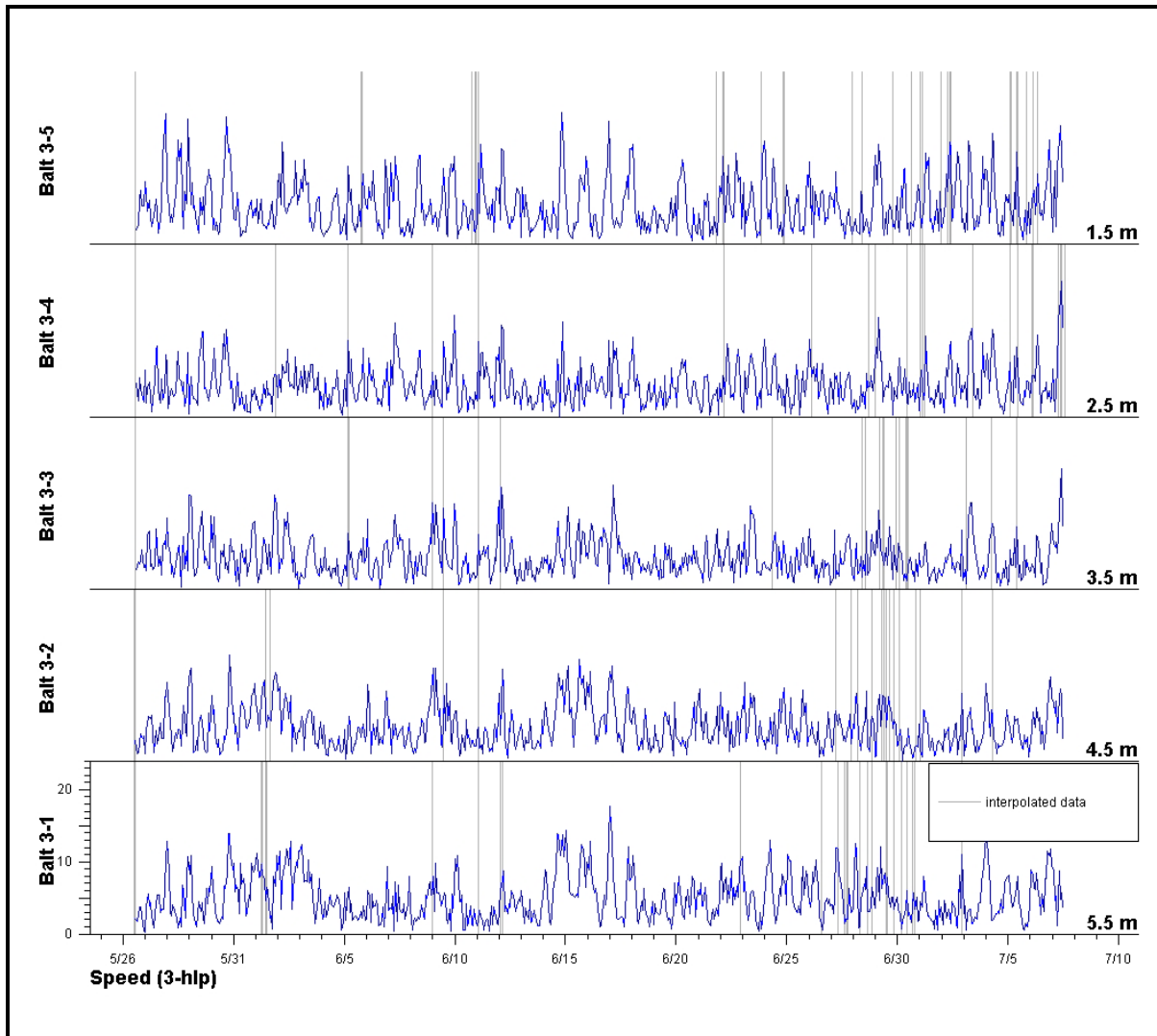


Figure 3.1-18. 3-HLP current magnitude time-series from the Fort McHenry Angle ADCP during the second deployment (5/26 thru 7/7/05).

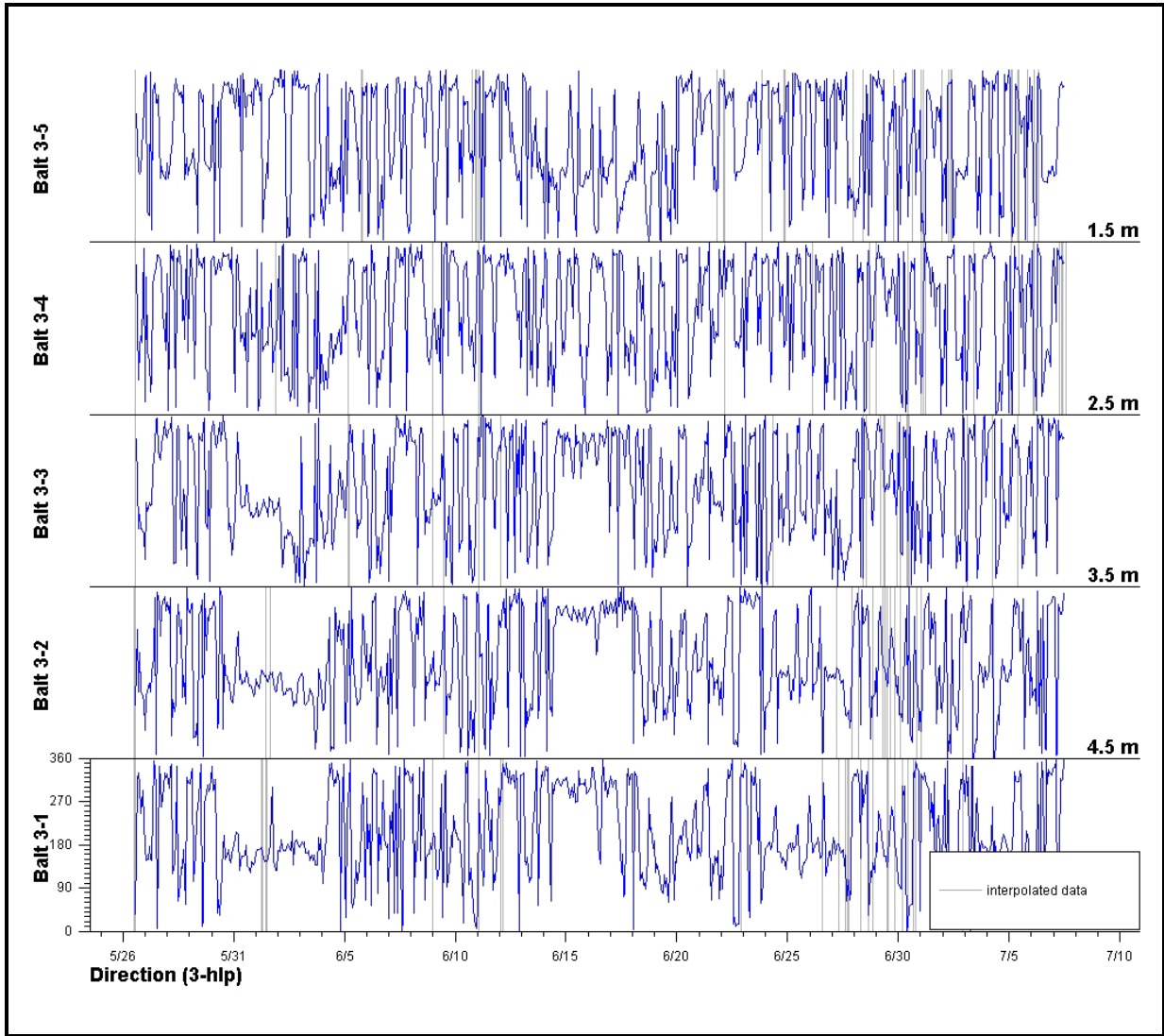


Figure 3.1-19. 3-HLP current direction time-series from the Fort McHenry Angle ADCP during the second deployment (5/26 thru 7/7/05).

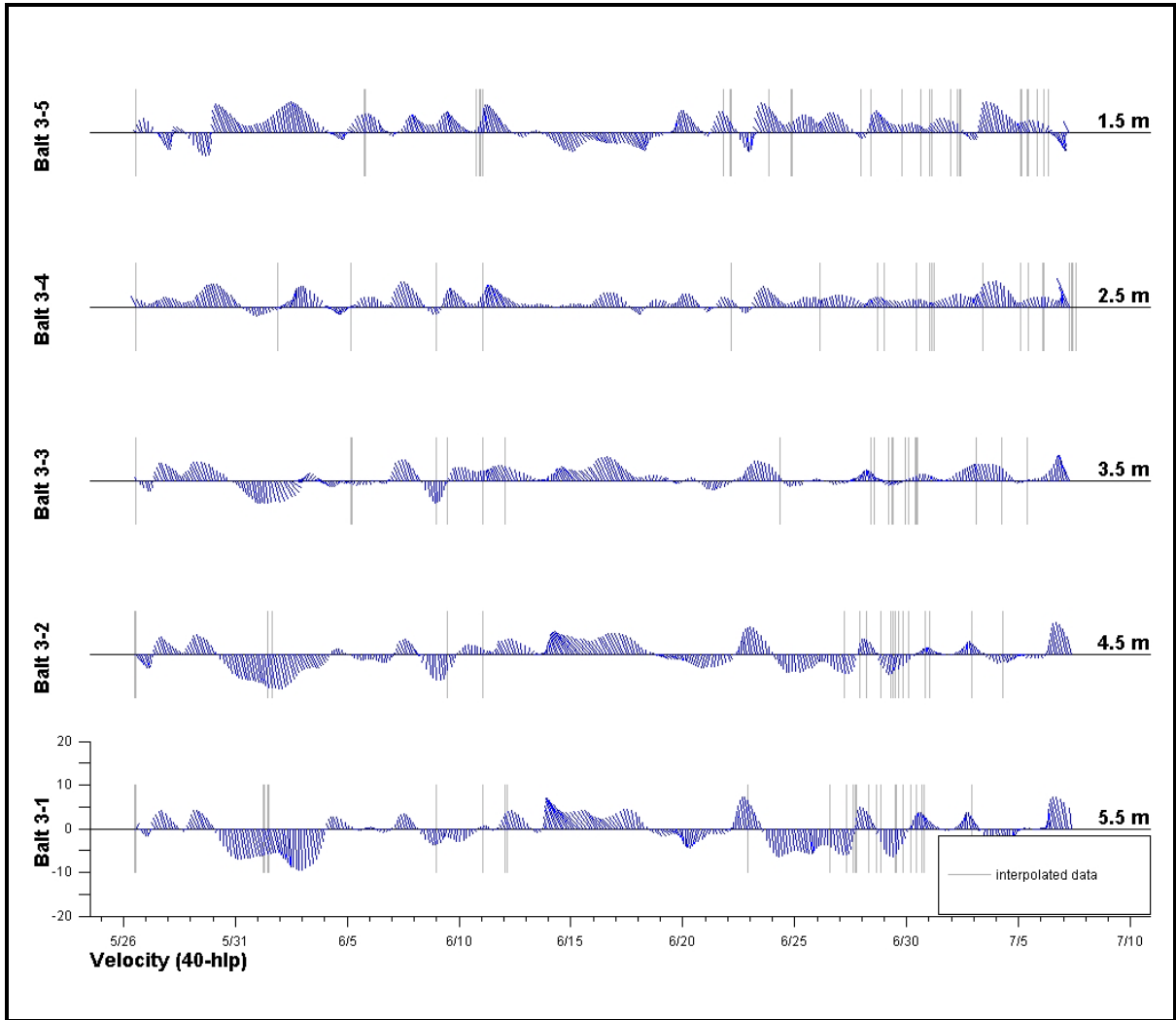


Figure 3.1-20. 40-HLP current magnitude and direction time-series from the Fort McHenry Angle ADCP during the second deployment (5/26 thru 7/7/05).

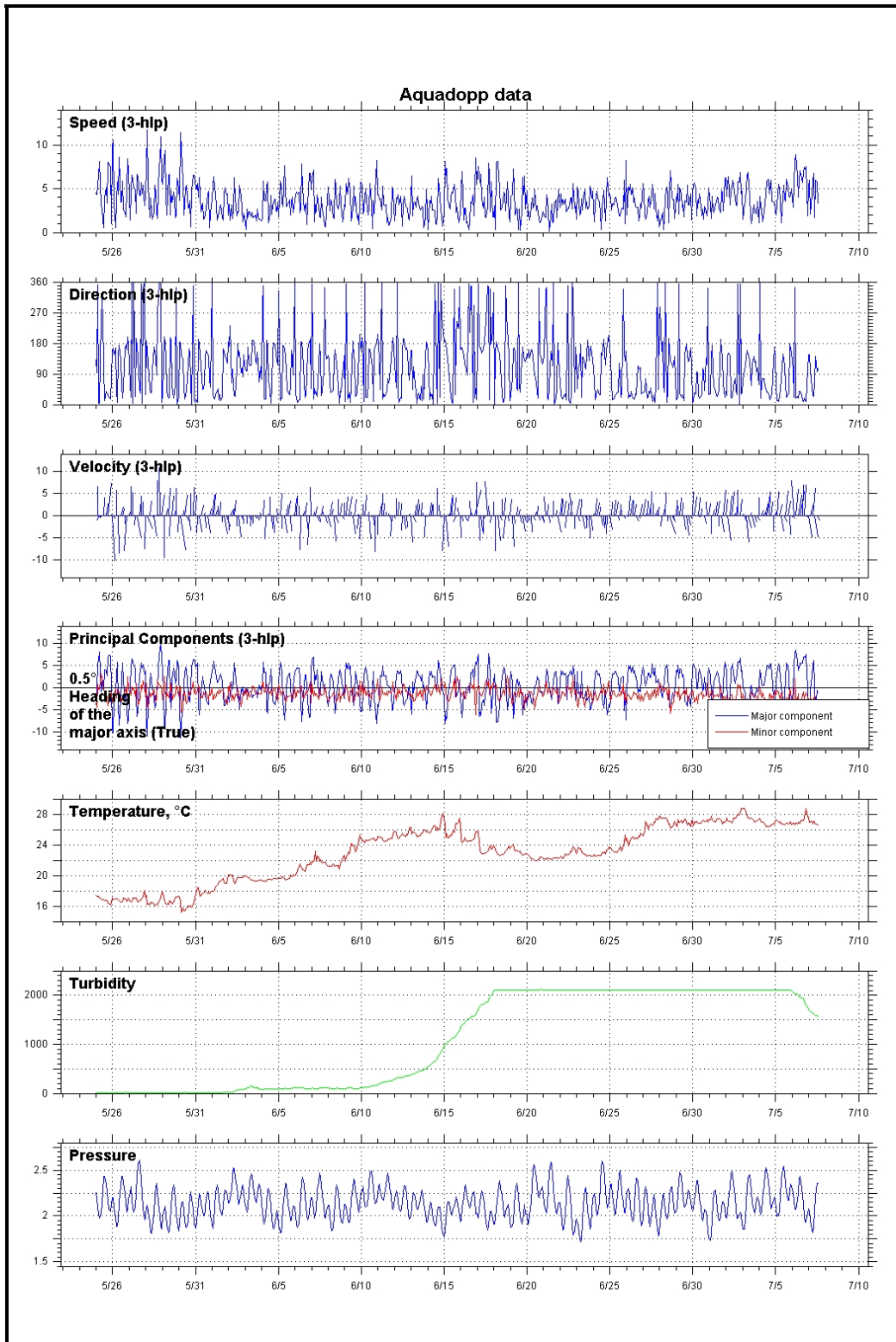


Figure 3.1-21. Near-bottom 3-HLP current magnitude and direction time-series from the Masonville Cove Aquadopp during the second deployment (5/24 thru 7/7/05). Time-series temperature, turbidity, and pressure data are also shown.

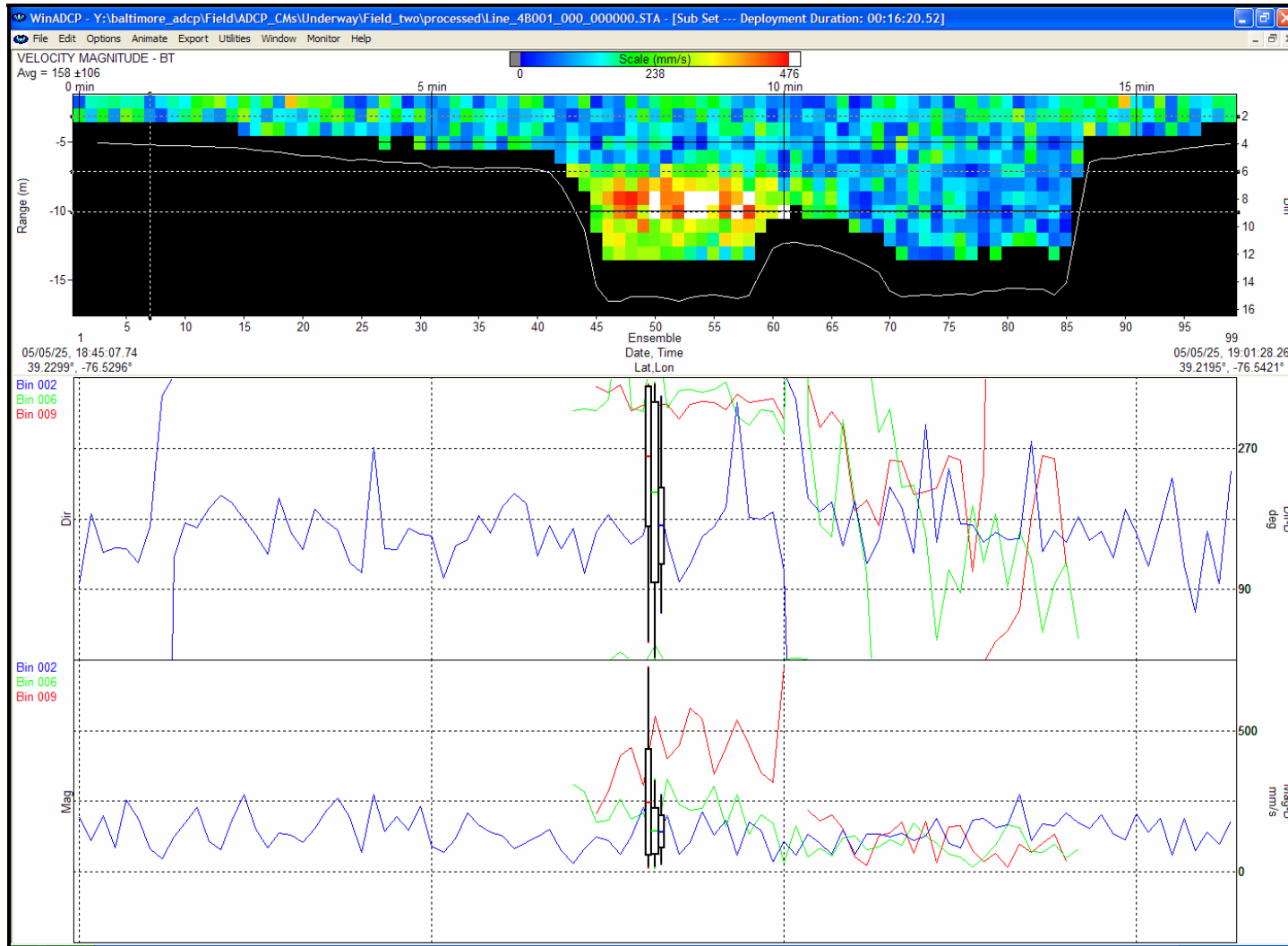


Figure 3.2-1 Close-up view of the WinADCP screen depicting the current magnitude and direction along-track contour and profile results from an ADCP transect acquired on 5/25/2005. A similar format and grid spacing was used to generate all of the following underway ADCP figures (Figures 3.2-2 thru 3.2-11).

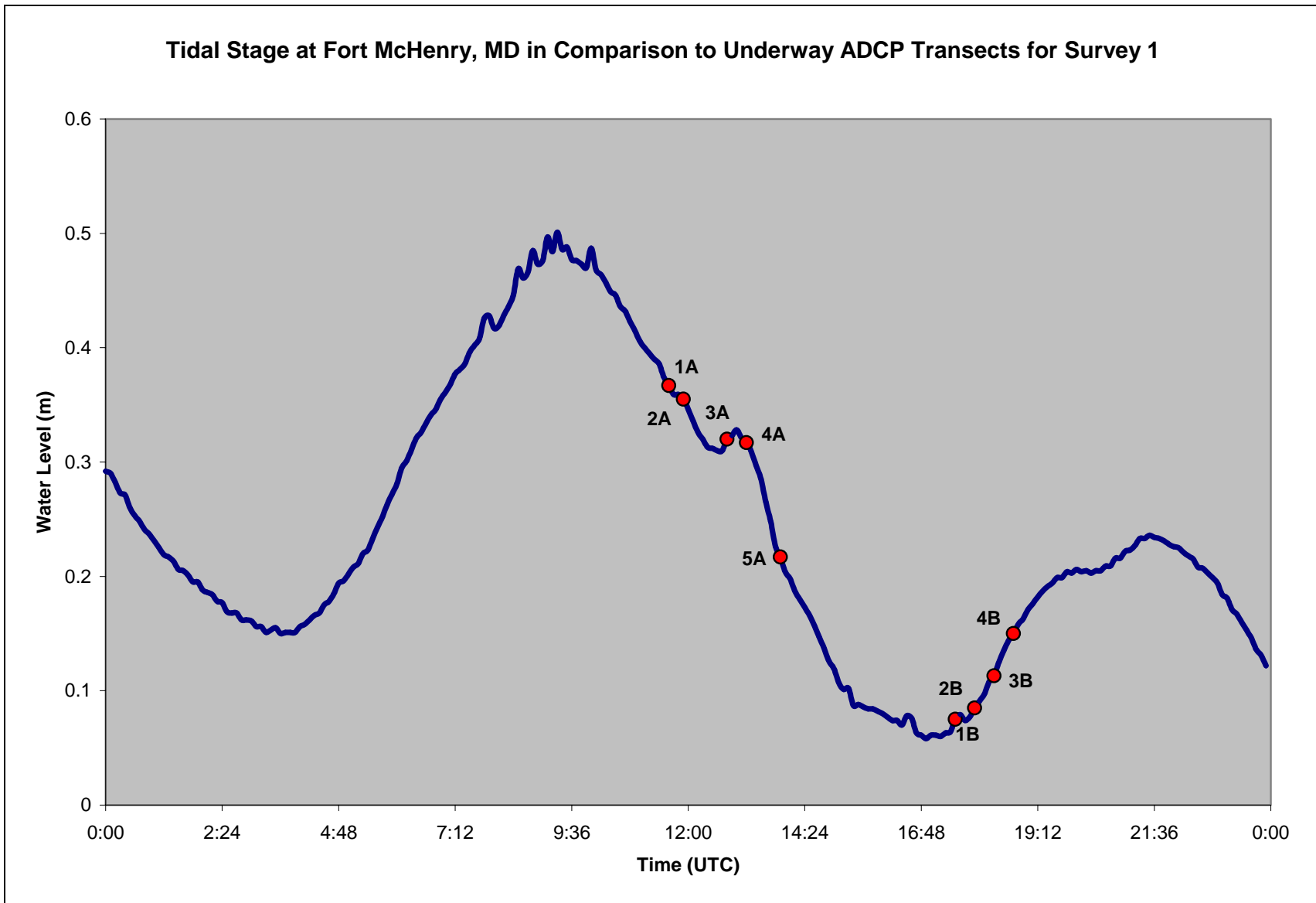
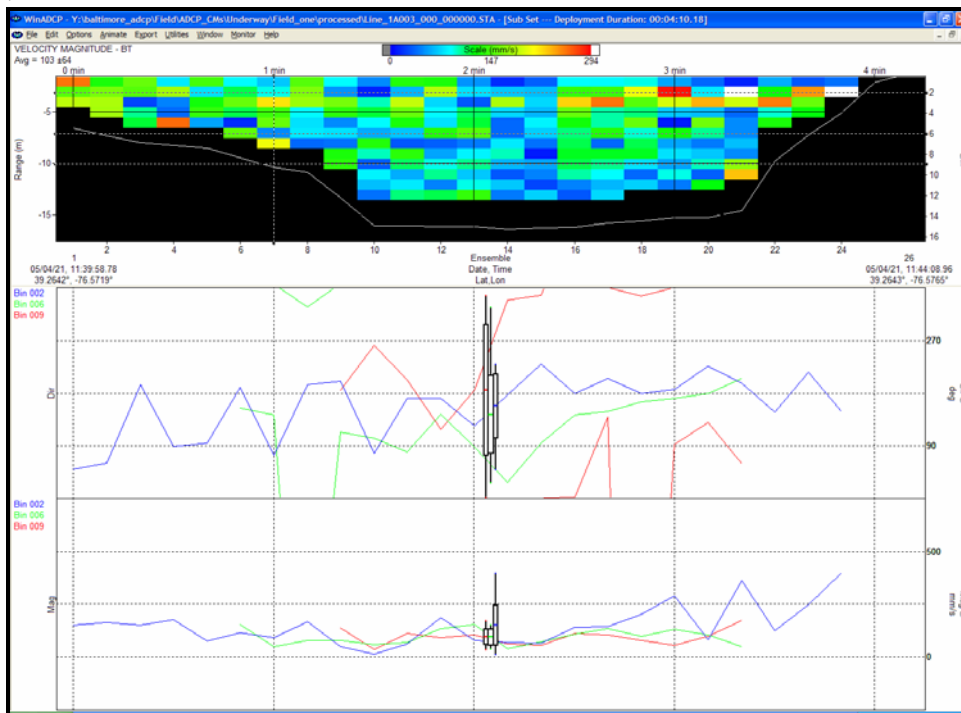
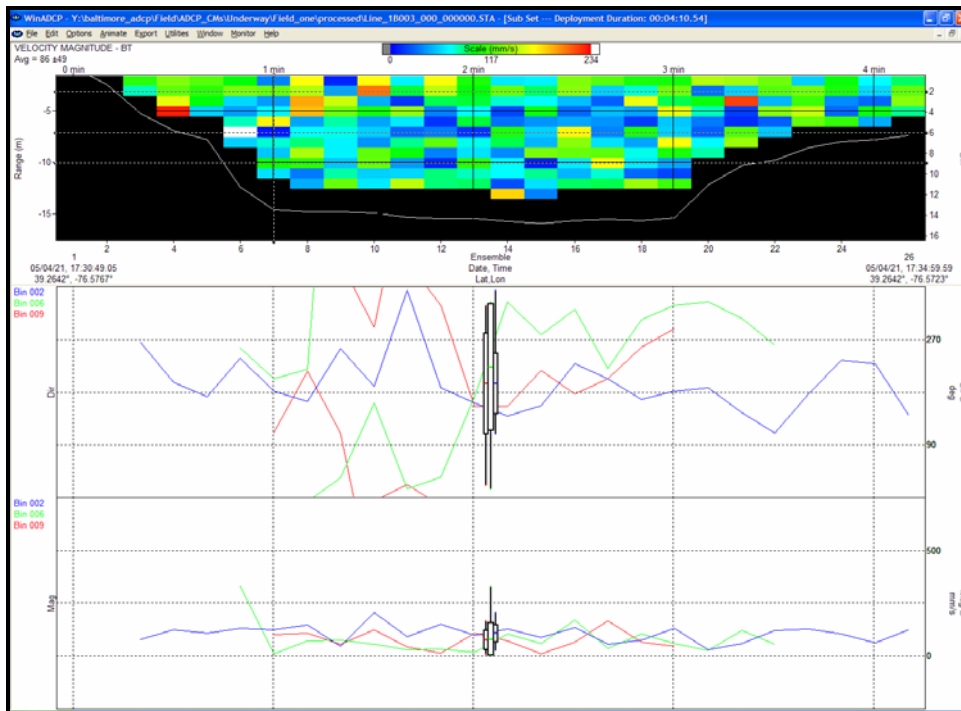


Figure 3.2-2. Indication of the Fort McHenry tidal stage relative to the underway ADCP transects that were conducted on 4/21/05

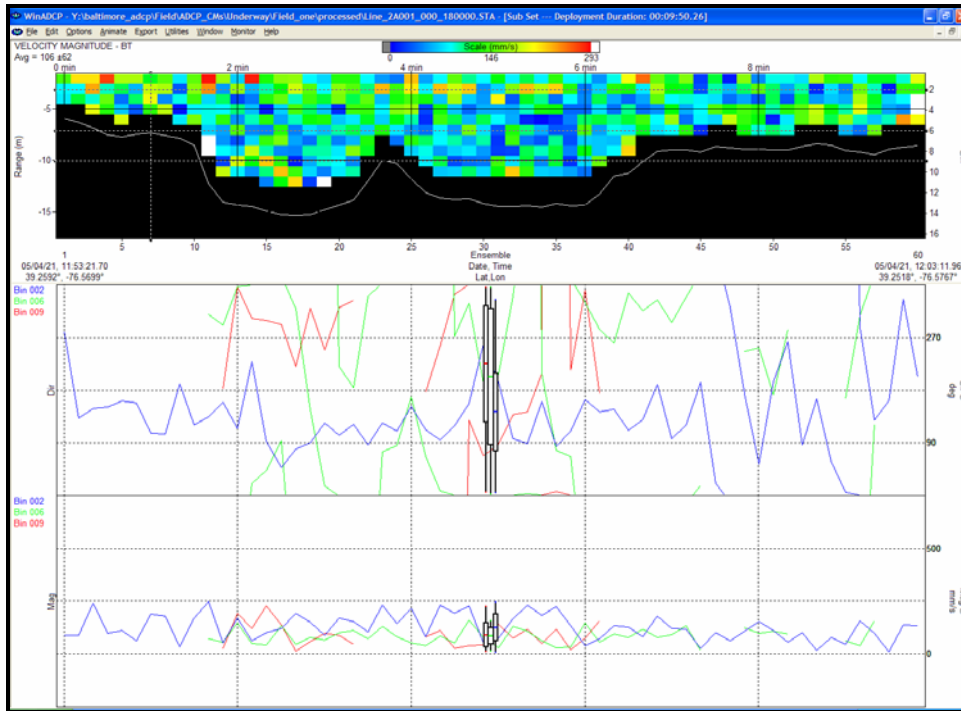


Transect - 1A003
 Start Time: 11:39 GMT
 End Time: 11:44 GMT
 Line Heading - 270 True

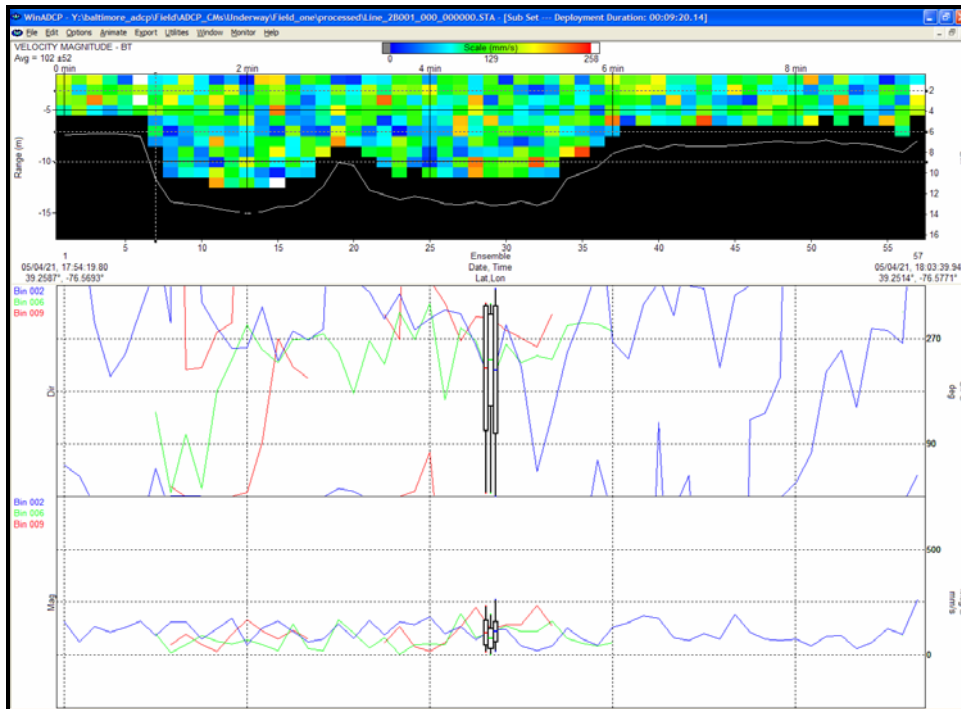


Transect - 1B003
 Start Time: 17:30 GMT
 End Time: 17:35 GMT
 Line Heading - 090 True

Figure 3.2-3. Current magnitude and direction along-track contour and profile results collected along underway ADCP Transect 1 on 4/21/05.

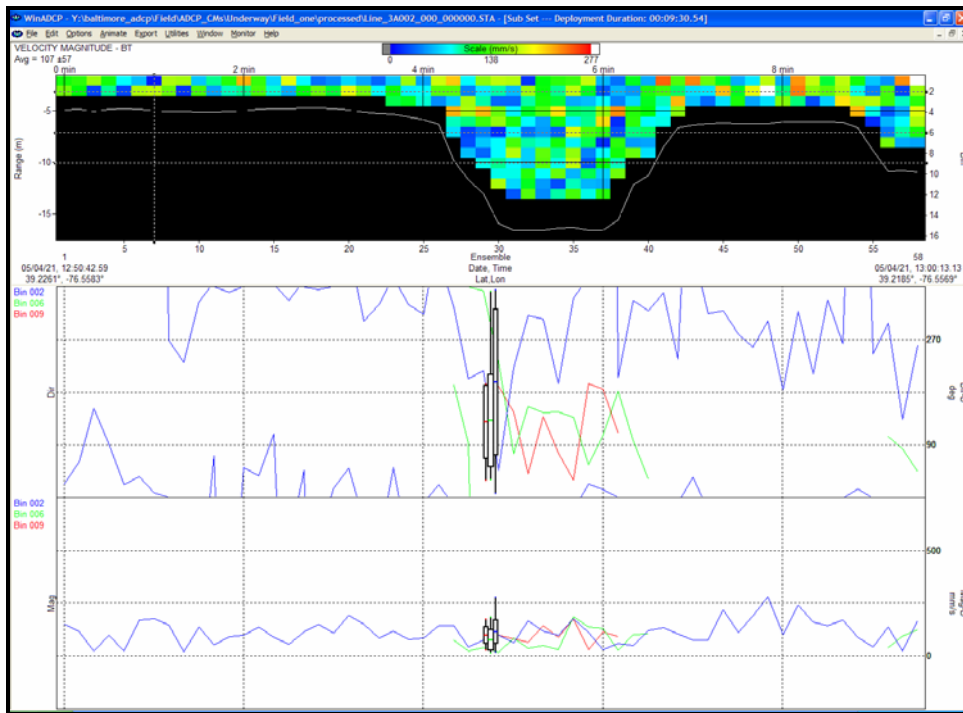


Transect - 2A001
 Start Time: 11:53 GMT
 End Time: 12:03 GMT
 Line Heading - 225 True

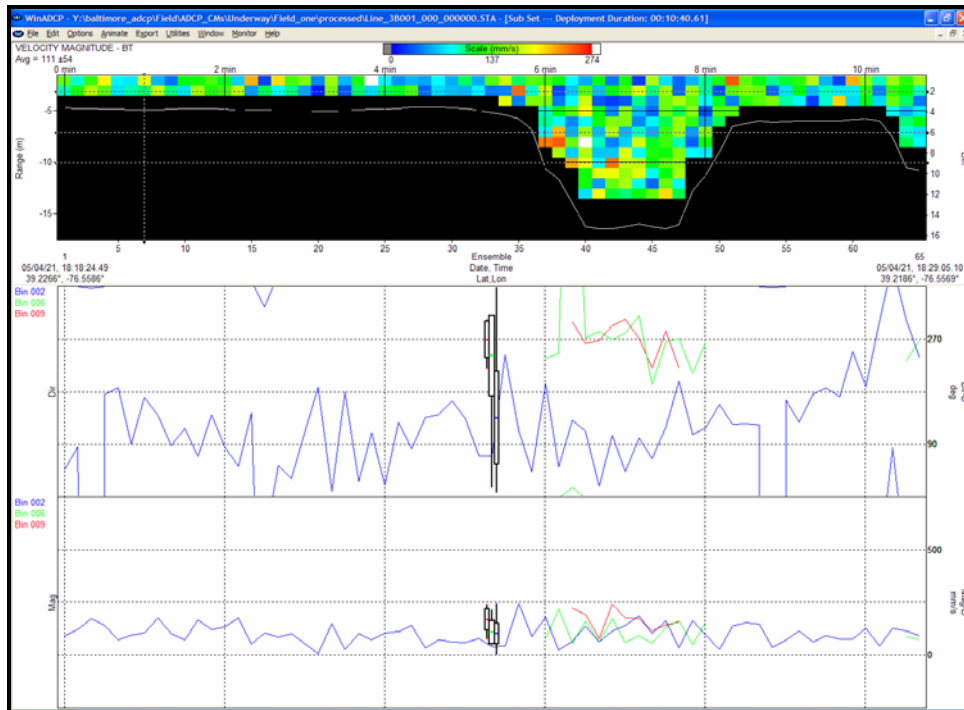


Transect - 2B001
 Start Time: 17:54 GMT
 End Time: 18:04 GMT
 Line Heading - 225 True

Figure 3.2-4. Current magnitude and direction along-track contour and profile results collected along underway ADCP Transect 2 on 4/21/05.

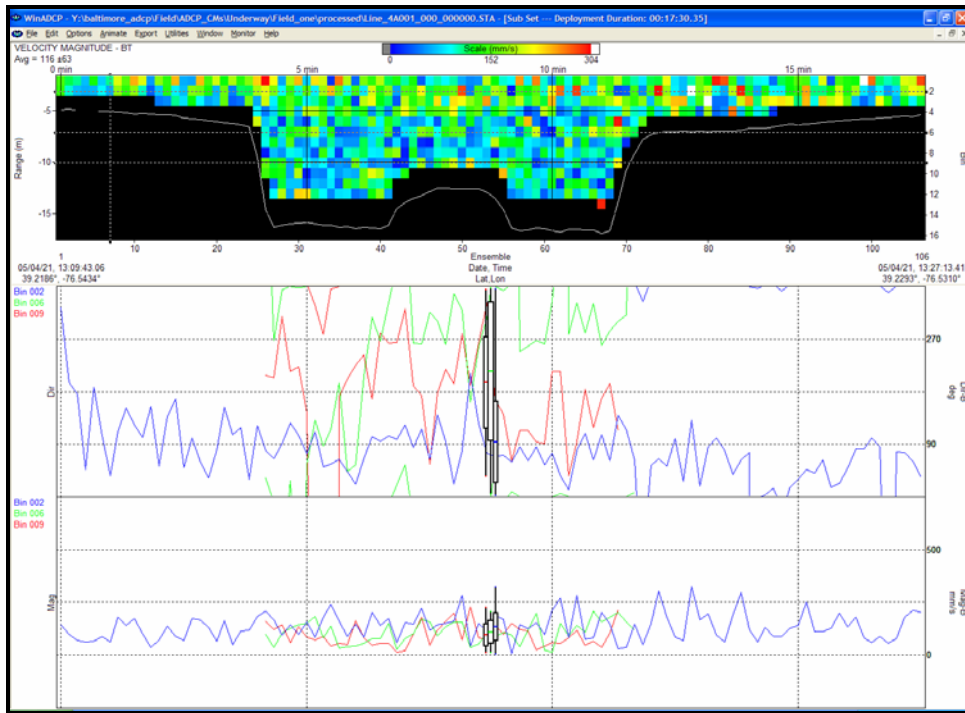


Transect – 3A001
Start Time: 12:50 GMT
End Time: 13:00 GMT
Line Heading – 175 True

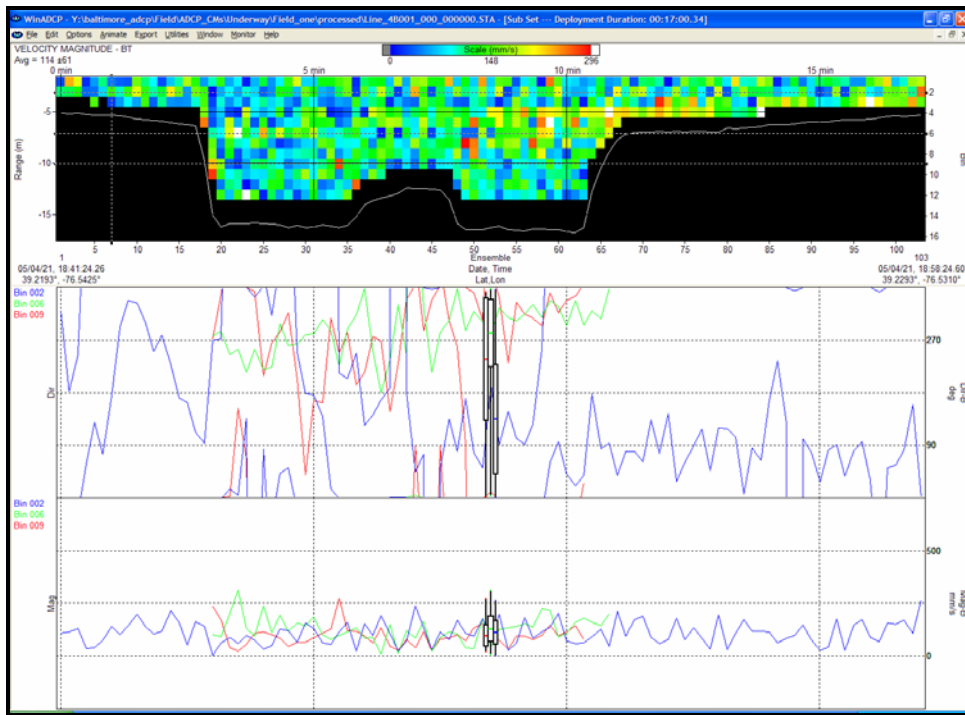


Transect – 3B001
Start Time: 18:18 GMT
End Time: 18:29 GMT
Line Heading – 175 True

Figure 3.2-5. Current magnitude and direction along-track contour and profile results collected along underway ADCP Transect 3 on 4/21/05.

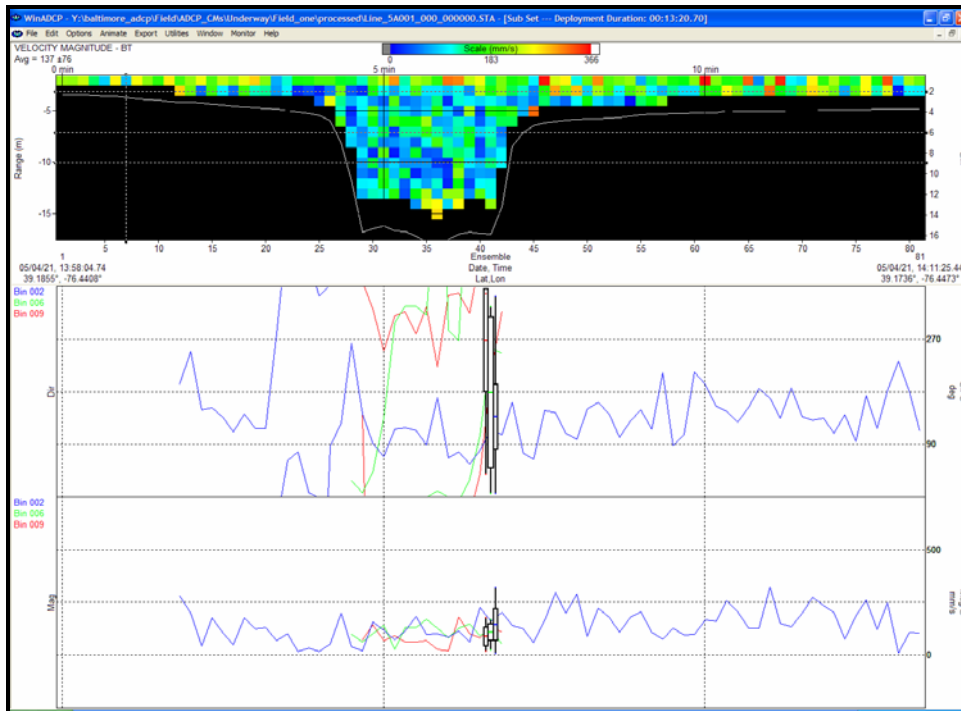


Transect – 4A001
 Start Time: 13:09 GMT
 End Time: 13:28 GMT
 Line Heading – 055 True

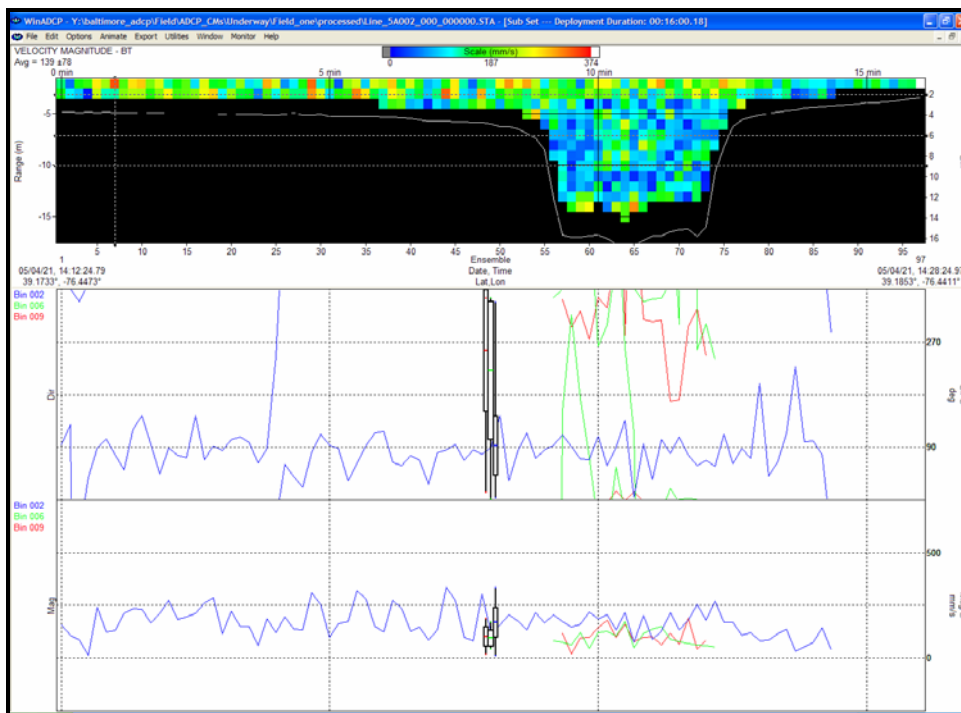


Transect – 4B001
 Start Time: 18:41 GMT
 End Time: 18:59 GMT
 Line Heading – 055 True

Figure 3.2-6. Current magnitude and direction along-track contour and profile results collected along underway ADCP Transect 4 on 4/21/05.



Transect – 5A001
Start Time: 13:58 GMT
End Time: 14:12 GMT
Line Heading – 195 True



Transect – 5A002
Start Time: 14:13 GMT
End Time: 14:28 GMT
Line Heading – 015 True

Figure 3.2-7. Current magnitude and direction along-track contour and profile results collected along underway ADCP Transect 5 on 4/21/05.

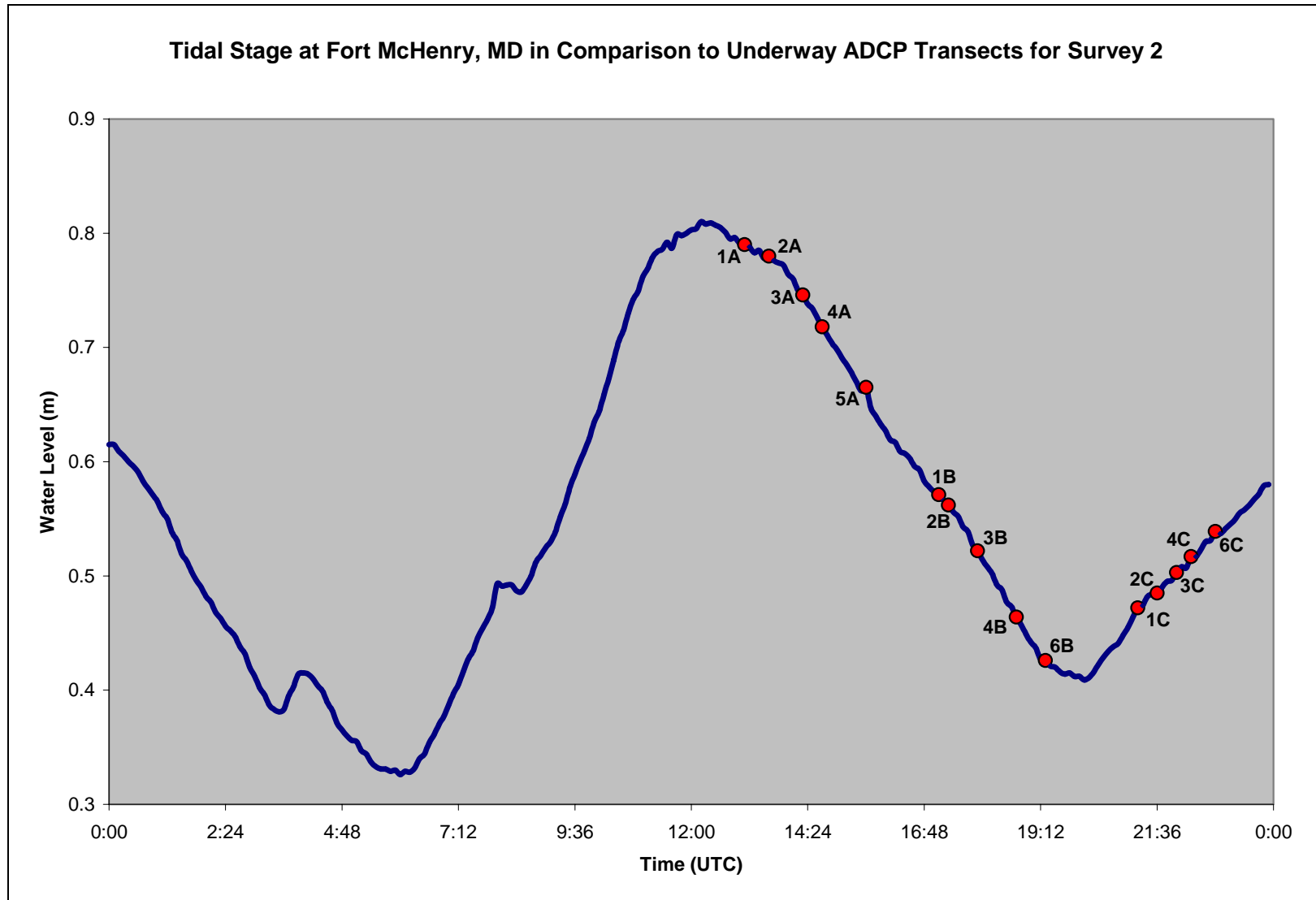
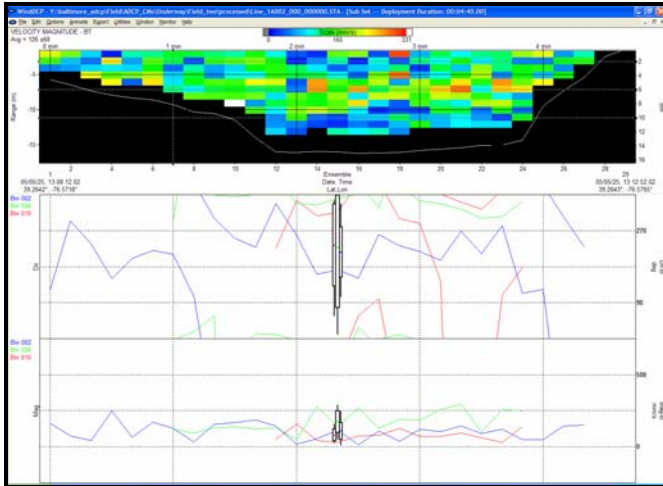
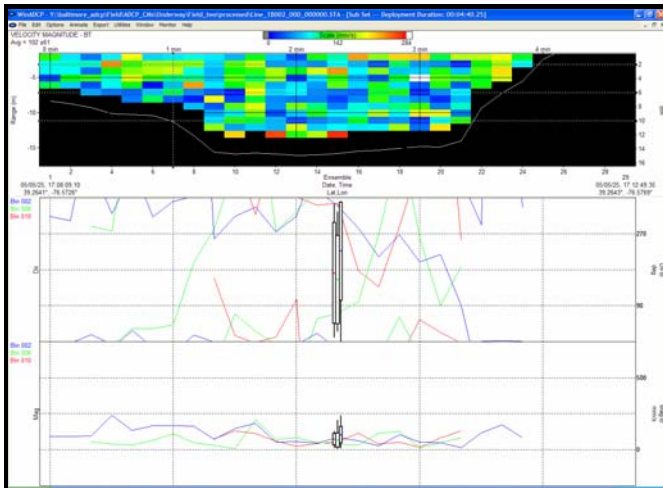


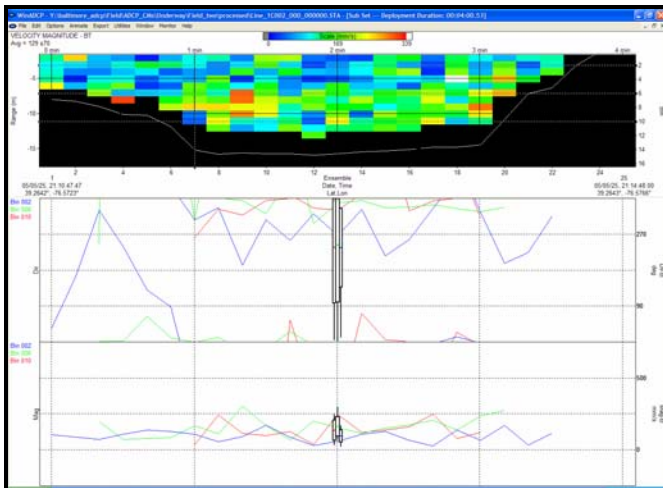
Figure 3.2-8. Indication of the Fort McHenry tidal stage relative to the underway ADCP transects that were conducted on 5/25/05.



Transect - 1A002
 Start Time: 13:08 GMT
 End Time: 13:13 GMT
 Line Heading – 270 True

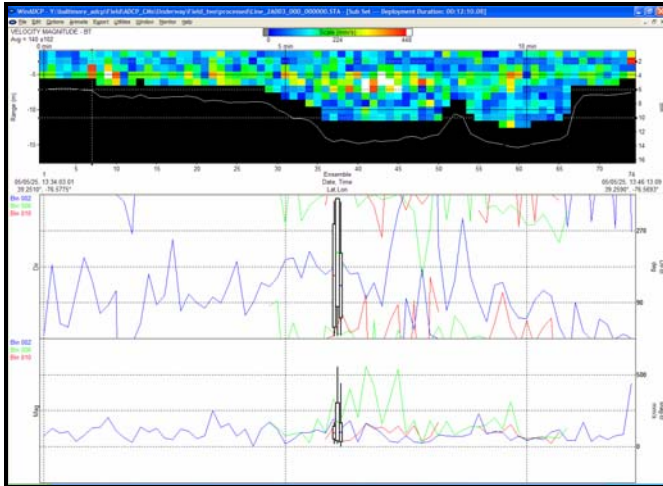


Transect – 1B002
 Start Time: 17:08 GMT
 End Time: 17:13 GMT
 Line Heading – 270 True

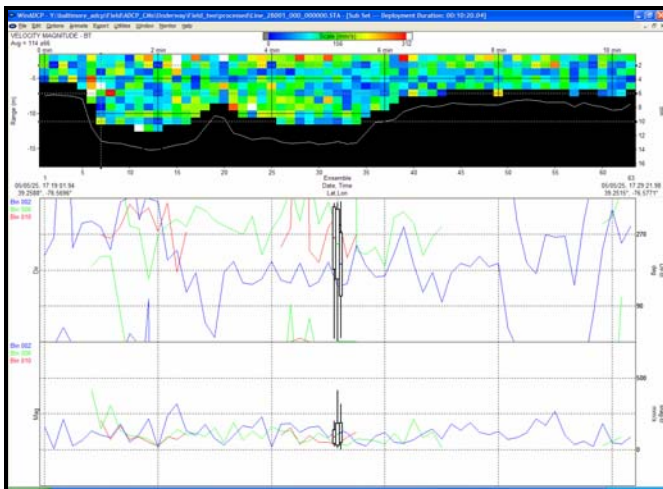


Transect – 1C002
 Start Time: 21:10 GMT
 End Time: 21:15 GMT
 Line Heading – 270 True

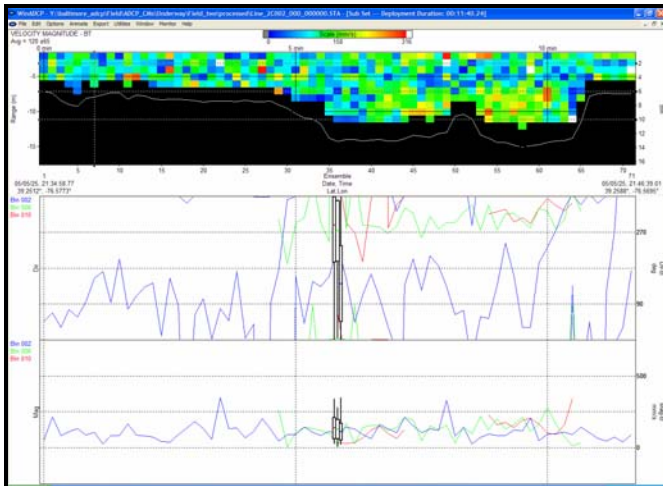
Figure 3.2-9. Current magnitude and direction along-track contour and profile results collected along underway ADCP Transect 1 on 5/25/05.



Transect - 2A003
 Start Time: 13:34 GMT
 End Time: 13:46 GMT
 Line Heading - 045 True

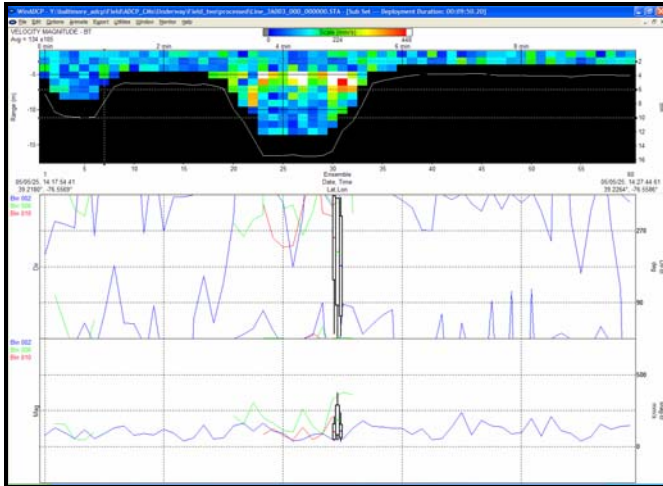


Transect - 2B001
 Start Time: 17:19 GMT
 End Time: 17:30 GMT
 Line Heading - 225 True

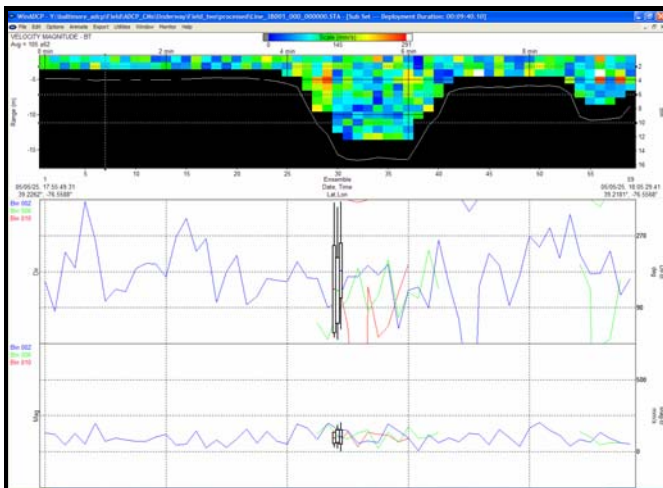


Transect - 2C002
 Start Time: 21:35 GMT
 End Time: 21:46 GMT
 Line Heading - 045 True

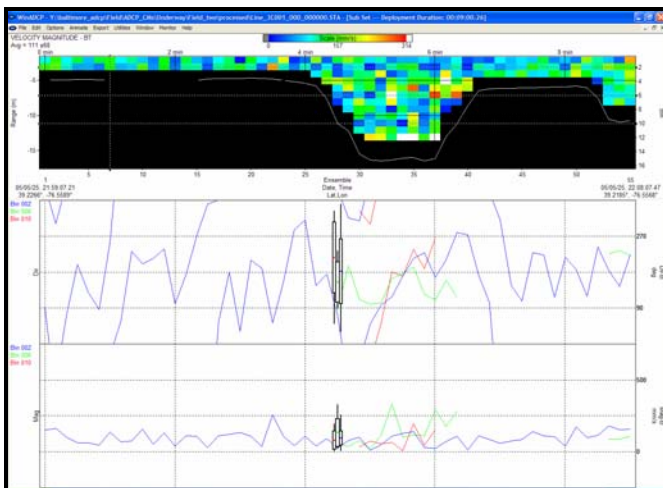
Figure 3.2-10. Current magnitude and direction along-track contour and profile results collected along underway ADCP Transect 2 on 5/25/05.



Transect – 3A003
 Start Time: 14:17 GMT
 End Time: 14:28 GMT
 Line Heading – 355 True

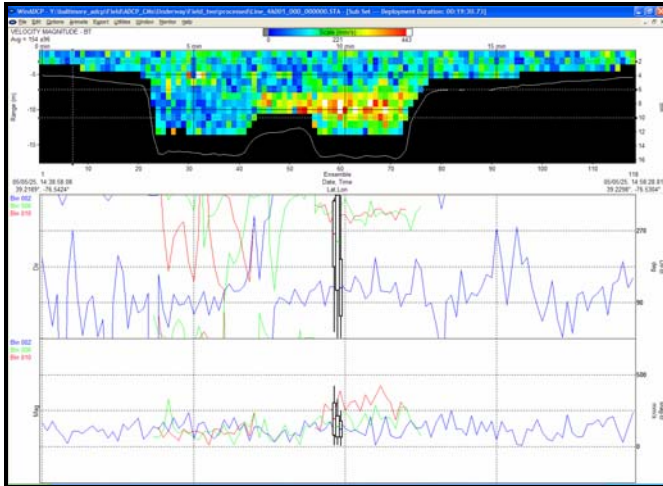


Transect – 3B001
 Start Time: 17:55 GMT
 End Time: 18:05 GMT
 Line Heading – 175 True

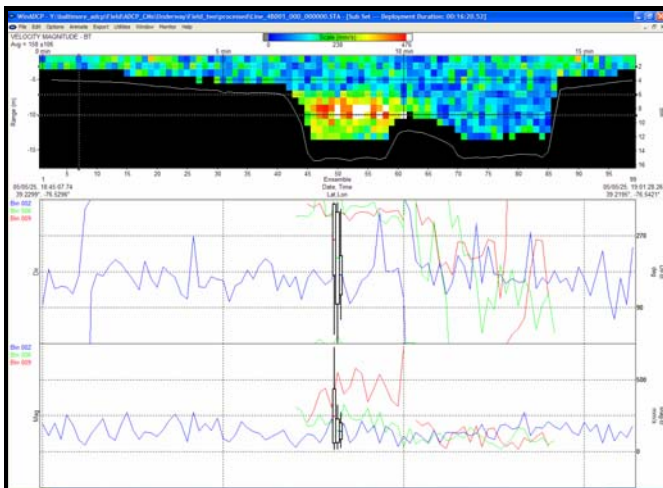


Transect – 3C001
 Start Time: 21:59 GMT
 End Time: 22:09 GMT
 Line Heading – 175 True

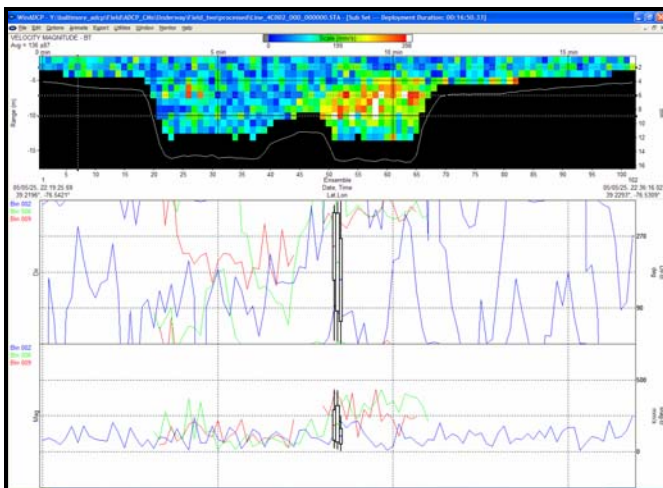
Figure 3.2-11. Current magnitude and direction along-track contour and profile results collected along underway ADCP Transect 3 on 5/25/05.



Transect – 4A001
 Start Time: 14:38 GMT
 End Time: 14:58 GMT
 Line Heading – 055 True

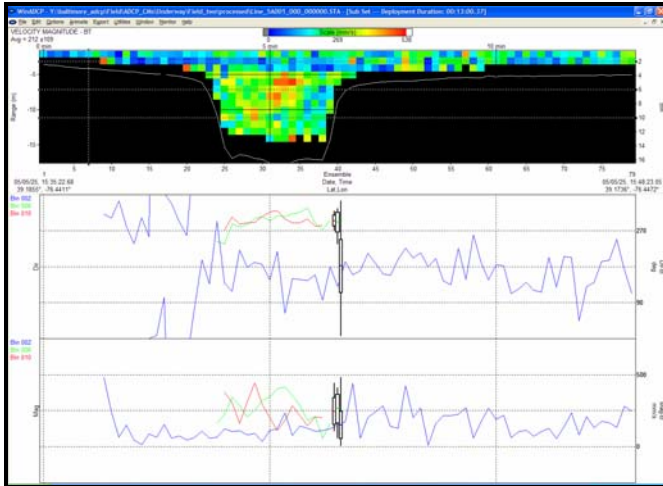


Transect – 4B001
 Start Time: 18:45 GMT
 End Time: 19:02 GMT
 Line Heading – 235 True

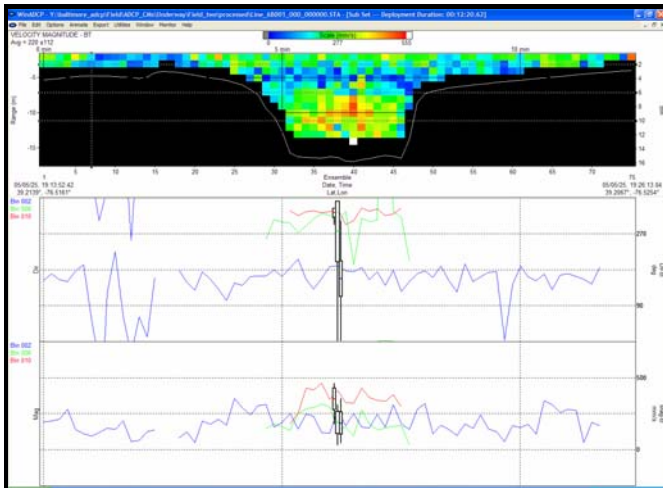


Transect – 4C002
 Start Time: 22:19 GMT
 End Time: 22:37 GMT
 Line Heading – 055 True

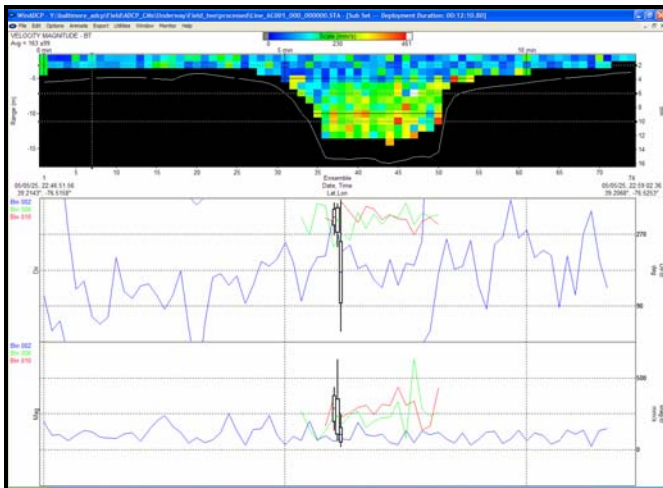
Figure 3.2-12. Current magnitude and direction along-track contour and profile results collected along underway ADCP Transect 4 on 5/25/05.



Transect – 5A001
 Start Time: 15:35 GMT
 End Time: 15:49 GMT
 Line Heading – 190 True



Transect – 6B001
 Start Time: 19:13 GMT
 End Time: 19:26 GMT
 Line Heading – 225 True



Transect – 6C001
 Start Time: 22:46 GMT
 End Time: 22:59 GMT
 Line Heading – 225 True

Figure 3.2-13. Current magnitude and direction along-track contour and profile results collected along underway ADCP Transects 5 and 6 on 5/25/05. Transect 6 was established further up the Harbor (near the Brewerton Angle) due to rough sea conditions along Transect 5.

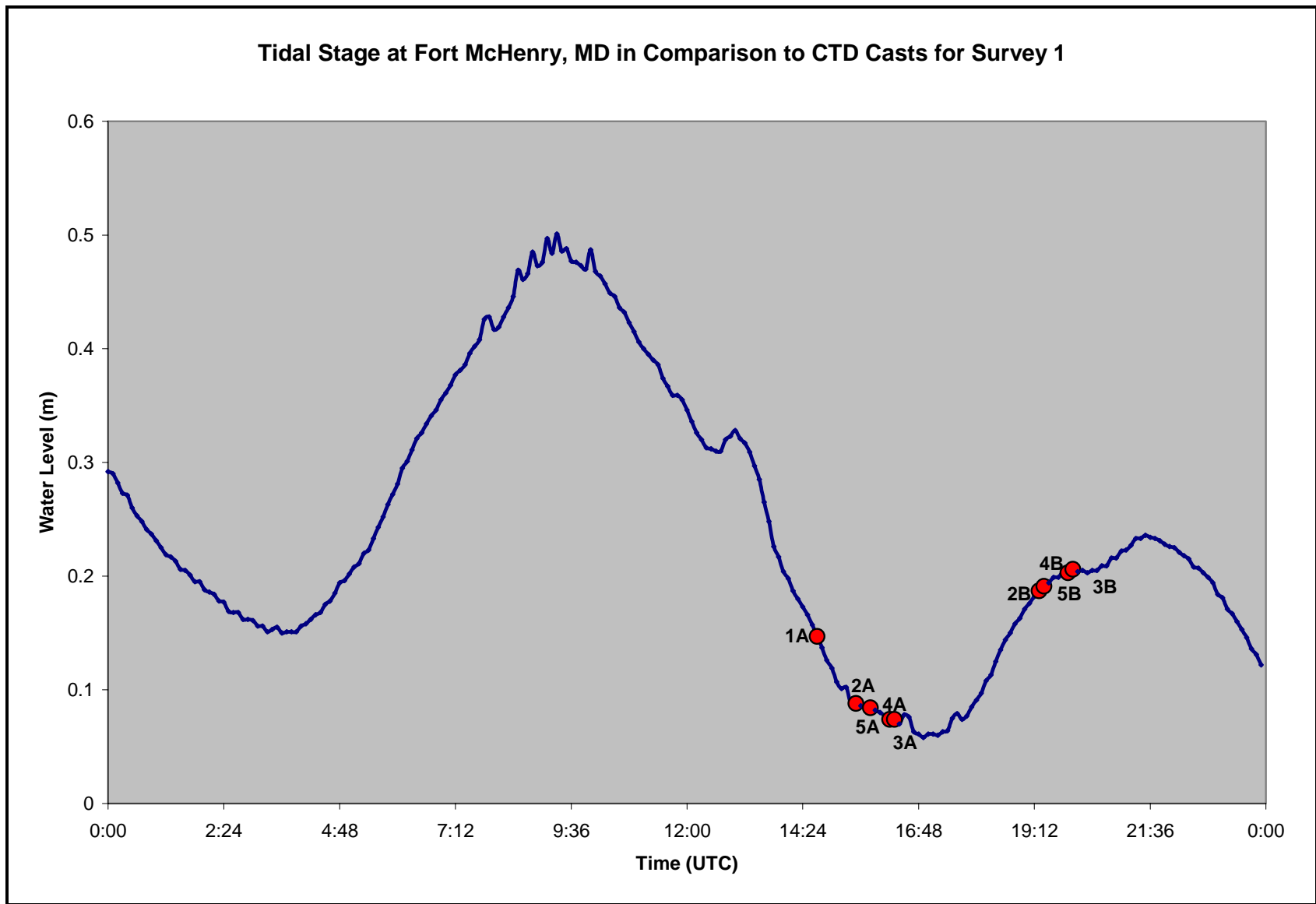


Figure 3.3-1. Indication of the Fort McHenry tidal stage relative to the CTD and water sample casts that were collected on 4/21/05

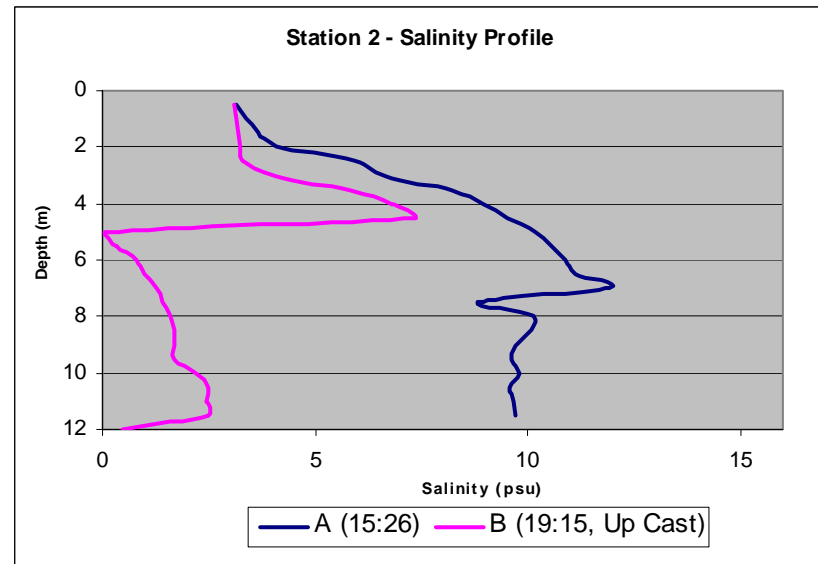
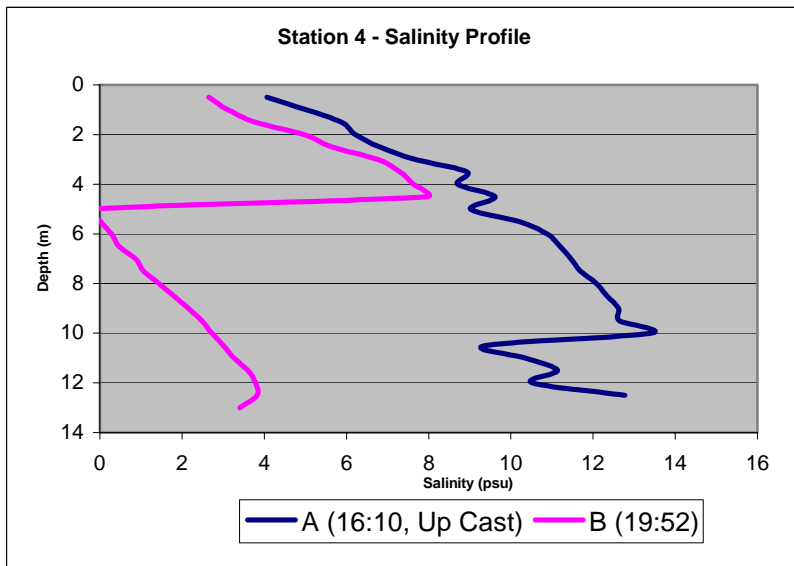
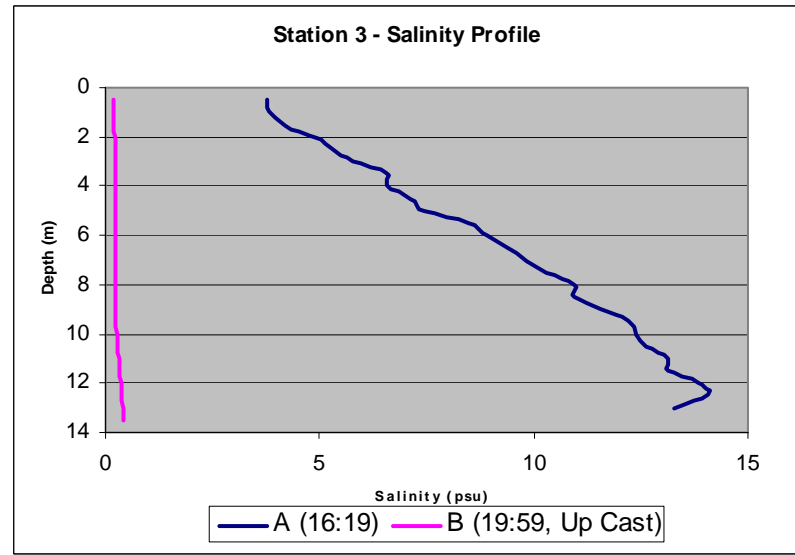
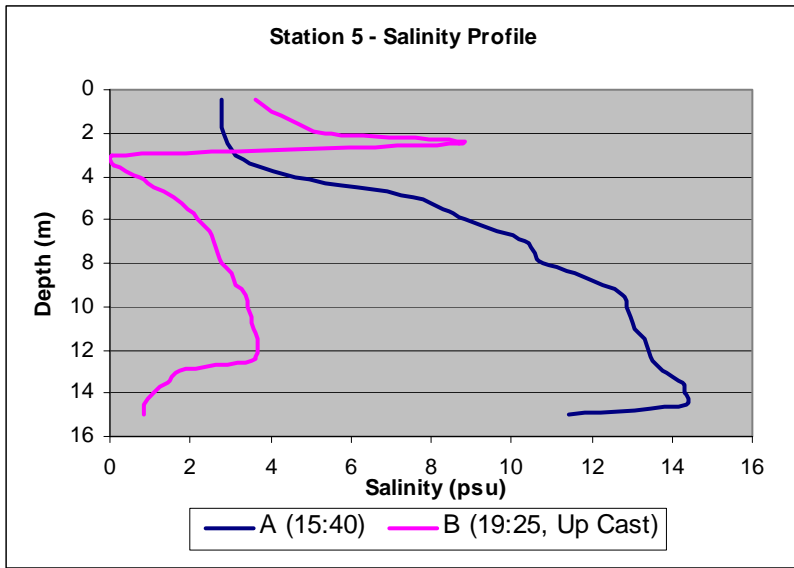


Figure 3.3-2. Salinity profile results from Stations 2, 3, 4, and 5 for the CTD casts collected on 4/21/05.

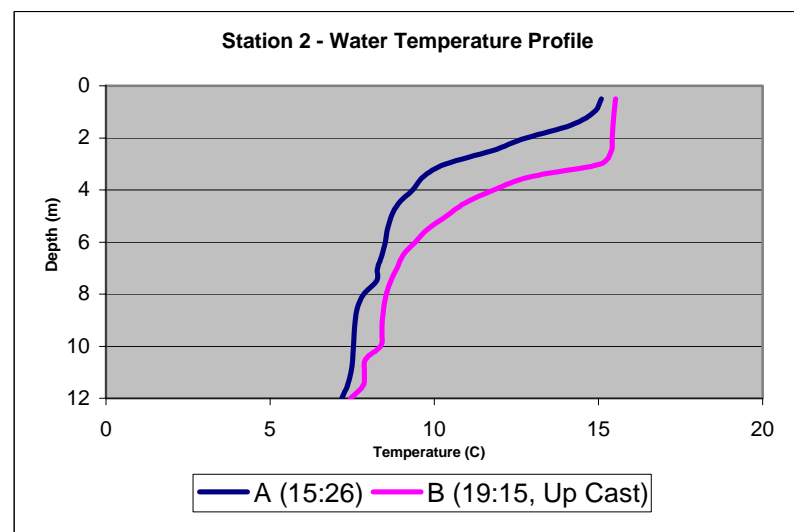
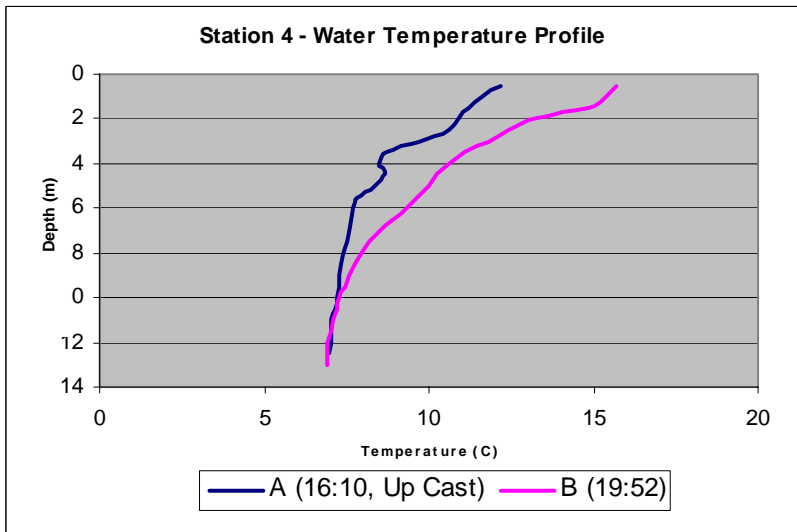
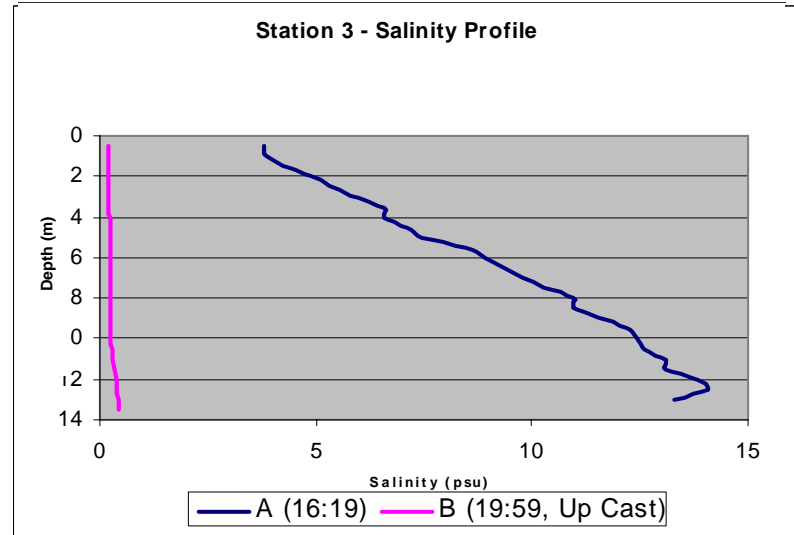
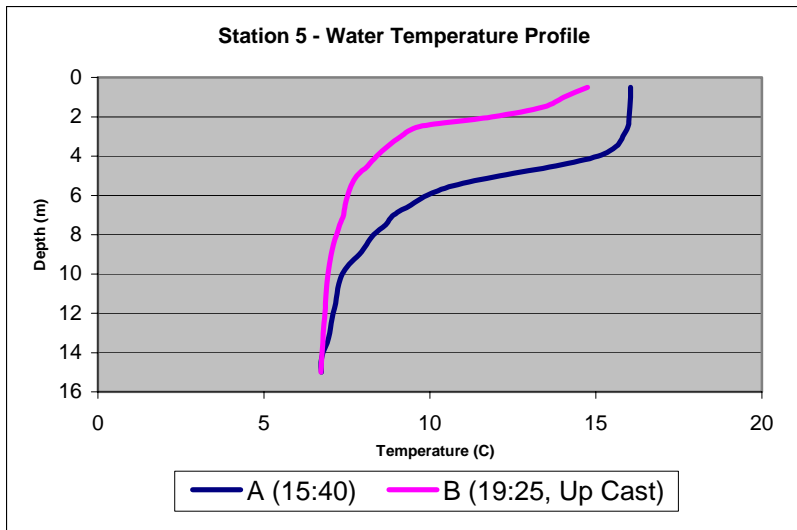


Figure 3.3-3. Water temperature profile results from Stations 2, 3, 4, and 5 for the CTD casts collected on 4/21/05.

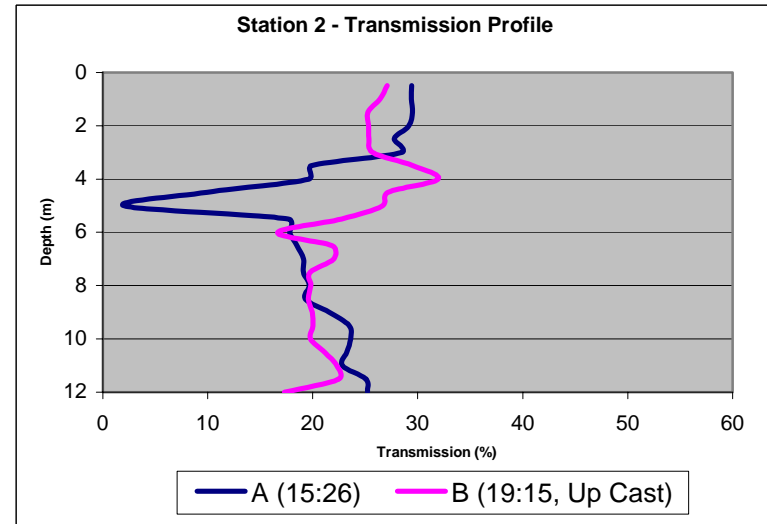
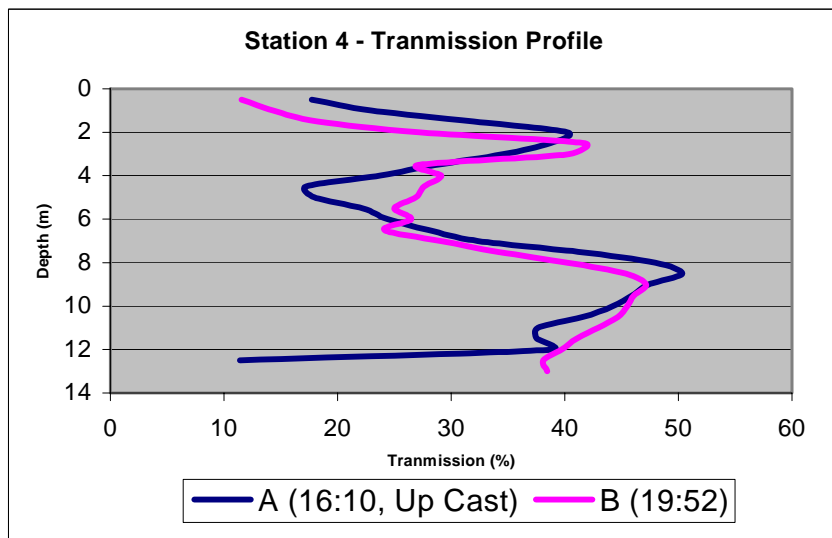
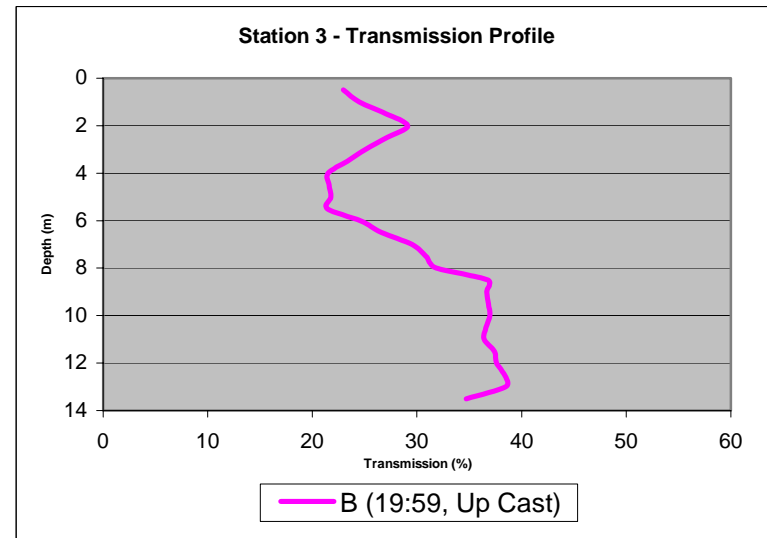
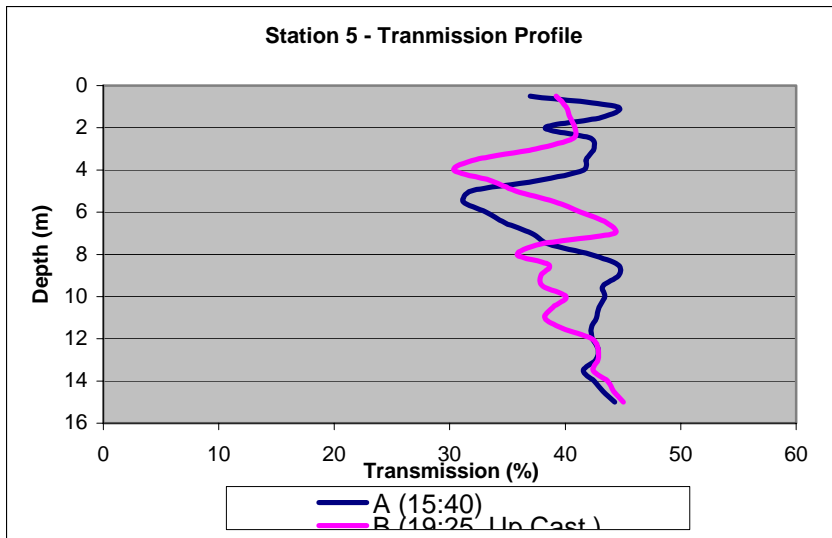


Figure 3.3-4. Transmissometer profile results from Stations 2, 3, 4, and 5 for the CTD casts collected on 4/21/05.

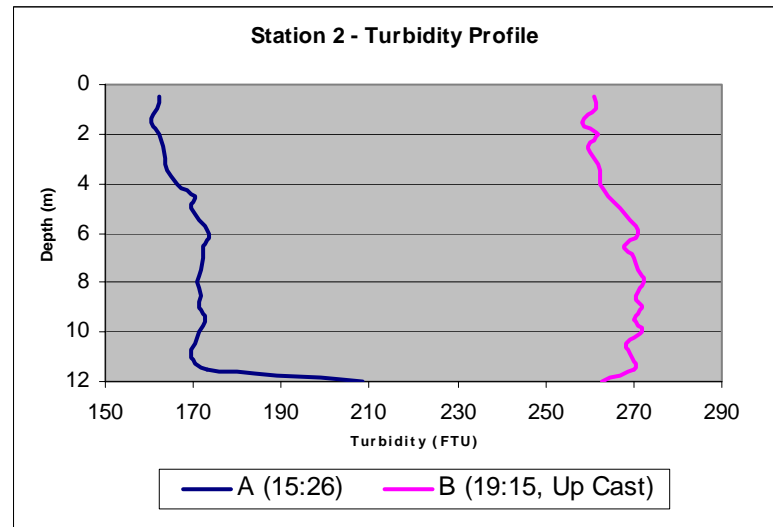
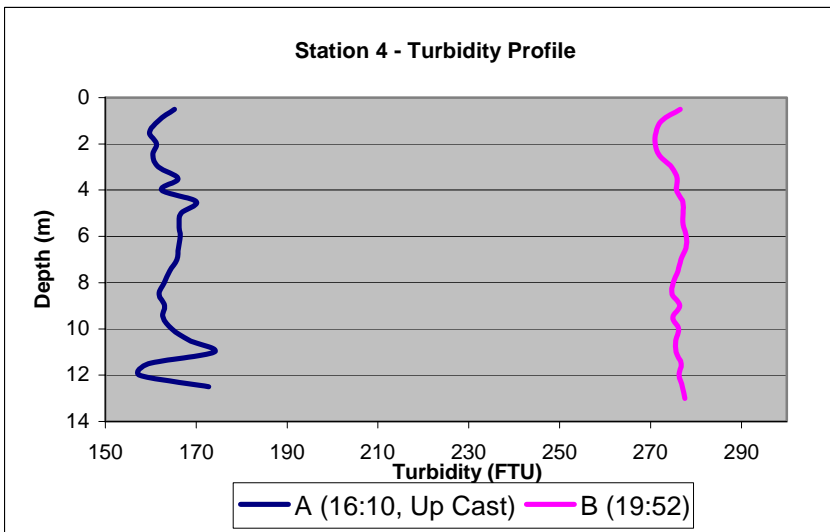
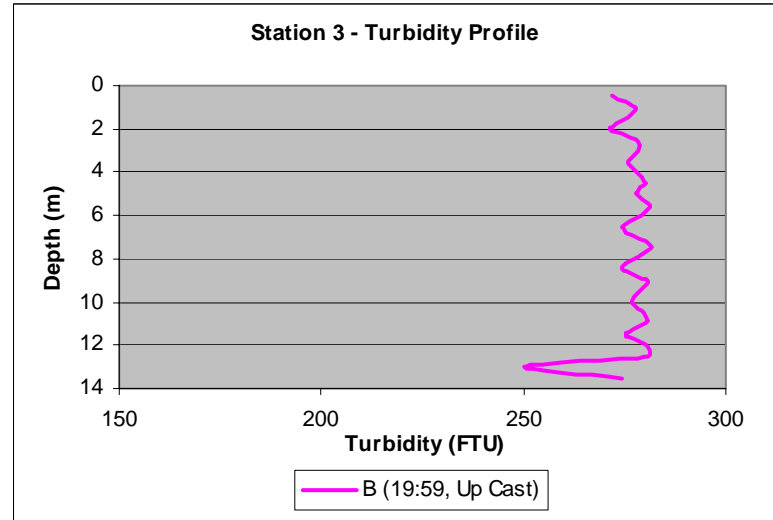
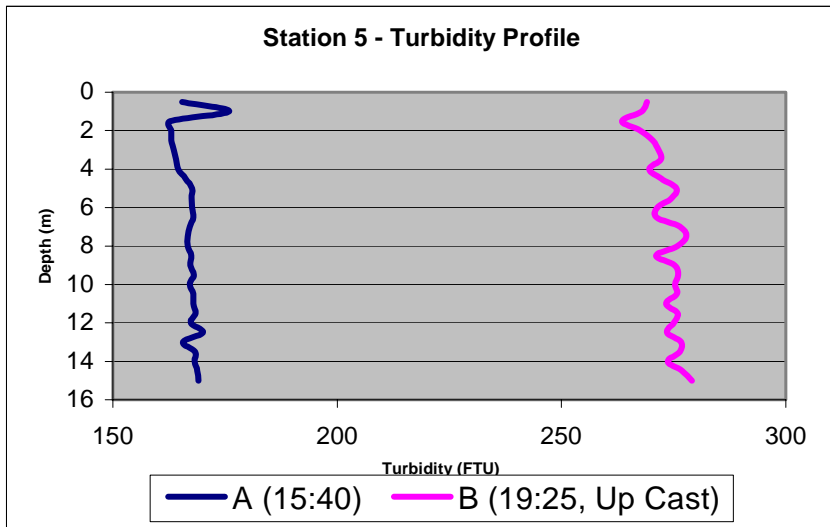


Figure 3.3-5. Turbidity profile results from Stations 2, 3, 4, and 5 for the CTD casts collected on 4/21/05.

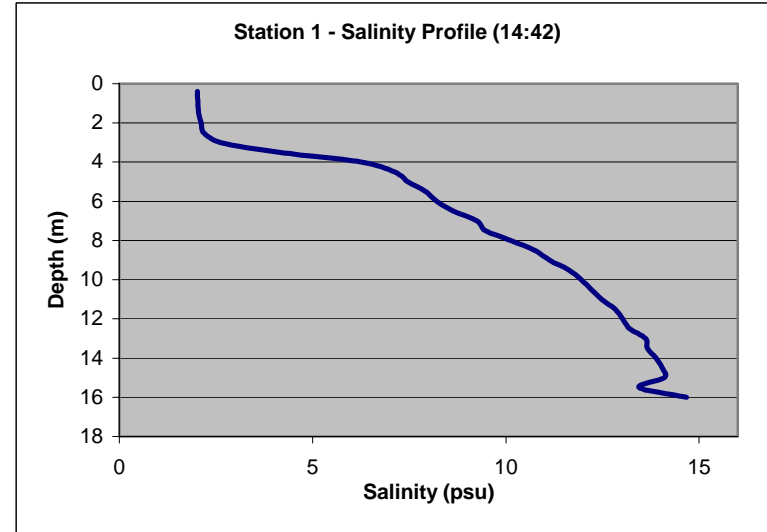
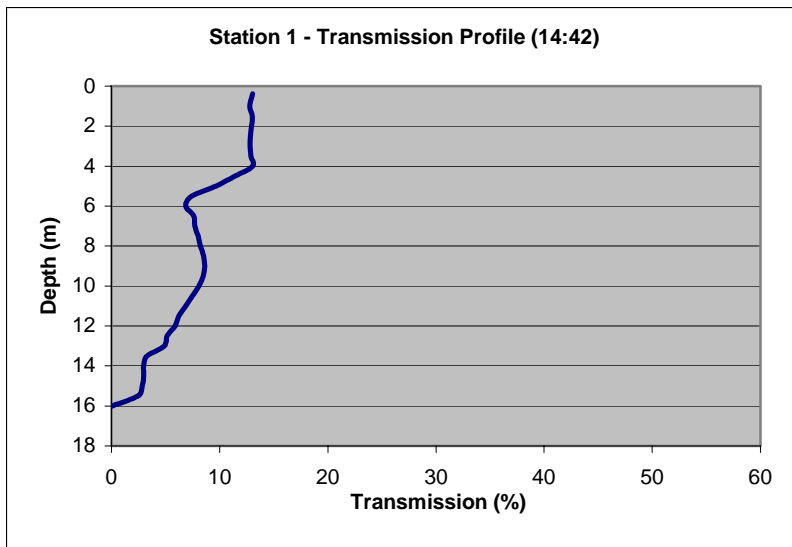
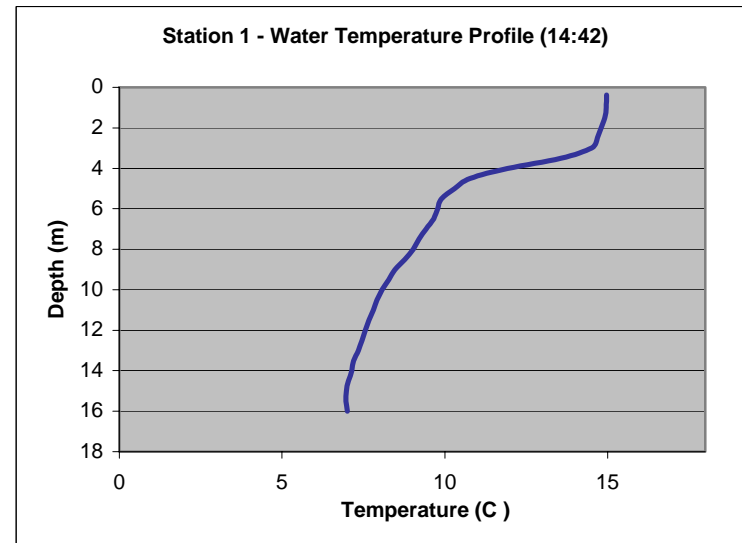
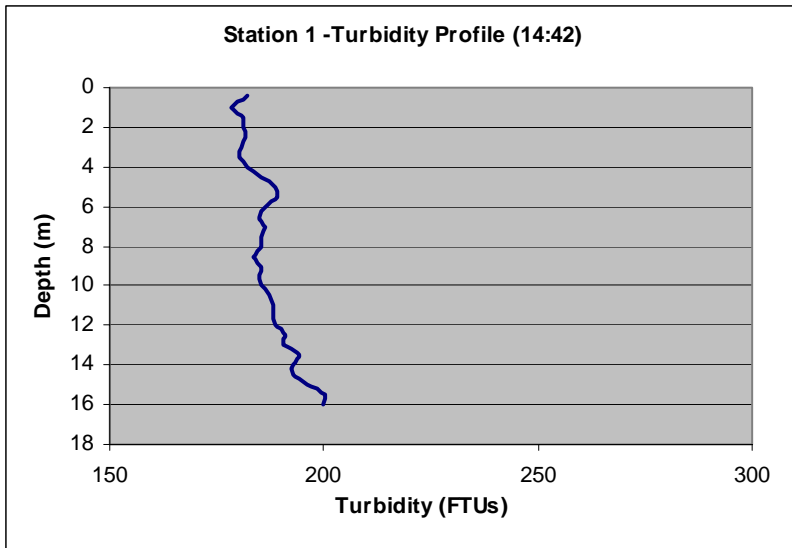


Figure 3.3-6. Turbidity, transmissometer, water temperature, and salinity profile results from Station 1 for the CTD cast collected on 4/21/05.

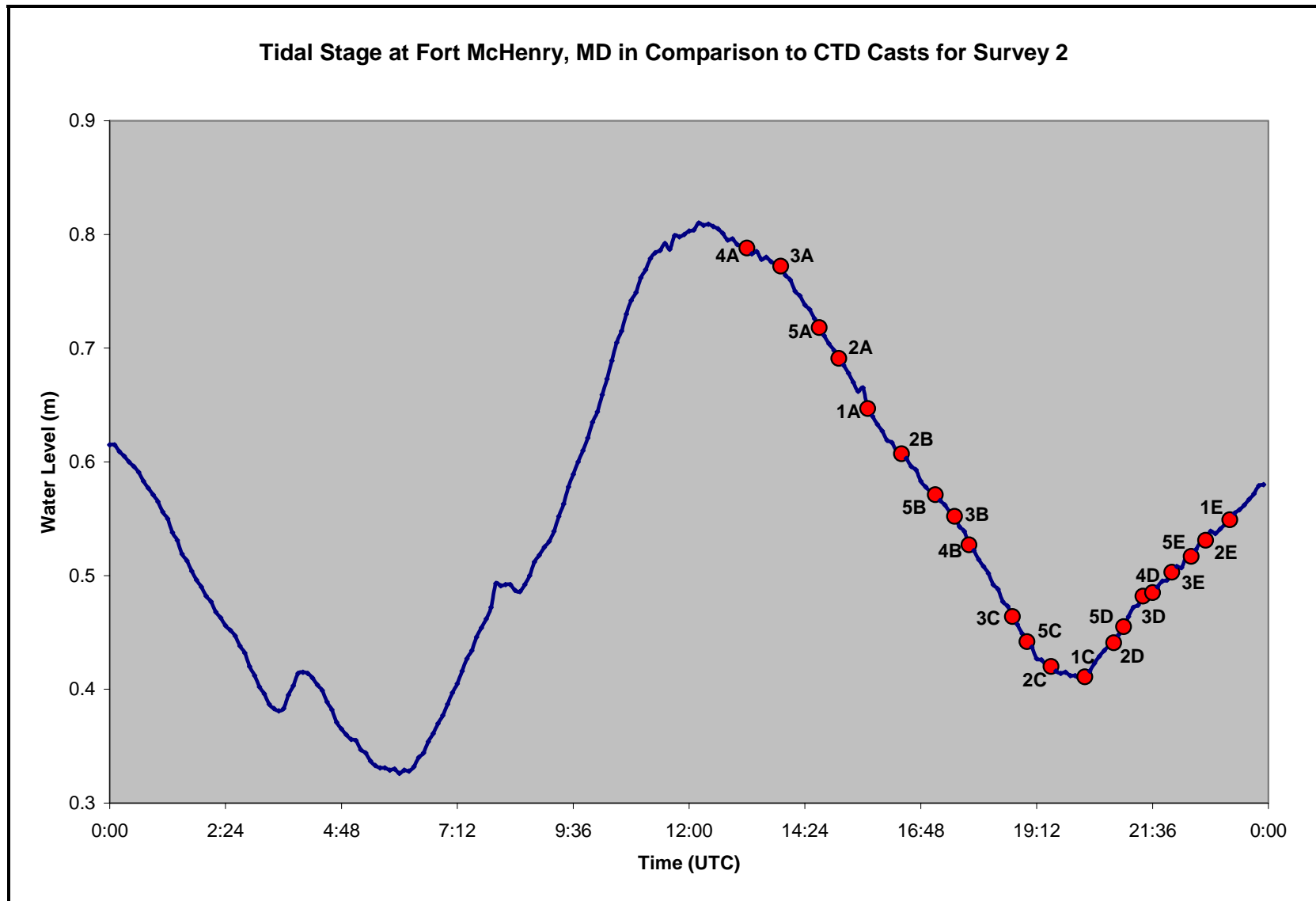


Figure 3.3-7. Indication of the Fort McHenry tidal stage relative to the CTD and water sample casts that were collected on 5/25/05

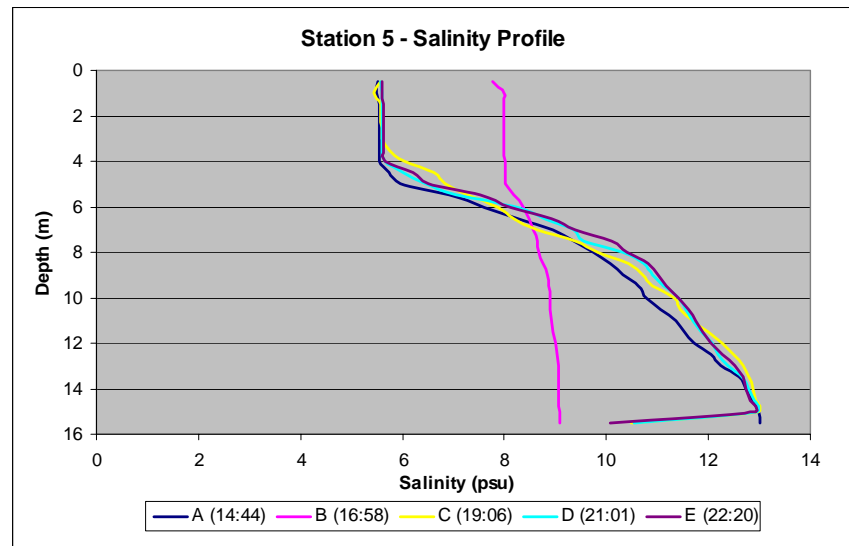
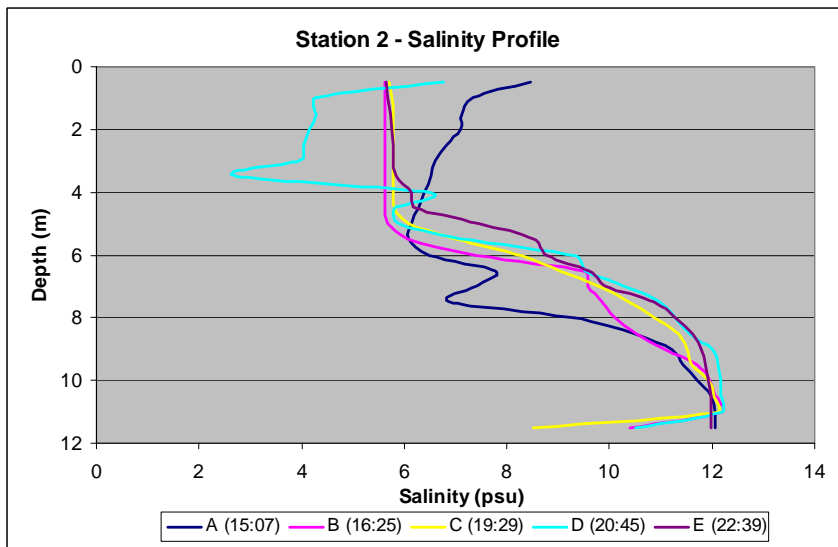
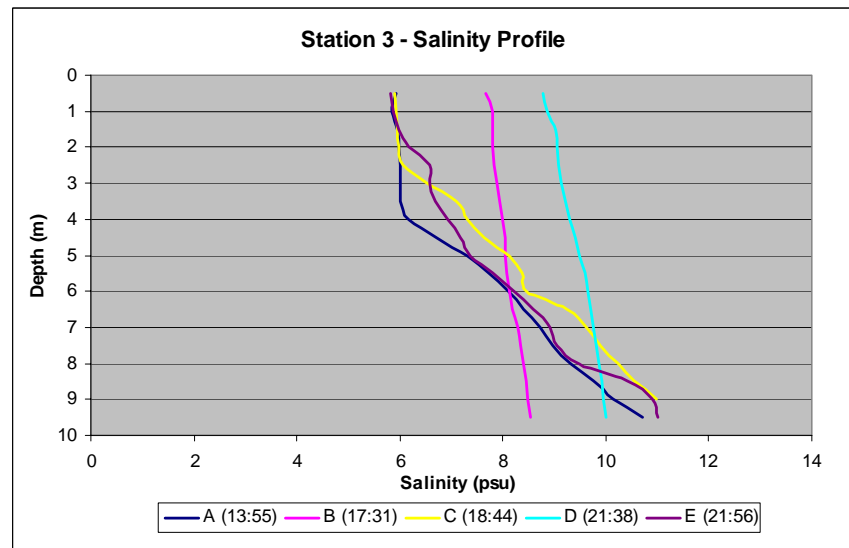
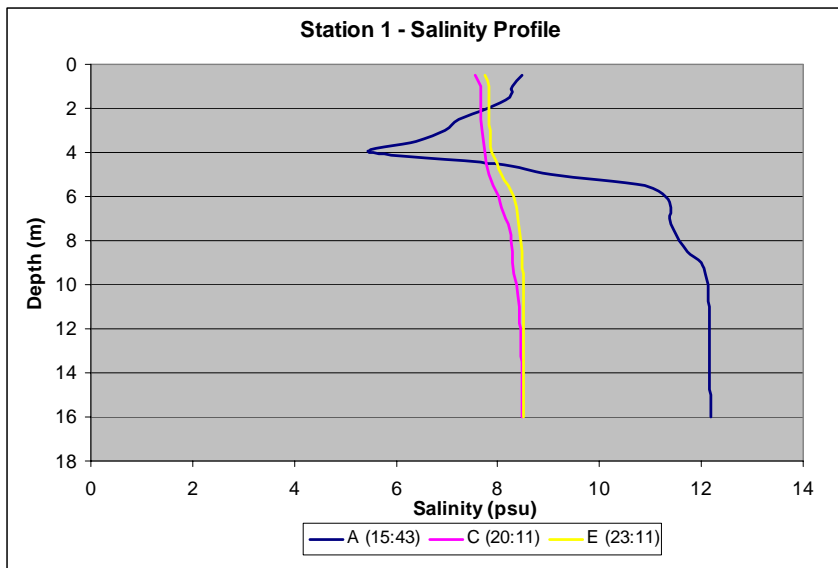


Figure 3.3-8. Salinity profile results from Stations 1, 2, 3, and 5 for the CTD casts collected on 5/25/05.

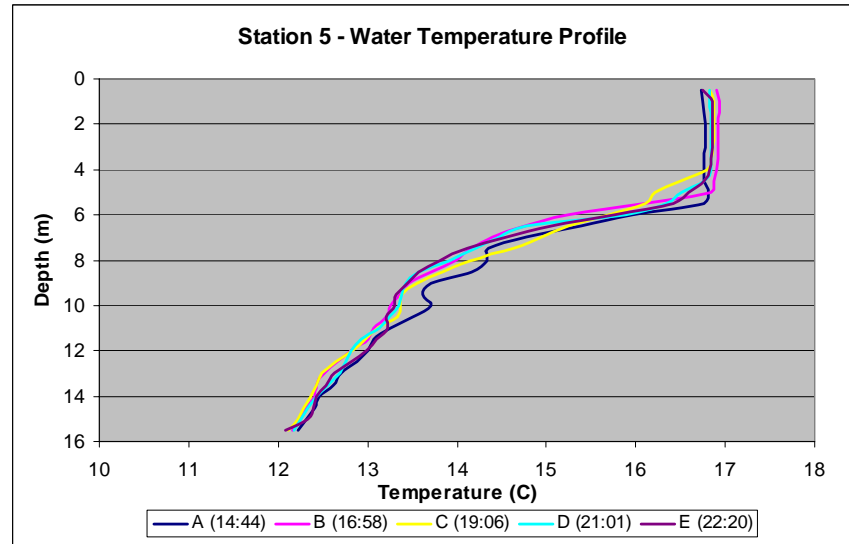
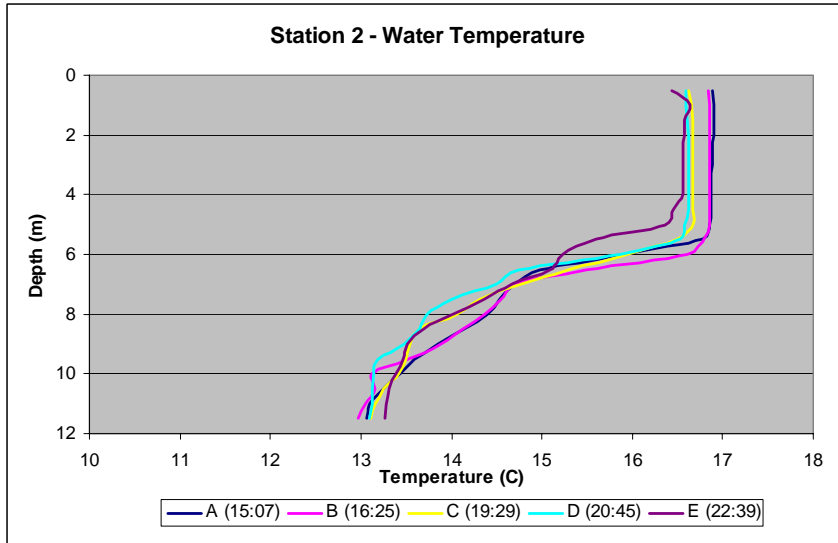
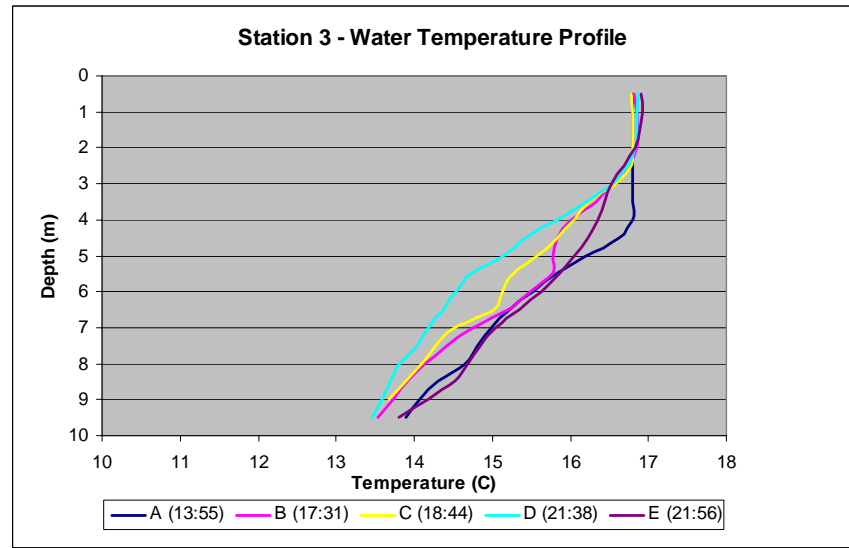
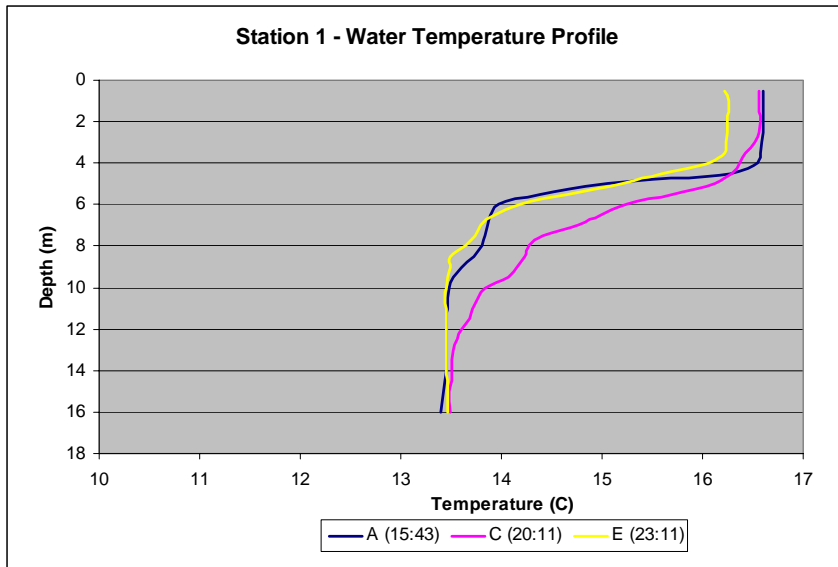


Figure 3.3-9. Water temperature profile results from Stations 1, 2, 3, and 5 for the CTD casts collected on 5/25/05.

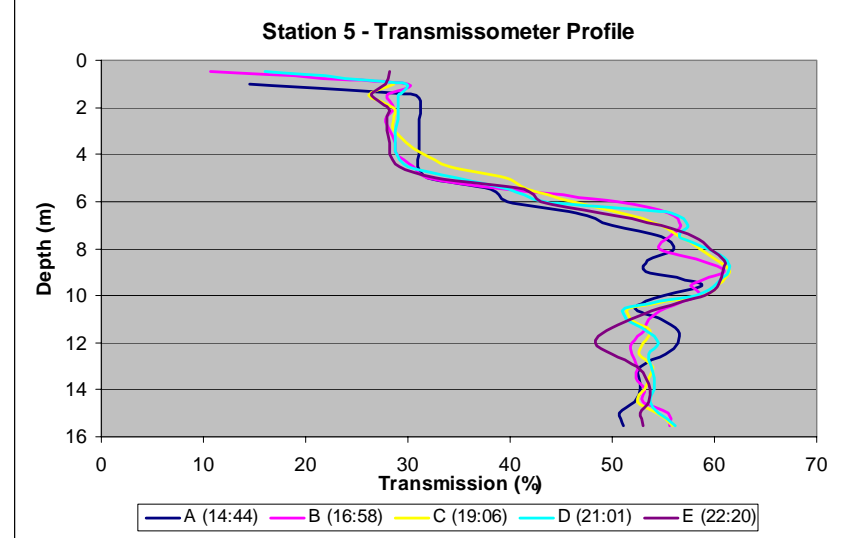
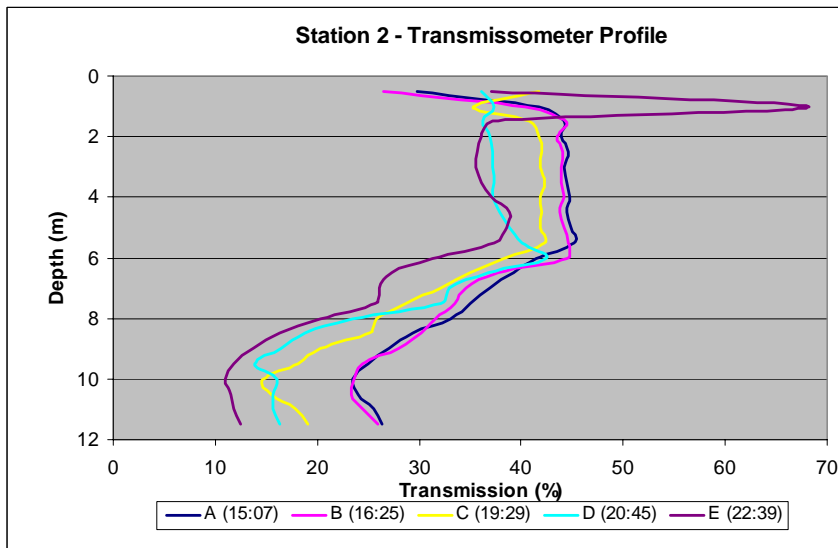
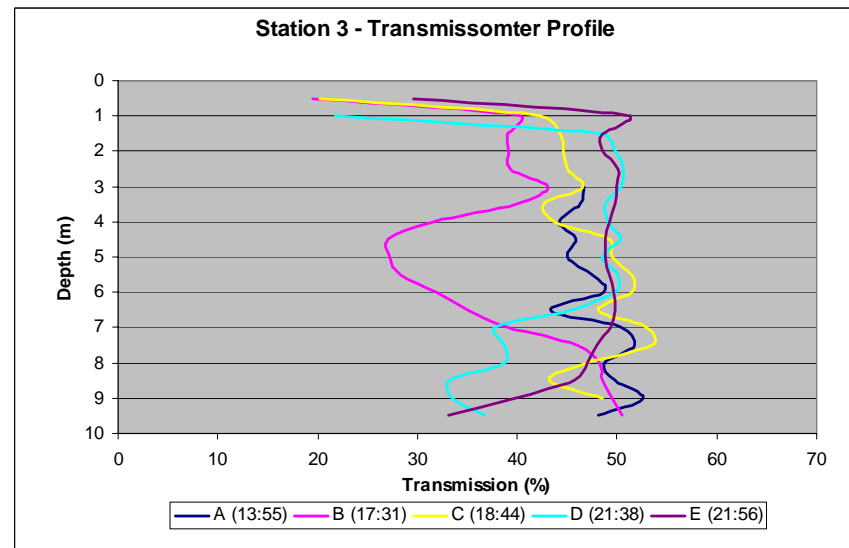
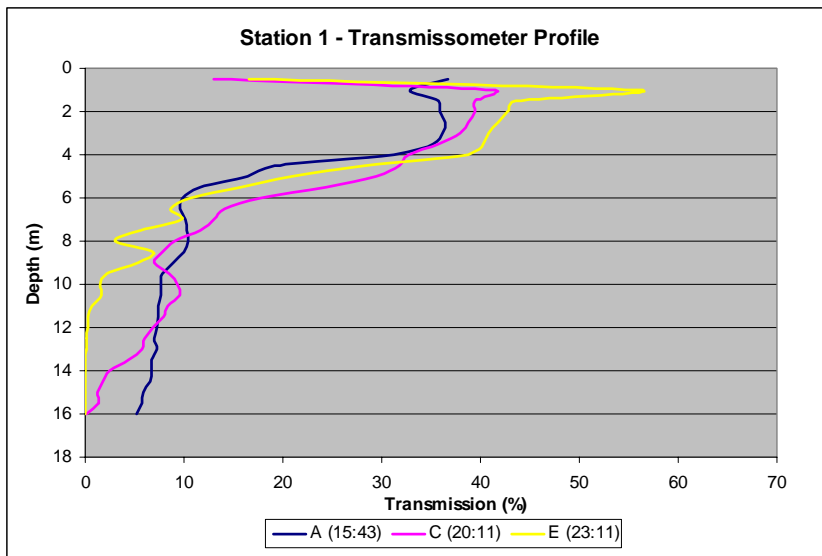


Figure 3.3-10. Transmissometer profile results from Stations 1, 2, 3, and 5 for the CTD casts collected on 5/25/05.

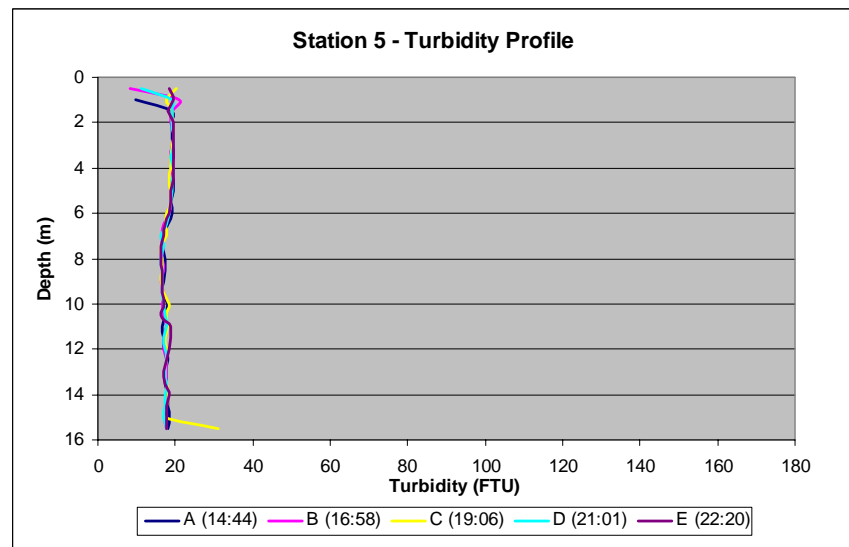
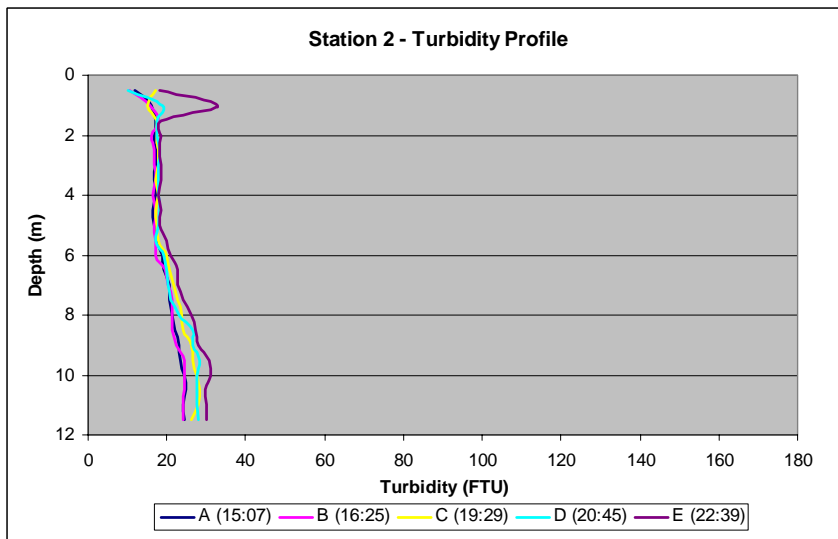
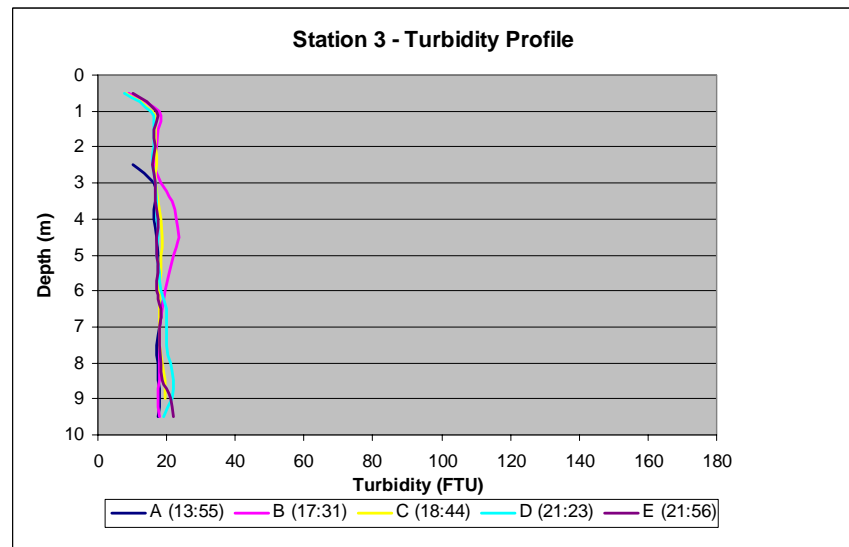
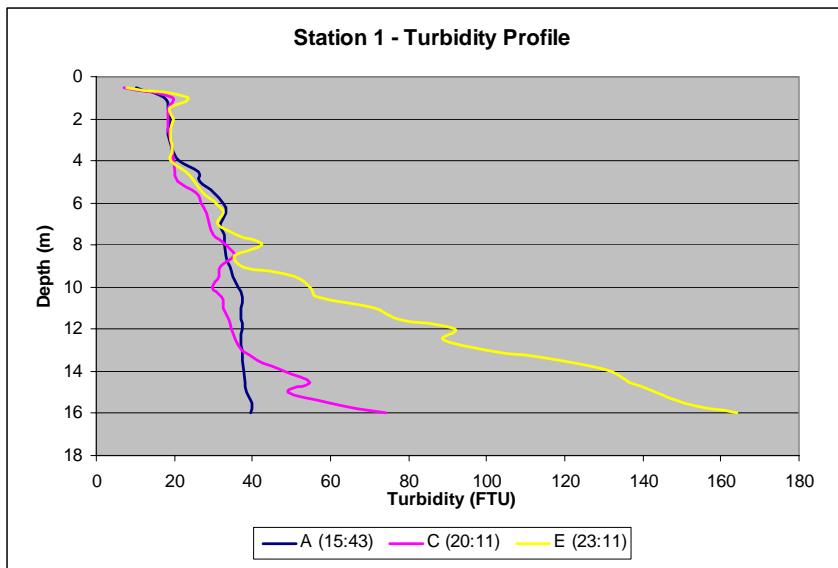


Figure 3.3-11. Turbidity profile results from Stations 1, 2, 3, and 5 for the CTD casts collected on 4/21/05.

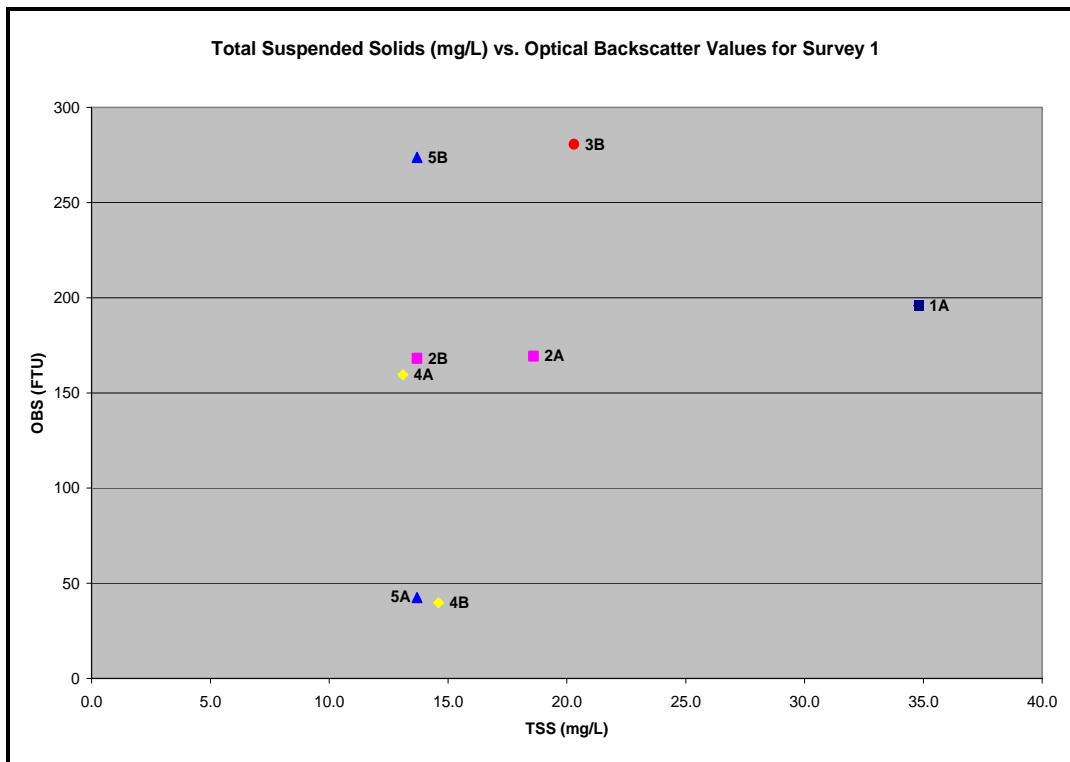
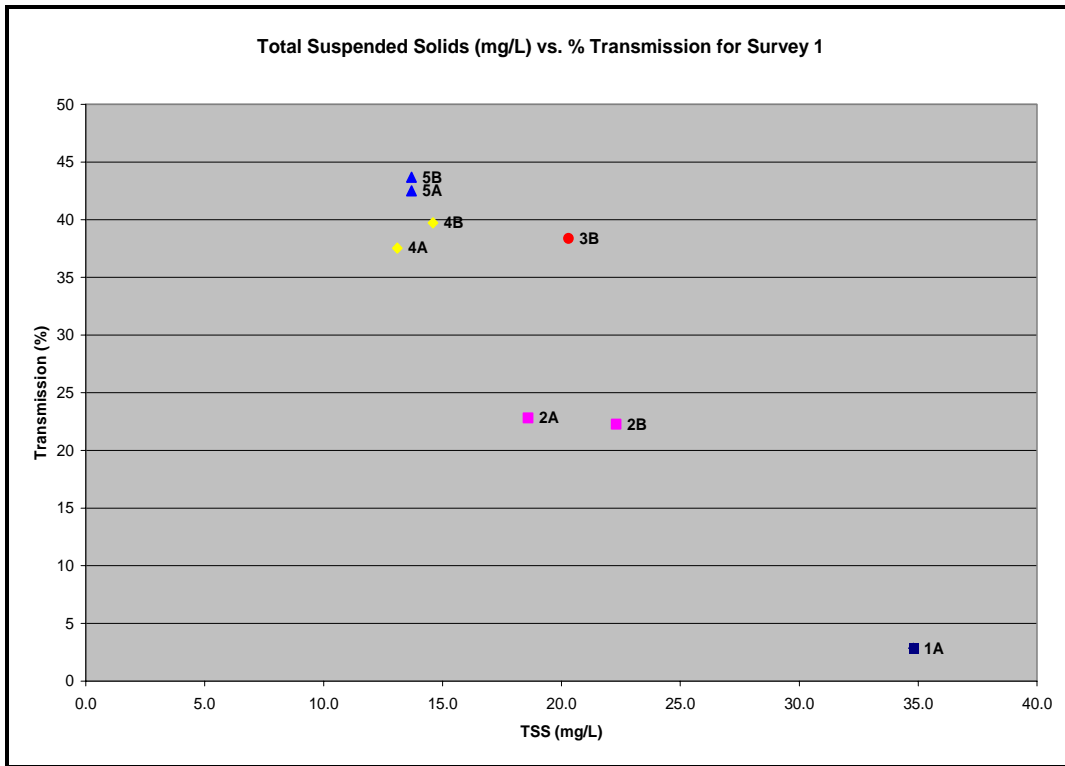


Figure 3.3-12 Total Suspended Solids (TSS) versus Turbidity and Transmission from the water samples and CTD profiles collected on 4/21/05.

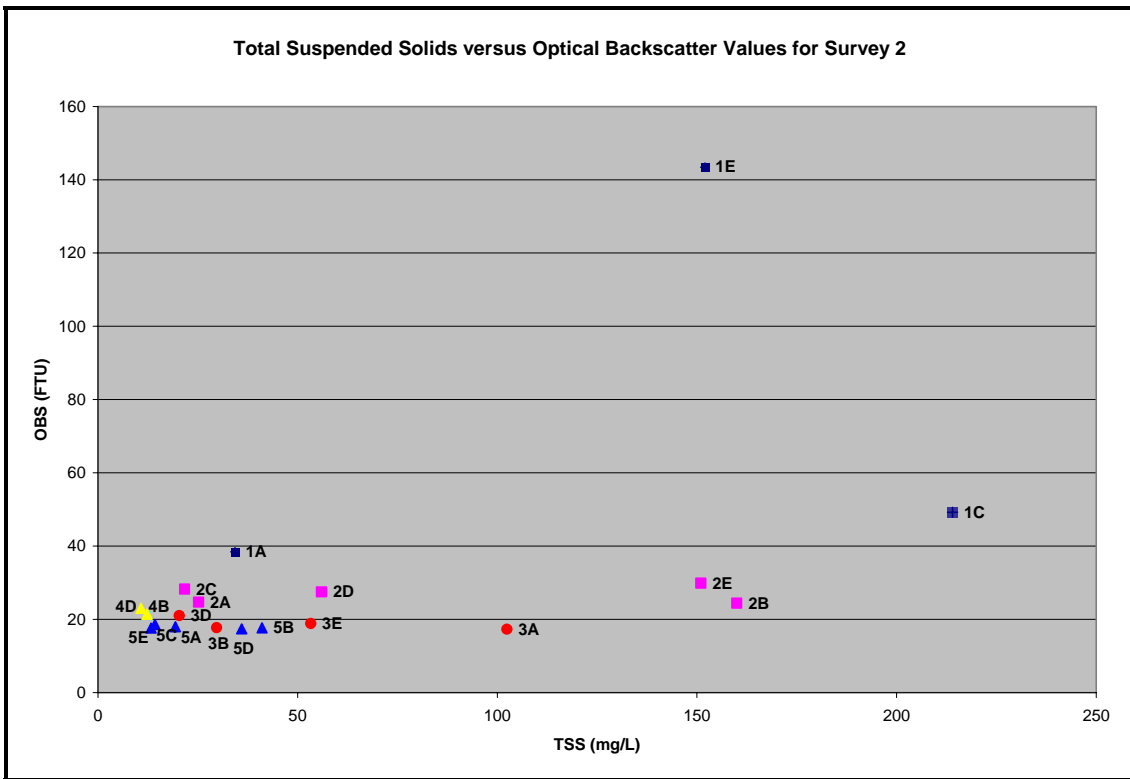
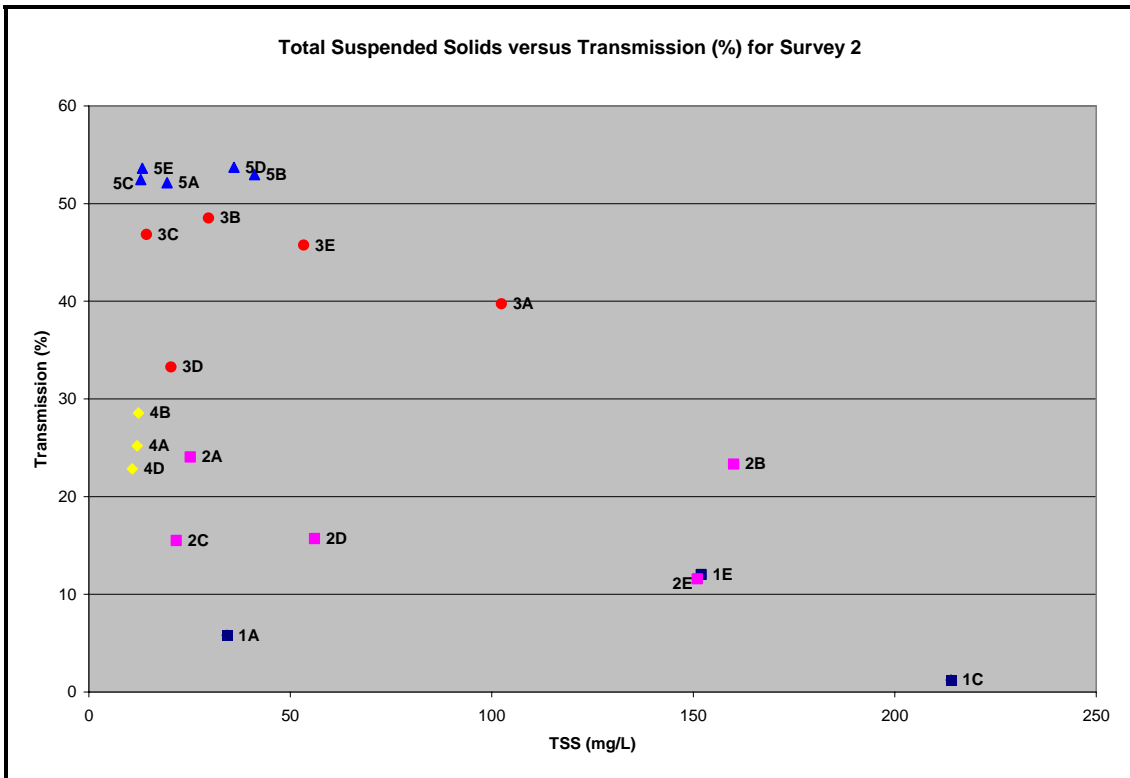


Figure 3.3-13 Total Suspended Solids (TSS) versus Turbidity and Transmission from the water samples and CTD profiles collected on 5/25/05.

THIS PAGE INTENTIONALLY LEFT BLANK

**Proposed Seagirt Borrow Patapsco River
Channels Hydrodynamics and Modeling
Presentation
and
Proposed Channel Depths Presentation
to
the Bay Enhancement Working Group**

THIS PAGE INTENTIONALLY LEFT BLANK



Masonville Dredged Material Containment Facility

Proposed Seagirt Borrow: Patapsco River
Channels Hydrodynamics and Modeling

Presented to:

Bay Enhancement Working Group

*Maryland Port Administration
December 5, 2006*

THE CHESAPEAKE BAY INSTITUTE
THE JOHNS HOPKINS UNIVERSITY

BULLETIN 1

A HYDRODYNAMIC STUDY OF THE BALTIMORE HARBOR SYSTEM

I. OBSERVATIONS ON THE CIRCULATION AND MIXING IN BALTIMORE HARBOR

by

William C. Boicourt and Peter L. Olson

This work contains results of work carried out for the State of Maryland, Department of Natural Resources, Water Resources Administration and Department of Health and Mental Hygiene, Office of Environmental Programs.

This report does not necessarily constitute final publication of the material presented.

Reference 82-10
October 1982

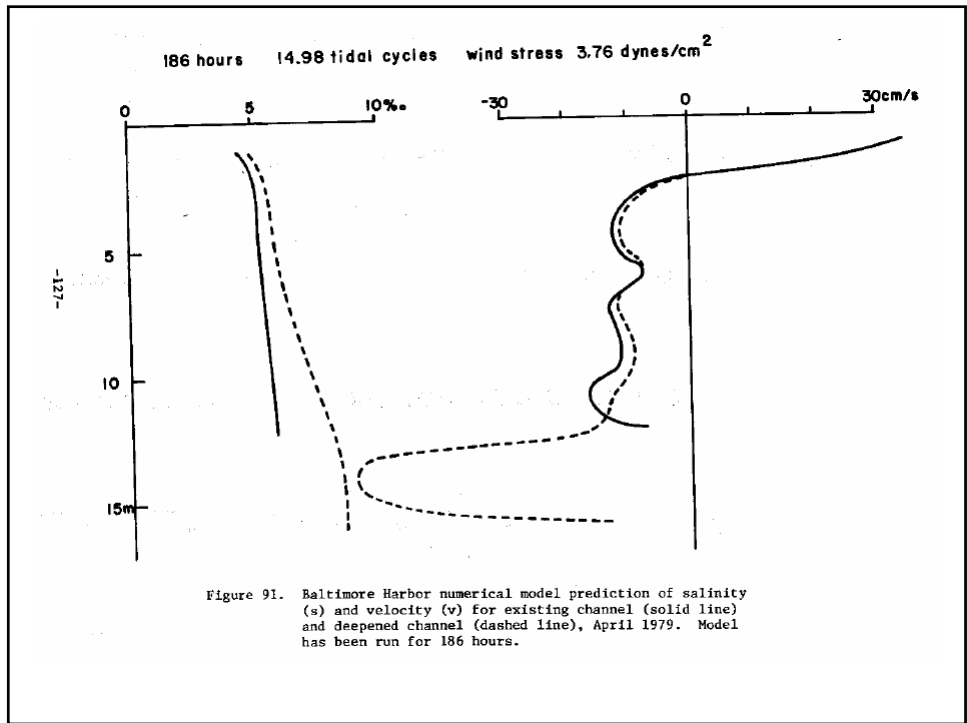
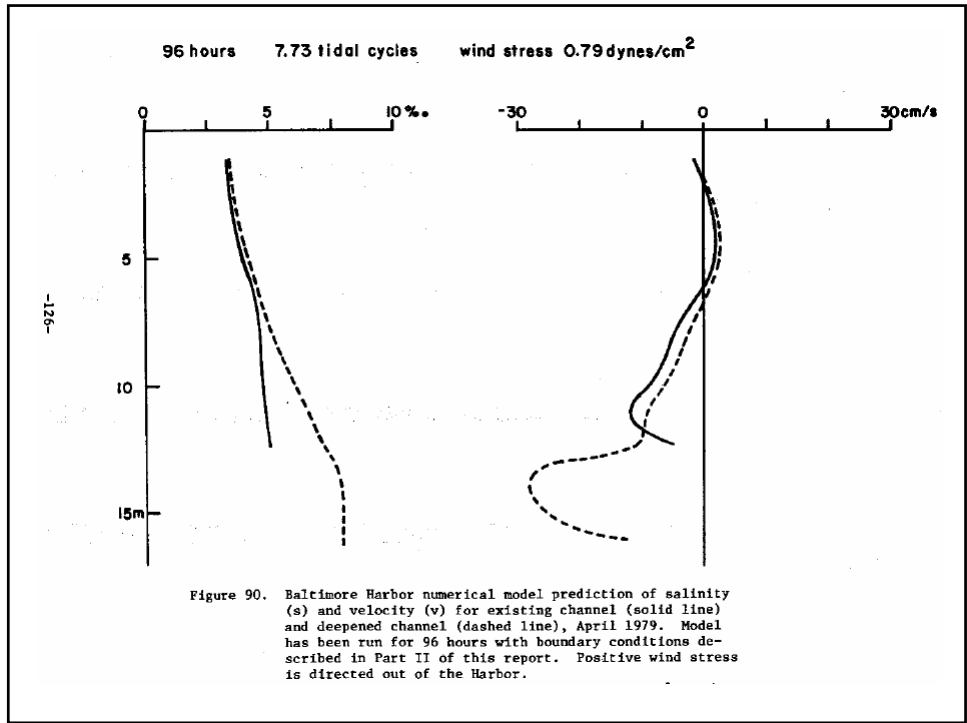
W. R. Taylor
Director

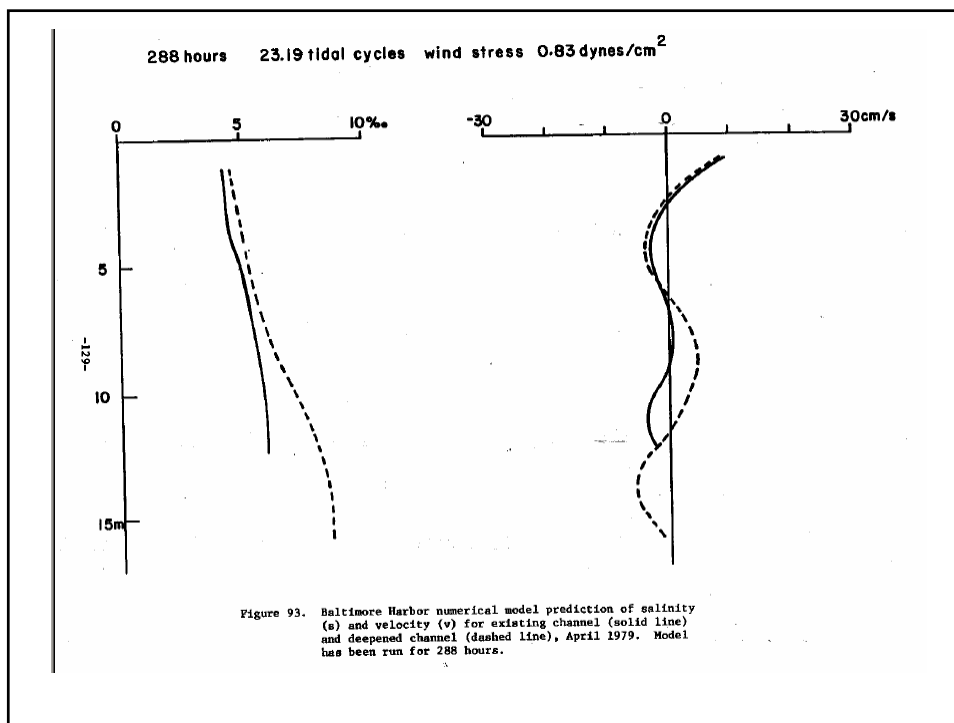
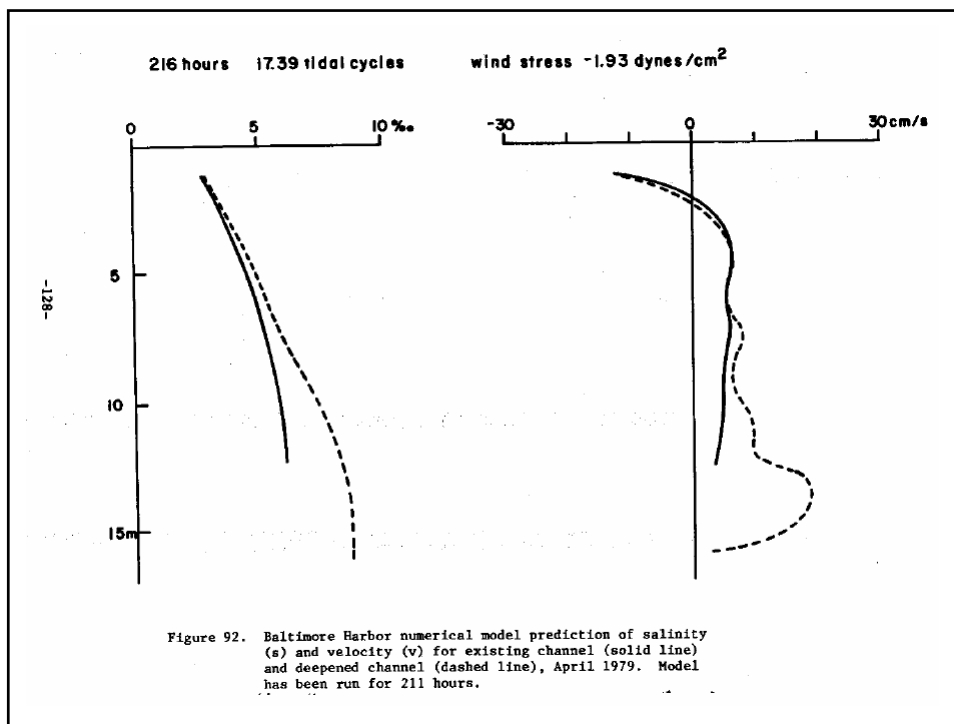
E. Channel Deepening and Lateral Homogeneity

... purposes of assessing the effects of the proposed deepening of the Baltimore Harbor navigation channels to the depth of 55 ft.

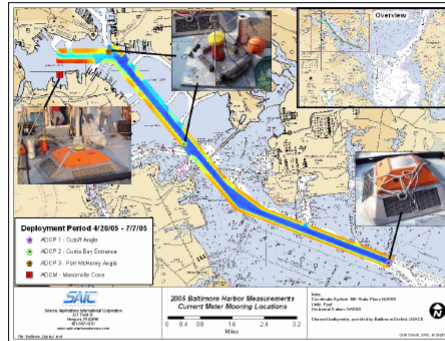
The primary result of channel deepening is to increase both the salt penetration into the Harbor, and the strength of the Harbor circulation. The reasons for this increase are described in Hansen and Festa (1976) and in Part II. The estuarine Rayleigh number R_a is the controlling parameter here. An increase in depth of the channel with a given density difference at the Outer Harbor boundary translates into a greater cross-sectional area through which to drive high-salinity water in the lower layer with approximately the same pressure-gradient force. At any point in the Harbor, the strength of the mixing-induced circulation is dependent on the vertical salt difference, and hence, there is an increase in the circulation velocity with the deepened channel. In addition, deepening the channel has the effect of lowering the influence of bottom friction on the inflowing water in the lowest layer.

5) The model has the capability of simulating effects due to a deepened harbor channel. We have carried out a sample, test-run of this capability using the same April, 1979 forcing data. Our results indicate no fundamental change in the structure of the circulation. The flow is dominated once again by the three-layer density driven component and by a two-layer flow characteristic of local wind forcing. The effect of increased channel depth on the circulation seems to be limited to an increase in velocity of about 10 to 20%. There is a more noticeable change in the salinity structure. Increased channel depth from 13 to 16.6 meters tends to increase the salinity by 25 to 35%. Most of this change is accommodated by an increase in the salinity in the deepened part of the channel; that is, the lowest 3 meters.





**DATA REPORT FOR THE
2005 WATER COLUMN MEASUREMENT PROGRAM
IN THE PATAPSCO RIVER, BALTIMORE HARBOR**

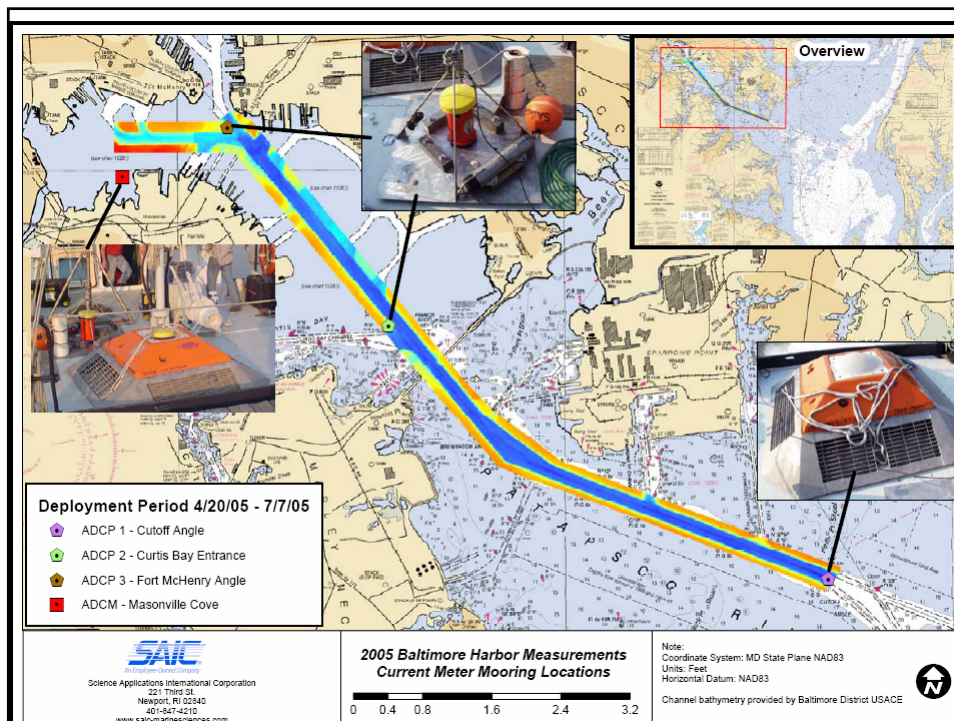


Prepared by:
Science Applications International Corporation
Admiral's Gate
221 Third Street
Newport, RI 02840

Prepared for:
Moffatt & Nichol
2700 Lighthouse Point East
Suite 501
Baltimore, MD 21224

September 2005
Contract No: 520820C
SAIC Project No. 01-0440-00-8918-500

SAIC REPORT NO. 695



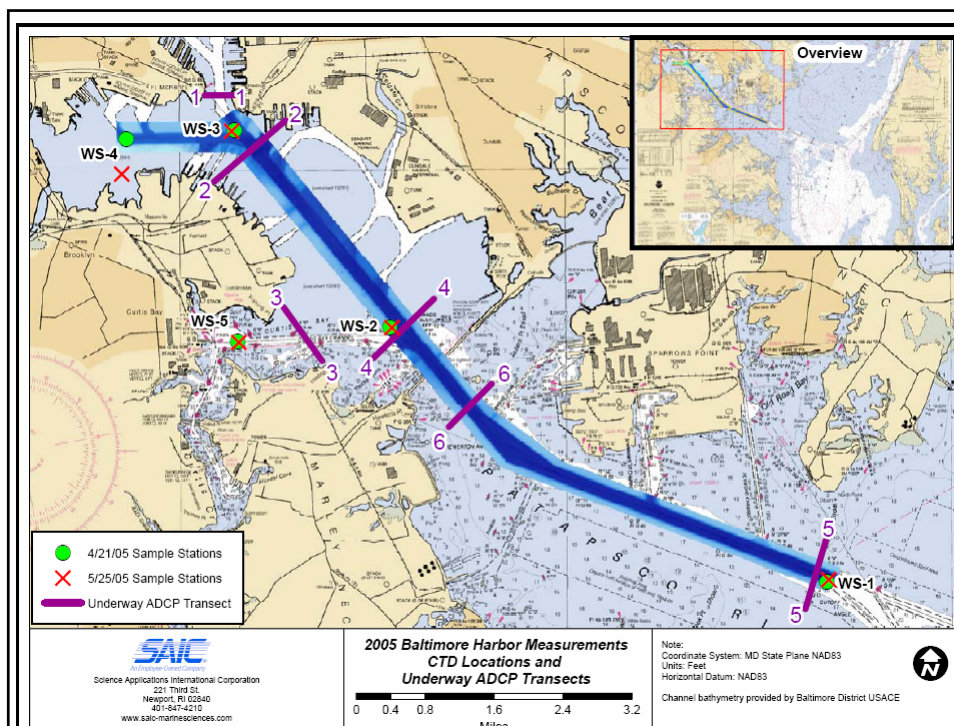


Table 3.1-1. Summary current statistics computed during both deployment periods from the Cutoff Angle ADCP data

Summary Current Statistics - Cutoff Angle ADCP (Approximate Water Depth - 16 m)								
Bin #	Approx Depth (m)	St.Dev. (3-HLP)	St.Dev. (40-HLP)	Ratio Var(40-HLP) / Var(3-HLP)	Max (3-HLP) (cm/sec)	Current Magnitude Min (3-HLP) (cm/sec)	Mean (3-HLP) (cm/sec)	Orientation of Principal axis °True, (3-HLP)
Deployment 1: 4/19/2005 - 5/26/2005								
1	13	8.4	7.0	0.7	43.7	0.1	11.5	295.8
2	12	9.1	7.8	0.7	53.8	0.2	12.7	306.9
3	11	9.9	8.7	0.8	62.7	0.2	14.0	306.8
4	10	10.9	9.8	0.8	61.0	0.6	15.3	305.6
5	9	11.2	10.2	0.8	69.7	0.1	16.5	304.4
6	8	11.3	10.1	0.8	70.9	0.1	17.4	303.6
7	7	11.3	9.6	0.7	61.6	0.5	17.7	303.3
8	6	10.9	8.7	0.6	57.0	0.3	17.2	302.2
9	5	10.1	7.8	0.6	61.9	0.2	15.9	303.2
10	4	8.8	6.7	0.6	51.8	0.1	13.3	307.5
11	3	6.9	4.3	0.4	44.3	0.3	10.4	315.4
12	2	5.1	2.5	0.2	29.0	0.2	9.3	322.5
13	1	4.8	2.1	0.2	25.0	0.1	9.8	316.3
Deployment 2: 5/27/2005 - 7/7/2005								
1	13	6.6	5.1	0.6	30.5	0.1	8.7	300.4
2	12	6.9	5.6	0.7	31.4	0.3	9.7	310.3
3	11	7.3	6.3	0.7	33.6	0.2	10.9	309.3
4	10	7.8	7.0	0.8	38.5	0.4	12.0	308.8
5	9	8.5	7.3	0.7	47.9	0.2	12.7	308.2
6	8	9.0	7.3	0.7	49.2	0.3	13.1	307.8
7	7	9.1	7.0	0.6	51.4	0.2	13.2	307.4
8	6	8.5	6.7	0.6	49.8	0.4	13.0	305.3
9	5	7.6	6.2	0.7	50.0	0.3	11.9	307.4
10	4	6.1	4.0	0.6	38.0	0.3	10.7	313.1

Table 3.1-2. Summary current statistics computed during both deployment periods from the Curtis Bay Entrance ADCP data

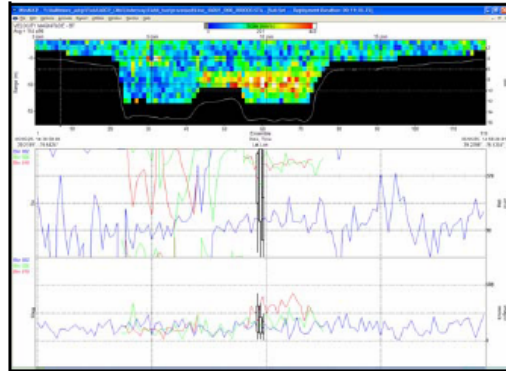
Summary Current Statistics - Curtis Bay Entrance ADCP (Approximate Water Depth - 12 m)								
Bin #	Approx Depth (m)	St.Dev. (3-HLP)	St.Dev. (40-HLP)	Ratio Var(40-HLP) / Var(3-HLP)	Max (3-HLP) (cm/sec)	Min (3-HLP) (cm/sec)	Mean (3-HLP) (cm/sec)	Orientation of Principal axis °True, (3-HLP)
Deployment 1: 4/9/2005 - 5/26/2005								
1	9	3.9	2.6	0.4	24.6	0.1	4.1	351.7
2	8	4.9	3.3	0.5	27.6	0.1	5.4	345.2
3	7	5.2	3.8	0.5	30.2	0.0	6.4	337.8
4	6	5.1	3.9	0.6	26.6	0.1	7.1	336.2
5	5	4.7	3.6	0.6	28.4	0.2	7.2	335.0
6	4	4.2	3.2	0.6	30.6	0.5	6.5	328.7
7	3	3.5	2.4	0.5	19.2	0.1	5.6	320.7
8	2	3.6	2.1	0.3	23.5	0.4	5.1	319.9
9	1	4.5	3.2	0.5	25.6	0.3	6.4	323.6
Deployment 2: 5/27/2005 - 7/7/2005								
1	9	3.4	2.0	0.3	23.5	0.0	4.0	348.9
2	8	3.8	2.7	0.5	25.4	0.1	4.5	348.2
3	7	4.3	3.3	0.6	32.9	0.0	5.1	341.7
4	6	4.6	3.6	0.6	33.6	0.1	5.7	337.5
5	5	4.0	3.2	0.6	26.7	0.4	5.8	334.5
6	4	3.1	2.2	0.5	18.1	0.0	5.3	327.0
7	3	2.5	1.3	0.3	14.0	0.1	4.7	328.5
8	2	3.1	2.0	0.4	18.1	0.1	5.0	335.4
9	1	4.1	3.2	0.6	23.0	0.1	6.8	331.6

Table 3.1-3. Summary current statistics computed during both deployment periods from the Fort McHenry Angle ADCP data

Summary Current Statistics - Fort McHenry Angle ADCP (Approximate Water Depth - 9 m)								
Bin #	Approx Depth (m)	St.Dev. (3-HLP)	St.Dev. (40-HLP)	Ratio Var(40-HLP) / Var(3-HLP)	Max (3-HLP) (cm/sec)	Min (3-HLP) (cm/sec)	Mean (3-HLP) (cm/sec)	Orientation of Principal axis °True, (3-HLP)
Deployment 1: 4/22/2005 - 5/24/2005								
1	5	4.5	3.5	0.6	21.8	0.2	7.3	327.6
2	4	4.1	3.3	0.6	20	0.1	6.7	340.1
3	3	3.3	2.7	0.7	18.4	0.3	5.6	331.7
4	2	2.9	1.8	0.4	16.1	0.1	4.8	325.5
5	1	3.5	2.3	0.4	20.8	0.1	5.4	332.2
Deployment 2: 5/26/2005 - 7/7/2005								
1	5	3.1	2.4	0.6	17.8	0.2	5	321.2
2	4	2.9	2.2	0.6	14.8	0.2	4.7	325.4
3	3	2.7	1.8	0.4	16.7	0.1	4.4	321.8
4	2	2.8	1.6	0.3	18.7	0.1	4.4	320.7
5	1	3.6	1.9	0.3	18.2	0.5	5.3	324.6

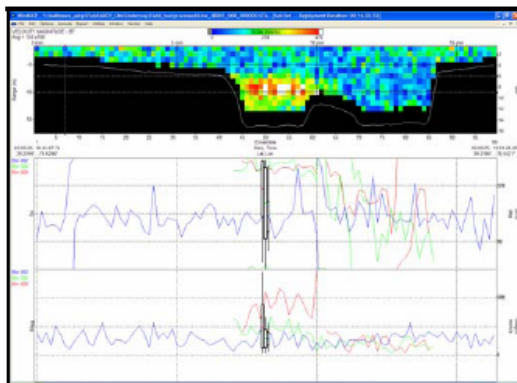
Table 3.1-4. Summary current statistics computed during both deployment periods from the Masonville Cove ADCM data

Summary Current Statistics - Masonville Cove ADCM (Approximate Water Depth - 3 m)								
Bin #	Approx Depth (m)	St.Dev. (3-HLP)	St.Dev. (40-HLP)	Ratio Var(40-HLP) / Var(3-HLP)	Max (3-HLP) (cm/sec)	Min (3-HLP) (cm/sec)	Mean (3-HLP) (cm/sec)	Orientation of Principal axis °True, (3-HLP)
Deployment 1: 4/20/2005 - 5/24/2005								
1	2.5	2	1	0.26	11.6	0.1	4	355.4
Deployment 2: 5/24/2005 - 7/7/2005								



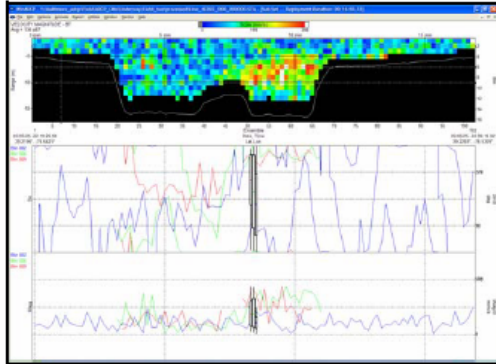
Transect – 4A001
 Start Time: 14:38 GMT
 End Time: 14:58 GMT
 Line Heading – 055 True

Figure 3.2-12. Current magnitude and direction along-track contour and profile results collected along underway ADCP Transect 4 on 5/25/05.



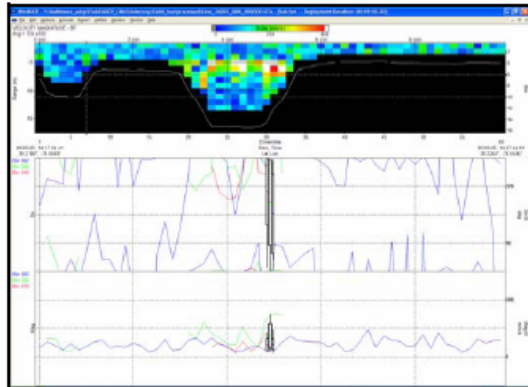
Transect – 4B001
 Start Time: 18:45 GMT
 End Time: 19:02 GMT
 Line Heading – 235 True

Figure 3.2-12. Current magnitude and direction along-track contour and profile results collected along underway ADCP Transect 4 on 5/25/05.



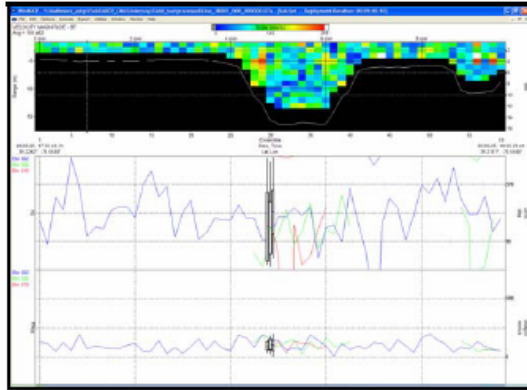
Transect – 4C002
 Start Time: 22:19 GMT
 End Time: 22:37 GMT
 Line Heading – 055 True

Figure 3.2-12. Current magnitude and direction along-track contour and profile results collected along underway ADCP Transect 4 on 5/25/05.



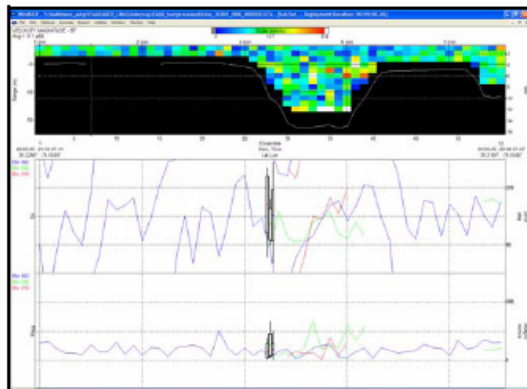
Transect – 3A003
 Start Time: 14:17 GMT
 End Time: 14:28 GMT
 Line Heading – 355 True

Figure 3.2-11. Current magnitude and direction along-track contour and profile results collected along underway ADCP Transect 3 on 5/25/05.



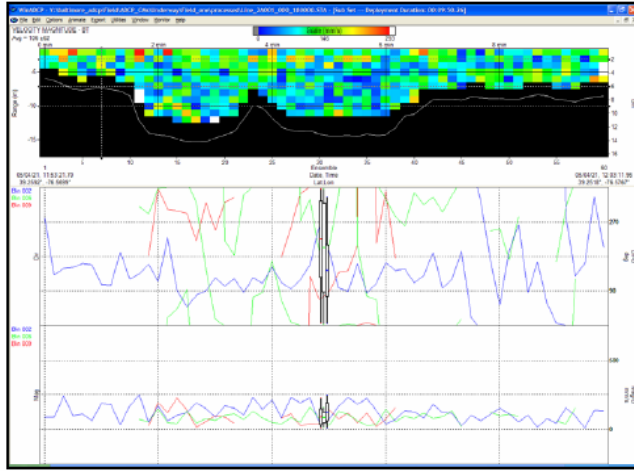
Transect – 3B001
 Start Time: 17:55 GMT
 End Time: 18:05 GMT
 Line Heading – 175 True

Figure 3.2-11. Current magnitude and direction along-track contour and profile results collected also underway ADCP Transect 3 on 5/25/05.



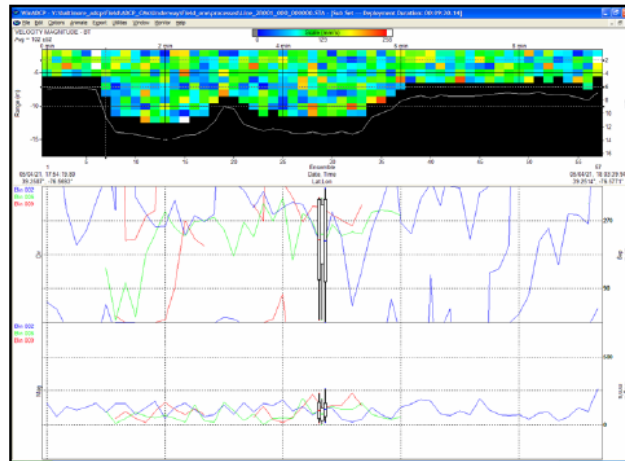
Transect – 3C001
 Start Time: 21:59 GMT
 End Time: 22:09 GMT
 Line Heading – 175 True

Figure 3.2-11. Current magnitude and direction along-track contour and profile results collected also underway ADCP Transect 3 on 5/25/05.



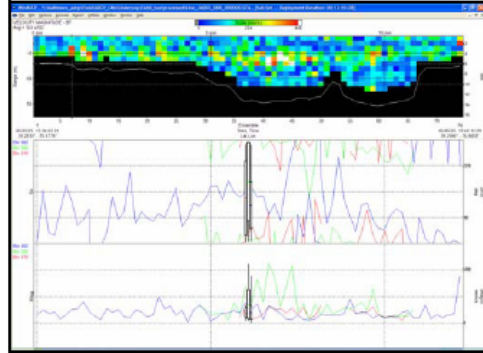
Transect - 2A001
 Start Time: 11:53 GMT
 End Time: 12:03 GMT
 Line Heading - 225 True

Figure 3.2-4. Current magnitude and direction along-track contour and profile results collected along underway ADCP Transect 2 on 4/21/05.



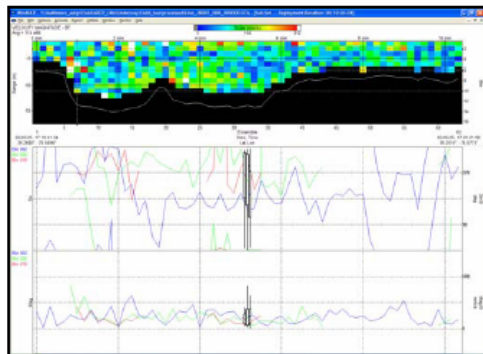
Transect - 2B001
 Start Time: 17:54 GMT
 End Time: 18:04 GMT
 Line Heading - 225 True

Figure 3.2-4. Current magnitude and direction along-track contour and profile results collected along underway ADCP Transect 2 on 4/21/05.



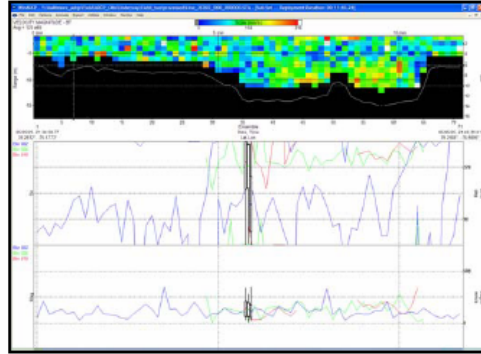
Transect - 2A003
 Start Time: 13:34 GMT
 End Time: 13:46 GMT
 Line Heading - 045 True

Figure 3.2-10. Current magnitude and direction along-track contour and profile results collected along underway ADCP Transect 2 on 5/25/05.



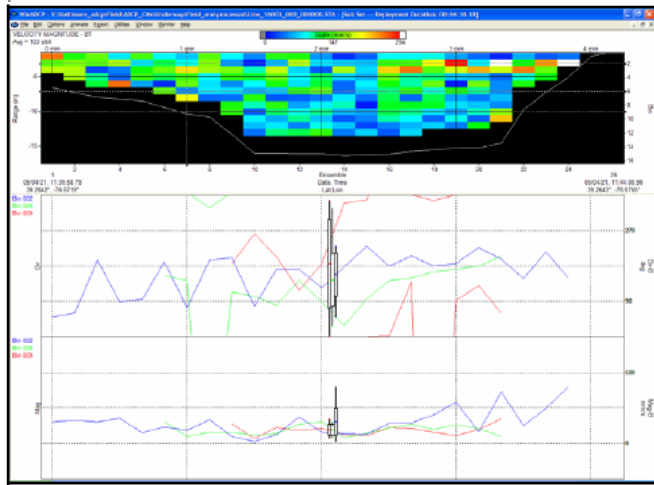
Transect - 2B001
 Start Time: 17:19 GMT
 End Time: 17:30 GMT
 Line Heading - 225 True

Figure 3.2-10. Current magnitude and direction along-track contour and profile results collected along underway ADCP Transect 2 on 5/25/05.



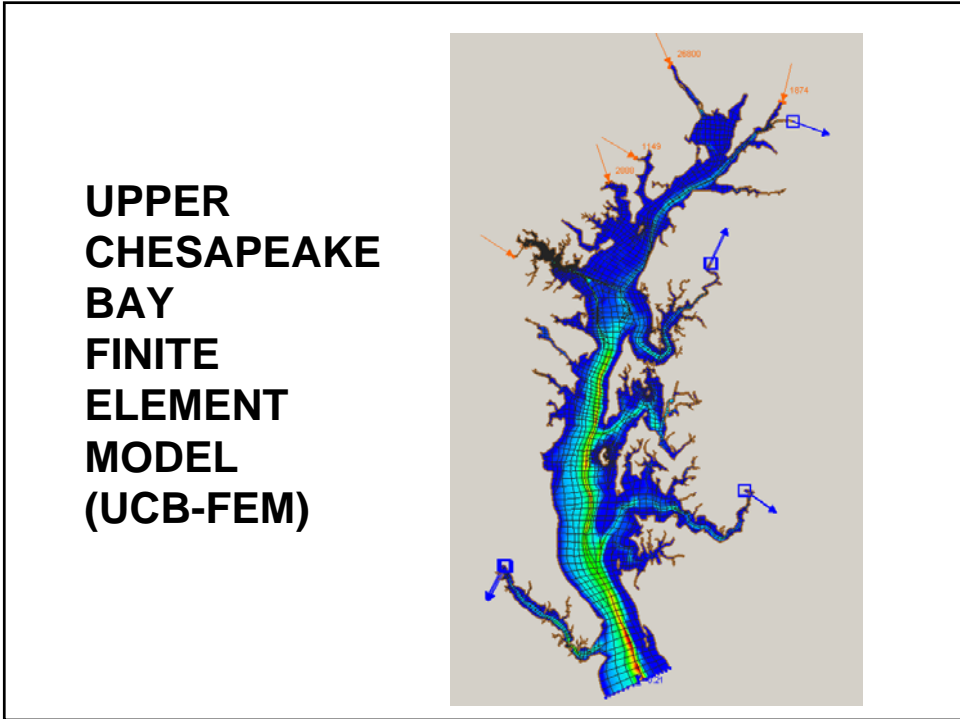
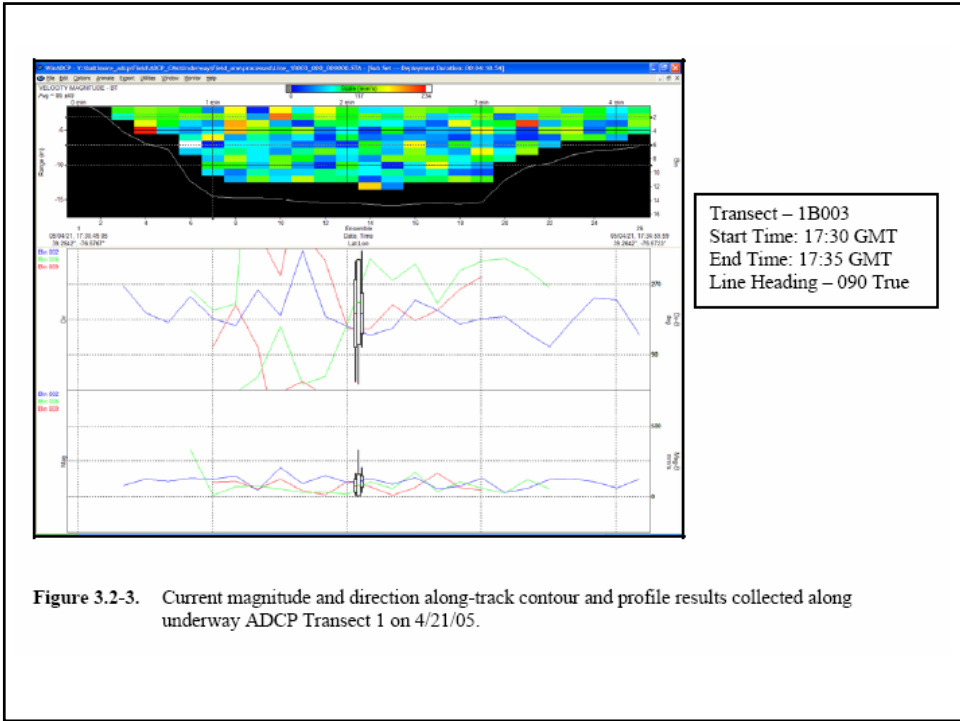
Transect - 2C002
 Start Time: 21:35 GMT
 End Time: 21:46 GMT
 Line Heading - 045 True

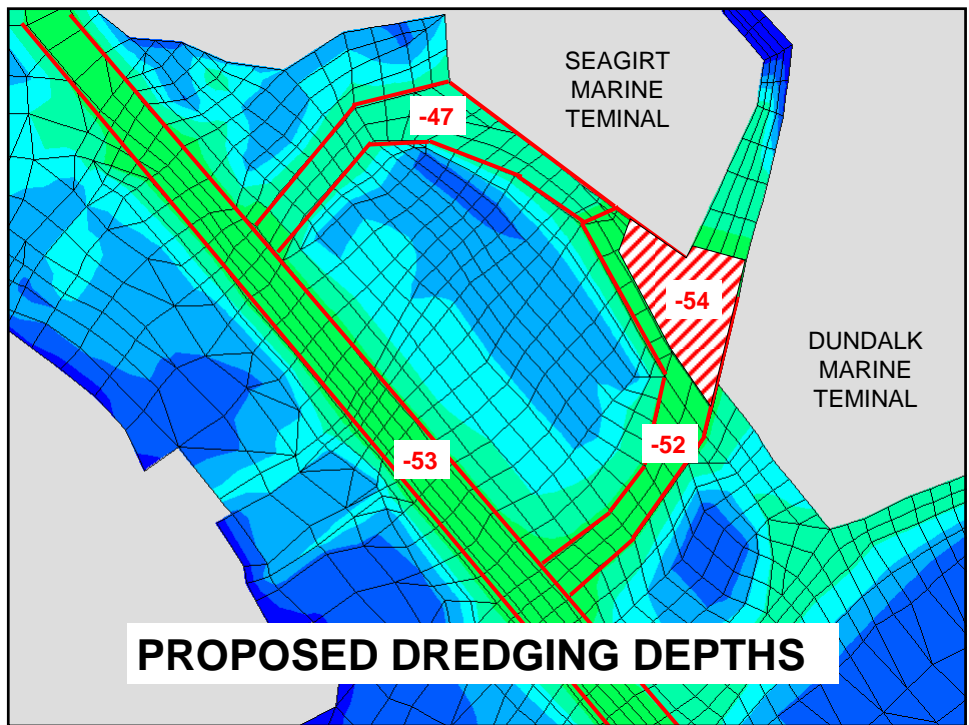
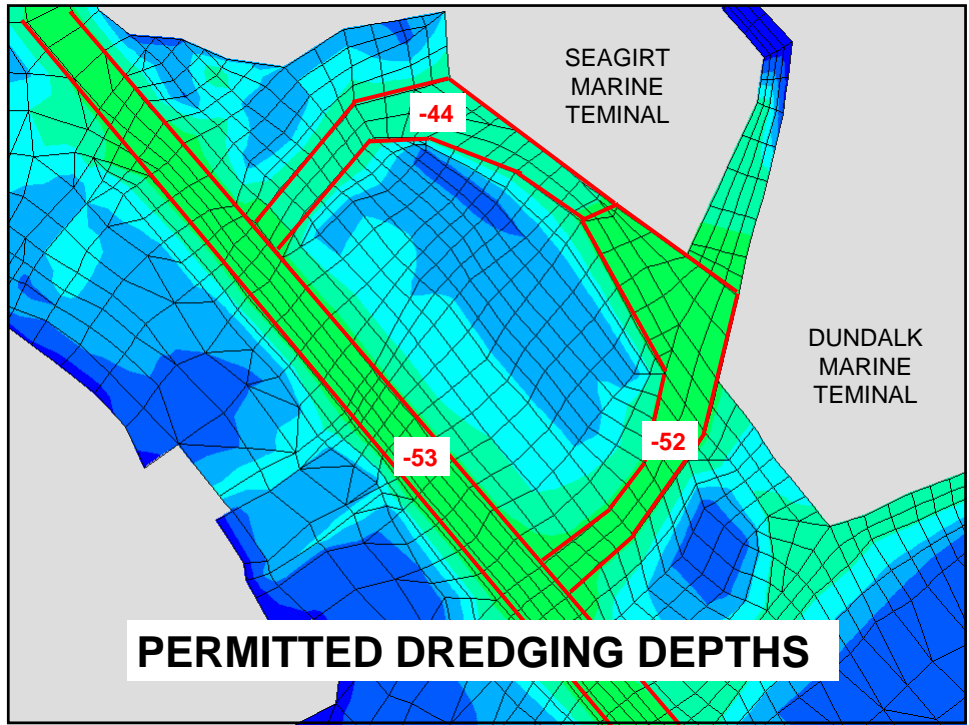
Figure 3.2-10. Current magnitude and direction along-track contour and profile results collected along underway ADCP Transect 2 on 5/25/05.

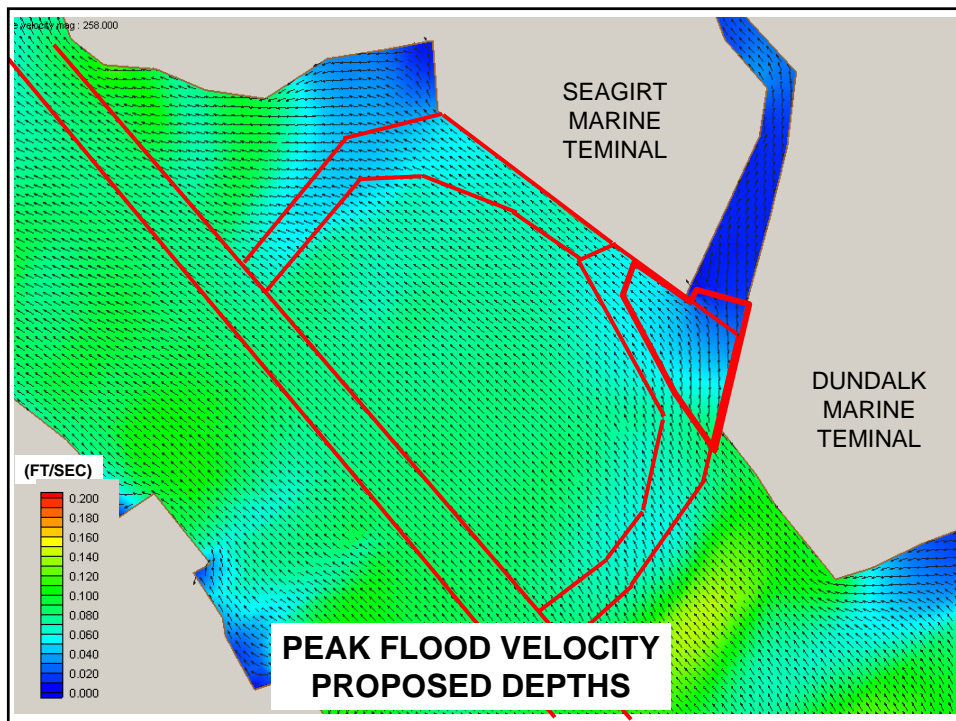
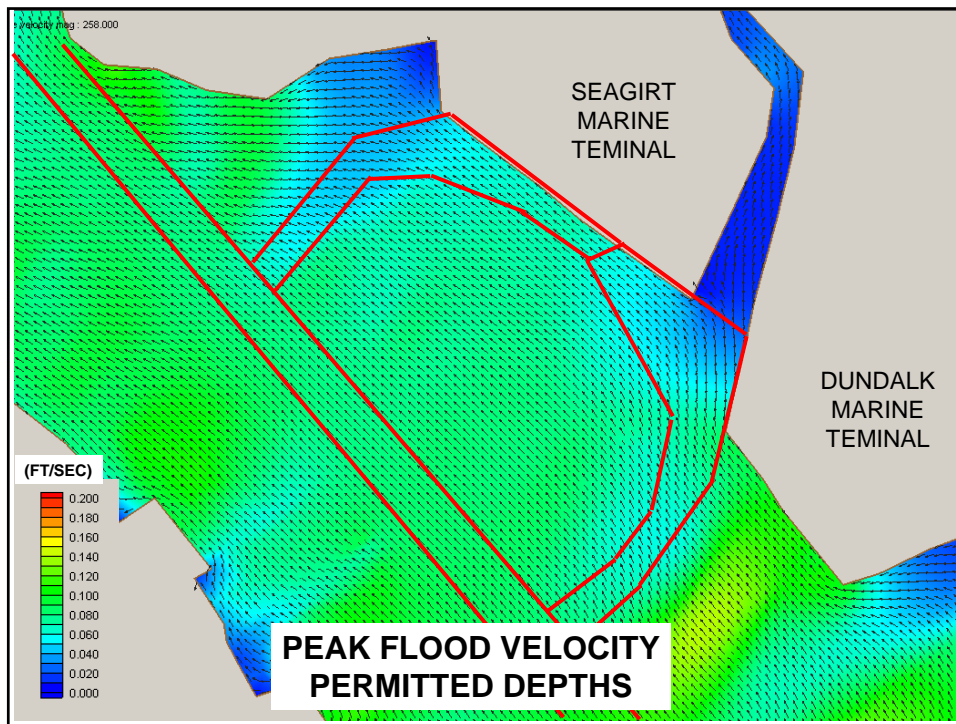


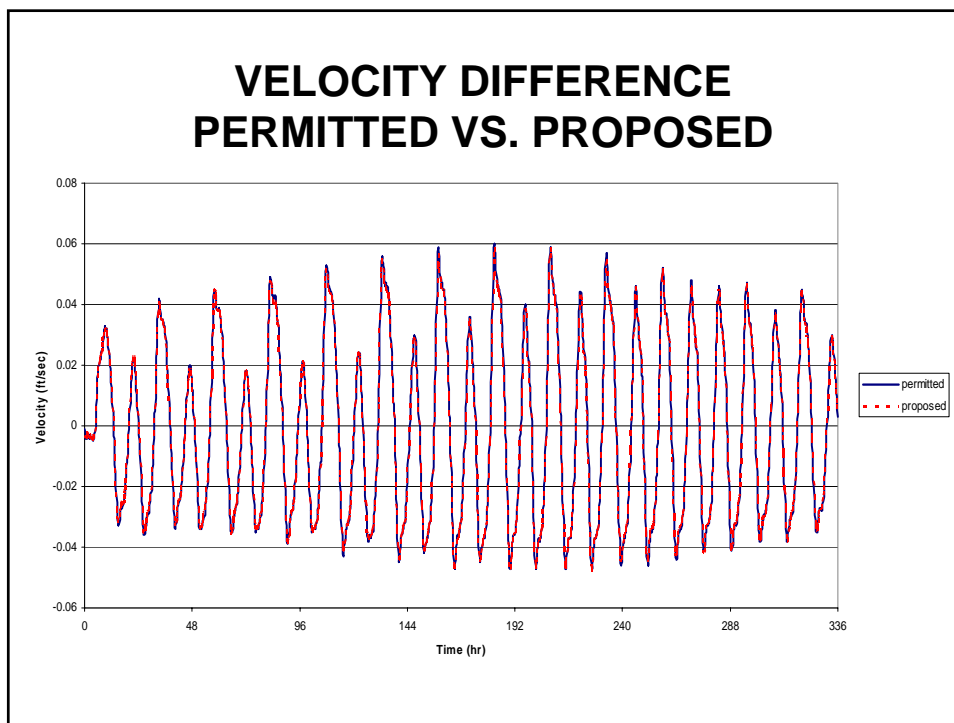
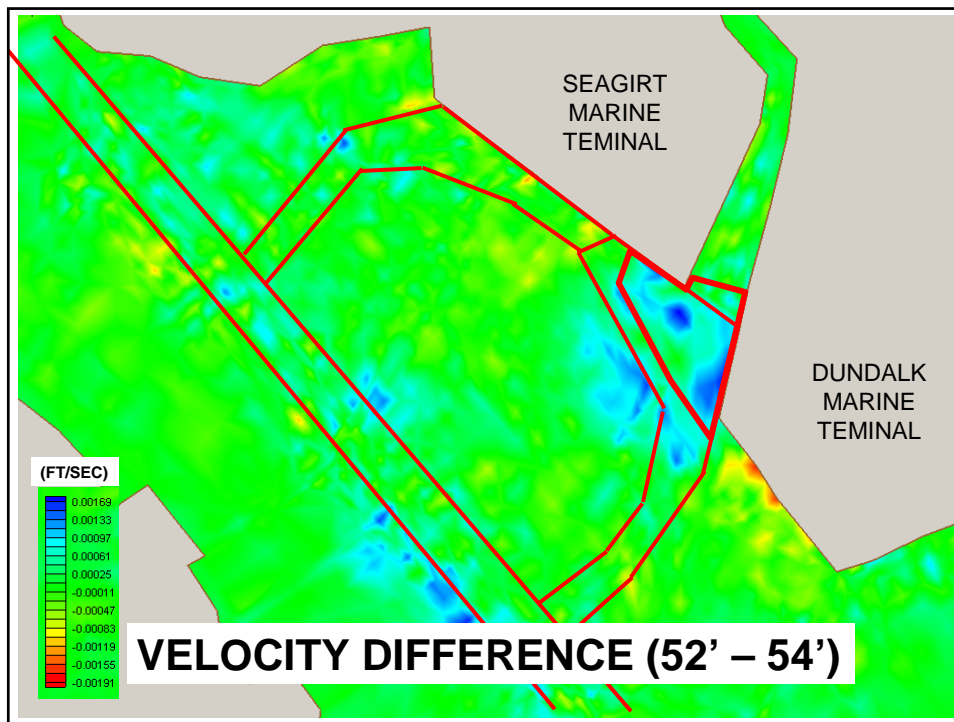
Transect - 1A003
 Start Time: 11:39 GMT
 End Time: 11:44 GMT
 Line Heading - 270 True

Figure 3.2-3. Current magnitude and direction along-track contour and profile results collected along underway ADCP Transect 1 on 4/21/05.









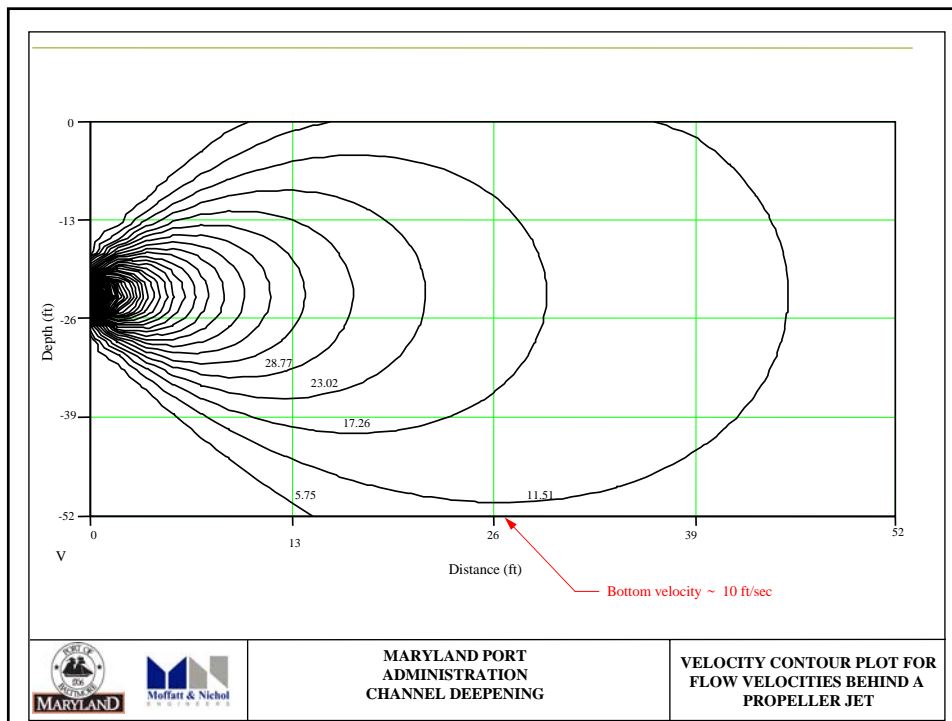
$$Q = V A$$

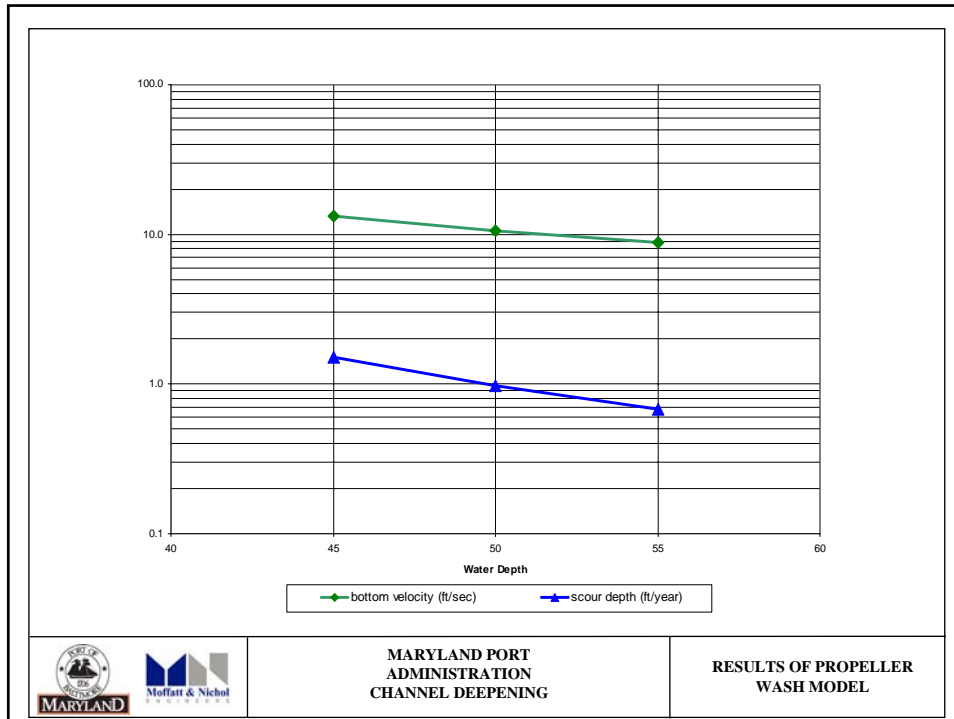
PERMITTED

$$Q = (0.057 \text{ FT/S})(52 \text{ FT}) \\ = 2.964 \text{ CFS}$$

PROPOSED

$$Q = (0.055 \text{ FT/S})(54 \text{ FT}) \\ = 2.970 \text{ CFS}$$





SUMMARY

- EQUIVALENT FLOW VELOCITY OBSERVED THROUGHOUT WATER COLUMN (TOP TO BOTTOM)
- THREE-LAYER FLOW OBSERVED IN BALTIMORE HARBOR WITH STRONGEST FLOW IN MIDDLE LAYER
- STRONG BOTTOM FLOW DUE TO SALT WEDGE ON FLOOD TIDE
- CHANGE TO AVERAGE FLOW VELOCITY DUE TO DEEPER DREDGING NEGLIGIBLE (2 TO 5 PERCENT)
- CHANGE TO TOTAL FLOW (Q) NEGLIGIBLE, INCREASES SLIGHTLY
- SHIP WAKE VELOCITIES STRONGER THAN MEASURED TIDAL FLOW (10 FT/SEC VS. 1 FT/SEC)

**Masonville Dredged Material Containment Facility
Proposed Seagirt Borrow: Patapsco River Channels Hydrodynamics and Modeling
Presented to Bay Enhancement Working Group
December 5, 2006**

The purpose of this hydrodynamics and modeling study of the Patapsco River is to evaluate the effects of deepening an area of the Dundalk West Access Channel to a maximum depth of -54 ft MLLW which is two feet deeper than the required depth of -52 ft MLLW. The deeper dredging would provide sand material for construction of the Masonville DMCF. The area of the channel deepening is approximately 41 acres.

Concerns were raised about whether the deeper channel would reduce flushing by causing water to be trapped in the deeper two-foot layer, thus creating poorer water quality, specifically as regards dissolved oxygen. To evaluate the flushing and subsequent water quality issues, a hydrodynamic study was made consisting of looking at measured current velocities in the river and numerical modeling of the proposed project.

Measured data were obtained from two sources: 1) Boicourt and Olson (1982) and 2) Science Applications International Corporation [SAIC (2005)]. Numerical modeling was performed using M&N's previously developed Upper Chesapeake Bay – Finite Element Model (UCB-FEM) based on the US Army Corps of Engineers (USACE) model RMA-2.

The Boicourt and Olson study included a substantial field measurement program that had current meters in place from late 1978 through late 1979. The study was performed to assess water quality impacts within the Harbor. A primary finding of the data analyses and model formulation effort was the complexity of the hydrodynamic structure within the Harbor, specifically, the existence of a density-driven, three-layer flow circulation. This circulation often dominates the flow to the point that semi-diurnal tidal current reversals are eliminated. A significant component of this three-layer flow is the existence of a layer of relatively high salinity on the bottom in the deeper channels.

The Boicourt and Olson study also evaluated the effects of dredging the shipping channels to a depth of 55 ft by using their hydrodynamic model. Primary conclusion of the modeling is that channel deepening increases both the salt penetration into the Harbor and the strength of the Harbor circulation, and specifically an increase in the circulation velocity in the deepened channel. The velocity increase is on the order of 10 to 20 percent.

As part of this Masonville EIS, SAIC and M&N prepared a water-column measurement program to provide the data to support M&N's hydrodynamic modeling effort. The 2005 measurement program that was developed consisted of four fixed long-term current measurement instruments and two days of transects along six lines and water sampling at five locations. See Attachment B-1 for details of the study.

Primary results of the 2005 data collection effort were a confirmation of the three-layer flow and other conclusions made by the Boicourt and Olson study. Primary flow direction was oriented along the channel, with comparable flow velocities throughout the water column from the

surface to the bottom. Maximum velocities were generally observed in the mid-water depths. Underway transect results were generally consistent with the stage of the tide, general inward flow on flood and outward flow on ebb. In some locations and during some transects, however, currents were weak and variable throughout most of the water column and showed a more mixed flow.

On April 21, 2005, Transect 4, nearest the Seagirt site, was aligned over the Fort McHenry Channel and the entrance to the Curtis Bay Channel. This transect showed on one run the lower and upper water column generally flowing outward, while the mid-water column flowed inward, then on another run the mid- and lower water column were flowing inward while the upper water column continued to flow outward.

On May 25, 2005, all of the transects except 3 showed the mid- and lower water column flowing inward, regardless of the tidal stage. This consistent inward flow was particularly evident in Transects 4, where a strong current of inward-flowing water was clearly seen in the lower to mid-water column and confined to the deeper waters of the Fort McHenry Channel. Similar flow was not observed in the adjacent Curtis Bay Channel. The near-surface currents were much weaker over these transects, and flowed either outward or to the south. A similar flow pattern was also observed over Transects 5 and 6, located further outside the Harbor across the Cutoff Angle or Brewerton Channel.

The UCB-FEM model finite element mesh used for the evaluation of the Seagirt dredging uses quadrilateral and triangular two-dimensional elements to represent the estuarial system. The southern boundary of the mesh is located in the Chesapeake Bay near the Hooper Island Light; the northern boundary is located at the Conowingo Dam on the Susquehanna River and Chesapeake City on the C & D Canal, resulting in total mesh length of roughly 90 nautical miles (nmi). A dense mesh was created for the Baltimore Harbor with additional refinement in the Seagirt project area to provide a more accurate simulation of conditions at the project site.

Water depths were adjusted to represent both currently permitted dredging depths and the deepened area in the Dundalk West Channel. Model results show negligible reduction in average current velocity through the water column, on the order of a maximum of 0.002 ft/sec (about 4 percent). When the total flow (Q) is computed by multiplying the average velocity (V) by the water depth for a one-foot width (A), the flow is higher with the deepened channel (2.970 cfs vs. 2.964 cfs), but still not significantly different.

Velocity modeling of ship propeller wash indicates that water movement due to ship traffic is much higher than tidal current velocity, about 10 ft/sec vs. 1 ft/sec. This high water velocity from the ship wake has ample ability to move the sediment off the bottom due to additional shear stress (resuspension) followed by sediment transport towards the sides of the channel. The relatively high water velocities as well as the physical movement of the ships would also serve to increase circulation in the water column within the channels. The propeller wash velocity modeling indicates that ship traffic would have a significant effect on channel depths and configurations during their passage through the shipping channels. Evidence of this effect is shown by hydrographic surveys of the Harbor channels that show channel conditions have deeper depths than dredged in the middle of the channel.

In summary, the following conclusions are made:

Comparable current speed is observed throughout the water column (top to bottom)

Three-layer flow is observed in Baltimore Harbor with faster speeds in the middle layer

Strong bottom flow due to salt wedge is observed on flood tide

Change to average flow velocity due to deeper dredging is negligible (2 to 5 percent)

Change to total flow (Q) is negligible, and increases slightly

Ship wake velocities are stronger than measured tidal flow (10 ft/sec vs. 1 ft/sec)

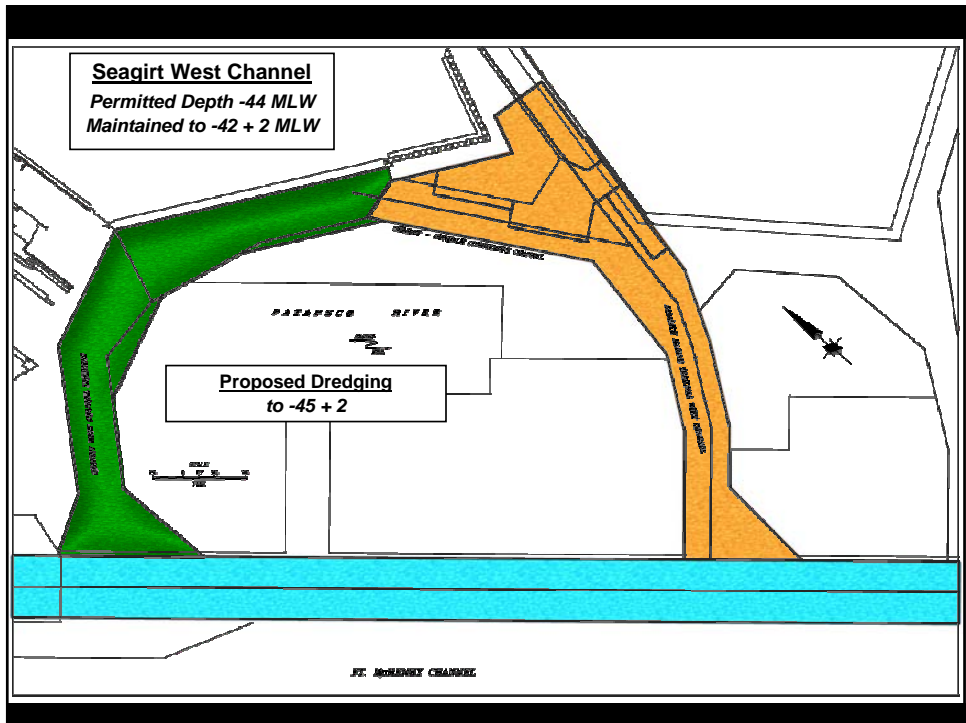
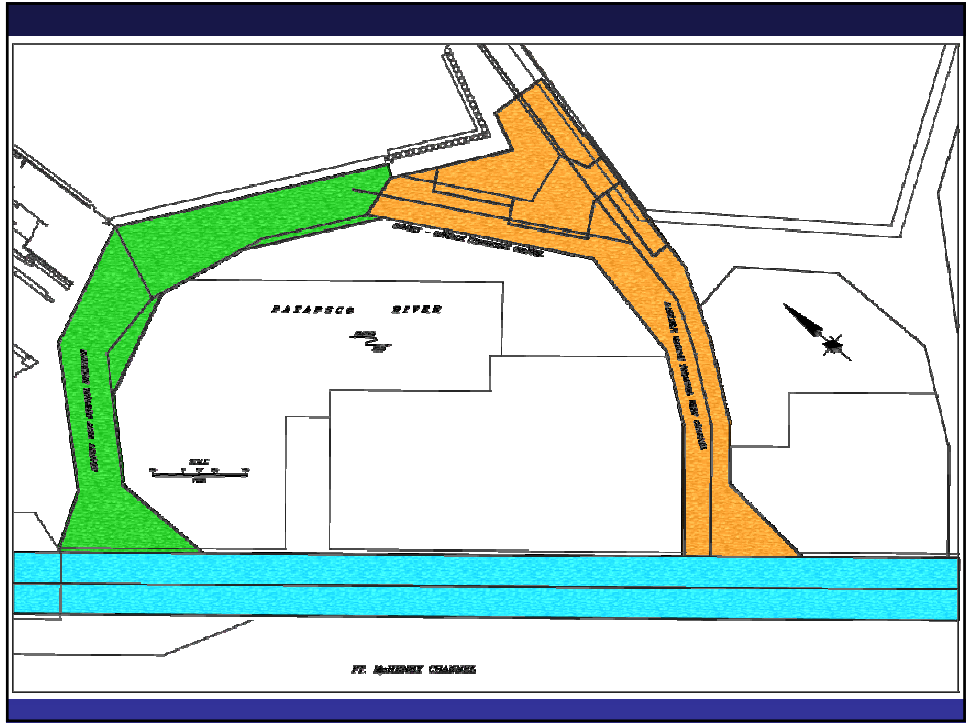
Seagirt Dredging

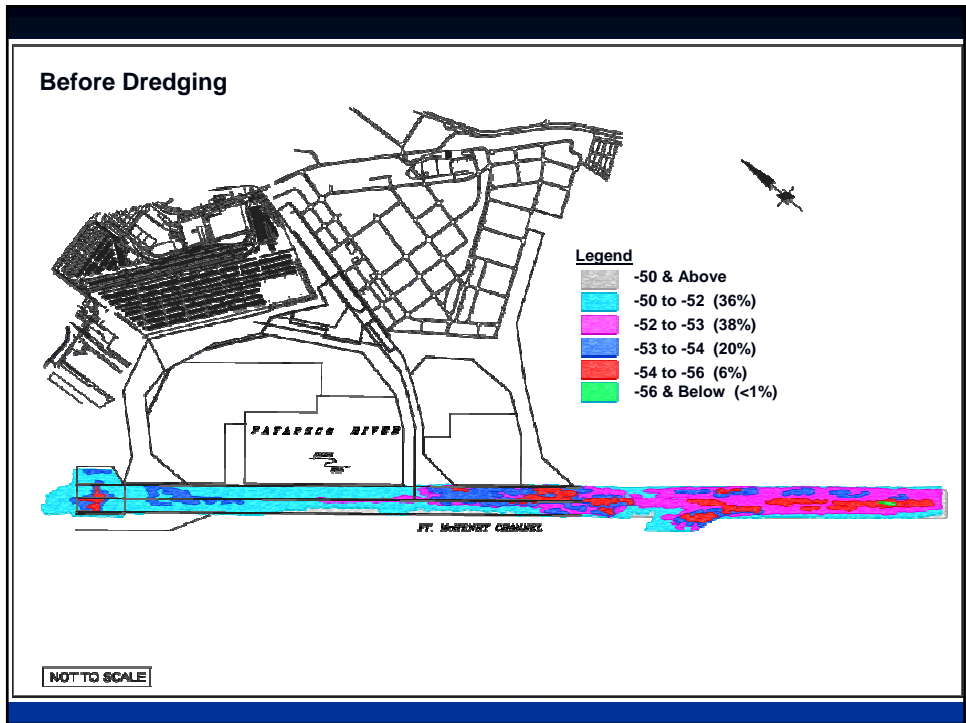
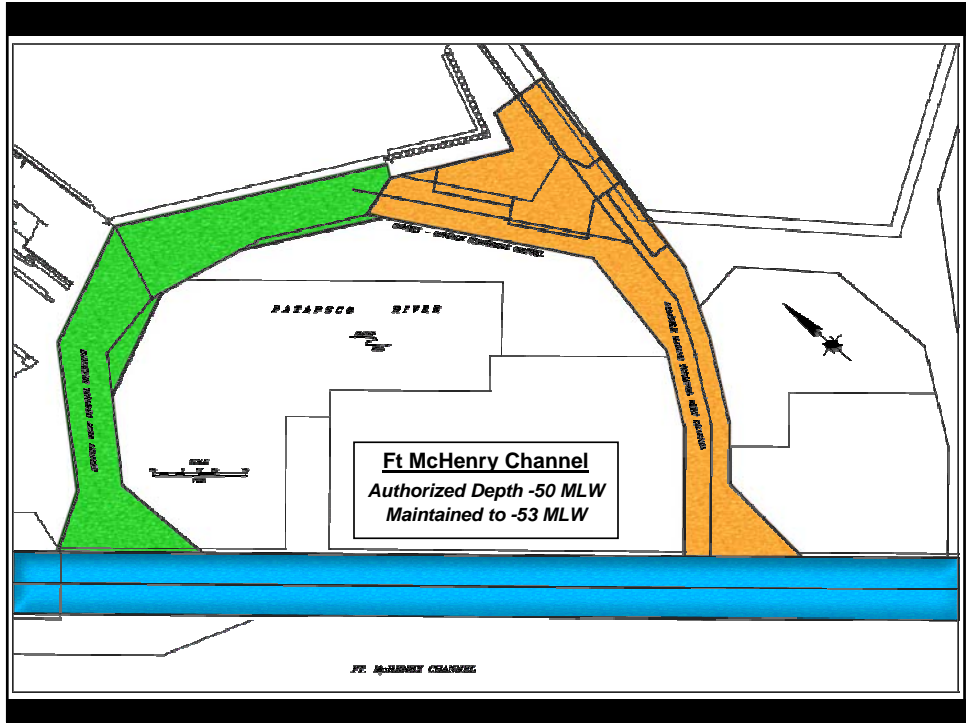
Proposed Channel Depths

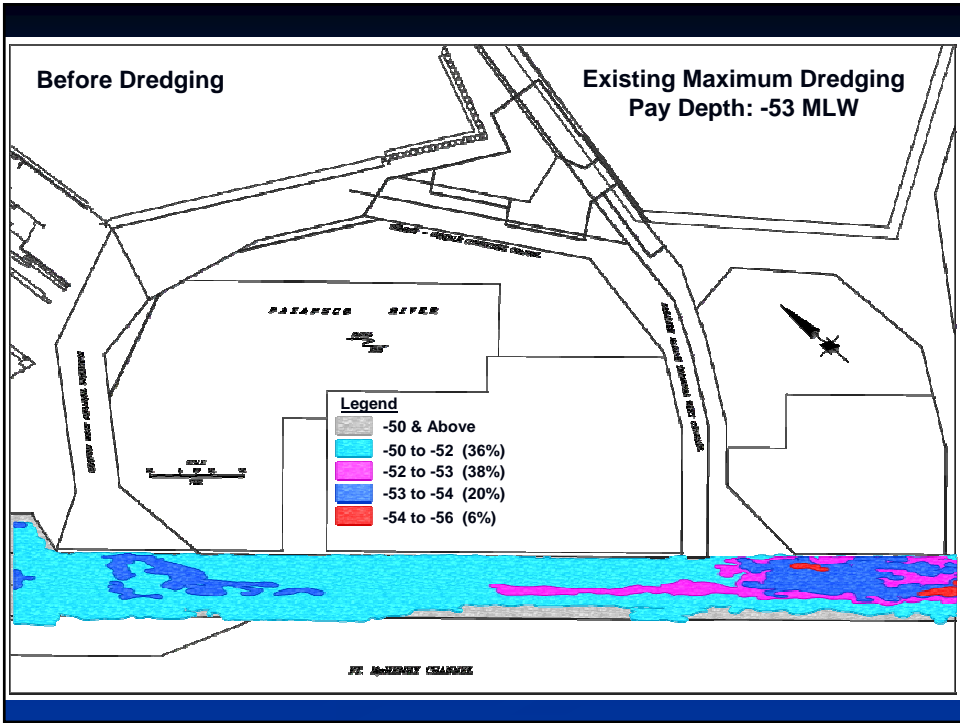
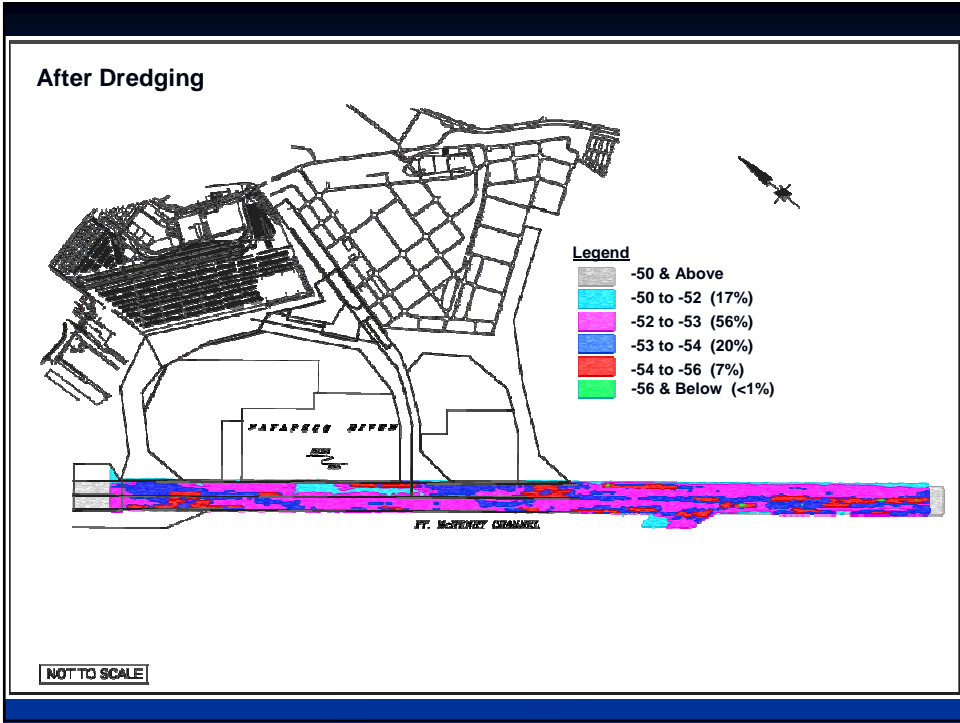
Presented to:
Bay Enhancement Working Group
December 05, 2006

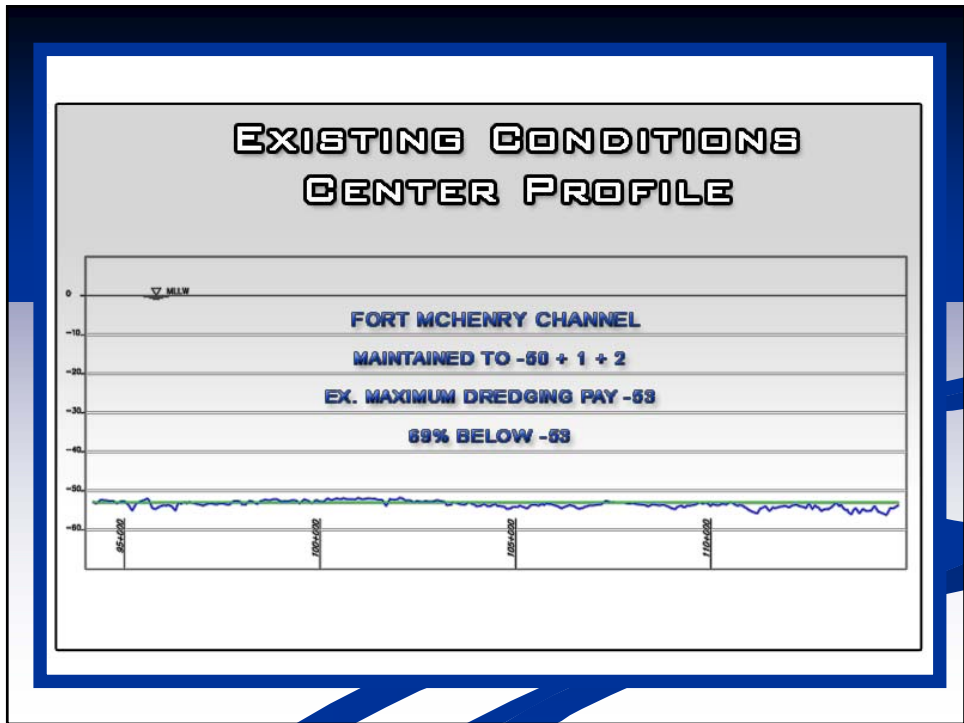
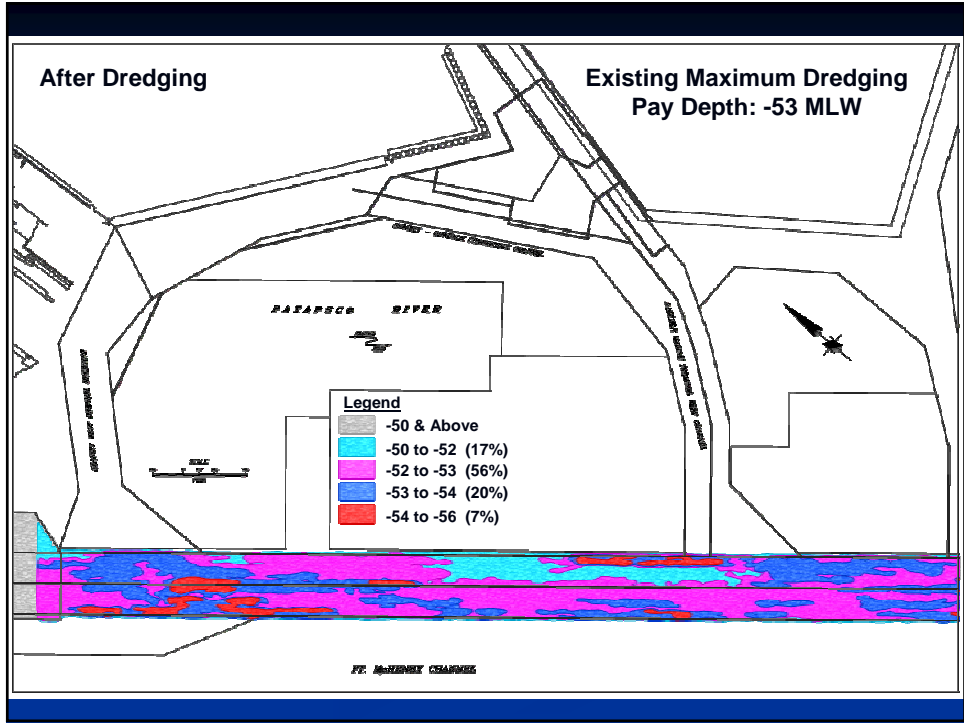
Seagirt Dredging

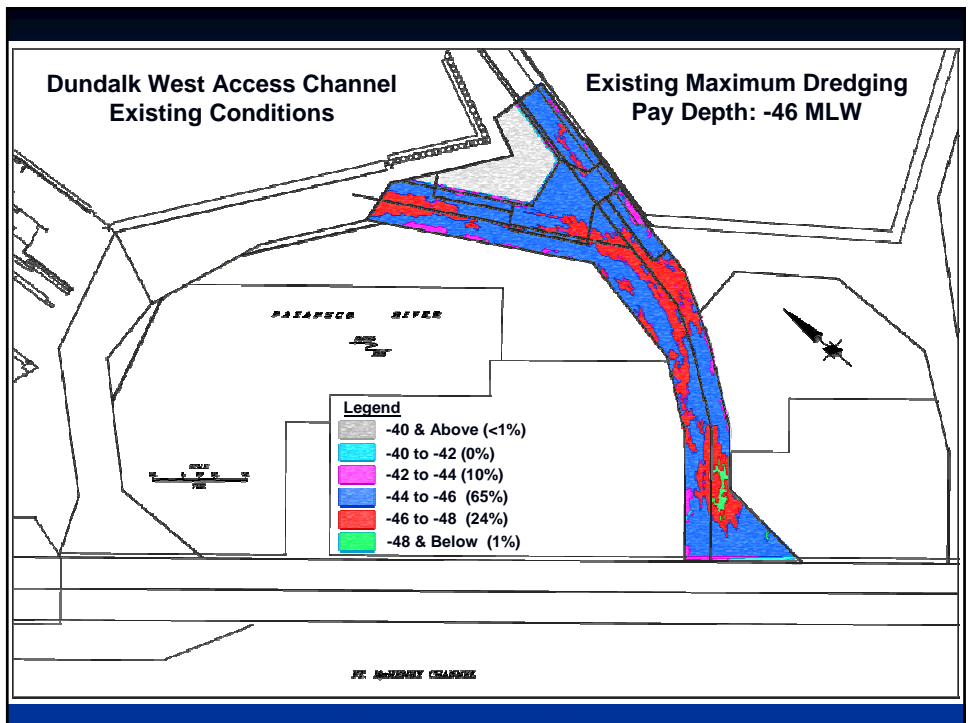
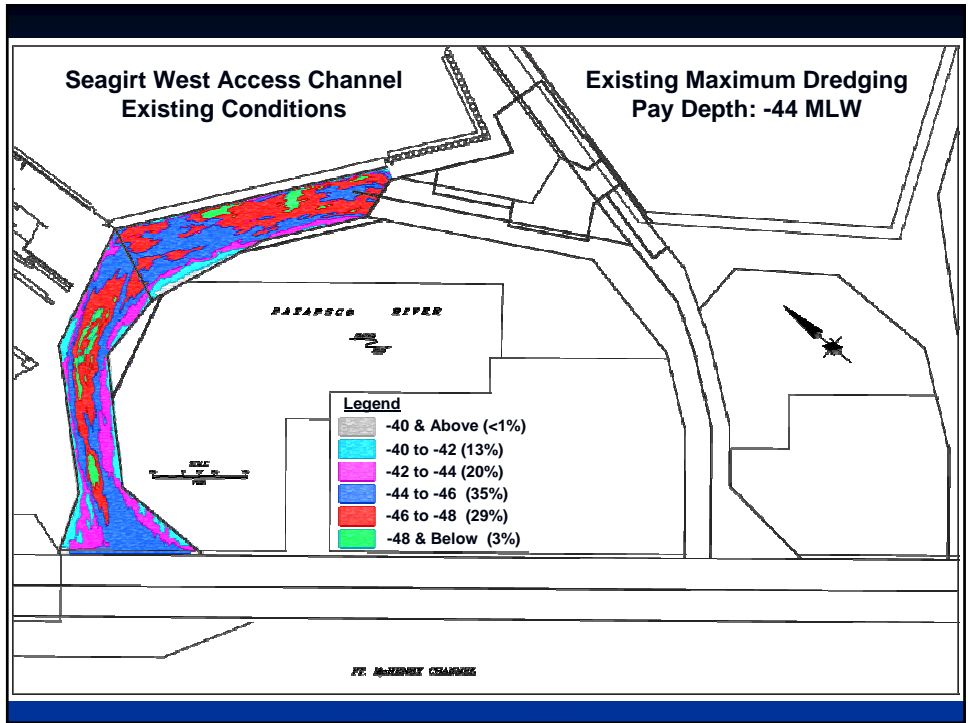
1. Permitted and Dredged Depths
2. Channel Hydrodynamics
3. Ships Effects (Props, Hull)
4. Existing Channel Conditions
 - a) Bathymetry
 - b) Centerline Profiles
 - c) Ships Effects
 - d) Channel Shoaling
5. Proposed Channel Geometries
 - a) Seagirt West Access Channel
 - b) Dundalk West Access Channel
 - Borrow Area at Dundalk











Summary of Existing Conditions

1. Bathymetry
 - a) Variable
 - Ft McHenry -49 to -58
 - Seagirt West -38 to -51
 - Dundalk West -42 to -50
 - Significantly Deeper at Channel Centerline
 - b) Ships Effect
 - Deeper at the Centerline
 - Hydraulic Connectivity at Centerline
 - c) Channel Shoaling
 - Shoaling occurs in the deeper sections

Proposed Channel Geometries

1. Seagirt West Access Channels
 - a) Dredge to -45+2
2. Dundalk West Access Channels
 - a) Dredge to -50+2
3. Borrow Area at Dundalk
 - a) Dredge to -52+2

December 12, 2006

Channel Depths for Masonville EIS

It is proposed that borrow material from the access channels being dredged at Seagirt and Dundalk Marine Terminals be used for dike building material at the proposed Masonville DMCF. The materials have been sampled and tested and have proved to be environmentally acceptable and structurally sound for construction.

The coarse grain material has been identified in the planned dredging areas at these terminals in the Dundalk West Channel. These materials are sand and gravel and located within the dredging template. Presently, these materials are to be dredged and placed at HMI. There are approximately 401,000 cy of material available above -53 ft MLLW, which is the maintenance depth for the Fort McHenry Channel. Additional dike building material is below that depth. If permits are modified to allow for a maximum dredging depth of -54 MLLW, approximately 68,000 cy more could be secured for construction. With a permitted maximum depth of -54, it is anticipated that material would be dredged to an average depth of -53. With possible fines for dredging below -54, the dredging contractor will not attempt to exceed that depth, thus raising the averaged dredged depth.

Questions regarding the possibility of creating an anoxic zone were raised since the borrow area would be dredged approximately 1-2 ft lower than the rest of the channel that connects this area with the Fort McHenry channel. After studying hydrographic surveys of this area, the following was observed:

- Ft. McHenry Channel has surveyed depths ranging from -49 to -58 ft.
- Dundalk West channel has depths ranging from -42 to -50.
- The loop channel, consisting of the Dundalk West, the Seagirt -Dundalk Connecting, and the Seagirt West channels all exit deeper than permitted depth due to ships traffic.

Evaluation and modeling of the potential 2 ft difference in channel depths led to the conclusion that no appreciable increase in the persistence of an anoxic zone should be anticipated due to this 2 ft. In addition, it is anticipated that ship traffic will help "churn" this area, which would reduce the significance of any depth difference. Also, not accounted into the modeling effort is that ship and tug operations and shoaling will impact the bottom significantly enough to make the difference even more insignificant. This impact is expected to occur within approximately 5 years.

Ft. McHenry Channel is authorized to -50 ft and , per USACE, is maintained to -50 ft + 1 ft of advanced maintenance + 2 ft of allowable overdredge, for a depth of -53 ft MLLW. Dundalk West is presently permitted to -52 and maintained to -44 ft + 2 ft.